DENITRIFYING ANAEROBIC METHANE OXIDATION (DAMO) MICROORGANISMS: INVESTIGATION OF THEIR OCCURRENCE AND ENRICHMENT

A THESIS SUBMITTED TO
THE GRADUATE SCHOOL OF NATURAL AND APPLIED SCIENCES
OF
MIDDLE EAST TECHNICAL UNIVERSITY

BY

DİLAN LAÇİN

IN PARTIAL FULFILLMENT OF THE REQUIREMENTS
FOR
THE DEGREE OF MASTER OF SCIENCE
IN
ENVIRONMENTAL ENGINEERING

SEPTEMBER 2021

Approval of the thesis:

DENITRIFYING ANAEROBIC METHANE OXIDATION (DAMO) MICROORGANISMS: INVESTIGATION OF THEIR OCCURRENCE AND ENRICHMENT

submitted by **DİLAN LAÇİN** in partial fulfillment of the requirements for the degree of **Master of Science in Environmental Engineering, Middle East Technical University** by,

Prof. Dr. Halil Kalıpçılar
Dean, Graduate School of **Natural and Applied Sciences** _____

Prof. Dr. Bülent İçgen
Head of the Department, **Environmental Engineering** _____

Assoc. Prof. Dr. Tuba Hande Bayramoğlu
Supervisor, **Environmental Engineering, METU** _____

Examining Committee Members:

Prof. Dr. İpek İmamoğlu
Environmental Engineering, METU _____

Assoc. Prof. Dr. Tuba Hande Bayramoğlu
Environmental Engineering, METU _____

Prof. Dr. Filiz B. Dilek
Environmental Engineering, METU _____

Assist. Prof. Dr. Harun Koku
Chemical Engineering, METU _____

Assoc. Prof. Dr. Bilge Alpaslan Kocamemi
Environmental Engineering, Marmara University _____

Date: 08.09.2021

I hereby declare that all information in this document has been obtained and presented in accordance with academic rules and ethical conduct. I also declare that, as required by these rules and conduct, I have fully cited and referenced all material and results that are not original to this work.

Name, Lastname: Dilan Laçin

Signature :

ABSTRACT

DENITRIFYING ANAEROBIC METHANE OXIDATION (DAMO) MICROORGANISMS: INVESTIGATION OF THEIR OCCURRENCE AND ENRICHMENT

Laçin, Dilan
Master of Science, Environmental Engineering
Supervisor: Assoc. Prof. Dr. Tuba Hande Bayramoğlu

September 2021, 256 pages

DAMO process has the potential of decreasing CH_4 emissions in the aquatic ecosystems, and the nitrite and nitrate levels in the natural ecosystems and receiving bodies. The seed source is very critical to enrich slowly growing DAMO microorganisms successfully in a short time. In this study, the occurrence and activity of DAMO microorganisms in different inoculum sources were investigated by activity tests and molecular analyses. Seed sources used in this study were paddy field soil (private rice field in Kızılırmak District, Çankırı, Turkey), freshwater sediment (Lake Eymir, Ankara, Turkey), anaerobic digester sludge (ASKİ Ankara Central Wastewater Treatment Plant) and return activated sludge of a biological nutrient removal system (İSKİ Ambarlı Advanced Wastewater Treatment Plant). Paddy field soil, freshwater sediment, and anaerobic digester sludge and their combinations were observed to show potential DAMO activity. Return activated sludge of a biological nutrient removal system was not observed to be a good choice for the enrichment of DAMO microorganisms due to its high biodegradable organic matter content which gives denitrifiers and methanogens great advantage over DAMO species.

The enrichment of both Damo-Bacteria and Damo-Archaea was also investigated in sequencing batch reactors (SBRs). Two enrichment studies were carried out, one at low influent concentrations and low hydraulic retention time (HRT), and the other at high influent nitrite and nitrate concentrations and high HRT. Higher DAMO-specific activities were obtained at high HRT and higher initial nitrite and nitrate concentrations. However, the enrichment of DAMO microorganisms cultivated in this study showed very low nitrite and nitrate removal rates although the molecular evidence supported their presence in the cultures. The main reason for the low activity of DAMO species was associated with SBR configuration, which did not facilitate gas transfer and availability of methane. The effect of granular activated carbon (GAC) on the activity of DAMO co-culture was investigated. The positive effect of GAC application was observed on both Damo-Bacteria and Damo-Archaea activity, which might be due to the increased dissolved methane availability and, in turn, improved contact between biomass and dissolved methane. Application of GAC decreased the time for enrichment by 3-fold.

This study is the first to report the occurrence and activity of DAMO microorganisms in Turkey, which are promising for the treatment of wastewaters with high CH_4 and nitrogen (N) content. Results revealed that enrichment of both DAMO species is possible. Improvement of the activity in shorter periods needs further investigation.

Keywords: Denitrifying anaerobic methane oxidation (DAMO), *M.oxyfera*, *M.nitroreducens*

ÖZ

DENİTRİFİYE ANAEROBİK METAN OKSİDASYONU (DAMO) MİKROORGANİZMALARI: VARLIKLARININ VE ZENGİNLEŞTİRİLMELERİNİN İNCELENMESİ

Laçin, Dilan
Yüksek Lisans, Çevre Mühendisliği
Tez Yöneticisi: Assoc. Prof. Dr. Tuba Hande Bayramoğlu

Eylül 2021, 256 sayfa

DAMO prosesi, sucul ekosistemlerdeki CH_4 emisyonlarını ve alıcı ortamlardaki nitrit ve nitrat seviyelerini azaltma potansiyeline sahiptir. Yavaş büyüyen DAMO mikroorganizmalarının kısa sürede başarılı bir şekilde zenginleştirilmesi için aşı kaynağı çok önemlidir. Bu çalışmada, farklı aşı çamuru kaynaklarında DAMO mikroorganizmalarının varlığı ve aktivitesi, aktivite testleri ve moleküler analizler ile araştırılmıştır. Bu çalışmada kullanılan aşı kaynakları, çeltik tarlası toprağı (Çeltik tarlası, Çankırı, Türkiye), tatlı su sedimanı (Eymir Gölü, Ankara, Türkiye), anaerobik çürütücü çamuru (ASKİ Ankara Merkezi Atıksu Arıtma Tesisi) ve biyolojik nutriyent giderim sistemi geri devir çamurudur (İSKİ Ambarlı İleri Atıksu Arıtma Tesisi). Çeltik tarlası toprağı, tatlı su sedimanı ve anaerobik çürütücü çamuru ve bu aşı çamurlarının kombinasyonlarında potansiyel DAMO aktivitesi gözlenmiştir. Biyolojik nutriyent giderimi sisteminin geri devir çamurunun, yüksek miktarda organik madde içermesi sebebiyle, DAMO mikroorganizmalarına kıyasla denitrifikasyon bakterilerine ve metanojenlere büyük

avantaj sağladığı ve DAMO mikroorganizmalarının zenginleştirilmesi için uygun bir seçim olmadığı gözlenmiştir.

Aynı zamanda, Damo-Bakteri ve Damo-Arke'nin birlikte zenginleştirilmesi, ardışık kesikli reaktörlerde (AKR) araştırılmıştır. Birinde düşük başlangıç nitrit ve nitrat derişimleri ve düşük hidrolik besleme süresi (HBS), diğerinde ise yüksek giriş nitrit ve nitrat derişimleri ve yüksek HBS kullanılan iki zenginleştirme çalışması yapılmıştır. Yüksek HBS ve yüksek başlangıç nitrit ve nitrat derişimlerinde daha yüksek DAMO spesifik aktiviteleri elde edilmiştir. Bununla birlikte, bu çalışmada DAMO mikroorganizmalarının kültürlerdeki varlıklarının moleküler çalışmalarla desteklemesine rağmen, zenginleştirilen DAMO mikroorganizmaları çok düşük nitrit ve nitrat giderim hızları göstermiştir. DAMO türlerinin düşük aktivitesinin ana nedeni, gaz transferini ve metanın çözünürlüğünü desteklemeyen AKR konfigürasyonu ile ilişkilendirilmiştir. Granüler aktif karbonun (GAK), DAMO ortak kültürünün aktivitesi üzerindeki etkisi araştırılmıştır. GAK uygulamasının hem Damo-Bakteri, hem de Damo-Arke aktivitesi üzerinde, çözünmüş metanın mevcudiyetinin ve buna bağlı olarak biyokütle ile çözünmüş metan arasındaki temasın artması kaynaklı olabileceği düşünülen, pozitif etkisi gözlenmiştir. GAK uygulaması zenginleştirme süresini 3 kat azaltmıştır.

Bu çalışma, yüksek CH_4 ve azot (N) içeriğine sahip atıksuların arıtımı için umut vadeden DAMO mikroorganizmalarının Türkiye'deki varlığını ve aktivitesini bildiren ilk çalışmadır. Sonuçlar, her iki DAMO türünün birlikte zenginleştirilmesinin mümkün olduğunu ortaya koymuştur. Aktivitelerin daha kısa sürelerde artırılması için daha fazla araştırma yapılması gerekmektedir.

Anahtar Kelimeler: Denitrifiye anaerobik metan oksidasyonu (DAMO), *M.oxyfera*, *M.nitroreducens*

To my family

ACKNOWLEDGMENTS

I would like to express my sincere gratitude and appreciation to Assoc. Prof. Dr. Tuba H. Ergüder Bayramoğlu for her patience, continuous support, and invaluable guidance during my master's study. I would also like to thank the examining committee members Prof. Dr. Filiz B. Dilek, Prof. Dr. İpek İmamoğlu, Assist. Prof. Dr. Harun Koku, Assoc. Prof. Dr. Bilge Alpaslan Kocamemi for their insightful comments and suggestions.

I gratefully acknowledge the financial support provided by the Scientific and Technological Research Council of Turkey (TUBİTAK) for the project (Project No: 118Y195) from which this thesis has emerged from.

Many thanks to all of the Envbiorg team members, Irmak Subaşı, Rayaan Harb, Nihan Kalaycıoğlu, Tercan Çataklı, Tuğba Çelik Çağlar, Ertan Hoşafçı and Simgenur Sağdıç for their valuable cooperation, support and friendship.

I am deeply grateful for the amazing people in my life, Yiğit Laçin, Sıla Laçin, Erdem Damar, Burak Akdemir and Özge Sevinç who always stand by me and help me through my anxiety, stress and problems during my master study. Thank you for all your encouragement, support, and constant source of inspiration.

Above all, I owe my deepest gratitude to my mother Betül Laçin, and my father Kenan Laçin for their endless support, unconditional love, and belief in me. Their tremendous understanding and encouragement kept me motivated and confident in everything I have accomplished in life including this Thesis.

TABLE OF CONTENTS

LIST OF TABLES

TABLES

LIST OF FIGURES

FIGURES

LIST OF ABBREVIATIONS

ABBREVIATIONS

AD : Anaerobic Digester

AMO : Anaerobic Methane Oxidation

ANAMMOX : Anaerobic Ammonium Oxidation

ANME : Anaerobic Methanotrophs

AOB : Ammonium Oxidizing Bacteria

CANON : Completely Autotrophic Nitrogen Removal Over Nitrite

CSTR : Continuously Stirred Tank Reactor

DAMO : Denitrifying Anaerobic Methane Oxidation

DEMON : Deammonification

DO : Dissolved Oxygen

FISH : Fluorescence *In Situ* Hybridization

FS : Freshwater Sediment

GAC : Granular Activated Carbon

GHG : Greenhouse Gas

HRT : Hydraulic Retention Time

MBfR : Membrane Biofilm Reactor

MBRs : Membrane Bioreactor

MCR : Methyl-coenzyme Reductase

M-DAMO : Metal-Dependent Anerobic Methane Oxidation

MSGLR : Magnetically Stirred Gas Lift Reactor

N-DAMO : Nitrogen-Dependent Anaerobic Methae Oxidation

OLAND : Oxygen-limited Autotrophic Nitrification-Denitrification

pMMO : Particulate Methane Monooxygenase

PS : Paddy Field Soil

RS : Return Activated Sludge

SBR : Sequencing Batch Reactor

S-DAMO : Sulfate-Dependent Anerobic Methane Oxidation

SRB : Sulfate-reducing Bacteria

WWTP : Wastewater Treatment Plant

CHAPTER 1

INTRODUCTION

Global warming, which is considered as one of the main concerns that humanity is facing today, is largely caused by the increase in greenhouse gas (GHG) concentrations since the onset of the industrial revolution. Methane accounts for 16% of the total global GHG emissions (IPCC, 2014) due to both natural and anthropogenic sources. It is considered the second important GHG with a global warming potential (GWP) of 25 due to its capacity to capture heat 25 times more effectively than CO_2 (IPCC, 2013). Therefore, understanding methane sources and sinks and reducing anthropogenic methane emissions are key steps in mitigating climate change.

Wastewater treatment with conventional techniques is one of the anthropogenic sources of methane and is also known to result in CO_2 and N_2O emissions (Gupta and Singh, 2012). Conventional wastewater treatment is also associated with limited nutrient recovery, high energy demand, and the need for external inputs (Ahn, 2006; Modin et al., 2007). Therefore, research in wastewater treatment is focused on the mitigation of GHG emissions, energy production, and recovery of valuable products such as methane, hydrogen, and volatile fatty acids in addition to nutrient removal. In this area of research, anaerobic treatment comes forward (Angenent et al., 2004; Haddadi et al. 2013; Torres et al., 2010). Anaerobic treatment was extensively studied regarding its potential in energy production and feasibility (Shin et al, 2016; Smith et al., 2015). Despite its many advantages, anaerobic treatment of wastewater results in the emission of methane (Bandara et al., 2011). Methane emissions also result from anaerobic digestion (AD) of wastewater treatment plant (WWTP) sludge due to considerable dissolved methane

concentrations in the supernatant which is recycled back to the plant (McCarty et al., 2011; Bandara et al., 2011). In other words, dissolved methane should be mitigated before it escapes into the atmosphere. Moreover, limited removal of nitrogen and phosphorus in anaerobic wastewater treatment and conventional treatment of wastewater with low carbon/nitrogen (C/N) ratio is another concern in wastewater treatment besides methane emissions (Wang et al., 2015). Nutrient-rich wastewater should be treated to prevent eutrophication in the receiving bodies before discharge. Therefore, there is a need for additional treatment processes which can contribute to nitrogen removal in the treatment of low carbon wastewaters such as AD supernatant, landfill leachate, and some industrial wastewaters containing very low carbon for nitrification/denitrification processes (Hou, 2013).

To these requirements, the nitrogen-dependent anaerobic methane oxidation (N-DAMO) or denitrifying anaerobic methane oxidation (DAMO) process was considered as a potential treatment for the main issues confronted in conventional wastewater treatment (nitrification-denitrification), which are the lack of carbon sources and substantial emission of GHGs (Wang et al., 2017). DAMO process, discovered in 2006 (Raghoebarsing et al., 2006), has become trending research in the field of anaerobic biotechnology since in this process CH_4 is oxidized and electrons are provided for denitrification, presenting a fundamental link between the nitrogen and carbon cycles (Wang et al., 2017). Major advantages related to the utilization of this mechanism include (1) the potential of decreasing CH_4 emissions in the aquatic ecosystems and (2) the potential of decreasing nitrogen levels in the natural ecosystems and receiving bodies (van Kessel et al., 2018; Lee et al., 2018).

DAMO is currently known to be carried out by two different microorganisms which are '*Candidatus* Methylomirabilis oxyfera (*M. oxyfera*) (Ettwig et al., 2009), a bacterial group that belongs to the NC10 phylum, and '*Candidatus* Methanoperedens nitroreducenss' (*M. nitroreducens*), an archaeal group related to anaerobic methanotrophic archaea (Haroon et al., 2013). *M. nitroreducens*

converts NO_3 to NO_2 by the pathway of reverse methanogenesis using CH_4 as an electron donor (Haroon et al., 2013; Cui et al., 2015). *M. oxyfera* further reduces NO_2 to N_2 gas using CH_4 as electron donor via an intra-aerobic pathway (Ettwig et al., 2010; Wu et al., 2011; Rasigraf et al., 2014). Thus, these two species together convert NO_3 and NO_2 via using CH_4.

After the first successful enrichment of Damo-Bacteria (Raghoebarsing et al., 2006), studies closely focused on cultivation (Ettwig et al., 2009; Kampman et al., 2014; Hu et al., 2014a; Hatamoto et al., 2014) and the factors affecting the activity of DAMO microorganisms (Hu et al., 2011; Hu et al., 2009; He et al., 2015a; He et al., 2015b; Luesken et al., 2012; Fu et al., 2017; Fu et al., 2015) for its applicability in wastewater treatment. Additionally, research has been conducted to investigate the occurrence and diversity of the DAMO microorganisms in various ecosystems. Anoxic environments where methane, nitrite, and nitrate coexist have been recognized as the potential habitat for the DAMO process to occur (He et al., 2014). Studies reported molecular evidence and Damo-Bacteria activity in various environments such as paddy field soil, freshwater lake, river sediments, marine sediments, various wetlands, and municipal and industrial WWTP sludge (Hu and Ma, 2016; Zhou et al., 2014; Hu et al., 2014a; Kojima et al., 2012; Shen et al., 2014; Ettwig et al., 2009; Chen et al., 2015a; Luesken et al., 2011). Nitrate-dependent anaerobic methane oxidation carried by Damo-Archaea (*M.nitroreducens*) was generally studied coupled to anaerobic ammonium oxidation (Anammox) process since two microorganisms can be partners in the total nitrogen removal from wastewater (Nie et al., 2019; Shi et al., 2013).

Enrichment of DAMO microorganisms is limited due to their slow growth metabolism (doubling time of 1 to 7 weeks depending on the media, temperature, and operational parameters) (Raghoebarsing et al., 2006; Hu et al., 2009; Ettwig et al., 2010; Luesken et al., 2012; Kampman et al., 2012; He at al, 2015b). This results in a long enrichment period and makes the recovery of DAMO microorganisms from inhibitory effects more difficult. Although several studies

successfully used mixed inoculum sources for the enrichment of DAMO microorganisms (Hu et al., 2009), the optimum seed source for the enrichment of DAMO co-culture (Damo-Archaea and Damo-Bacteria) and possible combinations of seed sources which can shorten the enrichment has never been studied. Since nitrite is quickly oxidized to nitrate, wastewater and anthropogenic discharges frequently carry a nitrate load which can be used as an electron acceptor by Damo-Archaea. In this process, Damo-Archaea supplies nitrite for Damo-Bacteria. Therefore, it is crucial to investigate the enrichment of DAMO co-culture consisting of both DAMO species (Li et al., 2018) for future applications of this process in wastewater treatment. Therefore, since slow growth is a major barrier in the cultivation of these organisms, and optimum inoculum can vary for Damo-Bacteria and Damo-Archaea, an appropriate seed source for the co-culture enrichment should be elucidated. Regardless of the progress made in DAMO research, there are much fewer studies on the occurrence and activity of Damo-Archaea or the co-existence of DAMO microorganisms. In addition, only a few studies focused on the enrichment of Damo-Archaea (Vaksmaa et al., 2017; Li et al., 2018). The co-existence and distribution of Damo-Archaea and Damo-Bacteria were reported few times in paddy fields and freshwater wetland (Ding et al., 2015; Xie et al., 2020; Zheng et al., 2020; Shen et al., 2019). Yet, there is a limited number of studies regarding the effect of inoculum source and optimum source of inoculum. Moreover, the literature lacks detailed studies regarding the impact of commonly occurring compounds encountered in wastewater on DAMO microorganisms and possible strategies to shorten the enrichment time.

The aim of this thesis study is to enrich Damo-Bacteria and Damo-Archaea. The primary objectives are;

- to investigate the presence of DAMO microorganisms and potential DAMO activity in different environments,

- to decide the optimum inoculum source which is favorable for both Damo-Bacteria and Damo-Archaea cultivation using individual or combinations of seed sources,
- to enrich DAMO microorganisms in Sequencing Batch Reactors (SBRs) using two different approaches and compare the enrichment progress with respect to activity and molecular composition and,
- to investigate the effect of granular activated carbon (GAC) on the activity of DAMO microorganisms as a possible strategy to overcome the slow growth

In this context, the occurrence and activity of DAMO microorganisms in different environments (inoculum sources such as paddy field, freshwater sediment, anaerobic digester sludge, return activated sludge from a biological nutrient removal system) were investigated through comparative physicochemical analysis of these sources, DAMO activity batch tests and molecular biological techniques. Moreover, 2 enrichment studies (Enrichment-1 and Enrichment-2) were conducted using SBRs which were inoculated with inoculum source combinations and operated with different operational conditions. The activity of microorganisms was determined using specific activity batch tests and fluorescence *in situ* hybridization (FISH) method. Finally, the GAC effect on reactor performance was investigated via activity tests for Enrichment-1 and Enrichment-2.

This thesis is divided into 5 chapters. Chapter 1 provides a brief introduction to the background information and an overview of the motivation and scope of the study conducted for this MS research and thesis. In Chapter 2, a detailed review of previous research on mechanisms and environmental occurrence of the DAMO process is presented and the potential application of DAMO in wastewater treatment is discussed in detail. Chapter 3 investigates the effect of inoculum sources on the occurrence and activity of DAMO microorganisms using individual and combinations of different inoculum sources. As a side note, this is the first study in which DAMO occurrence and activity were reported in Turkey. In

Chapter 4, DAMO enrichment is presented focusing on the performance of the enrichment SBRs, activity tests, and molecular composition of microorganisms and, the findings on the GAC effect on the DAMO process are illustrated. Finally, Chapter 5 provides an overview of the findings of this research and proposes ways forward for future research.

CHAPTER 2

LITERATURE REVIEW

2.1 Carbon (C) and Nitrogen (N) Cycles

Inorganic carbon is present in the form of carbonate in sedimentary rocks, carbon dioxide, and methane in the atmosphere and mainly present as bicarbonate in the water (Moomaw, 2014) and organic carbon is stored in living and dead organisms found in the biosphere. Although these sub-cycles are interconnected, the carbon cycle consists of short-term biogenic processes such as respiration, photosynthesis, and air-sea exchange of carbon and long-term processes which are occurring over millions of years by the exchange of carbon between rocks and the ocean, atmosphere, biosphere, and soils (Berner, 2003). Understanding the global carbon cycle is important since carbon makes up 50% of the dry weight of life on the planet and carbon exchange processes regulate the energy flow on earth, living forms, and industry. In other words, plants transform radiant energy into chemical energy in the form of organic matter; this energy supports food chains in natural ecosystems and anthropogenic activities by fossil fuels for heating, transportation, and generation of electricity. Finally, the interest in carbon cyle has gained more importance since human activities have altered the global carbon cycle significantly over the past 200 years (Wahlen, 1993), and understanding the consequences of the use of fossil fuels leading to climate change is essential for articulating economic, energy, technology, trade, and security policies.

Carbon dioxide and methane are considered the two most important GHGs (Houghton, 2003). Although its lifetime in the atmosphere is much shorter than that of carbon dioxide, methane absorbs long-wave radiation emitted from the surface

affecting the atmospheric temperature directly (Hansen et a1, 1988). It also has impacted the ozone concentration in the troposphere and the stratosphere (Johnston 1984). Considering both direct and indirect impact, the net heating effect of methane is 25 times more than that of carbon dioxide over 100 years (IPCC, 2013). It has 72 times higher global warming potential in 20 years due to its short lifetime (Deutzman, 2011). It is therefore vital that we understand how global methane cycling occurs, what microbial metabolism is involved, and how it is regulated by environmental factors, including anthropogenic activities.

Methane emissions result from both natural and anthropogenic sources. Natural sources account for 21–47% (Liu et al., 2008) of global methane emissions and mainly consist of marine and freshwater sediments (Kirschke et al., 2013). Methane is produced naturally by thermal decomposition of buried organic material (Reeburgh, 2007), and the majority of recent methane production results from the activity of strictly anaerobic microorganisms, in anoxic habitats (Reeburgh, 1996) which constitutes 69% of the global methane production (Conrad, 2009). Methanogenesis is the final step in the anaerobic degradation of organic matter performed by the methanogenic archaea, using H_2, CO_2, or the methyl groups of organic compounds as electron acceptors (Thauer, 1998). Methanogenic reactions of typical substrates (hydrogen, formate, acetate) are given in Equation 2.1 to 2.3 (Pan et al., 2016);

$4H_2 + CO_2 \rightarrow CH_4 + 2\,H_2O$ (Equation 2.1)

$4HCOOH \rightarrow CH_4 + 3CO_2 + 2H_2O$ (Equation 2.2)

$CH_3COOH \rightarrow CH_4 + CO_2$ (Equation 2.3)

Anthropogenic sources, account for about 45–80% (Liu et al., 2008) of the global emissions, including fossil fuel burning, agriculture, cattle breeding, landfills, and WWTPs (Daelman et al., 2012; Gupta and Singh, 2012; Bogner et al., 2008).

Atmospheric methane concentrations increased from about 700 ppb in the pre-industrial age to nearly 1800 ppb in 2008 (Rigby et al., 2008).

As for CH_4 sink mechanisms, methane undergoes photochemical oxidation in the troposphere and biological oxidation in the environment. In photochemical oxidation hydroxyl radical plays a critical role in the oxidation (Prinn, 2003). However, biological oxidation of methane being approximately 1.5 times (Tate, 2015) higher than chemical oxidation plays a vital role in mitigating the methane emissions since methane is continuously converted to CO_2 by methanotrophs in the ecosystems. These methanotrophs are classified as aerobic methanotrophs and anaerobic methanotrophs (Murrel and Jetten, 2009) that can carry out the anaerobic oxidation of methane using various electron acceptors (Raghoebarsing et al., 2006; Ettwig et al., 2008; 2009). The anaerobic methane oxidation process is considered a major sink for methane (Conrad et al., 2009) since it consumes 7–25% of the global methane production (Knittel and Boetius 2009; He et al., 2014) and 90% of the methane formed by methanogenic archaea in anaerobic marine sediments (Reeburgh et al., 1993). There are various mechanisms of anaerobic methane oxidation such as sulfate dependent anaerobic methane oxidation (S-DAMO) by anaerobic methanotrophic archaea and sulfate-reducing bacteria (Hinrichs et al. 1999; Boetius et al. 2000; Cui et al., 2015), anaerobic methane oxidation through Mn^{4+} and Fe^{3+} as electron donors (Beal et al., 2009; Cai et al., 2018b), anaerobic methane oxidation via humic substances (Valenzuela et al., 2017) and nitrogen dependent denitrifying anaerobic methane oxidation (DAMO) (Raghoebarsing et al., 2006).

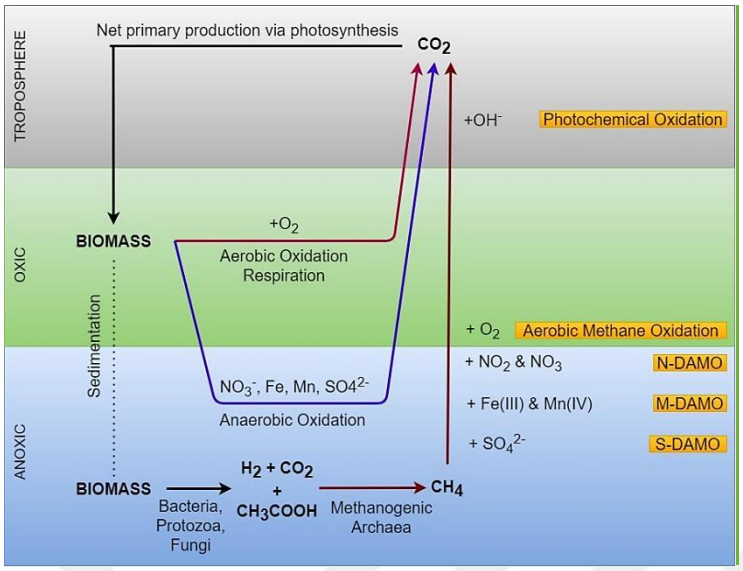

Figure 2.1 Global methane cycle (Modified from Thauer et al., 2010)

Nitrogen (N) has also significant importance as a nutrient present in the environment. N is mostly present in the atmosphere and the ocean as nitrogen gas which can only be fixed by nitrogen-fixing bacteria in aquatic and terrestrial environments, while most microorganisms can only take up oxidized and reduced inorganic and organic forms of N (Duce et al., 2008). N_2 fixation is vital for maintaining biological productivity in ecosystems since it replaces biologically available nitrogen that is lost by the sink mechanisms in the ecosystems (Jetten, 2008).

Sink mechanisms for reactive nitrogen are conversion to nitrogen gas by denitrification and anaerobic ammonium oxidation (Anammox) (Duce et al., 2008). In addition, microbial conversions taking place in the global N cycle also includes aerobic ammonium oxidation by bacteria and archaea, aerobic nitrite oxidation, dissimilatory nitrate and nitrite reduction to ammonium (Jetten et al., 2008) and finally, denitrification coupled to anaerobic methane oxidation (DAMO) discovered recently (Ettwig et al., 2009; Haroon at al., 2013). Denitrification which is the reduction of nitrate through nitrite to nitric oxide, nitrous oxide, and nitrogen

gas, is one of the major sources of nitric oxide (NO) and nitrous oxide (N_2O) emissions to the atmosphere (Jetten, 2008). Nitrous oxide is a GHG with a GWP of 298 and is emitted both naturally and from anthropogenic sources. Moreover, anthropogenic N_2O emissions constitute 40% of the global N_2O emissions (IPCC, 2013).

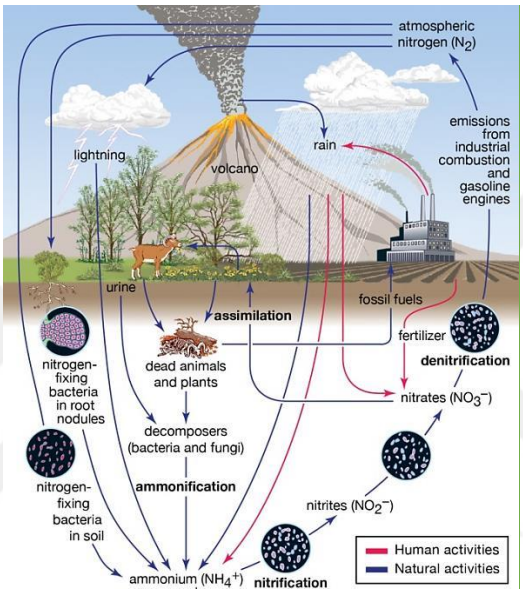

Figure 2.2 Nitrogen cycle (Britannica, 2020)

Similar to the C cycle, the N cycle has also been heavily impacted by humans since the industrial revolution (Galloway et al., 2008) due to the rising demand for nitrogen in agriculture and industry. The atmospheric concentrations of N_2O have increased since 1750 to 324 ppb and exceeded the pre-industrial levels by about 20% (IPCC, 2013). NH_3 and NO_x emissions to the atmosphere by anthropogenic activities also affect tropospheric O_3 and aerosols through atmospheric chemistry contributing to global warming (Duce et al., 2008). Atmospheric nitrogen input is due to emissions from the increased combustion of fossil fuels and the production and use of fertilizers (Duce et al., 2008). In addition, anthropogenic activities also increased the input of reactive nitrogen to the rivers, oceans, and groundwater by

direct wastewater discharges causing eutrophication in the ecosystems, by fertilizer application to agricultural land (Galloway et al., 2008). This input leads also to acidification (Guo et al., 2010), shifts in species composition, and loss of biodiversity (Tomassen et al., 2003), and the presence of nitrogen oxides can also constrain methane production, and encourage methane consumption (Barnard et al., 2006). Nitrate contamination of water sources is becoming a problem leading to the risk of degradation of drinking water sources and eutrophication of continental and coastal aquifers (Hou, 2013).

2.2 Denitrifying Anaerobic Methane Oxidation: DAMO

As presented above in detail, the input fluxes of nitrate resulted from agricultural activities and wastewater discharges, and methane generated by anaerobic decomposition of organic matter has an increasing environmental impact on a global scale. Recently in 2006, it was discovered that methane and nitrogen cycles are linked to each other in a very unique way called nitrogen dependent anaerobic methane oxidation (N-DAMO) or denitrifying anaerobic methane oxidation (DAMO) (Raghoebarsing et al., 2006). These two terms are used interchangeably. This process became a significant addition to the huge biodiversity and metabolic ability of nitrogen and carbon exchange mechanisms in the microbial world.

Anaerobic Methane Oxidation (AMO): A Brief History

In the past, methane was known to be utilized as a carbon and energy source by aerobic bacteria in a reaction mechanism that starts with the oxidation of methane with O_2 to methanol, limited to aerobic ecosystems. Anaerobic oxidation of methane (AMO) was considered impossible due to the non-polar C-H bond of methane (Thauer and Shima, 2008). Later, AMO coupled to sulfate reduction was observed in 1976 (Reeburgh, 1976). Microorganisms responsible for this process, namely, sulfate-dependent anaerobic methane oxidation (S-DAMO) microorganisms, were identified and their presence was proven in marine

environments and freshwater (Hinrichs et al., 1999; Boetius et al., 2000). These microorganisms were called anaerobic methanotrophs (ANME) (Hinrichs et al., 1999) and divided into 3 phylogenetic clusters (ANME-1, ANME-2, and ANME-3). ANME (Knittel et al. 2005) often forms consortia with sulfate-reducing bacteria (SRB) to catalyze S-DAMO. AMO coupled with metal ion reduction was also discovered in which manganese (Mn^{4+}) and iron (Fe^{3+}) are used as electron acceptors (Beal et al., 2009). This new pathway that involves metal reduction is called metal-dependent anaerobic methane oxidation (M-DAMO). It is suggested that S-DAMO exists largely in ecosystems where it plays a significant part in the biogeochemical cycling of carbon and sulfur and M-DAMO may play an important role in global marine ecosystems due to the high manganese and iron content provided from rivers (Beal et al., 2009). Stoichiometric reaction for S-DAMO is given in Equation 2.4. Stoichiometric reactions for M-DAMO which is carried out using (Mn^{4+}) and (Fe^{3+}) as electron acceptors are given in Equation 2.5 and 2.6, respectively. Very recently, evidence was reported for the anaerobic methane oxidation in wetland sediments coupled to N_2O reduction mediated by humic substances due to their electron-transferring capacity (Valenzuela et al., 2017).

$$CH_4 + SO_4^{2-} \rightarrow HCO_3^- + HS^- + H_2O \quad \text{(Equation 2.4)}$$

$$CH_4 + 8Fe(OH)_3 + 15H^+ \rightarrow HCO_3^- + 8Fe^{2+} + 21H_2O \quad \text{(Equation 2.5)}$$

$$CH_4 + 4MnO_2 + 7H^+ \rightarrow HCO_3^- + 4Mn^{2+} + 5H_2O \quad \text{(Equation 2.6)}$$

2.2.1 Metabolic pathways and mechanisms of DAMO process

N-DAMO (from now on called DAMO) is carried out by two different microorganisms which are a bacterial group (from now on called as Damo-Bacteria) that belongs to the NC10 phylum, and an archaeal group (from now on called as Damo-Archaea) related to anaerobic methanotrophic archaea (Haroon et al., 2013).

'*Candidatus* Methylomirabilis oxyfera' (*M.oxyfera)* belongs to the NC10 phylum which is a candidate phylum of prokaryotes considered important in biogeochemical cycles and evolutionary history (Ettwig et al., 2009). There are few other members of this phylum recently cultured and difficult to enrich such as *M. sinica*, *M. limnetica*, and *M. Lanthanidiphyla* (Graf et al., 2018; He et al., 2016).

Damo-Bacteria have a polygonal cell shape and are observed as distinct from other bacteria by their cell shape (Figure 2.3a) (Wu et al., 2012b). It is reported as a Gram-negative rod bacterium with a diameter of 0.25–0.50 μm and a length of 0.8–1.1 μm (Ettwig et al., 2010). In addition, the intracytoplasmic membranes (ICMs) are not present in its cell which is common in other bacterial methanotrophs. It is hypothesized that it is energetically disadvantageous for Damo-Bacteria to produce ICMs which do not comply with its slow metabolism (Wu et al., 2012a).

The specific maximum growth rate (μ_{max}) of Damo-Bacteria was reported as 0.009-0.0018 h^{-1} with a biomass yield of 0.055–0.094 g COD/g COD, equivalent to a doubling time of 5.7-16 days (Harb et al., 2019; Guerrero-Cruz et al., 2019; Chen et al., 2014b).

Based on the complete genome analysis, and isotopic labeling experiments (Ettwig et al. 2010), it is suggested that Damo-Bacteria encodes, transcribes, and expresses all the genes involved in the aerobic methane oxidation; however, lacks the genes required for the reduction of nitrous oxide (N_2O) to dinitrogen gas (N_2) during complete denitrification. *M. oxyfera* reduces NO_2 to N_2 gas using CH_4 as an electron donor via an intra-aerobic pathway. In this pathway (Figure 2.4a), oxygen to be used for the oxidation of methane is produced in the cell by metabolizing nitrite via nitric oxide into oxygen and dinitrogen gas (Ettwig et al.,2010; Wu et al., 2011; Rasigraf et al., 2014) using nitrite reductase (nir) and putative nitric oxide dismutase (nod) enzymes. The oxidation of methane via internally produced O_2 is the same as the mechanism of aerobic methanotrophs catalyzed by the particulate methane monooxygenase (pMMO) complex (Ettwig et al.,2010). Oxygen produced in NO dismutation is used to hydroxylate methane to produce methanol and water

via pMMO complex. The remaining O_2 produced in the cell is consumed in respiration via terminal respiratory oxidases (Wu et al. 2011).

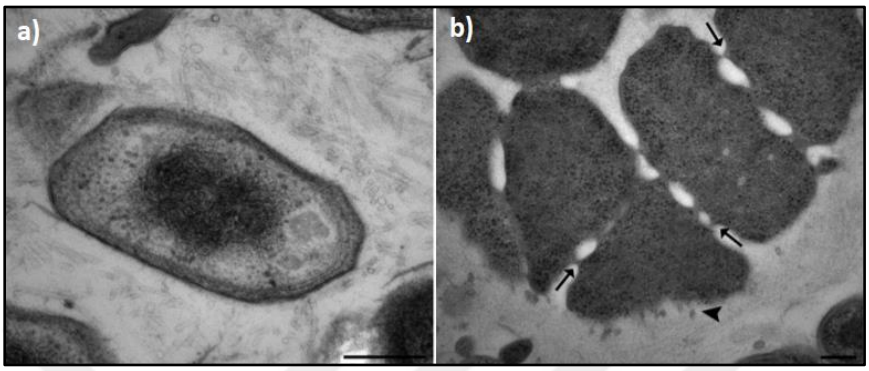

Figure 2.3 Transmission electron micrographs of a) 'Candidatus Methylomirabilis oxyfera' (Damo-Bacteria) and b) 'Candidatus Methanoperedens Nitroreducens' (Damo-Archaea) cells showing putative cell-to-cell contacts (arrows) and tubules (arrowhead). Scale bar = 200 nm (Gambelli et al., 2018)

Damo-Archaea was first affiliated with Methanosarcinales which is distantly related to ANME-2 and methanogens (Ettwig et al., 2010). Later, the microorganisms responsible for the conversion of NO_3 to NO_2 via nitrate reductase (Nar) enzyme are classified under the ANME-2d population. ANME-2d lineage was named Candidatus Methanoperedenaceae and Damo-archaea was named as '*Candidatus* Methanoperedens Nitroreducens'. Damo-Archaea was shown to have the pathway of reverse methanogenesis using nitrate as the terminal electron acceptor (Haroon et al., 2013; Cui et al., 2015). In the pathway (Figure 2.4b), Methyl-coenzyme reductase (MCR), the well-known enzyme of methanogenesis, functions in a reverse mode catalyzing the activation of methane (Haroon et al., 2013). It is recently reported that Damo-Archaea can transform around 10% of the produced nitrite to ammonium, preventing nitrite accumulation and toxicity (Ettwig et al., 2016).

Damo-Archaea aggregates are observed to have slightly irregular coccoid cells with approximately 1.5 μm diameter and are typically found as sarcina-like clusters (Figure 2.3b) (Gambelli et al., 2018; Haroon et al., 2013). Damo-Archaea is also reported to perform chromium and selenium reduction coupled to AMO (Lu et al., 2016; Luo et al., 2018). Since the discovery of Damo-Bacteria and Damo-Archaea is very recent, physiology and key enzymes should be investigated further (Ding et al., 2021). Recently it was observed that AMO by '*M. nitroreducens*' was found to comply with the first-order kinetic model while the nitrate reduction to nitrite was well described by the Monod kinetic model (Lu et al., 2019). For Damo-Archaea, the specific maximum growth rate (μ_{max}) was reported as 0.0015 h^{-1} with a biomass yield of 0.071 g COD/g COD, equivalent to a doubling time of 19 days in a modeling study (Chen et al., 2014b).

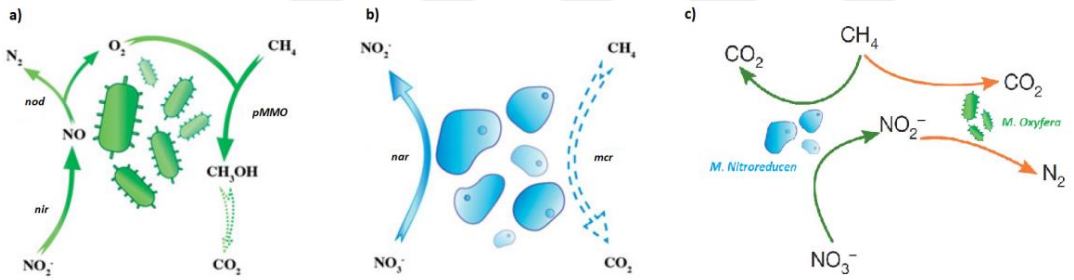

Figure 2.4 Metabolic pathways and overall reactions of a) Damo-Bacteria, b) Damo-Archaea and, c) Syntophic relationship of Damo species (Modified from Liu et al., 2019a; Haroon et al., 2013)

Reactions carried out by Damo-Archaea (*M.nitroreducens*) and Damo-Bacteria (*M.oxyfera*) are shown in Equation 2.7 ($\Delta G^0 = -503$kJ/mol CH_4) and Equation 2.8 ($\Delta G^0 = -928$ kJ/mol CH_4), respectively.

$$CH_4 + 4\,NO_3^- \rightarrow 4\,NO_2^- + 2\,H_2O + CO_2 \qquad \text{(Equation 2.7)}$$

$$3\,CH_4 + 8\,NO_2^- + 8\,H^+ \rightarrow 4\,N_2 + 10\,H_2O + 3\,CO_2 \qquad \text{(Equation 2.8)}$$

Since Damo-Archaea cannot further reduce the nitrite to NO, N_2O, or N_2 (Haroon et al., 2013), Damo-Bacteria coexists with Damo-Archaea in the natural habitat and enrichment cultures where nitrate is supplied as the electron acceptor (Figure 2.4c) (Vaksmaa et al., 2016; Liu et al., 2020; Nie et al., 2020). However, Damo-Archaea is estimated to have a lower methane affinity than that of Damo-Bacteria probably due to different enzyme complexes used to activate methane (Ding et al., 2021).

2.3 Nitrogen removal Technologies

2.3.1 Conventional wastewater treatment

Nitrogen is removed from wastewater using biological or physical-chemical methods. At municipal wastewater concentrations (typically 50 mg N/L), biological treatment is preferred (Mulder, 2003) where the removal of nitrogen is performed with a two-step process involving nitrification and denitrification. A schematic diagram of a conventional nitrogen removal treatment system can be seen in Figure 2.5.

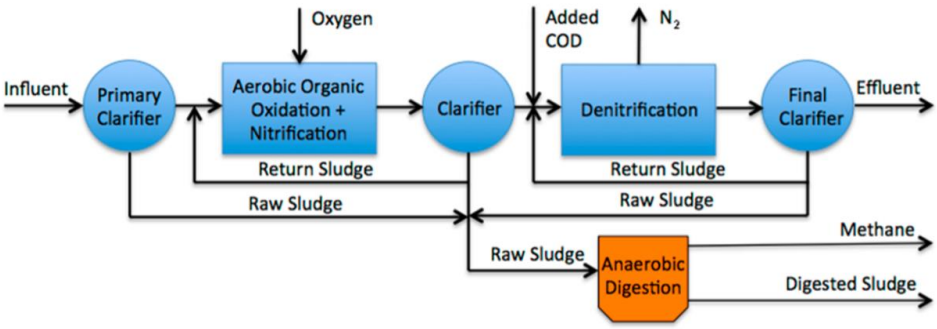

Figure 2.5 Conventional wastewater treatment system schematic (McCarty, 2018)

During nitrification, ammonia is oxidized to nitrite, and nitrite is oxidized to nitrate by strictly aerobic chemolithoautotrophic microorganisms. These microorganisms use ammonia or nitrite as an energy source and molecular oxygen as an electron acceptor and carbon dioxide as the carbon source. Ammonium oxidation is performed by various microorganisms such as Nitrosomonas, Nitrosococcus, Nitrosopira, Nitrosovibrio, and Nitrosolobus which are under the beta subdivision of the Proteobacteria. This reaction is catalyzed by ammonia monooxygenase and hydroxylamine oxidoreductase enzymes (Rahimi et al., 2020). Then, nitrite is oxidized to nitrate by Nitrobacter, Nitrospira, Nitrospina, Nitrococcus, and Nitrocystis (Ahn, 2006). Nitrification rate depends on the reactor configuration, substrate type, and influent ammonium concentration. The process is performed at oxygen concentrations of 1– 3 mg O_2/L. Nitrifying bacteria grow slowly and control the sludge retention time (SRT) in conventional activated sludge systems as a rate-limiting step (Tchobanoglous et al., 2014). The conversion is catalyzed by nitrite oxidoreductases (Rahimi et al., 2020).

Following nitrification, denitrification takes place which is performed by heterotrophic microorganisms under anoxic conditions where nitrite and nitrate are reduced to dinitrogen gas and nitrous oxide. Since denitrification is a respiratory process, an electron donor is needed as an energy source (Hou et al., 2013). During denitrification, nitrite and/or nitrate is used as electron acceptors and organic matter (methanol, acetate, glucose, ethanol, etc.) as carbon and energy source. In conventional wastewater treatment, denitrification can be performed as pre-anoxic denitrification where wastewater COD is utilized as electron donor or post-anoxic denitrification where an external electron acceptor (methanol, acetate, glucose, ethanol, lactic acid, or organic wastes) is added (Ahn, 2006). Denitrifiers include alpha and beta classes of the Proteobacteria, such as Pseudomonas, Alcaligenes, Paracoccus, and Thiobacillus.

Representative equations of ammonium oxidation by Nitrosomonas (Equation 2.9) and nitrite oxidation by Nitrobacter (Equation 2.10), the overall nitrification

(Equation 2.11) (Ahn, 2006) and denitrification (Equation 2.12) reaction are presented below (Dahab and Lee, 1988).

$55\ NH_4^+ + 76\ O_2 + 109\ HCO_3^- \rightarrow C_5H_7O_2N + 54NO_2 + 57\ H_2O + 104\ H_2CO_3$ (Equation 2.9)

$400\ NO_2^- + NH_4^+ + 4H_2CO_3 + HCO_3^- + 195\ O_2 \rightarrow C_5H_7O_2N + 3H_2O + 400NO_3^-$ (Equation 2.10)

$NH_4^+ + 1.83\ O_2 + 1.98\ HCO_3^- \rightarrow 0.021\ C_5H_7O_2N + 0.98\ NO_3^- + 1.04\ H_2O + 1.88\ H_2CO_3$ (Equation 2.11)

$CH_3COOH + 1.18\ NO_3^- + 1.18\ H^+ \rightarrow 0.12\ C_5H_7O_2N + 1.4\ CO_2 + 2.5\ H_2O + 0.53\ N_2$ (Equation 2.12)

There are several drawbacks to be mentioned concerning the conventional nitrification and denitrification systems which are listed below.

- There is a risk of GHG emissions such as N_2O, CO_2, and CH_4 (Compos et al., 2016). N_2O emissions are generated during both nitrification and denitrification (Ahn, 2006). Nitrous oxide released from WWTPs accounts for 2.8 % of all GHG emitted from all anthropogenic sources (Gupta and Singh, 2012). The organic content in the wastewater is either converted into biomass or released as CO_2 and CH_4 from sludge digesters (Gupta and Singh, 2012). CO_2 is also released due to the breakdown of organic matter in the activated sludge process and the primary clarifiers (Keller and Hartley, 2003). CO_2 emissions from conventional WWTPs differ from 0.2 to 0.25 kg CO_2/m^3 wastewater (Campos et al., 2016).
- Conventional wastewater treatment is not suitable for the treatment of wastewater with a low C/N ratio such as effluent of anaerobic municipal wastewater treatment, AD supernatant, landfill leachate, and some industrial wastewaters (Hou, 2013). The addition of an external electron donor would be required (Ahn, 2006; Modin et al., 2007) which is a considerable burden that

might cause deterioration of effluent water quality by excessive biomass of bacterial cells and remnant carbon source (Boley et al., 2000).

- During nitrification, pH decreases; thus external chemical addition such as lime is needed (Ahn, 2006).
- Large size reactor or long hydraulic retention time (HRT) are required to complete ammonium removal due to low nitrification rate, resulting in high operational cost (Shoda, 2017).
- Other challenges include a slow reaction rate due to long start-up time and HRT, a drop of productivity at low temperatures, and the requirement of oxygen control (Rahimi et al., 2020).

2.3.2 New perspectives

Due to the above-mentioned concerns regarding the conventional wastewater treatment, research in wastewater treatment focused on sustainable nitrogen removal, mitigation of GHG emissions, energy production, and recovery of valuable products such as methane gas, hydrogen gas, and volatile fatty acids (Ahn, 2006; Modin et al., 2007).

In this area of research, numerous potential nitrogen removal processes have been studied to increase the sustainability of nitrogen removal (Rahimi et al, 2020). Some of these processes are simultaneous nitrification and denitrification, partial nitrification and denitrification, aerobic deammonification, Anammox, and DAMO (Ge et al., 2015; Shoda, 2017; van Kessel et al., 2018; Harb et al., 2021).

A great discovery in the field of anaerobic biotechnology was made in 1995. Anaerobic ammonium oxidation (Anammox) process was reported which uses nitrite as the electron acceptor, ammonium as electron donor, and carbon dioxide as a carbon source to convert ammonia to nitrogen gas (Strous et al., 1999). Anammox bacteria are autotrophic bacteria, belonging to the group of Planctomycetes. This process gained attention due to its potential in the

applications for wastewater with a low C/N ratio since it does not require a carbon source. However, nitrate is a by-product of the Anammox process which leads to incomplete nitrogen removal (Luesken et al., 2011; Du et al., 2019). Several processes were developed for the utilization of Anammox in nitrogen removal such as completely autotrophic nitrogen removal over nitrite (CANON), one-stage Anammox, oxygen-limited autotrophic nitrification-denitrification (OLAND), and deammonification (DEMON). In these systems, the biomass consists of ammonium oxidizing bacteria (AOB) and Anammox bacteria. AOB nitrify ammonium, thereby remove oxygen and produce nitrite while nitrite and the remaining ammonium are removed by the Anammox bacteria (Rahimi et al., 2020). While these processes provide similar results to conventional nitrification/denitrification, about 50% less energy is required for oxygen supply compared to nitrification-denitrification and 90% less GHG emitted compared to conventional wastewater treatment (Ahn, 2006; Hu et al., 2013).

Anaerobic treatment (methanogenesis, dark fermentation, microbial electrochemical technologies) comes forward regarding their potential in energy production, feasibility with respect to no oxygen supply, lower operational costs, smaller space requirements, and less sludge handling costs (Angenent et al., 2004).

AD is considered a suitable technology for both waste treatment and energy recovery. It is one of the oldest biotechnologies used to produce energy from organic wastes such as municipal or industrial wastewater, food waste, agricultural residues, manure, and slurry (Nikolausz and Kretzschmar, 2020). Biodegradable waste is converted to methane gas by AD systems under anaerobic conditions. During AD, series of complex microbiological processes, various types of bacteria work in syntrophy to go through four stages: hydrolysis, acidogenesis, acetogenesis, and methanogenesis (Gonzalez-Fernandez et al., 2015). Anaerobic digestion is applied in WWTPs to stabilize the properties of the sludge, reduce the volume of the sludge, and produce the energy gas methane. However, the digestion liquid usually contains very low organic content (180-280 mg/L) (Zhang et al., 2011) and very high ammonium content (1000–1500 mg/L), constituting 10–20%

of the WWTP total nitrogen (Wang et al., 2017) and theoretical dissolved methane (10-25 mg/L) (Cookney et al., 2016) constituting around 45-50% of the total methane produced in the system (Liu et al., 2014). Subsequently, recirculation of reject water can cause high ammonium and dissolved methane input to the WWTP in which dissolved methane is released into the environment and contribute to GHG accumulation in the atmosphere and reduce the system's methane yield (Velasco et al., 2018). Methane accounts for 16% of the total global GHG emissions (IPCC, 2014) due to both natural and anthropogenic sources. Methane released from WWTPs accounts for 9% of all emitted from all anthropogenic sources (EPA, 2006).

2.3.2.1 Anaerobic Biotechnology: Potential of DAMO

DAMO, which plays an important role in global carbon and nitrogen cycles, has also potential biotechnological applications in wastewater treatment. Since its discovery, much research has been conducted to investigate DAMO process for the future utilization to treat nitrogenous pollutants in wastewater (Hu et al., 2014; Luesken et al., 2011; Shen et al., 2012) and remove dissolved methane from effluents digesters (Kampman et al., 2012). Moreover, based on the stoichiometry of Damo-Bacteria and Damo-Archaea which is thermodynamically favorable under standard conditions, DAMO process is considered as an alternative treatment strategy for the biological denitrification of nitrate-contaminated waters with low carbon content. These include AD supernatant, landfill leachate, and some industrial wastewaters containing very low carbon for conventional nitrification/denitrification processes such as mineral processing, electroplating, semiconductor manufacturing, and power plants. The treatment for this type of wastewater normally requires an external electron donor (Hou, 2013). However, methane is a potentially inexpensive and widely available electron donor for wastewater or landfill leachate, as it is generated onsite due to the anaerobic digestion of sludge and during the degradation of organic waste in landfills.

Therefore, nitrate can be converted to dinitrogen gas and removed from the wastewater using methane as an electron donor by DAMO process (Modin et al., 2007). DAMO process was considered as a potential treatment applied to the main issues confronted in conventional wastewater treatment (nitrification-denitrification), which are the lack of carbon sources and substantial emission of GHGs (Wang et al., 2017). Moreover, it is also suggested for the treatment of groundwater contaminated with nitrate as a bioremediation technique (Luo et al., 2018).

Ultimately, there are several studies involving DAMO and Anammox which report the removal of methane and nitrogen from digestate simultaneously without requiring external carbon addition (Kampman et al., 2012; Zhu et al., 2011 and Shi et al., 2013). The establishment of an integrated DAMO-Anammox system was studied for complete nitrogen removal in which Damo-Archaea reduces nitrate to nitrite preventing the accumulation of nitrate in the system while Anammox removes ammonium and nitrite (Lu et al., 2018). This integration is also promising to remove dissolved methane from wastewaters (Luesken et al., 2011) such as the AD liquor and landfill leachate. A conceptual diagram suggested as a DAMO-Anammox integrated system is given in Figure 2.6.

However, nitritation and organic matter degradation are required to partially convert the ammonium to nitrite and the organic matter into methane before complete nitrogen removal by DAMO-Anammox processes (Harb et al., 2021; Wang et al., 2017; van Kessel et al., 2018). Two integration strategies are suggested with combined Nitritation-DAMO-Anammox processes such as 1) side-stream treatment of the anaerobic digester liquor before it is recirculated into the main wastewater line, and 2) main-stream treatment with activated sludge process followed by combined DAMO-Anammox (Wang et al., 2017).

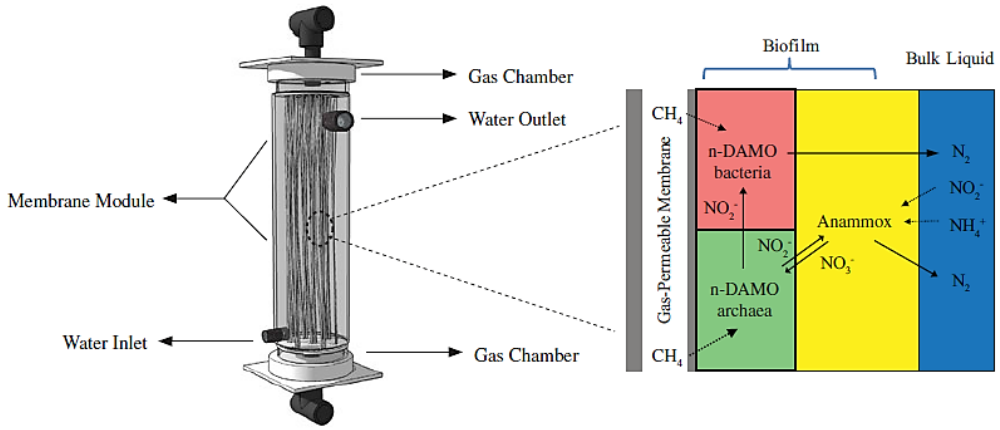

Figure 2.6 Methane-based membrane bioreactor treating the effluent from partial nitritation coupling DAMO and Anammox processes (Liu et al., 2019a)

2.4 DAMO research in the field of wastewater treatment

After the discovery of DAMO microorganisms (Raghoebarsing et al., 2006), DAMO research has gained interest from many researchers. Studies regarding DAMO research can be grouped into three such as 1) studies investigating the occurrence and diversity of DAMO species, 2) studies focusing on the cultivation and factors that affect the activity of DAMO microorganisms, 3) lac-scale research on the applicability of DAMO in wastewater treatment coupling Anammox. In the present literature review, regarding this thesis study, studies investigating the occurrence and diversity of DAMO species and research focusing on the cultivation and factors that affect the activity of DAMO microorganisms are addressed.

2.4.1 Occurrence and diversity of DAMO species

Research has been conducted to investigate the occurrence and diversity of the DAMO microorganisms in ecosystems. Anoxic environments where methane,

nitrite, and nitrate coexist have been recognized as the potential habitat for the DAMO process to occur (He et al., 2014). DAMO activity was also observed in anoxic-oxic interphase in freshwaters where counter gradients of methane and nitrate occur (Thauer and Shima, 2006).

DAMO process was observed in environments with high CH_4 concentration and oxygen-limited ecosystems (Zhu et al., 2015; Bhattacharjee et al., 2016). Wetlands and agricultural lands have been stated as sources of methane due to plant-derived organic substances acting as the carbon source for methane production (Lu, 2005; Wang et al., 2012). In addition to high methane content, the application of nitrogen-rich fertilizers makes the agricultural fields a favorable habitat for DAMO species (Lu, 2005).

Studies mostly focus on the presence of Damo-Bacteria in various environments such as paddy field soil (Hu and Ma, 2016; Shen et al., 2014; Wang et al., 2012; Zhou et al., 2014; Hu et al., 2014; Wang et al. 2012; Zhu et al. 2013); freshwater lake and river sediments (Hu et al., 2014b; Kojima et al., 2012; Shen et al., 2014; Liu et al., 2014; Raghoebarsing et al., 2006; Ettwig et al., 2009; Zhu et al., 2013; Shen et al., 2016), various wetlands (Wang et al., 2016); water reservoirs (Zhu et al. 2013), coastal tidal land (Li-Dong et al. 2014; Zhu et al. 2013), saline lakes (Yang et al. 2012), and marine sediments (Chen et al., 2014a). In these ecosystems, molecular evidence and evidence of Damo-Bacteria activity were reported. However, it was reported that total inorganic nitrogen content, ammonium content, and organic content affect the distribution of DAMO species in the sediments (Shen et al., 2013). DAMO presence and distribution are also affected by the soil depths and season (Zhu et al., 2018). Moreover, molecular surveys showed the extensive presence of Damo-Bacteria in return activated sludge, anaerobic sludge, municipal and industrial WWTPs sludge samples, and digestate collected from an anaerobic digestion facility (Hu et al., 2009; Luesken et al., 2011; Hu and Ma, 2016; Xu et al., 2017; Hatamoto et al., 2014).

Recently DAMO activity was suggested in marine ecosystems based on the high methane reservoir in marine sediments (Orcutt et al. 2011) indicating the availability of methane as an electron donor. However, there is only few research on the distribution and diversity of DAMO process and the associated environmental factors in the marine ecosystem (Chen et al., 2014a).

There are much fewer studies on the occurrence and activity of Damo-Archaea or the co-existence of DAMO microorganisms. The co-existence and distribution of Damo-Archaea and Damo-Bacteria were reported few times in paddy fields and freshwater wetlands (Ding et al., 2015; Xie et al., 2020; Zheng et al., 2020; Shen et al., 2019).

High diversity has been observed for DAMO microorganisms in different niches (Han and Gu, 2013; Zhang et al., 2018; Chen et al., 2019; Mayr et al., 2020). In some enrichment cultures, Damo-Bacteria and Damo-Archaea were observed simultaneously active (Xie et al., 2018; Liu et al., 2019a; Raghoebarsing et al., 2006) while in other studies Damo-Bacteria or Damo-Archaea was not enriched or significantly lower in abundance (Ettwig et al., 2008; Hu et al., 2015). This suggests that different ecosystems might be favorable for Damo-Bacteria and Damo-Archaea (Xie et al., 2020).

2.4.2 Cultivation of DAMO Species

DAMO microorganisms are reported to have a very slow growth rate with a doubling time of 1 to 7 weeks depending on the media, temperature, and operational parameters (Raghoebarsing et al., 2006; Hu et al., 2009; Ettwig et al., 2010; Luesken et al., 2012; Kampman et al., 2012; He at al, 2015). Therefore, the application of the DAMO process in large-scale wastewater treatment is limited by the growth metabolism.

The reported maximum specific growth rate of DAMO species was 0.121/d and 0.028/d for Damo-Bacteria and Damo-Archaea, respectively (He et al., 2013; Yu et

al., 2017). Furthermore, the reported nitrate removal rate is almost lower than 80 mg N/L·d while the average nitrite removal rate is 70–80 mg N/L·d (Allegue et al., 2018; Hatamoto et al., 2017). These maximum removal rates were achieved in lab-scale studies using a downflow hanging sponge (DHS) reactor and membrane bioreactor (MBR). As the engineering application requirement of nitrogen removal rate is about 1000 mg N/L·d for side-stream nitrogen removal from anaerobic sludge digestion liquor (Lu et al., 2020), the DAMO process is still in the development stage and it has been only tested on a bench-scale so far (Wang et al., 2017). In addition, the studies on DAMO are mostly conducted with synthetic wastewater (Raghoebarsing et al., 2006; Ettwig et al., 2008; Ettwig et al., 2009; Hu et al., 2009; He et al., 2014; Wang et al., 2016; Bhattacharjee et al., 2016; Hatamoto et al., 2014; Hatamoto et al., 2017).

Enrichment studies mostly focused on shortening the enrichment time and improving biomass retention. The effects of reactor configuration (Hu et al., 2014), inocula type (He et al., 2014), and type of nitrogen feed (Hu et al., 2011) on the enrichment of DAMO species have been investigated. Moreover, there are few studies concerning the effects of temperature (Hu et al., 2009; Kampman et al., 2014; He et al., 2015b), pH (He et al., 2015b; Zhu et al., 2012), salinity (He et al., 2015b), dissolved oxygen (DO) (Luesken et al., 2012), heavy metals (He et al., 2015a; Kampman et al., 2014) and HRT (Kampman et al., 2014; Hatamoto et al., 2014) on the growth and activities of the DAMO. Parameters affecting the cultivation and the activity of DAMO species are discussed below.

2.4.2.1 Seed source

Since anoxic ecosystems contaminated with methane and nitrogen are a potential source for the enrichment of DAMO organisms, most of the enrichment studies were performed using eutrophic freshwater sediments (Raghoebarsing et al., 2006; Ettwig et al., 2008; Ettwig et al., 2009; Kampman et al., 2012; He et al., 2014; Wang et al., 2016). Municipal and industrial WWTP sludge also has the potential

to contain DAMO species already adapted to treatment conditions (Luesken et al., 2011). Therefore, WWTP sludge was also used as an inoculum source in the cultivation studies (Hu et al., 2009; Luesken et al., 2011; Kampman et al., 2014; He et al., 2014). Damo-Bacteria and other NC10 phylum species were detected in various WWTP sludge samples (Luesken et al., 2011). Methanogenic sludge was also suggested as an appropriate seed source due to significant amounts of methane produced in the AD process and nitrite is detected in methanogenic sludge (He et al., 2014). Agricultural soil and peatlands which are usually infiltrated by groundwater containing high nitrate concentrations are also potential ecosystems where methane and nitrogen are present together (Zhu et al., 2012). Paddy soil samples tested for the target gene of Damo-Bacteria resulted in the detection and successful enrichment of Damo-Bacteria (Hatamoto et al., 2014).

Combined seed sources were suggested to have an advantage over using a sole inocula source for the enrichment of Damo-Bacteria-Archaea co-culture (Li et al., 2018). Seed sources such as the mixture of freshwater lake sediment, paddy soil, and methanogenic sludge from a local WWTP; the combination of municipal wastewater sludge containing primary sludge, secondary sludge, and digested secondary sludge, and a mixture of municipal wastewater treatment sludge and freshwater sediment have also been used in the cultivation studies (Li et al., 2018; Kampman et al., 2014; Hu et al., 2009) (Table 2.1).

Optimum source of inoculum was investigated for Damo-Bacteria enrichment using methanogenic sludge, paddy soil, and freshwater sediment; concluding that paddy soil was the optimum inoculum for the enrichment of *M.oxyfera* (He et al., 2014). Similarly, Damo-Bacteria presence and activity were investigated by comparative analyses using paddy field soil, cornfield soil, and anaerobic WWTP sludge, suggesting that paddy field soil and cornfield soil are suitable inoculum sources for cultivation (Hu and Ma, 2016). The studies on the co-enrichment of DAMO microorganisms are limited. The co-existence and distribution of Damo-Archaea and Damo-Bacteria were reported a few times in a paddy field and a freshwater wetland (Ding et al., 2015; Xie et al., 2020; Zheng et al., 2020; Shen et

al., 2019). It is recently suggested that different ecosystems might be favorable for Damo-Bacteria and Damo-Archaea (Xie et al., 2020). It should be noted that only a few studies focused on the enrichment of Damo-Archaea (Vaksmaa et al., 2017; Li et al., 2018).

Table 2.1 Summary of some of the DAMO enrichment studies

Inocula	Reactor Configuration	N Type	Temperature (°C)	pH	Composition (%)	
					Damo-Archaea	Damo-Bacteria
Freshwater sediment[1]	SBR	NO_2^-, NO_3^-	25	7	10	80
Freshwater sediment (ditch sediment)[2]	CSTR	NO_2^-, NO_3^-	30	7.3–7.6	0	70
Freshwater sediment (ditch sediment)[3]	SBR	NO_2^-, NO_3^-	30	6.9-7.5	0	70
Mixture of sediments from a freshwater lake, anaerobic digester sludge and return sludge[4]	SBR	NO_3^-	35	-	40	30
Industrial wastewater treatment plant [5]	SBR	NO_2^-	20-23	6.8-7.3	-	60-70
Mixture of methanogenic sludge, paddy soil, Freshwater sediment[6]	SBR	NO_2^-	30	7.0-7.2	-	50
Freshwater sediment[7]	SBR	NO_2^-	30	7.0-8.0	-	70-80
Mixture of digested primary sludge, secondary sludge and digested secondary sludge[8]	MBR	NO_2^-, NO_3^-	20	6.5–8	-	60-70
Freshwater sediment[9]	MBR	NO_2^- or NO_3^-	10-25	7	-	73
River sediment[10]	SBR	NO_2^-, NO_3^-	35	7.5	0	73

[1] Raghoebarsing et al., 2006; [2] Ettwig et al., 2008; [3] Ettwig et al., 2009; [4] Hu et al., 2009; [5] Luesken et al., 2011; [6] He et al., 2014; [7] Kampman et al., 2012; [8] Kampman et al., 2014; [9] Wang et al., 2015; [10] Bhattacharjee et al., 2016

2.4.2.2 Reactor configuration

For slow-growing microorganisms, SBRs are reported as suitable due to the homogeneous distribution of substrates and biomass (Strous et al., 1999). Therefore, SBRs are used in the first DAMO cultivation studies (Raghoebarsing et al., 2006; Ettwig et al., 2009; Hu et al., 2009; Luesken et al., 2011). However, it is seen that methane gas-liquid phase mass transfer in the SBR reactor has a limiting effect on the DAMO activity (Fu et al., 2019). Up-flow continuous reactors and batch reactors (Hatamoto et al., 2014), continuous stirred tank reactors (CSTRs) (Ettwig et al., 2008; Hu et al., 2014), MBRs (Wang et al., 2016; Kampman et al., 2014), DHS reactor (Hatamoto et al., 2017) and a magnetically stirred gas lift reactor (MSGLR) (Hu et al., 2014) were also operated (Table 2.1).

Biomass loss has a vital influence on nitrogen removal activity due to the slow growth rate (Lai et al., 2018). MBR is beneficial to cultivate slow-growing microorganisms by separating HRT and SRT and effectively retaining biomass (Maaz et al., 2019). MBRs are suggested to increase the activity of DAMO enrichment cultures due to improved biomass retention (Kampman et al., 2012; Kampman et al., 2014). However, membrane fouling should be addressed when using MBR (Lu et al., 2020). Optimum reactor configuration was investigated using a MSGLR, an SBR, and a CSTR which concluded that MSGLR is an effective reactor type due to high gas-liquid mass transfer and effective mixing of liquid-solid phases and relatively less biomass washout (Hu et al., 2014). Another comparison was performed using an up-flow reactor with a continuous supply of methane and a batch reactor which revealed that the continuous upflow reactor configuration achieved nitrite and nitrate removal efficiency more than two times compared to the batch reactor (Hatamoto et al., 2014) suggesting continuous methane supply might have better results in DAMO cultivation due to improved availability of methane.

Membrane Biofilm Reactor (MBfR) configuration was also stated as effective since recirculation of gas might also help to increase the activity through improved methane supply (Xie et al., 2018). Limited mass transfer between gas-liquid phases and liquid-solid phases can also be overcome with the MSGLR (Hu et al., 2014).

Damo-Bacteria can grow in granular sludge. Therefore, modeling studies were conducted using one-dimensional granular sludge reactors and MBfRs (Winkler et al., 2015; Chen et al., 2016; Castro-Barros et al., 2017). Granular systems make Damo-Bacteria remain in the inner layers resulting in less exposure to nitrite inhibition (Winkler et al., 2015). In addition, granular systems such as MBfR can sustain biomass effectively. However, it was also reported that dissolved methane can not reach the inner parts of the granule which negatively affects the DAMO performance (Chen et al., 2016). Recently, in a study, integration of GAC to an MBR system improved the nitrate and methane removal performance due to the porous structure of GAC which absorbed methane and increase the soluble methane availability for DAMO microorganisms, and helped microorganisms' retention (Lu et al., 2020).

Finally, HRT is reported to have an important effect on the cultivation of DAMO species. Shorter HRT applied at decreased influent nitrite concentrations was observed to lead to an increase in the nitrite consumption rates (Kampman et al., 2014; Hatamoto et al., 2014). Shorter HRTs were reported to result in effective removal of nitrogen and dissolved methane, and washing out of the possible inhibitory by-products (Kampman et al., 2014). In the literature, the DAMO enrichment studies generally conducted at low HRTs as 1.4-15 days and using short cycle durations (1-3 days) (Hu et al., 2014; Kampman et al., He et al., 2014; Etttwig et al., 2009; Hatamoto at al., 2014). However, few studies used long HRTs such as 90-120 days with high initial N concentrations (Fu et al., 2017; Li et al., 2018). Although there is no comparison in the literature concerning the effects of long and short HRTs, it was observed that shorter enrichment periods were achieved using long HRTs (Fu et al., 2017; Li et al., 2018).

2.4.2.3 Nitrogen feed

Nitrogen feed used in the cultivation studies contributes to the understanding of electron acceptors used by Damo-Bacteria and Damo-Archaea and reaction mechanisms based on the final microbial composition of DAMO species in the enrichment culture (Hu et al., 2011; Hatamoto et al., 2014). As expected, nitrite-fed reactors achieve a much higher abundance of Damo-Bacteria than Damo-Archaea (Table 2.1) (Hu et al., 2011; Hatamoto et al., 2014) since nitrite is the electron acceptor used by Damo-Bacteria. However, nitrate-fed reactors generally show higher lag periods and lower nitrogen consumption rates (Hatamoto et al., 2014). For the co-cultures of Damo-Bacteria and Damo-Archaea, nitrate reduction by Damo-Archaea was indicated as the limiting step since nitrite removal rate by Damo-Bacteria was reported 2 times higher than the nitrate removal rate of Damo-Archaea (Li et al., 2018). Unlike nitrite-fed enrichment cultures, using nitrate as the N source results in the enrichment of both Damo-Archaea and Damo-Bacteria with a similar microbial composition (Hatamoto et al., 2014; Li et al., 2018). This is because Damo-Archaea reduces nitrate to nitrite and Damo-Bacteria further reduces nitrite to nitrogen gas by using methane as the electron and no nitrite accumulation occurs suggesting that the system of Damo-Archaea and Damo-Bacteria live under nitrate and methane conditions (Li et al., 2018). However, it is reported that even though Damo-Bacteria is enriched under nitrate conditions, NC10 bacterial communities differ depending on the influent nitrogen type used (nitrite or nitrate) (Hatamoto et al., 2014).

It has been initially observed in the literature that nitrite causes a toxic effect at a concentration of 1 mM NO_2-N (He et al., 2014; Hu et al., 2011; Hatamoto et al., 2014). However, this level of nitrite did not inhibit the activities of *M. oxyfera* in most studies (Ettwig et al., 2008; Ettwig et al., 2009; Ettwig et al., 2010; Luesken et al., 2011; Hu et al., 2014). Moreover, nitrogen feed supplied in DAMO enrichment studies includes NO_2-N in the range of 0.5-15 mM nitrite (Harb et al., 2021; Ettwig et al., 2008; Raghoebarsing et al., 2006; Luesken et al., 2011) and

NO_3-N in the range of 0.5-22 mM (Hatamoto et al., 2017; Kampman et al., 2014; Bhattacharjee et al., 2016). Recently in a study investigating the effect of nitrite on DAMO activity, 950 mg/L NO_2-N (67 mM) was reported to completely inhibit the activity in a short-term exposure (Lou et al., 2019). In addition, the nitrogen removal performance of DAMO culture was completely inhibited at concentrations of 650 mg/L (46 mM) NO_2-N in the long-term inhibition experiments. Therefore, the reasons behind the different nitrite toxicity levels require further investigation.

It should also be noted that there is still a lack of understanding of the appropriate initial concentrations used in the cultivation of DAMO species. Even though low initial substrate concentrations are suggested for the enrichment of slowly-growing microorganisms, recent enrichment studies using higher NO_3-N initial concentrations (3.6 mM) have achieved comparatively shorter enrichment periods (Fu et al., 2017; Li et al., 2018).

2.4.2.4 pH

DAMO cultivation was conducted using pH ranges between 6.5 and 8.0 (Table 2.1) (Ettwig et al., 2009; Luesken et al., 2011; He et al., 2014; Kampman et al., 2014). Studies revealed that DAMO microorganisms prefer slightly more alkaline conditions (Zhu et al., 2012; He et al., 2015; Zhu et al., 2012). The optimum pH for DAMO species was reported as pH 7.6 (He et al., 2015), as shown in Figure 2.7. As it was also reported previously for most heterotrophic denitrifying bacteria (Tang et al., 2011), DAMO microorganisms also perform best at pH of 7.0-8.0 (He et al., 2015). Yet, Damo-Bacteria is observed to be present in environments with lower (pH 6-7) and higher (pH 9) pH values despite being less active (He et al., 2015; Zhu et al., 2012; Xu et al., 2018). Both low and high pH inhibited Damo-Bacteria activity, however low pH caused a stronger inhibition than high pH (Lou et al., 2019). Similarly, Damo-Archaea activity is reported to decrease when pH is below 6.5 and above 7.5 (Lou et al., 2019).

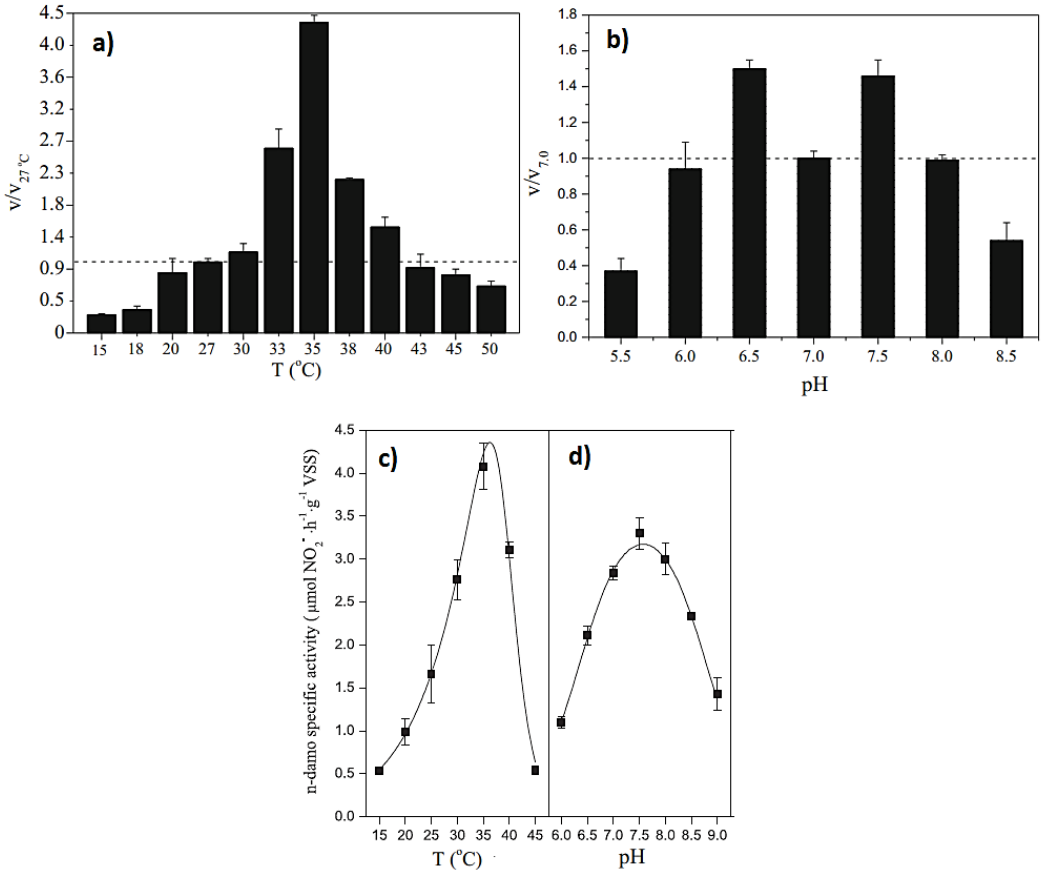

Figure 2.7 The short-term effects of temperature and pH on DAMO species; a) Effect of temperature on Damo-Archaea (v/v 27 °C on y-axis refers to the ratio of the NO_3-N consumption rate at different temperatures to consumption rate at 27°C) (Lou et al., 2019), b) Effect of pH on Damo-Archaea (v/v 7.0 on y-axis refers to the ratio of the NO_3-N consumption rate at different pH values to consumption rate at pH 7.0) (Lou et al., 2020), c) Effect of temperature on Damo-Bacteria, and d) Effect of pH on Damo-Bacteria (He et al., 2015)

2.4.2.5 Temperature

DAMO enrichment studies were carried out at temperatures between 10-45 (Hu et al., 2009; Luesken et al., 2011; He et al., 2014; Hatamoto et al., 2017; Wang et al., 2015) (Table 2.1). Yet, few studies have investigated the effects of temperature on the growth and activity of DAMO species (Hu et al., 2009; Li et al., 2018, He et al., 2015).

The optimum temperature for Damo-Bacteria was reported to be about 35 °C after short-term and long-term incubation at temperatures ranging from 15 °C to 45 °C (He et al., 2015). Similarly for Damo-Archaea, the optimum temperature was reported as 35 °C after a short-term investigation at temperatures ranging from 15 °C to 50 °C (Lou et al., 2020). The effect of temperature was also at 20 °C, 35 °C and 45 °C (Hu et al., 2009); and of 22 °C and 30 °C (Li et al., 2018). Results revealed that DAMO activity was lower at lower temperatures and lower temperatures may inhibit the growth of Damo-Archaea. However, despite the lower enrichment temperatures of 20°C (Wang et al., 2015) and 10-25 °C (Kampman et al., 2014), DAMO culture was reported to be enriched achieving similar nitrite and nitrate removal rates to those reported by other studies at 30-35 °C (Raghoebarsing et al. 2006; Luesken et al. 2011; Zhu et al., 2012). Studies testing DAMO activity at higher temperatures (45 °C) also achieved lower nitrogen consumption compared to 35 °C which is recognized as suitable for DAMO microorganisms (Hu et al., 2009; He et al., 2015). However, it is argued that DAMO microorganisms can operate at a wide range of temperatures (Ding et al., 2016) suggesting that process can be acclimated and then be used to treat wastewater with various temperatures.

2.4.2.6 Salinity

The effect of salinity was studied on DAMO microorganisms (He et al., 2015). It was revealed that increasing the salt concentrations from 0 to 15 g NaCl/L resulted

in the reduction of DAMO activity (He et al., 2015). It was suggested previously that salinity disrupts the nitrite reductase, NO dismutase, and methanol dehydrogenase (Wu et al., 2011) and cell osmotic pressure causes the inhibition of DAMO microorganisms under high salinity conditions (He et al., 2015). The indirect effect of salinity is also reported as the decrease in methane solubility which is the electron donor for DAMO species. However, recovery from inhibition due to high salinity (20 g NaCl/L) was also reported suggesting that DAMO process can exist in marine ecosystems (He et al., 2015). DAMO species were detected in saline lakes (32 and 84 g/L NaCl) (Yang et al. 2012) and marine sediments (Chen et al., 2015a; Li-Dong et al. 2014).

2.4.2.7 CH_4

AMO rates are reported as higher in ecosystems where high CH_4 fluxes are sustained by advective transport than in diffusion-dominated ecosystems due to high flows of CH_4-rich medium (Boetius and Wenzhöfer, 2013).

According to the Damo-Archaea (Equation 2.7) and Damo-Bacteria (Equation 2.8) stoichiometry, NO_3:CH_4 (Equation 2.7) and NO_2:CH_4 (Equation 2.8) ratio are 1.7 and 2.5, respectively (Raghoebarsing et al., 2006). Since methane has low solubility (10-25 mg/L) (Cookney et al., 2016; Islas-Lima et al., 2004; He et al., 2013), most of the DAMO cultivation studies were conducted with excess methane supply (Raghoebarsing et al., 2006; Kampman et al., 2014; Luesken et al., 2011; Chen et al., 2016) with concentrations of 95%:5% (CH_4:CO_2) (Raghoebarsing et al., 2006; Ettwig et al., 2008; Ettwig et al., 2009; Luesken et al., 2011; Bhattacharjee et al., 2016).

The effect of partial pressure of methane on anaerobic methane oxidizers was investigated (Nauhaus et al., 2002; Cai et al., 2018a; Ding et al., 2016). Results revealed that an increase in methane partial pressure from 0 atm to 1.5 atm improved the microbial activity significantly (Cai et al., 2018a; Ding et al., 2016).

In a modeling study for MBfR, lower surface methane loadings (0-0.0001 g $CH_4/m^2.h$) resulted in lower availability of methane, and the abundance of DAMO microorganisms decreased in the culture (Chen et al., 2014b). Paraffin oil was successfully used to increase the solubility of methane which consequently contributed to the DAMO activity in the culture (Fu et al., 2015).

In the DAMO enrichment studies targeting the cultivation of both Damo-Bacteria and Damo-Archaea, methane affinity is also an important factor determining the composition of target microorganisms (Guerrero-Cruz et al., 2019). Methane affinity of Damo-Archaea (0.5 mM) (Lu et al., 2019) is reported to be much lower than that of Damo-Bacteria (2.6 ± 0.7 μM) (Ding and Zheng, 2021). In other words, in methane-limited conditions, unsatisfactory nitrogen removal performance can be observed for Damo-Archaea (Lu et al., 2019).

2.4.2.8 Dissolved Oxygen

DAMO species are present in a wide range of aquatic environments such as agricultural fields and WWTP sludges where there is regular oxygen exposure. Yet, these species thrive under such conditions (Guerrero-Cruz et al., 2019; Raghoebarsing et al. 2006; Ettwig et al. 2008; Hu et al. 2011; Luesken et al. 2011).

The detrimental effect of oxygen on Damo-Bacteria has been reported (Luesken et al., 2012). The addition of oxygen at 2% or 8% is shown to decrease the CH_4 and NO_2 conversion rates in the enrichment culture, causing methane oxidation without denitrification (Luesken et al., 2012) and suppression of the protein biosynthesis and cell division processes. On the contrary, under low oxygen concentrations (0.7%), increased activity was reported which returned to its original level after oxygen had been removed. Moreover, the addition of 1.1% O_2 increased methane consumption rate by 118% and nitrite consumption rate by 58% suggesting that the addition of oxygen may facilitate the growth of bacteria and the specific activity. It is recognized that Damo-Bacteria has the ability to conduct methane oxidation

through a strictly O_2-dependent reaction catalyzed by pMMO complex (Ettwig et al. 2010). However, it is still unclear whether *M. oxyfera* could use external O_2 to oxidize methane or not.

There is very limited information regarding the effect of oxygen on Damo-Archaea. However, many studies investigated the oxygen tolerance of methanogens which are phylogenetically the closest relatives of *M.nitroreducens* and are traditionally considered to be strict anaerobes. It is known that enzymes, specifically the MCR complex of the core methane metabolism, become inactivated upon exposure to oxygen (Guerrero-Cruz et al., 2018). Strong inhibitory effect of oxygen was reported on Damo-Archaea with increasing O_2 concentrations from 0 to 1.15 mg/L and 0 mg/L was reported as the optimal concentration for Damo-Archaea (Lou et al., 2020).

2.4.2.9 Organic Matter

There are not many studies investigating the effects of organic matter on DAMO process. Besides, there are limited studies that used real wastewater as feed (Kampman et al., 2012; Kampman et al., 2014). In a study where two SBRs were operated, one SBR was fed with a medium containing 10% (by volume) filtered activated sludge process effluent with (1.3 mg BOD (Biological Oxygen Demand) and 3.8 mg N/L), and the other was fed with synthetic wastewater. Results revealed that the maximum nitrite consumption rate in the SBR fed with activated sludge effluent was 11% higher and the addition of effluent did not upset the enrichment. The reason for the high nitrite consumption observed in the SBR fed with activated sludge effluent was discussed to be the addition of growth factors that are absent in the SBR fed with synthetic wastewater (Kampman et al., 2012). Similarly, the addition of low COD concentrations (24 mg/L) was reported to indirectly affect the Damo-Bacteria due to the excretion of growth factors by the heterotrophic bacteria which are utilized by Damo-Bacteria. However, a decrease in DAMO microorganisms was observed when COD concentrations increased from 24 mg/L

to 140 mg/L suggesting that high COD can support heterotrophic denitrifiers over Damo-Bacteria due to the competition over nitrite especially under high nitrite concentrations (He et al., 2018).

2.4.2.10 Heavy Metals

Copper (Cu) is stated as a key element for pMMO enzyme that facilitates methane oxidation (Glass and Orphan, 2012; Wu et al., 2011). Expectedly, copper addition is reported to stimulate *M. oxyfera* activity, resulting in a considerable enhancement in nitrite removal (Hatamato et al., 2018; He et al., 2015; Kampman et al., 2014). A copper concentration of 10 µmol/L and 16 µmol/L is observed to enhance the activity of the Damo-Bacteria in an SBR (He et al., 2015; Jiang et al., 2018). On the other hand, copper concentrations exceeding 25 µmol/L (He et al., 2015) and 79 µmol/L (Jiang et al., 2018) is reported to have an inhibitory effect on Damo-Bacteria. Iron (Fe^{2+}) is also observed to increase the Damo-Bacteria at a concentration of 20 µmol/L (He et al., 2015) and 900 µmol/L (Jiang et al., 2018) since the iron activates the enzymes responsible for the nitrite reduction. The effect of molybdenum (Mo) was investigated (He et al., 2015; Jing et al., 2018). While He et al. (2015) reported no effect, improvement of the removal of NO_2 and the development of Damo-Bacteria was reported at 5 mg/L of Mo. Conversely, 1 mg/L Mo concentrations created an inhibitory effect on the microbial activity (Jiang et al., 2018) Other trace metal elements such as zinc (Zn), cobalt (Co), manganese (Mn), and nickel (Ni) were found to not affect the specific activity (He et al., 2015).

2.4.2.11 Sulfate

The effect and mechanism of sulfate on the Damo-Bacteria were recently investigated (Li et al., 2020). The results showed that the performance of the Damo-Bacteria was promoted at sulfate concentrations from 0 to 80 mg/L SO_4^{2-}/L.

The highest CH_4 and NO_2 removal activity were observed at a sulfate concentration of 80 mg/L. However, further increase of concentrations from 80 to 200 mg/L inhibited the activity of Damo-Bacteria (Li et al., 2020).

CHAPTER 3

INVESTIGATION OF THE OCCURRENCE AND ACTIVITY OF DENITRIFYING ANAEROBIC METHANE OXIDATION (DAMO) PROCESS IN DIFFERENT SEED SOURCES

3.1 INTRODUCTION

DAMO process has the potential of decreasing CH_4 emissions in the aquatic ecosystems and the nitrogen levels in the natural ecosystems and receiving bodies (van Kessel et al., 2018). Anoxic environments, where methane, nitrite, and nitrate coexist, and anoxic-oxic interphase in freshwaters, where counter gradients of methane and nitrate occur, have been recognized as the potential habitat for DAMO species (He et al., 2014; Thauer and Shima, 2006; Zhu et al., 2012).

Wetlands and agricultural lands have been stated as sources of methane due to plant-derived organic substances acting as the carbon source for methane production (Wang et al., 2012). In wetland soils, oxygen is usually depleted rapidly on the surface, leaving the bulk of the soil anoxic (Zheng et al., 2020). Therefore, methane can be oxidized anaerobically in anoxic soil layers using electron acceptors such as sulfate (Knittel and Boetius, 2009), manganese/iron (Beal et al., 2009), and nitrite/nitrate (Ettwig et al., 2010; Haroon et al., 2013). However, DAMO is thermodynamically favored over S-DAMO in environments where nitrite, nitrate, and sulfate co-exist (Shen et al., 2019). In addition to high methane content, the application of nitrogen-rich fertilizers makes the agricultural fields a favorable habitat for DAMO species (Lu, 2005). Especially, paddy field soil carries substantial methane and nitrate (Zhou et al., 2014). Additionally, the intertidal marsh is reported to be a large source of methane which is also suffering from a considerable loading of anthropogenic nitrogen (Zheng et al., 2016).

Considering the methane and nitrogen sources, potential ecosystems were identified and investigated for the presence and diversity of DAMO species using molecular surveys, activity experiments, and enrichment studies (Xie et al., 2018). Consequently, DAMO activity was reported in various environments such as wetlands, agricultural lands, marine ecosystems, rivers, lakes, and WWTP sludge samples (Xie et al., 2018) (Table 3.1).

As seen in Table 3.1, there are much fewer studies on the occurrence and activity of Damo-Archaea than that of Damo-Bacteria or the co-existence of DAMO microorganisms. In addition, only a few studies focused on the enrichment of Damo- Archaea (Vaksmaa et al., 2017; Li et al., 2018). However, it is hypothesized that since nitrite is quickly oxidized to nitrate, and anthropogenic activities and discharges frequently carry a nitrate load to the environment, it is also crucial to investigate various ecosystems for the Damo-Archaea activity for their methane removal potential where nitrate is used as electron donor (Li et al., 2018). Damo-Archaea was generally studied coupled to the Anammox process (Nie et al., 2019; Shi et al., 2013). Although few studies include Damo-Archaea, different abundances of Damo-Bacteria and Damo-Archaea were observed in different niches, and the distribution of species in the ecosystem varies (Han and Gu, 2013; Zhang et al., 2018; Chen et al., 2020). In some enrichment cultures, Damo-Bacteria and Damo-Archaea were observed simultaneously active (Xie et al., 2018; Liu et al., 2019a; Raghoebarsing et al., 2006) while in other studies one was not enriched or significantly lower in abundance (Ettwig et al., 2008; Hu et al., 2015). Variations that were observed in niches and enrichment cultures suggest that different ecosystems might be favorable for Damo-Bacteria and Damo-Archaea (Xie et al., 2020).

Table 3.1 Detection of DAMO species in various ecosystems

Ecosystem	Detection method	DAMO species	Reference
Constructed wetland sediments	Molecular Techniques	Damo-Archaea	Wang et al., 2019
Wastewater treatment plant sludge		Damo-Archaea	Xu et al., 2020
Lake		Damo-Archaea, Damo-Bacteria	Ding et al., 2015
River		Damo-Archaea, Damo-Bacteria	Ding et al., 2015
Reservoir		Damo-Bacteria	Wang et al., 2016
Estuary		Damo-Bacteria	Zhang et al., 2018
Lake		Damo-Bacteria	Deutzmann et al., 2011; Kojima et al., 2012
Paddy field soil		Damo-Bacteria	Zhou et al., 2014; Wang et al., 2012
Saline lakes		Damo-Bacteria	Yang et al., 2012
Paddy field soil		Damo-Archaea, Damo-Bacteria	Vaksmaa et al., 2017
River Sediment		Damo-Bacteria	Shen et al., 2013
The sediment of a drinking reservoir		Damo-Bacteria	Liu et al., 2020
Sea sediments		Damo-Bacteria	Chen et al., 2014c
Marsh sediments	Molecular techniques and Activity experiments	Damo-Archaea, Damo-Bacteria	Zheng et al., 2020; Chen et al., 2020
Upland soil		Damo-Bacteria	Zhu et al., 2018
Freshwater wetlands		Damo-Archaea, Damo-Bacteria	Xie et al.,2020
Paddy field soil		Damo-Bacteria	Shen et al., 2014
Natural and urban wetland, paddy field		Damo-Bacteria	Hu et al., 2014
Paddy and corn field soil, WWTP sludge		Damo-Bacteria	Hu and Ru Ma, 2016
Paddy field soil		Damo-Archaea, Damo-Bacteria	Ding et al., 2015

Table 3.1 Detection of DAMO species in various ecosystems (continued)

Ecosystem	Detection method	DAMO species	Reference
Anoxic canal sediment	Enrichment Studies	Damo-Archaea, Damo-Bacteria	Raghoebarsing et al., 2006
Lake sediments, AD sludge, return sludge mixture		Damo-Archaea, Damo-Bacteria	Hu et al., 2009
Methanogenic sludge, activated sludge mixture		Damo-Archaea, Damo-Bacteria	Ding et al., 2014
Freshwater river sediment		Damo-Archaea, Damo-Bacteria	Ding et al., 2017a
Lake sediment, paddy field soil, AD sludge mix		Damo-Archaea, Damo-Bacteria	Li et al., 2018
River sediment, activated sludge, AD sludge mix		Damo-Archaea, Damo-Bacteria	Lou et al., 2019
Sediments from a ditch draining agricultural land		Damo-Bacteria	Ettwig et al., 2009
Wastewater treatment plant sludge samples		Damo-Bacteria	Luesken et al., 2011
Peatland		Damo-Bacteria	Zhu et al., 2012
Methanogenic sludge		Damo-Bacteria	He et al., 2015
Paddy field soil		Damo-Bacteria	He et al., 2015
Coastal sediment		Damo-Bacteria	He et al., 2015
Freshwater sediment		Damo-Bacteria	He et al., 2015

Although community dynamics of DAMO species, their contributions to carbon and nitrogen cycling, and underlying controlling mechanisms are still unclear (Zheng et al., 2020), some pieces of evidence were collected regarding the relative abundance of species in different ecosystems and factors influencing their distribution. The abundance of Damo-Archaea (4.2×10^3 - 3.9×10^{10} copies/g soil) was significantly higher than that for Damo-Bacteria (4.5×10^5 - 6.4×10^6 copies/g soil) in wetlands and marsh sediments (Chen et al., 2019; Xie et al., 2020). On the contrary, the abundance of Damo-Bacteria was one to two orders of magnitude higher than that of NC10 phylum bacteria in the paddy field soil and the river sediment (Vaksmaa et al., 2017).

Inorganic nitrogen content, ammonium content, and organic content were observed to be affecting the distribution of DAMO species in the sediments (Shen et al., 2013). Comparative analysis revealed that low NH_4 and high NO_2 content were suitable for the growth of *M. oxyfera* (Damo-Bacteria) (Hu and Ma, 2016). Temperature, nitrogen source, and phosphorus contents are also reported as critical environmental factors that affected the abundance of Damo-Bacteria. In contrast, nitrogen availability is suggested to be the only factor affecting *M. nitroreducens* (Damo-Archaea) (Xie et al., 2020). The analysis demonstrated that the DO in the sediment and moisture content in the upland soils were also important factors affecting the distribution of Damo-Bacteria (Shen et al., 2013; Zhu et al., 2018).

DAMO presence and distribution are also stated to be affected by the season and the soil depth (Zhu et al., 2018; Shen et al., 2013; Zhu et al., 2018). The temporal distribution of Damo-Bacteria in a paddy soil core reported higher abundance (1.09×10^9 copies /g soil) in summer than winter (8.6×10^7 copies /g soil) (Wang et al., 2012). The vertical distribution of Damo-Bacteria in a paddy soil core was the highest in 30–70 cm (Wang et al., 2012). Damo-Bacteria was also detected in the deeper layers (90–100 cm), whereas they could not be recovered from the upper layer (0–30 cm) (Hu et al., 2014; Zhu et al., 2018). On the contrary, one study reported Damo-Bacteria to be more abundant in surface (0–30 cm) and Damo-Archaea in sub-surface (30–60 cm) soil layers (Zheng et al., 2020). Therefore,

factors affecting the vertical distribution of both DAMO species are still unclear and yet to be discovered for different ecosystems (Zheng et al., 2020).

Ecological relationships (competition or cooperation) between microorganisms in the nitrogen cycle (nitrifying and denitrifying bacteria) and DAMO species are suggested to affect the relationships between *M. oxyfera* and *M. nitroreducens* and their niche differentiation (Xie et al., 2018).

DAMO process studies are still in the level of lab-scale due to the slow growth metabolism (Raghoebarsing et al., 2006). Since optimum inoculum can vary for DAMO species, an appropriate source for the co-culture enrichment should be elucidated. Previously, the optimum source of inoculum was only investigated for Damo-Bacteria enrichment using methanogenic sludge, paddy soil, and freshwater sediment; concluding that paddy soil was the optimum inoculum for the enrichment of *M.oxyfera* (He et al., 2014). Similarly, Damo-Bacteria presence and activity were investigated by comparative analysis using paddy field soil, cornfield soil, and, sludge from the anaerobic tank of a WWTP suggesting that paddy field soil and cornfield soil as the suitable inoculum sources (Hu and Ma, 2016). Although several studies successfully used mixed inoculum sources for the enrichment of DAMO microorganisms (Table 3.1), the optimum seed source for the enrichment of DAMO co-culture and possible combinations of seed sources that can shorten the enrichment has never been studied.

The primary objective of this part of the thesis is to investigate the presence of DAMO species and potential DAMO activity in different environments. It is also to investigate any synergistic effect in nitrite or nitrate removal by using combinations of seed sources and to decide the optimum inoculum source which is favorable for both DAMO species. To this purpose, the occurrence and activity of DAMO microorganisms in different environments were investigated through comparative physicochemical analyses, batch reactor tests, and molecular biological techniques. In this study, paddy field soil with long-term fertilization, freshwater sediment from an hyper-eutrophic lake, anaerobic digester sludge of a conventional WWTP,

and return activated sludge from a biological nutrient removal system were chosen as potential seed sources.

3.2 MATERIALS AND METHODS

3.2.1 Site description and sample collection

Freshwater sediment (FS) samples were collected from three locations at 30-50 cm depth from Lake Eymir (Ankara, Turkey) which is a highly eutrophic lake (Beklioglu et al., 2017). The sediment samples were mixed to form a composite sample and mixed with ambient water taken from the sampling point to make a homogeneous slurry. Solid impurities were removed by sieving (18 mesh, 1mm).

The paddy field soil (PS) samples were taken from a private rice field (Kızılırmak District, Çankırı, Turkey) which has been fertilized for more than 40 years. The samples were taken from 30-50 cm soil depth from two locations. Soil samples were mixed and sieved (18 mesh, 1 mm) and distilled water was added to obtain a homogeneous slurry. Stainless steel soil core sampling device (Soil moisture equipment corp. Model 2800) was used in sediment and paddy field soil sampling (Figure 3.1). The sampling sites for FS and PS are presented in Figure A.1 in Appendix A.

Two different WWTP sludge samples were collected one being from the anaerobic digester recycle line of ASKİ Ankara Central WWTP (Sincan, Ankara, Turkey) and the other from the return activated sludge line of anaerobic/anoxic/oxic (A2O) process for biological nutrient removal (BNR) in İSKİ Ambarlı Advanced WWTP (Ambarlı, İstanbul, Turkey).

Figure 3.1 Soil core sampling device

All seed samples were collected in April 2019. Information specific to the sampling sites are summarized in Table 3.2. After collection, sludge and sediment samples were stored in plastic containers without headspace to prevent air contact and PS samples were stored in sealed plastic bags. All collected seed samples were immediately transported to the laboratory. Each seed sample was divided into three parts. The first part of each seed sample was used to prepare seed stocks which were used as inoculum in the batch experiments to determine the potential DAMO activity. The second part was stored in the refrigerator at 4 ^{0}C for physicochemical analyses and the last part was stored in the refrigerator at -20 ^{0}C for the molecular analyses

Table 3.2 Information on sampling sites in this study

Seed source	Abbreviation	Location	Geographic coordinates
Freshwater sediment	FS	Eymir Lake, Ankara	39 ° 48'51.16 "N, 32 ° 49'14.76" E 39 ° 49'4.53 "N, 32 ° 49'13.88" E 39 ° 49'19.70 "N, 32 ° 49'46.16" E
Paddy field soil	PS	Paddy Field, Kızılırmak-Çankırı	40 ° 21'2.05 "N, 33 ° 58'48.82" E 40 ° 21'0.05 "N, 33 ° 58'45.23" E
Anaerobic digester sludge	AD	ASKİ Ankara Central WWTP, Ankara	39 ° 53'41.01 "N, 32 ° 27'26.97" E
BNR WWTP return activated sludge	RS	İSKİ Ambarlı Advanced WWTP, İstanbul	40 ° 59'16.59 "N, 28 ° 41'14.00" E

3.2.2 Batch reactor experiments

Batch reactor experiments were conducted to determine the activity of DAMO microorganisms in the sampled four seed sources. For this purpose, one set of reactors were operated.

The experiments were carried out in serum bottles (reactors) with 120 mL total and 70 mL effective volume. A total of 24 batch reactors, namely, 12 test reactors and 12 control reactors, were conducted (Figure 3.2). Each test reactor was inoculated with different inoculum sources (individual or combination of the 4 different seed sources) which are shown in Table 3.3. Test reactors and their control counterparts were inoculated with the same inoculum source. The preparation of inoculum sources is explained below in detail.

Figure 3.2 Control and test reactors used in batch reactor experiments

Table 3.3 Individual and combined inocula used in the batch reactor experiments

Seed Stock No	Reactors		Inoculum Source [a]
	Test (T)	Control (C)	
1	T1	C1	PS
2	T2	C2	FS
3	T3	C3	AD
4	T4	C4	RS
5	T5	C5	FS-PS
6	T6	C6	FS-AD
7	T7	C7	FS-RS
8	T8	C8	FS-PS-AD
9	T9	C9	FS-PS-RS
10	T10	C10	RS-AD
11	T11	C11	RS-PS
12	T12	C12	RS-AD-PS

[a] PS: Paddy Field Soil, FS: Freshwater Sediment, AD: Anaerobic Digester Sludge, RS: Return Activated Sludge

3.2.2.1 Preparation of inoculum sources

Average VS concentrations of the 4 main seed sources were 40.3±4.4, 20.8 ±2.1, 14.5±0.2, and 15.6±0.4 g/L for paddy field soil (PS), freshwater sediment (FS), anaerobic digester sludge (AD), and return activated sludge (RS), respectively.

Before inoculation, these 4 seed sources were used to prepare 12 seed stocks, each to be used as an inoculum source in different test and corresponding control reactor pairs, as shown in Table 3.3. These 12 seed stocks include 4 individual seed sources (seed stocks 1-4; PS, FS, AD, RS) and their combinations (seed stocks: 5-12). While preparing the seed stocks, which are composed of more than one seed source (Seed Stocks: 5-12), each seed source was added in required volumes to give an equal amount of VS (600 mg) in each seed stock. As abovementioned, AD sludge, that is the seed stock-3, has the lowest VS concentration of 14.5 g/L. Therefore, all other seed stocks were diluted to achieve the same VS concentration of 14.5 g/L before they were used as inoculum sources. The details of the preparation of 12 seed stocks are given in Table A.1. After the dilution of the seed

stocks, 12 inoculum sources, with the same VS concentration (14.5 g/L), were obtained (Table A.1).

3.2.2.2 Reactor set-up and operation

All Inoculum sources were flushed with Corgon (95% Argon, 5% CO_2) prior to inoculation. Each reactor was then inoculated with 20 mL of the related inoculum source (Table 3.3). The initial VS concentration in each reactor was 4.2 g/L. 50 mL basal medium (Ettwig et al. 2009) was added to all reactors. Medium components are presented in Table 3.4.

Nitrite and nitrate were added to both control and test reactors but methane was added only to the test reactors. Except for methane, all conditions were the same in control and test reactors. The initial nitrite and nitrate concentrations in the reactors were 10 and 30 mg N/L, respectively (Ding et al., 2015). The reactor contents were adjusted to a pH range of 7-8. To maintain anaerobic conditions and remove DO, the reactor contents were purged with Corgon gas (95% Ar, 5% CO_2 mixture) for 3 minutes and closed with rubber stoppers (ISOLAB, rubber turn over flange-15.9 mm). The headspace of the reactors was vacuumed and purged with Corgon for 3 min for three cycles. Then, 30 mL CH_4:CO_2 (95%:5%) gas mixture was added into each reactor adjusting the total pressure at 1.6 atm and methane partial pressure approximately at 0.6 atm. Reactors were incubated on an orbital shaker (80 rpm) at 35 ± 2 °C.

Table 3.4 Basal medium components and concentrations obtained in the reactors (Ettwig et al. 2009)

Medium Components	**Concentration (g/L)**
$KHCO_3$	0.5
KH_2PO_4	0.05
$CaCl_2 \cdot 2H_2O$	0.3
$MgSO_4 \cdot 7H_2O$	0.2
Acidic Trace Element Solution	0.5 mL
Alkaline Trace Element Solution	0.2 mL
Acidic Trace Element Solution	**Concentration (g/L)**
HCl	100 mM
$FeSO_4 \cdot 7H_2O$	2.085
$ZnSO_4 \cdot 7H_2O$	0.068
$CoCl_2 \cdot 6H_2O$	0.12
$MnCl_2 \cdot 4H_2O$	0.5
$CuSO_4$	0.32
$NiCl_2 \cdot 6H_2O$	0.095
H_3BO_3	0,014
Alkaline Trace Element Solution	**Concentration (g/L)**
NaOH	10 mM
SeO_2	0.067
$Na_2WO_4 \cdot 2H_2O$	0.050
Na_2MoO_4	0.242

The incubation lasted for 15 days. That incubation period was selected because it is equal to the commonly reported doubling time for DAMO microorganisms (Raghoebarsing et al., 2006). Therefore, microbial growth was not taken into account in the activity measurement.

To determine the DAMO activity, 3 mL of reactor content was sampled periodically (Day 0, 5, 8, 10, and 15) by a syringe and filtered through 0.45 μm pore-sized syringe-filters. Nitrite, nitrate, and sulfate were then measured in duplicate. According to the results of NO_2 and NO_3 analyses performed on Day 5, a second N source addition was performed on Day 8. On Day 8, 3 mL of medium solution was added to the reactors to achieve 10 mg/L NO_2-N and 30 mg/L NO_3-N initial concentrations.

3.2.3 Calculation methods

Potential DAMO activity was estimated by both nitrogen (nitrite and nitrate) analysis and methane analysis results.

3.2.3.1 Calculation of Damo-Bacteria and Damo-Archaea activity in the reactors

As stated above, nitrite and nitrate were added to both control and test reactors, but methane was added only to the test reactors. Therefore, the nitrite and nitrate consumptions in the control reactors were attributed to the other heterotrophic and autotrophic denitrification activities. However in the test reactors, since there is methane supply, DAMO activity is also possible in addition to the heterotrophic and/or autotrophic denitrification activities. It is to be noted that, the term "heterotrophic denitrification" used in this thesis refers to the denitrification of organic carbon other than methane. A conceptual schematic of the DAMO activity calculation is presented in Figure 3.3. Therefore, nitrite and nitrate consumptions in the test reactors were considered to be the total denitrification consisting of

heterotrophic and autotrophic denitrification and DAMO activity. Damo-Archaea converts nitrate to nitrite which results in an increase in the nitrite concentration in the reactor. Thus, produced nitrite was included in the calculations of nitrite consumption by Damo-Bacteria as additional nitrite input (Figure 3.3).

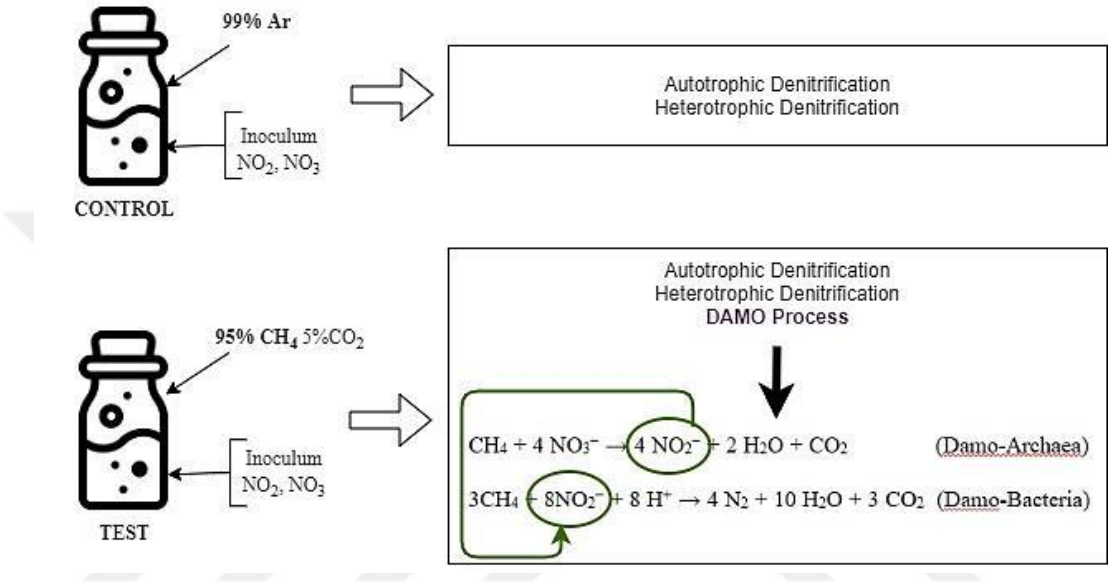

Figure 3.3 Conceptual schematic of the DAMO activity calculation approach

The potential activity of Damo-Bacteria and Damo-Archaea was estimated from the total nitrate and total nitrite consumptions (μmol) over 15 days incubation period via using the Equations 3.1, 3.2, and 3.3 as follows;

$$\Delta N = N_{effluent} - N_{influent} \quad \text{(Equation 3.1)}$$

$$\Delta NO_3\text{-}N_{Damo\text{-}Arch} = \Delta NO_3\text{-}N_{test} - \Delta NO_3\text{-}N_{control} \quad \text{(Equation 3.2)}$$

$$\Delta NO_2\text{-}N_{Damo\text{-}Bact} = \Delta NO\text{-}N_{2_{test}} - \Delta NO_2\text{-}N_{control} + \Delta NO_2\text{-}N_{Damo\text{-}Arch}$$
(Equation 3.3)

Where;

$\Delta NO_{3_{\text{Damo-Arch}}}$: nitrate consumed by Damo-Archaea

$\Delta NO_{2_{\text{Damo-Bact}}}$: nitrite consumed by Damo-Bacteria

$\Delta NO_{2_{\text{Damo-Arch}}}$: nitrite produced by Damo-Archaea

$\Delta NO_{3_{\text{test}}}$: nitrate consumed in the test reactor

$\Delta NO_{2_{\text{test}}}$: nitrite consumed in the test reactor

$\Delta NO_{3_{\text{control}}}$: nitrate consumed in the control reactor

$\Delta NO_{2_{\text{control}}}$: nitrite consumed in the control reactor

Similarly, in the rate calculations, nitrite and nitrate consumption rates (μmol/d) of DAMO microorganisms were calculated by using nitrite consumption rate in test reactors and control reactors. Both nitrite and nitrate were rapidly consumed in most test reactors in between Day-0 and Day-5. Thus, rate calculations were performed based on the second feeding conditions of the reactors. Therefore in the calculations (Equation 3.4 and Equation 3.5), N concentration, measured at Day-8 and Day-10 were used (See Table E.1 for the concentrations). Nitrite and nitrate consumption and production trends in test and control reactors are presented in Figure E.1 to E.4. Nitrite consumption by Damo-Bacteria was calculated using the trends in test and control reactors which are presented in Figure E.1 and E.2. Nitrate consumption by Damo-Archaea was calculated using the trends in test and control reactors which are presented in Figure E.3 and E.4.

$$r_{NO_3,\text{Damo-Arch}} = r_{NO_3,\text{test}} - r_{NO_3,\text{control}} \quad \text{(Equation 3.4)}$$

$$r_{NO_2,\text{Damo-Bact}} = r_{NO_2,\text{test}} - r_{NO_2,\text{control}} + r_{NO_2,\text{Damo-Arch}} \quad \text{(Equation 3.5)}$$

Where;

$r_{NO_3,test}$: consumption rate of nitrate in the test reactor/phase

$r_{NO_3,control}$: consumption rate of nitrate in the control reactor/phase

$r_{NO_2,test}$: consumption rate of nitrite in the test reactor/phase

$r_{NO_2,control}$: consumption rate of nitrite in the test/control reactor

$r_{NO_2,Damo\text{-}Bact}$: nitrite consumption rate of Damo-Bacteria

$r_{NO_3,Damo\text{-}Arch}$: nitrate consumption rate of Damo-Archaea

$r_{NO_2,Damo\text{-}Arch}$: nitrite production rate of Damo-Archaea

3.2.3.2 Calculation of methane consumption rate in the reactors

The DAMO activity of the test reactors was also calculated considering the consumption rate of methane (μmol/d) in the headspace. Methane content in the headspace was estimated by GC analysis and headspace volume as given in Equation 3.6. In the calculations, headspace volume change due to liquid sampling was taken into account (He et al., 2015). For example, headspace volume was 50 mL while gas sampling was conducted at Day-5 and was 53 mL while gas sampling was conducted at Day-10 due to liquid sampling (3 mL) performed after gas sampling at Day-5. Therefore, during headspace CH_4 content calculations (Equation 3.6), headspace volume on Day-10 (53 mL) was taken into account in the calculations.

$$CH_{4\,\text{headspace}}\ (\mu\text{mol}) = \frac{CH_4\ (\mu\text{mol})\ \times \text{Headspace volume}\ (\mu\text{L})}{\text{Injection volume}\ (100\ \mu\text{L})} \quad \text{(Equation 3.6)}$$

Assuming that liquid and gas phases were in equilibrium, dissolved methane content in the effective liquid volume was calculated based on the measured methane content in the headspace (µmol) and the mole fraction solubility coefficient for CH_4 (Wilhelm et al., 1977) using the Equation 3.7 presented below. The mole fraction solubility coefficient of CH_4 is 0.000021 at temperatures of 0 to 75 ^{0}C (Wilhelm et al., 1977). Calculation of mole fraction solubility coefficient of CH_4 is given in Appendix B.

$$CH_{4\,liquid}\ (\mu mol) = CH_{4_{headspace}}\ (\mu mol) \times MFSC \qquad \text{(Equation 3.7)}$$

Where;

- $CH_{4\,liquid}$ is the amount of methane dissolved in the liquid phase in equilibrium with the amount in headspace (µmol)
- $CH_{4\,headspace}$ is the amount of methane in the gas phase (µmol)
- MFSC is the ratio of dissolved methane to methane in the gas phase at temperatures from 0 to 75 ^{0}C and at 1 atm pressure.

Then, the total amount of methane in liquid and headspace was calculated as presented below in Equations 3.8 and 3.9 and used in the methane consumption calculations (Ettwig et al., 2008).

$$\text{Total } CH_{4\,in\,reactor}\ (\mu mol) = CH_{4_{headspace}}\ (\mu mol) + CH_{4_{liquid}}\ (\mu mol)$$

(Equation 3.8)

$$CH_{4\,Consumed} = \text{Total } CH_{4_{initial}} - \text{Total } CH_{4_{final}} \qquad \text{(Equation 3.9)}$$

3.2.4 Analytical methods

3.2.4.1 Physio-chemical analyses

Total solid (TS), Volatile solid (VS), Total suspended solid (TSS) and Volatile suspended solid (VSS) contents were determined according to the Standard Methods (APHA, AWWA, WEF, 2005) with triplicate analyses.

Ammonia, nitrite, and nitrate were extracted from soil and sediment samples with 2 M KCl (Estefan et al., 2013; Ding et al., 2015; Wang et al., 2012; Shen et al., 2013). Nitrite, nitrate, phosphate, and sulfate were determined with an Ion chromatograph (IC) (Dionex) (Reino et al., 2018). For the routine analyses during batch reactor experiments, nitrite, nitrate, and ammonia analyses were conducted in duplicates. The Nessler Method (Hach Nessler Reagent) was used for the ammonia analyses when the sample amount was sufficient. Ammonia was measured with test kits (Lovibond, VARIO Ammonia Test Kits) when the sample volume is low. IC method and calibration curves for the ions analyzed by IC and ammonia calibration conducted for the Nessler Method are presented in Appendix H.

Soluble COD (sCOD) analysis was conducted according to the USEPA approved reactor digestion method using medium-range COD kits (Hach, 2012).

All samples were filtered through 0.45 μm pore-sized filter paper (Sartorius) prior to ammonia, sCOD, and TOC analyses. For IC analysis, the samples were filtered through a 0.22 μm filter (Sartorius). TS, VS, TSS, VSS, sCOD, TOC, and NH_3-N analyses were run in triplicates for each measurement.

CO_2, CH_4, N_2 gases were measured with a gas chromatograph (GC) equipped with a Thermal Conductivity Detector (Trace GC Ultra: Thermo Electron Corporation) (Ettwig et al. 2008). Calibration curves and methods used in GC analyses were given in Appendix H.

DO and pH were analyzed by DO meter and pH meter, respectively. The temperature of the hot room used was measured with a thermometer. Soil pH was measured at a soil/water ratio of 1:2.5 using a pH meter (Shen et al., 2013; Wang et al., 2012).

Medium components except for acidic and alkaline trace metal solutions were sterilized by autoclaving. Acidic and alkaline trace metal solutions were sterilized by filtration through 0.22 μm filter paper.

For the routine analyses of batch reactor experiment, headspace gas samples of 100 μl were taken for immediate analysis by GC on Day 0, 5, 10, 15 to measure CH_4, N_2, and CO2 in duplicate. A liquid sampling of 3 mL was conducted at Day 0, 5, 8, 10, 15, and analysis for nitrite and nitrate were conducted with IC run in duplicates.

Calibration and analytical method validation were carried out for the IC, GC, Nessler methods. Limit of detection (LOD) and limit of quantification (LOQ) were calculated using Equation 3.10 and 3.11 presented below (Magnusson and Örnemark, 2014; Dettmer-Wilde and Engewald, 2014).

$$\mathrm{LOD} = \frac{3.3\sigma}{s} \quad \text{(Equation 3.10)}$$

$$\mathrm{LOQ} = \frac{10\sigma}{s} \quad \text{(Equation 3.11)}$$

Where;

s: the slope of the calibration curve

σ: standard deviation of the lowest analyte concentration

3.2.5 Fluorescence In Situ Hybridization (FISH)

Fluorescence In Situ Hybridization (FISH) analyses was performed for seed samples obtained from four different sites to identify and quantify the (targeted)

species (Nielsen et al., 2009). For this purpose, approximately 5 ml of samples were used.

Solid phase was separated by centrifugation (10000 g for 5 min) and then the supernatant was discarded. Centrifuged solid samples were fixed with an equal volume of 4% paraformaldehyde (PSA) in phosphate-buffered saline (PBS) and left overnight at 4°C. PSA and solid were separated by centrifugation (10000 g for 5 min) and fixed biomass was dissolved in 5 mL 1:1 PBS/EtOH. Dehydration was carried out with sequential wash with 50%, 80%, and 99% ethanol. Permeabilization was performed using lysozyme and incubation for 1 hr at 37 ^{0}C.

Four different hybridization mixtures composed of different probes were used in the FISH analyses of the biomass samples taken from four sampling sites. Therefore, for each sample, 4 slides were prepared. The hybridization mix contents used on these slides are given in Figure C.1. Hybridization was carried out in a hybridization buffer (40% formamide) at 46°C for at least 5 h (He et al., 2014; Hatamoto et al., 2014). After hybridization, the biomass on slides was washed at 48°C for 20 min with a washing buffer containing the same components as the hybridization buffer. The 16S rRNA-targeted oligonucleotide probes used in this study are given in Table 3.5.

Prepared slides were observed via Carl Zeiss Axio Vision A1 UV microscope and at least 3 representative microscopy images were captured for each probe. Microscopic visualization is explained in detail in Appendix D.

For quantitative determination of General Bacteria, General Archaea, NC10 Phylum bacteria, Damo-Archaea, and Damo-Bacteria, images captured for each slide were analyzed via ImageJ software. Pixel areas were determined using ImageJ for specific probes using 3 representative images (captured from the same slide). The average pixel area obtained from image analysis of 3 representative images was used in the quantification of the target microorganisms. A visual summary of ImageJ analysis is represented in Figure D.1. Methods used in

quantification are given in Appendix D in detail. Summary data for the quantification of representative images are presented in Appendix D.

Table 3.5 The 16S rRNA-targeted oligonucleotide probes used in this study

Probe	**Label**	**Target Species**	**Reference**
EUB Mix (EUB338, EUB338 II, EUB338 III)	GFP	General Bacteria	Knittel et al., 2005
DARCH-915 (S-Darc-0915-a-A-20-GTG CTC CCC CGC CAA TTC CT)	GFP	General Archaea	Ettwig et al., 2009
NC10-1027 (S-*-DBACT-1027-a-A-18-TCT CCA CGC TCC CTT GCG)	Cy5	NC10 phylum bacteria	Ettwig et al., 2009
DBACT-193 (S-*-DBACT-0193-a-A-18-CGC TCG CCC CCT TTG GTC)	Alexa Fluor 350	Damo-Bacteria (*M. oxyfera*)	Ettwig et al., 2009
DARCH-872 (S-*-Darc-872-a-A-18- GGC TCC ACC CGT TGT AGT)	GFP and Cy5	Damo-Archaea (*M. nitroreducens*)	Hu et al., 2015

3.3 RESULTS AND DISCUSSION

3.3.1 Physicochemical characteristics of the collected samples

The physicochemical properties of the collected sediment, soil, and sludge samples, including the pH, moisture content, TS, VS, NH_4^+-N, NO_2-N, NO_3-N, and sCOD content, are shown in Table 3.6.

Significant differences were observed in the chemical properties of the potential seed sources (Table 3.6). pH values of the FS and sludge samples are close to each other ranging from 7.35 to 7.46. In agricultural fields, nitrogen-rich fertilization directly or indirectly can cause acidification and a decrease in soil pH (Matsuyama et al., 2005; Guo et al., 2010; Shen et al., 2013). Unexpectedly, despite the long-term (around 20 years) fertilization, paddy field soil has a relatively higher pH value (8.35) than other seed sources. The type of fertilizer used in the region might have been a factor in high pH.

NH_4^+-N and NO_3^--N were found in all seed sources, and no NO_2^--N was detected in FS and AD. In addition, NO_2^--N was observed at a very low concentration in PS, which was parallel with the previous studies on soil and sediment (Shen et al., 2013; Zhu et al., 2018; Hu and Ma, 2016). This result was attributed to the rapid oxidation of nitrite to nitrate in the environment.

Table 3.6 Results of physicochemical analyses of seed sources

Parameter	Unit	FS	PS	AD	RS
pH	-	7.35	8.35	7.44	7.46
Moisture Content	%	89.2	24.2	98.1	98.5
TS	g/L	188.7± 7.6	433.3± 48.2	27.6± 0.3	30.7± 0.6
VS	g/L	20.8± 2.1	40.3± 4.4	14.5±0.2	15.6± 0.4
NH_4^+-N	mg/L	0.45±0.02	0.44±0.03	942.43±110.99	39.97±1.78
	mg N/kg[b]	3.48±0.14	0.48±0.04	45217.7±5325.3	2474.8±110.1
NO_2^--N	mg/L	ND[a]	0.07±0.002	ND[a]	0.37±0.02
	mg N/kg[b]	ND[a]	0.1±0.002	ND[a]	26.4±1.55
NO_3^--N	mg/L	1.07±0.01	0.07±0.0002	7.87±0.14	0.06±0.004
	mg N/kg[b]	10.2±0.1	0.1±0.0003	439.4±7.8	4.4±0.3
sCOD	mg/L	274±24.7	162±19.3	743±90.7	1733±25.2
	mg/kg[b]	2601±236	215.2±26	41496±5065	124940±1814

[a] ND: Not detected

[b] mg/kg dry weight is calculated using the moisture content

PS was also found to have a relatively low NO_3^--N concentration (0.51 ± 0.002 mg N/kg) compared to other seed sources despite the fertilization. Fertilization practices to improve agricultural productivity causes an increase in nitrogen load in fields which makes these areas become habitats for DAMO microorganisms (Wang et al., 2012; Ding et al., 2015; Hu and Ma, 2016). Therefore, high nitrate content was expected in the soil samples taken from the paddy field (Wang et al., 2012; Shen et al. 2013; Hu and Ma, 2016). However, low nitrite and nitrate contents were observed. This might be due to the fact that sampling was conducted after the ventilation and ploughing of the field before fertilizer application. NO_x-N concentration in paddy field soil sample (1.04 mg N/kg) is relatively low compared to previous research, where NO_x-N was found to be ranging from 0.27 to 26.97 mg N/kg in paddy field samples (Zhou et al., 2014; Ding et al., 2015; Shen et al., 2014; Hu and Ma, 2016). Differences can also be due to sampling depth since high nitrate content was observed in the upper layer of soil samples (Ding et al., 2015; Zhang et al., 2012; Wang et al., 2012), due to the season (Zhou et al., 2014), leaching of nitrogen to deeper layers of soil (Ding et al., 2015; Wang et al., 2015) and agricultural practices (Hu and Ma, 2016).

In the sediment sample, owing to the hyper-eutrophic state of the lake (Öğün, 2012), NH_4^+-N and NO_3^--N concentrations were found to be higher compared to PS, providing a potentially suitable condition for the growth of Damo-Archaea. Previous literature reports NH_4^+-N and NO_3^--N concentrations ranging from 0 to 3.74 mg/L and 0.01 to 3.09 mg/L, respectively (Liu et al., 2020; Yang et al., 2012). In this study, NH_4^+-N and NO_3^--N concentrations in the sediment samples are measured as 0.45±0.02 mg/L and 1.07±0.01 mg/L. High nitrate content together with low ammonium content can be due to nitrification occurring under aerobic conditions in the upper soil.

FS has a sCOD content that is nearly equal to the sCOD value (250 mg/L) of low-strength domestic wastewater (Tchobanouglus et al., 2014). This high value may be due to the potential discharge of wastewaters into the canal connecting Eymir Lake to Mogan Lake which is another lake in the region (Beklioglu et al., 2017). PS was

found to have 162 mg/L sCOD content which is expected due to plant-derived organic substances (Wang et al., 2012).

3.3.2 Molecular identification of the microbial species in seed sources

FISH analysis was used to investigate the distribution and relative abundance of targeted species such as *M. oxyfera*, *M. nitroreducens*, and NC10 Phylum bacteria in the total microbial population in collected samples, that is 4 different seed sources. The relative compositions of target species to total microbial population were determined based on FISH analyses as shown Figure 3.4. Sample FISH images of the four seed sources are shown in Figure 3.5 and Figure 3.6. Approximately 45%, 65%, 58%, and 50% of the cells in AD, FS, PS, and RS, respectively were general bacteria and 55%, 35%, 42%, and 50% were general archaea. FISH results (Figure 3.4) revealed that general archaea (55%) were higher than general bacteria (45%) only in AD due to the methanogenic content of the AD sludge (Westerholm and Schnürer, 2019). Yet, RS also has a very high general archaea content of 50%.

As shown in Figure 3.4, both Damo-Bacteria (*M. oxyfera*) and Damo-Archaea (*M.nitroreducens*) were observed in all seed sources. The NC10 phylum proportion to the total microbial population was the highest in FS (28%), followed by RS (22%). NC10 phylum composition in PS and AD was found to be 15% of the total culture. NC10 phylum mediates the anaerobic methane oxidation coupled to nitrite reduction (He et al., 2016). Consequently, NC10 phylum being the highest in FS (28%) was consistent with the batch reactor experiments' results, since the highest nitrite removal rate was observed in FS (Figure 3.4, Table 3.9).

The proportion of *M.nitroreducens* to total culture followed the order of AD>PS>RS>FS and the proportion of *M.oxyfera* to total culture followed the order of RS>AD>FS>PS. Although not in the same order, nitrite and nitrate consumption was mostly observed in the reactors containing AD, PS, and FS. However,

although DAMO species was detected in RS, DAMO activity was not observable in the reactors containing RS (to be discussed in Section 3.3.3). This might reveal that DAMO process was overshadowed by other predominant microorganisms in the RS.

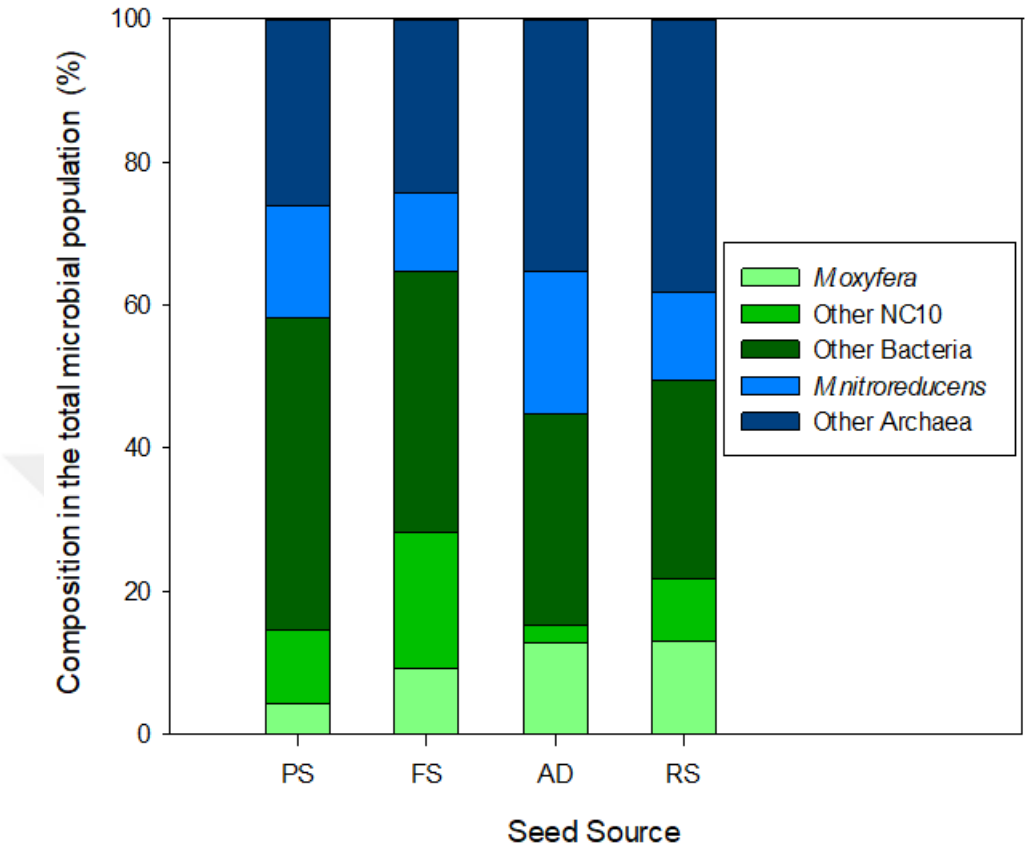

Figure 3.4 Relative composition of microbial communities in the seed sources ("Other Bacteria" refers to bacteria composition in total microbial population excluding NC10 phylum bacteria; "Other NC10" refers to NC10 phylum bacteria composition in total microbial population excluding *M.oxyfera* (Damo-Bacteria); "Other Archaea" refers to archaea composition in total microbial population excluding Damo-Archaea; Shades of the green show the total bacterial composition in the microbial population; Shades of the blue show the total archaeal composition in the microbial population, see Appendix D for the detailed method of calculation of each species)

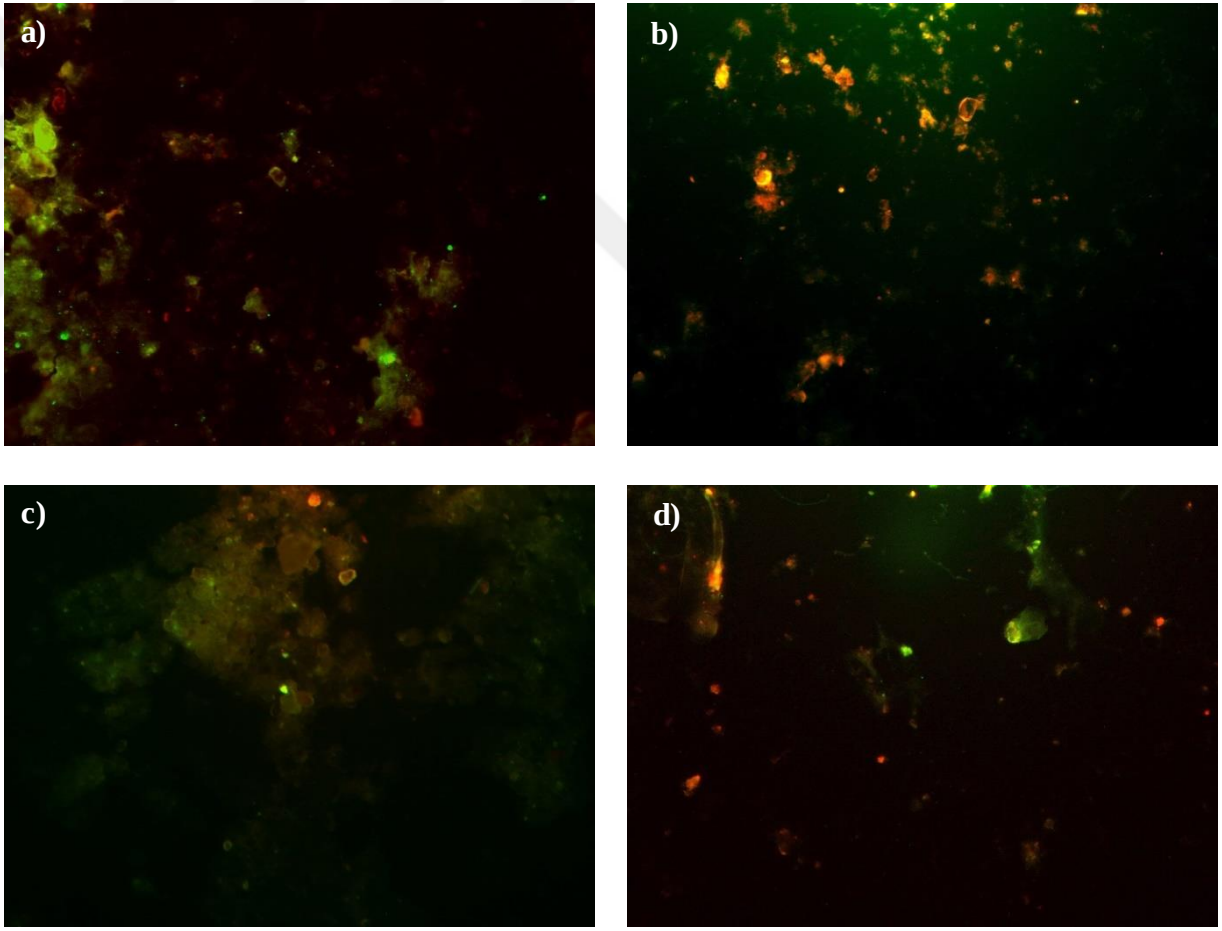

Figure 3.5. FISH images of the seed sources a) AD, b) FS, c) PS and d) RS. The NC10 phylum bacteria was hybridized with NC10-1027 probe (Cy5, orange), and Damo-Archaea (*M. nitroreducens*) was hybridized with DARCH-915 probe (GFP, green)

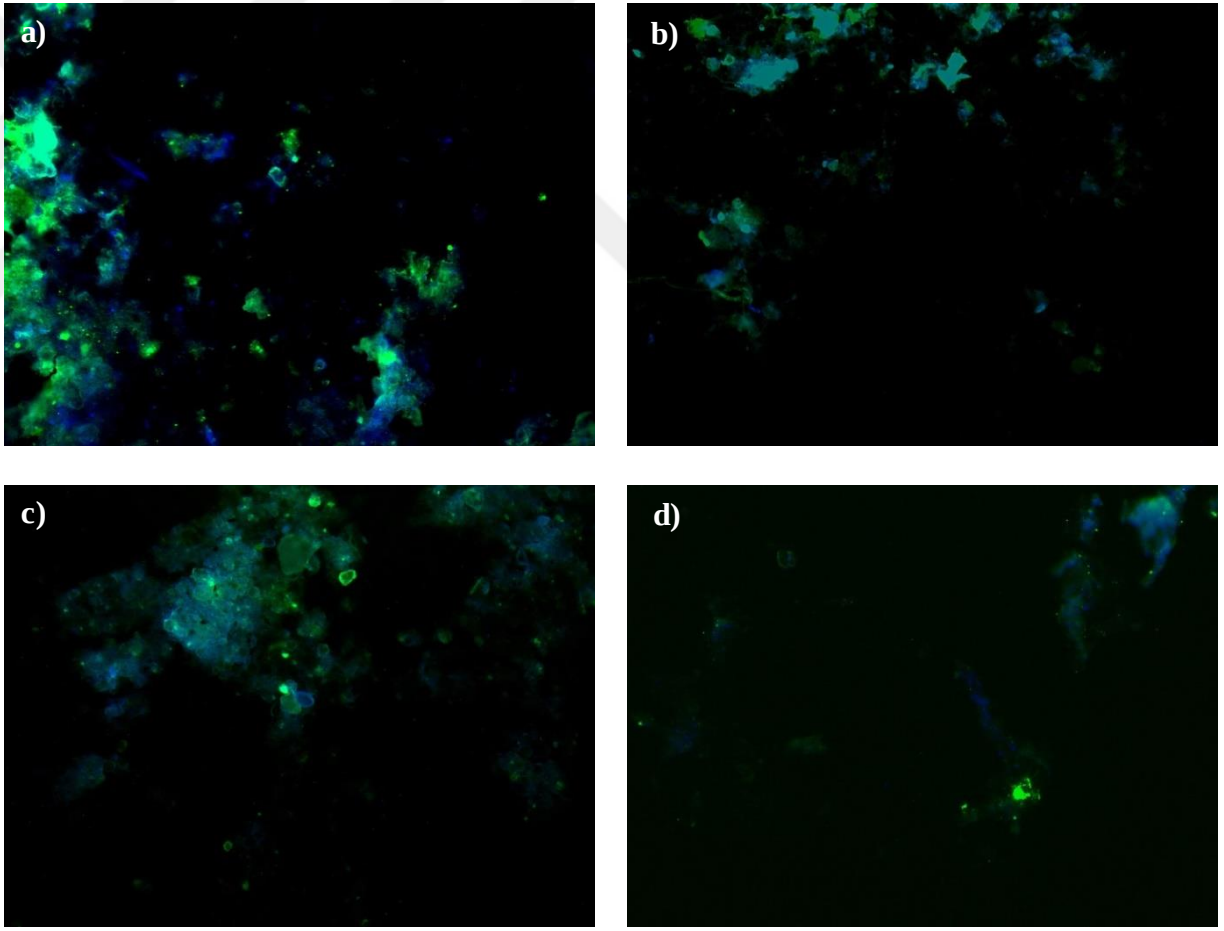

Figure 3.6. FISH images of the seed sources a) AD, b) FS, c) PS and d) RS. Damo-Bacteria (*M.oxyfera*) was hybridized with DBACT-193 probe (Alexa Fluor 350, blue), and Damo-Archaea (*M. nitroreducens*) was hybridized with DARCH-915 probe (GFP, green)

The activity detected in FS and PS (to be mentioned in Section 3.3.3) might be due to the fact that DAMO species are already acclimatized to nitrite, nitrate, and methane fluxes in the natural ecosystems, and they are already active. As mentioned previously, the absence of DAMO activity in the RS, on the other hand, maybe due to the high microbial diversity in this seed source, the lack of acclimatization of DAMO species to the conditions, and the competition of other microorganisms with DAMO species and the influence of the interspecies relationships in the seed source.

Molecular studies revealed that, in addition to the presence and diversity of the DAMO microorganisms in the seed sources, the interspecies relationship among Damo-Bacteria, denitrifiers, and nitrifiers, which are affecting DAMO by either providing nitrite/nitrate or competing for nitrite/nitrate, is another factor to be considered. Moreover, this ecological relationship between DAMO microorganisms and other microorganisms in the nitrogen cycle, creating competition or cooperation, also affects the nitrite and nitrate levels and methane emissions in the ecosystems (Xie et al., 2020).

The use of microbial community analyses, quantitative PCR, and phylogenetic analyses of the 16S rRNA and pmoA genes is suggested for the identification and quantification of *M. nitroreducens, M. oxyfera,* and to assess the relative abundance of DAMO species in different seed sources before the enrichment. The relative abundance of Damo-Bacteria and Damo-Archaea in the seed source also contributes to the decision-making process in the feeding strategy during enrichment. It should be noted that a preliminary activity test, as performed in this study, might be meaningful for better selection of the seed sources before enrichment.

3.3.3 Potential DAMO activities in the seed sources

3.3.3.1 Overall evaluation of the results

Results are represented in Figure 3.7 showing total nitrite, nitrate, and methane consumption in the test and control reactors over the 15 days. The total nitrite and nitrate consumption (μmol) was calculated for Damo-Bacteria and Damo-Archaea, respectively (as mentioned in Section 3.2.3.1). The change in nitrite and nitrate concentrations in test and control reactors is given in Table E.1.

It should be reminded that the only difference between test reactors and their control counterparts is the methane added to the test reactors. Thus, nitrite and nitrate removal observed in control reactors was attributed to autotrophic denitrification and heterotrophic denitrification other than DAMO. Any additional nitrite and nitrate removal observed in the corresponding test reactor was due to DAMO activity.

According to the results (Figure 3.7b and 3.7c), reactors inoculated with PS, FS, and their combinations were the ones that showed the highest DAMO activity. However, in reactors containing wastewater treatment sludge (AD and RS) in the inoculum, low or no DAMO activity was observed (Figure 3.7).

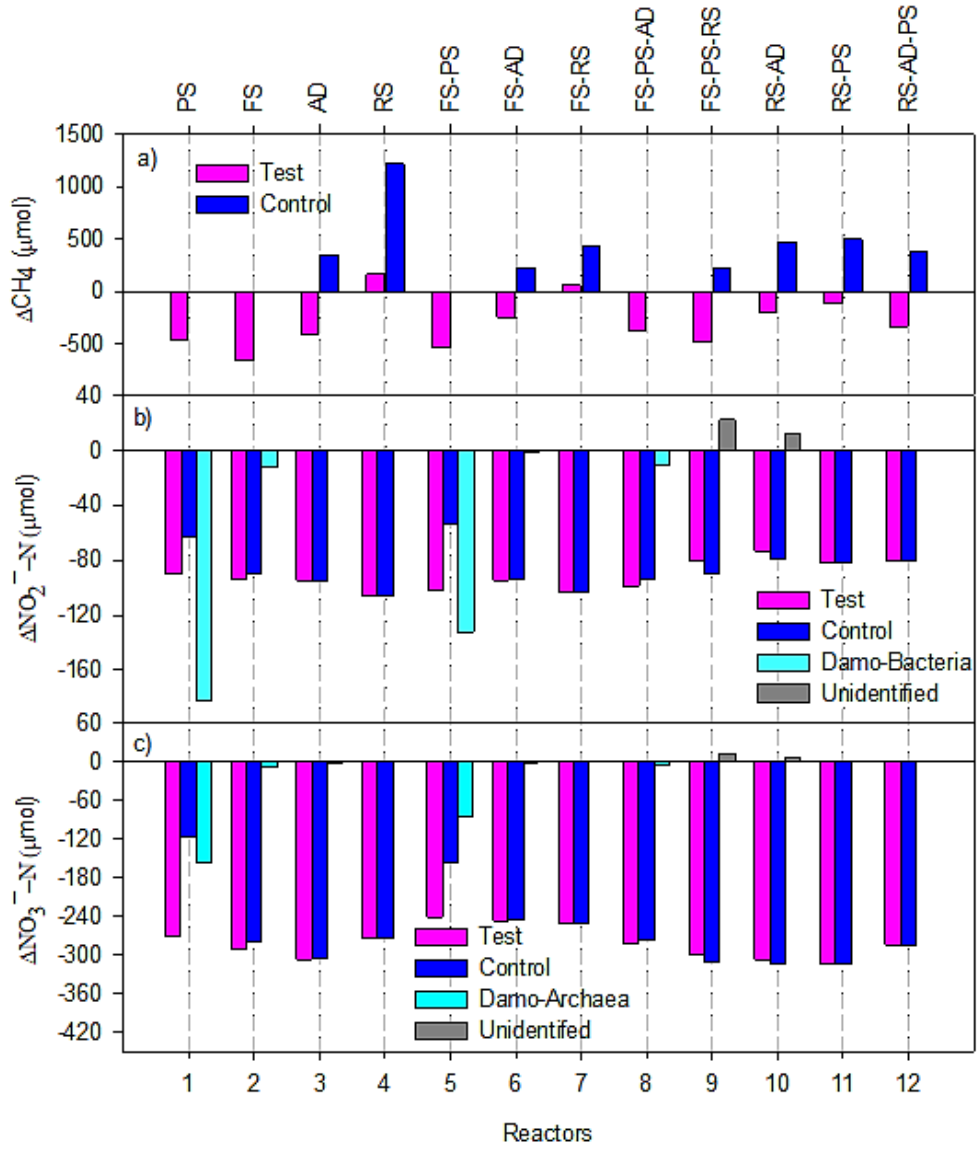

Figure 3.7 Comparison of the a) total CH_4 conversion in the test and control reactors, b) total NO_2^--N conversion in the test and control reactors and estimated Damo-Bacteria activity, c) total NO_3^--N conversion in the test and control reactors, and estimated Damo-Archaea activity, between Day-0 and Day-15. The top x-axis shows the reactor content with respect to the seed source.

Both total nitrite and nitrate consumption was in the order of T1 (PS) > T5 (FS, PS) > T2 (FS) > T8 (FS, PS, AD), and very low or no nitrite/nitrate consumption was observed in the other reactors. T1 (PS) reactor had the highest consumption of NO_2^--N (182.60 μmol) and NO_3^--N (155.44 μmol) between Day-0 and Day-15 due to DAMO process. In T2 (FS) reactor, NO_2^--N consumption (12.72 μmol) and NO_3^--N (9.05 μmol) consumption due to DAMO activity were estimated close to each other and much lower than the T1 reactor. Expectedly, T5 (FS-PS) and T8 (FS-PS-AD) reactors which were inoculated with the combination of PS and FS content, DAMO activity was also observed. In T5 reactor, NO_2^--N and NO_3^--N consumption due to DAMO process was measured respectively as 132.60 and 84.57 μmol. In T8 reactor, 10.72 μmol NO_2^--N and 5.82 μmol NO_3^--N were consumed by Damo-Bacteria and Damo-Archaea, respectively.

Methane consumption and production in the test and control reactors are shown in Figure 3.7a. In the majority of the test reactors, except T4 (RS) and T7 (FS-RS) reactors, methane consumption was detected. The highest consumption was observed in T1 (PS), T2 (FS), and T5 (PS-FS) reactors with 463, 654, and 531 μmol of CH_4 consumption, respectively. On the other hand, methane production was observed in T4 (RS) and T7 (FS-RS) reactors. Moreover, as can be seen in Figure 3.7a, methane production was observed in most of the control reactors (C3, C4, C6, C7, C9, C10, C11, and C12). However, in C1 (PS), C2 (FS), C5 (PS-FS), and C8 (PS-FS-AD), no methane was detected. Methane analysis results over the 15-day incubation period are presented in Table F.1, and the graphs showing the methane trend in the test reactors are given in Figure F.1. In the batch reactor experiment, to differentiate the DAMO activity from other autotrophic and heterotrophic denitrification, it was initially assumed that DAMO activity is not present in the control reactors since there is no methane in the headspace. The possibility of DAMO was then realized in control reactors which methane production was observed in (C3, C4, C6, C7, C9, C10, C11, and C12). However, methane was gradually produced and partial pressure of CH_4 was lower in control reactors (221-493 μmol CH_4 production at the end of 15 days), except C4 (1216

μmol CH_4 production at the end of 15 days) compared to their test counterparts (968-1272 μmol CH_4 in the headspace at the beginning of the batch reactor experiment). Thus, DAMO activity, which may occur in the control reactors, was neglected in the calculations. Nevertheless, it can be said that the estimation of NO_2^--N and NO_3^--N consumption by Damo-Bacteria and Damo-Archaea is relatively more reliable in the test reactors compared to their control counterparts (C1, C2, C5, C8) where biomass was never in contact with methane. In other words, since there was no addition of methane to control reactors and no methane production occurred in C1, C2, C5, and C8, DAMO activity was not present in these reactors. Therefore the difference between test and control reactors in terms of nitrite and nitrate consumption is due to DAMO microorganisms. As a matter of fact, T1 (PS), T2 (FS), T5 (PS-FS) and T8 (PS-FS-AD) reactors were the ones which the highest total nitrite and nitrate consumption due to DAMO proses (Figure 3.7b and Figure 3.7c).

sCOD consumption over the 15-days incubation period was observed for test and control reactors. Table 3.7 shows the initial and final sCOD concentrations and removal efficiencies (%) for test and control reactors. sCOD consumption for test reactors varied between 43-135 mg/L while in control reactors it was between 84-211 mg/L. Among test reactors, the highest consumption (135 mg/L) was detected in T4 (RS) reactor and the lowest (43 mg/L) was observed in T8 (FS-PS-AD) reactor. Similarly, in control reactors, the highest consumption (211 mg/L) was detected in C4 (RS) reactor. However, among control reactors, the lowest sCOD consumption of 84 mg/L was observed in C1 (PS) reactor. In addition to that, sCOD consumption in the test and control reactors was compared. In control reactors (except C2 (FS)), relatively more sCOD consumption was observed. It can be speculated as DAMO process was being prominent and competitive for NO_x (NO_2 and NO_3)in the reactors where methane was applied. Another possibility is that methane addition negatively affected heterotrophic denitrification. Similarly, in the control rectors (C9, C10, and C11) that all include RS in the seed source, higher total NO_x consumption was observed compared to their test counterparts.

This might also suggest that in the test reactors heterotrophic denitrification activity was somehow suppressed.

It was previously assumed that in the test reactors, the denitrifying activity is the total of DAMO process and other heterotrophic/autotrophic denitrification processes. However, in the control reactors, nitrite and nitrate were removed by other denitrification processes since DAMO process cannot occur without methane. Expectedly, as seen in Figure 3.8, there is nitrite and nitrate consumption in the test and control reactors and there is also sCOD consumption in the test reactors; therefore, heterotrophic denitrification possibility was assessed in the test reactors.

Table 3.7 Average initial and final sCOD concentrations and removal efficiencies in test and control reactors [a]

No	Inoculum Source	Initial Concentration (mg/L)	Final Concentration (mg/L)		Removal (%)	
			Test	Control	Test	Control
1	PS	176.3	112.0	92.0	36	48
2	FS	238.3	115.0	122.0	52	49
3	AD	334.0	280.0	226.0	16	32
4	RS	401.3	266.7	190.3	34	53
5	FS-PS	254.0	161.3	131.3	36	48
6	FS-AD	350.0	289.7	277.0	17	21
7	FS-RS	285.3	193.3	129.0	32	55
8	FS-PS-AD	285.7	242.7	139.3	15	51
9	FS-PS-RS	201.3	121.0	84.3	40	58
10	RS-AD	376.3	300.7	269.7	20	28
11	RS-PS	231.3	154.3	80.3	33	65
12	PS-AD-RS	289.3	210.3	143.3	27	50

[a] Average results of triplicate analyses

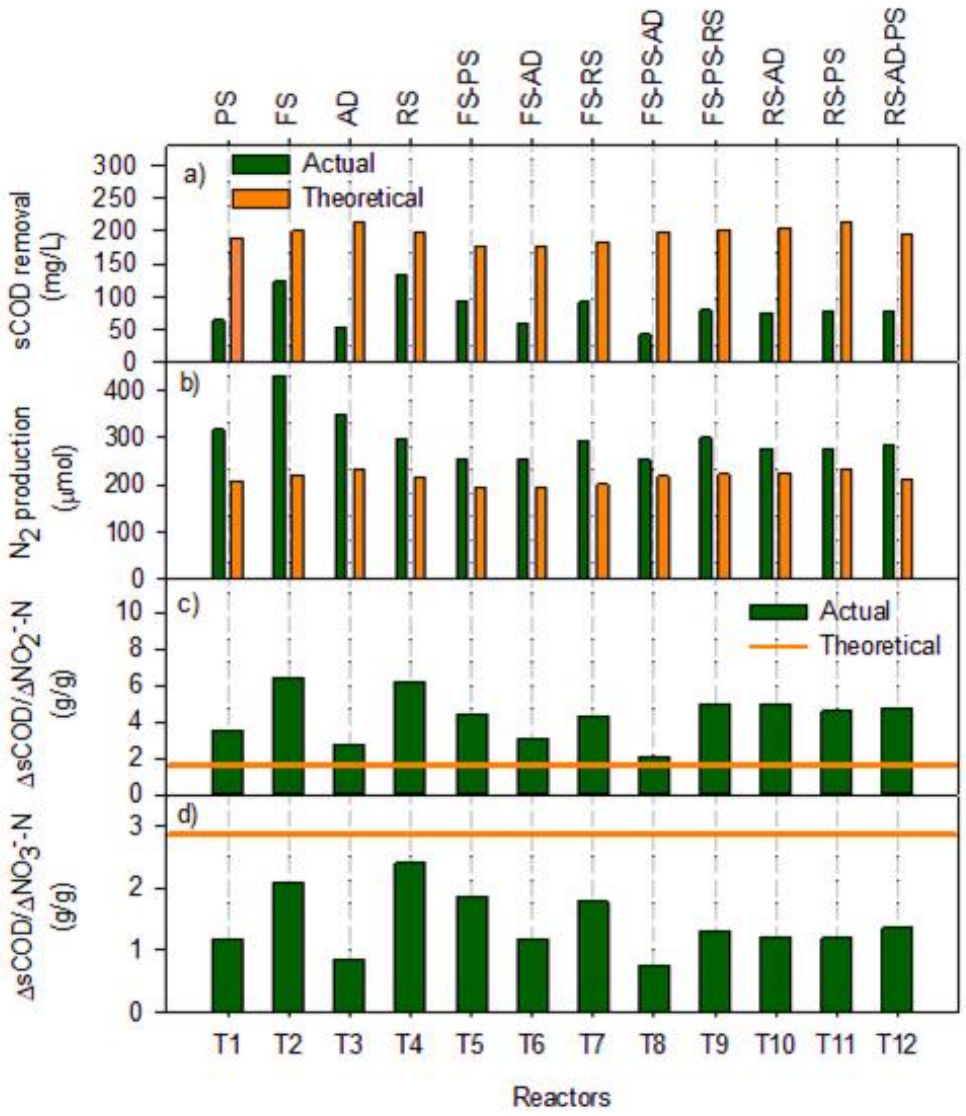

Figure 3.8 Comparison of the actual and theoretical a) sCOD consumption (all NO_x-N was assumed to be consumed with heterotrophic denitrification), b) N_2 gas production between Day-0 and Day-15 (all NO_x-N was assumed to be consumed with heterotrophic denitrification), c) $\Delta sCOD/\Delta NO_2^-$-N ratio (all NO_2 was assumed to be consumed with heterotrophic denitrification), d) $\Delta sCOD/\Delta NO_3^-$-N ratio (all NO_3 was assumed to be consumed with heterotrophic denitrification). The top x-axis shows the reactor content with respect to inoculum.

In Table 3.8, sCOD equivalence of nitrite and nitrate, and theoretical N_2 production during heterotrophic denitrification of sCOD is presented. As seen in Table 3.8, consumption of 2.86 g sCOD with heterotrophic denitrification results in the consumption of 1 g N when nitrate is used as the electron acceptor. Similarly, consumption of 1.71 g sCOD via heterotrophic denitrification results in the consumption of 1 g N when nitrite is used as the electron acceptor.

Table 3.8 sCOD equivalence of Nitrogen (N) and theoretical N_2 production from heterotrophic denitrification of 1 g sCOD

Reduction Reactions used in calculations		**Theoretical Ratio[a]**	
		g sCOD/g N	**mol N_2/g sCOD**
$2NO_3^- + 12H^+ + 10e^- \rightarrow N_2 + 6H_2O$	$O_2 + 4H^+ + 4e^- \rightarrow 2H2O$	2.86	0.016
$2NO_2^- + 8H^+ + 6e- \rightarrow N_2 + 4H_2O$	$O_2 + 4H^+ + 4e^- \rightarrow 2H_2O$	1.71	0.016

[a] Theoretical ratios were calculated using electron equivalent and molar mass on an electron transfer basis

In order to understand if NO_x content was removed only via heterotrophic denitrification or not, the required sCOD amounts were calculated. To this purpose, using Table 3.8, sCOD equivalents (g) for only nitrite removal, for only nitrate removal, and both nitrate and nitrite removal were calculated, considering that only heterotrophic denitrification prevails. The actual and theoretical sCOD consumption in the test reactors over 15-days of incubation was compared (Figure 3.8a). For the test reactors, the ratio of ΔsCOD/ΔNO_2^--N was calculated assuming that all NO_2 was consumed with heterotrophic denitrification. The ΔsCOD/ΔNO_2-N ratio was compared to the theoretical ratio of 1.71 for heterotrophic denitrification (Figure 3.8c). Finally, the ratio of ΔsCOD/ΔNO_3^--N was calculated assuming that all NO_3 was consumed with heterotrophic denitrification. The ΔsCOD/ΔNO_3-N ratio was also compared to the theoretical ratio of 2.86 for heterotrophic denitrification (Figure 3.8d). In addition, theoretical nitrogen gas

production was calculated assuming all sCOD removal was due to heterotrophic denitrification and compared with the actual N_2 production (Figure 3.8b).

As seen in Figure 3.8a, sCOD removal in all reactors has been observed to be lower (31-78%) than the theoretical value calculated for each reactor using the required sCOD if all NO_x (NO_2 and NO_3) was consumed by heterotrophic denitrification. Similarly, more N_2 gas was produced (14-48%) in all of the test reactors than the theoretical amount expected. $\Delta sCOD/\Delta NO_2^-$-N ratio in all reactors was higher than the theoretical value (1.71) (Figure 3.8c), indicating that less nitrite was consumed than expected with the heterotrophic denitrification, or sCOD might have been removed for the heterotrophic denitrification of nitrate or anaerobic fermentation. However, on the assumption that all nitrate was removed due to heterotrophic denitrification, $\Delta sCOD/\Delta NO_3^-$-N ratio in all reactors was much lower than that of expected with heterotrophic denitrification (Figure 3.8d). This, along with the comparison of theoretical and actual sCOD removal, and N_2 production in the test reactors shows that NO_x removal was not only through heterotrophic denitrification. Especially, other possible denitrification processes than heterotrophic denitrification might have contributed to nitrate removal such as DAMO process (Raghoebarsing et al., 2006) or autotrophic denitrification where other electron donors (NH_4, H_2, Mn^{2+}, Fe^{2+}, Fe^o, S^o, HS^-) (Di Capua et al., 2019) are used.

Nitrite and nitrate consumption rates, and actual and theoretical methane consumption rates by DAMO species are presented in Table 3.9. Theoretical methane consumption rate was calculated using the stoichiometric reactions of Damo-Bacteria (Equation 2.7) and Damo-Archaea (Equation 2.8) and compared with the actual methane consumption rates observed in the batch reactor experiments. Nitrite consumption rates of Damo-Bacteria were calculated using the trends in test and control reactors which are presented in Figure E.1 and E.2. Nitrate consumption rates of Damo-Archaea were calculated using the trends in test and control reactors which are presented in Figure E.3 and E.4. As shown in Table

3.9, no Damo-Bacteria and Damo-Archaea activity were detected in T4, T7, T10, T11, and T12 reactors.

CH_4 consumption rates were calculated for the reactors (T1, T2, T3, T5, T6, T8, T9, T10, and T12) which show a linear methane consumption trend which is defined as $R^2 > 0.90$. The graphs showing the methane trends in the test reactors are shown in Figure F.1. In T4 (RS) and T7 (FS-RS), methane concentrations fluctuated and methane production was observed instead of consumption (Figure F.1, Figure 3.7). Additionally, in T11 (RS-PS), consecutive methane consumption and production were detected through the measurements at Day-0, 5, 10, 15 (Figure F.1). Therefore, no linear trend was observed (Figure F.1) to be used in the rate calculations although there is net methane consumption (Figure 3.7a). Methane consumption was observed in all reactors inoculated with FS except T7 which also had RS content in the inoculum source.

Table 3.9 Nitrite, nitrate, and methane consumption rates of test reactors[a]

Reactor	Inoculum source	Damo-Bacteria nitrite consumption rate (µmol N/d)	Damo-Archaea nitrate consumption rate (µmol N/d)	Actual methane consumption rate (µmol/d)	Theoretical methane consumption rate (µmol/d)
T1	PS	59.6	48.0	30.0	34.4
T2	FS	71.3	65.6	42.1	43.1
T3	AD	27.2	26.1	26.8	16.7
T4	RS	Nd	Nd	Nc	-
T5	FS-PS	22.0	17.0	33.0	12.5
T6	FS-AD	34.5	17.2	15.4	17.2
T7	FS-RS	Nd	Nd	Nc	-
T8	FS-PS-AD	23.7	19.1	22.9	13.7
T9	FS-PS-RS	14.0	5.0	30.2	6.5
T0	RS-AD	Nd	Nd	13.1	-
T11	RS-PS	Nd	Nd	Nc	-
T12	RS-AD-PS	Nd	Nd	20.9	-

[a] Nd: DAMO activity was not detected,

Nc: Methane consumption rate was not calculated since CH_4 concentration did not show a linear trend which is defined as $R^2 > 0.90$,

[b] Theoretical methane consumption rate was calculated using the stoichiometric reactions of Damo-Bacteria (Equation 2.7) and Damo-Archaea (Equation 2.8). For Damo-Bacteria stoichiometric molar ratio of CH_4:NO_2 is 3:8 and for Damo-Archaea stoichiometric molar ratio of CH_4:$NO_3$is 1:4.

DAMO activity was low according to total nitrite and nitrate consumption in the reactors containing AD in the inoculum (except T8) (Figure 3.7). However, considering the rate calculations, DAMO activity was also detectable in the reactors containing AD. Nitrite consumption rate by Damo-Bacteria was in the order of T2 (FS) > T1 (PS) > T6 (FS-AD) > T3 (AD) > T8 (FS-PS-AD) > T5 (FS-PS) > T9 (FS-PS-RS). Nitrate consumption was in the order of T2 (FS) > T1 (PS) > T3 (AD) > T8 (FS-PS-AD) > T6 (FS-AD) > T5 (FS-PS) > T9 (FS-PS-RS).

The highest nitrite removal rate of 71.3 μmol N/d was calculated for T2 reactor inoculated with FS. T1 and T6 reactors inoculated with PS and a combination of FS and AD followed the T2 reactor (Table 3.9). Nitrate consumption was also the highest in T2 reactor with a rate of 48.0 μmol N/d, followed by T1 (PS) and T3 (AD) reactors. Although nitrite and nitrate removal due to DAMO activity was not observable in T10 and T12 reactors, methane removal was still observed.

In reactors, where DAMO activity was observable (T1, T2, T5, T8), comparatively more NO_2^--N was consumed than NO_3^--N through DAMO activity (Figure 3.7). Moreover, rate calculations revealed that nitrite consumption rate of Damo-Bacteria was higher (14.0-71.3 μmol N/d) than nitrate consumption by Damo-Archaea (5.0-65.6 μmol N/d) (Table 3.9). In consistence with these results, nitrate reduction by Damo-Archaea was indicated as the limiting step since nitrite removal rate by Damo-Bacteria was previously reported to be 2 times higher than nitrate removal rate of Damo-Archaea (Li et al., 2018).

As seen in Table 3.9, theoretical and actual CH_4 consumption rates were very close to each other in T1 (PS), T2 (FS), and T5 (FS-AD) which are the reactors where DAMO activity was detected based on nitrite and nitrate consumption. On the other hand in T3, T5, T6, T8, and T9 actual consumption was higher than the theoretical value, suggesting that other AMO mechanisms are occurring in the culture.

3.3.3.2 Evaluation of the effect of seed sources (RS, AD, PS, FS)

According to the total nitrite and nitrate consumption in test and control reactors and estimated DAMO activity (Figure 3.7), reactors inoculated with PS, FS, and their combinations were the ones that showed the highest DAMO activity. However, reactors containing wastewater treatment sludge (AD, RS) in the inoculum such as T3 (AD), T4 (RS), T6 (FS-AD), T7 (FS-RS), and T12 (RS-AD-PS) showed very low or no NO_x (NO_2 and/or NO_3) consumption by DAMO process. Moreover, in T9 (FS-PS-RS), T10 (RS-AD), and T11 (PS-AD-RS), total NO_x consumption was measured higher in their control counterparts where DAMO process is not expected.

Considering the initial sCOD content in the seed sources, WWTP sludge samples contain much more sCOD compared to the PS and FS (Table 3.9). Therefore, for the reactors which contain wastewater sludge in the inoculum, the main removal mechanism for nitrite and nitrate might be heterotrophic denitrification. To assess this possibility and differentiate DAMO activity from other NO_x removing mechanisms, results were evaluated with respect to each seed source (RS, AD, PS, FS) and its effects on the reactors which contain its combinations. In this manner, sCOD consumption, CH_4 consumption and production; total nitrite and nitrate removal; and nitrite, nitrate, and methane consumption rate results were discussed.

Return Activated Sludge (RS)

The highest sCOD consumption was observed in the reactors inoculated with only RS (T4 and C4) (Table 3.7). Other reactors containing RS in the inoculum also showed high sCOD consumption in both test and control reactors. The sCOD consumption closest to the theoretical value (sCOD consumption if all NO_x was consumed by heterotrophic denitrification) was observed in T4 (RS) reactor among all reactors (Figure 3.8). Although the sCOD removal was lower than the theoretical sCOD in T4 (RS) (Figure 3.8a); actual sCOD consumption (135 mg/L)

corresponds to approximately 70% of the theoretical COD consumption (197 mg/L) value, indicating the major denitrification activity as the heterotrophic denitrification.

Theoretical N_2 production due to heterotrophic denitrification in this reactor (T4) was 30% lower than the actual N_2 production (Figure 3.8b), indicating that other mechanisms are contributing to N_2 production. In T4 reactor, the actual $\Delta sCOD/\Delta NO_2\text{-}N$ ratio is 3.6 times the theoretical value (1.71) which is the second-highest after T2 (FS) reactor. This indicated that biodegradable sCOD might have been removed for the heterotrophic denitrification of nitrate and/or for anaerobic fermentation.

Actual $\Delta sCOD/\Delta NO_3^-\text{-}N$ ratio in T4 was very close to the theoretical value although it was slightly lower. Among all reactors, the highest $\Delta sCOD/\Delta NO_3^-\text{-}N$ ratio corresponding to 84% of the theoretical value, where all nitrate is removed due to heterotrophic denitrification, was observed in T4 (RS) (Figure 3.8d). This suggested that either most of the nitrate was removed by heterotrophic denitrification or organic matter was removed by potential anaerobic fermentation.

Considering anaerobic fermentation, in all the control reactors containing RS in the inoculum, methane production was observed (Figure 3.7a). Moreover, among the test reactors containing RS, methane production was observed in T4 (RS) and T7 (FS-RS) as well (Figure 3.7a). C4 (RS) reactor had the highest methane production among the control reactors and T4 (RS) showed the highest methane production in their test counterparts. The high general archaea content (50%) of RS (Figure 3.4) well explains that observation.

Low NO_x consumption, high sCOD consumption, and methane production observed in reactors containing RS suggest that RS supported heterotrophic denitrification and anaerobic fermentation more than DAMO process. Yet, FISH analyses revealed the existence of DAMO microorganisms in RS. Therefore, in the reactors containing RS, DAMO was overshadowed due to the high biodegradable organic content of the seed source (RS) supporting other heterotrophic

microorganisms which were the highest among all the seed sources with sCOD of 1733 mg/L (Table 3.9). In addition to high biodegradabe sCOD, the high biomass content of the sludge is also an organic source for the denitrifiers which can use biomass decay products (He et al., 2014). Therefore, there is a high possibility of DAMO microorganisms being out-competed by denitrifiers which are more dominant and active in the inoculum. Finally, although being not high as in AD (942 mg/L), ammonium content of RS (40 mg/L) (Table 3.6) might have supported the Anammox process, which is another possible competition factor for Damo-Bacteria (Zhu et al., 2011; He et al., 2014).

Among the reactors, which have been inoculated with RS, only T9 (PS-FS-RS) showed both NO_x and CH_4 removal associated with DAMO process, with the lowest theoretical methane consumption rate (6.5 μmol/d) (Table 3.9). The highest difference between the actual (30.2 μmol/d) and theoretical (6.5 μmol/d) methane consumption rates was also observed in T9 reactor. Therefore methane consumption in this reactor can be due to another removal mechanism such as S-DAMO and M-DAMO. The DAMO activity in T9 was potentially due to biomass introduced from FS and PS. In addition to T9, T10 (RS-AD) and T12 (PS-AD-RS) reactors containing RS in the inoculum also showed methane consumption. The observation of methane consumption along with no NO_x consumption in these reactors might also be due to other methane oxidation mechanisms such as S-DAMO, M-DAMO.

Although RS supported heterotrophic denitrification and anaerobic fermentation more than DAMO process, in the previous enrichment studies high denitrification rates were shown to decrease over time due to the decrease in organic matter of the inoculum source (Ettwig et al. 2009; Hu et al. 2009; He et al., 2014). Therefore, even though DAMO activity was not detected, RS sludge remains a potential inoculum source.

Anaerobic Digester Sludge (AD)

Compared to RS, in the reactors which contain AD, a different fashion was observed in sCOD consumption. Unlike RS, relatively low sCOD consumption was observed among all test reactors containing AD in the inoculum.

Theoretical and stoichiometric ratio comparison for the heterotrophic denitrification supported DAMO activity in the reactors containing AD (Figure 3.8a). sCOD consumption in T3 (AD) was 73% lower than the theoretical value calculated using the required sCOD if NO_x was to be consumed by heterotrophic denitrification. Similarly, it was observed that 34% more N_2 was produced in T3 (AD) than the amount of N_2 to be produced as a result of heterotrophic denitrification (Figure 3.8b). Therefore, there were other mechanisms involved in the NO_x consumption different than heterotrophic denitrification.

On the assumption that all nitrate is removed due to heterotrophic denitrification, $\Delta sCOD/\Delta NO_3^-$-N ratio in T3 (AD) was 2.5 times higher than that expected with heterotrophic denitrification (Figure 3.8d). Comparison of theoretical and actual sCOD removal, N_2 production, and $\Delta sCOD/\Delta NO_3^-$-N ratio in T3 (AD) suggested that NO_x removal was not only through heterotrophic denitrification and especially nitrate was potentially consumed by DAMO microorganisms.

On the contrary, total nitrite and nitrate consumption by DAMO process over the 15-d period was very limited in the reactors inoculated with AD. However, this approach might have caused an underestimation in the NO_x removal by DAMO process since both nitrite and nitrate were quickly consumed in some reactors containing AD between Day-0 and Day-5.

In all the control reactors containing AD in the inoculum, methane production was observed (Figure 3.7a). However, methane production was much lower than methane production in control reactors containing RS in the inoculum. In addition, none of the test reactors containing AD produced showed methane (Figure 3.7a). As mentioned earlier, methane production possibility in the test reactors was

neglected in the calculations since it was not detected. However, assuming that methane production observed in control reactors should also be expected in test reactors, it can be said that, produced methane should have been consumed by methane oxidation mechanisms. On this assumption, part of sCOD consumption in the test reactors was also due to anaerobic fermentation. Therefore, even less sCOD must have been used for heterotrophic denitrification. Consequently, more NO_x might have been removed by other mechanisms than heterotrophic denitrification. Therefore, there is another possibility of underestimation of DAMO activity in the reactors containing AD.

More methane production observed in the reactors containing RS than in the reactors containing AD was unexpected since anaerobic digesters are enriched with methanogenic archaea. Moreover, molecular results also revealed the slightly higher archaea content of the AD (55%) than that of RS (50%). Thus, high methanogenic activity is expected in AD. However, lower anaerobic fermentation might be due to the low sCOD concentration (743 mg/L) (Table 3.6) of the AD which may not be enough for methanogenic activity. On the other hand, RS had a sCOD content of 1733 mg/L which supported methanogens. Additionally, the sCOD content of AD and RS might have been different in terms of acetate (HAc). Since AD was obtained after the anaerobic digestion biodegradable sCOD content might have been lower than RS. Moreover, ammonia inhibition in the AD sludge is considered as another factor. It is generally agreed that total ammonia nitrogen (TAN) of around 1700–1800 mg/l inhibits the methanogenic activity in the anaerobic digestion (Yenigün and Demirel, 2013). Yet, the initial NH_4^+-N concentration (942.4 mg/L) in AD is lower than the inhibitory concentration; thus, this possibility was discarded.

Supporting the discussion above, rate calculations revealed Damo-Activity in T3 (AD), although they were lower than detected in T1(PS) and T2(FS). Nitrite was consumed by Damo-Bacteria with a rate of 27.2 μmol N/d and nitrate was consumed by Damo-Archaea with a rate of 26.2 μmol N/d. Moreover, in T3 (AD) reactor, actual and theoretical methane consumption rates for DAMO species were

26.8 and 16.7 μmol/d, respectively. In T3 reactor, the actual methane consumption rate was not as close to the theoretical rate as in T1(PS) and T2(FS). Similar to T3 (AD), a higher actual methane consumption rate observed in T4 (RS) might be due to other methane oxidation mechanisms such as S-DAMO, M-DAMO.

In addition to T3 (AD), both NO_x and CH_4 removal due to DAMO activity was also detected in T6 (FS-AD) and T8 (PS-FS-AD).

In all reactors where DAMO activity was observed, the removal rate of nitrite was found to be higher than that of nitrate (Table 3.9). However, no difference was observed between nitrite and nitrate removal rates in T3 (AD). This was associated with a possible competition for nitrite between Damo-Bacteria and other microorganisms that use nitrite as the electron acceptor. In the physicochemical analysis of the seed sources, the highest NH_4^+-N content was detected in AD (Table 3.6), which is approximately 20 times higher than the NH_4^+-N concentration of RS. Moreover, nitrite was not detected in AD (Table 3.6). The undetectable NO_2^--N and high amount of NH_4^+-N (942 mg/L) in AD indicate that there may be competition for nitrite between Anammox and Damo-Bacteria when AD is used in the inoculum. Therefore, this competition might be the reason for the low activity of Damo-Bacteria.

Paddy Field Soil (PS)

In the reactors containing PS in the inoculum, actual sCOD removal has been observed to be 66% lower than the theoretical sCOD value to be consumed if all NO_x was consumed by heterotrophic denitrification. Similarly, theoretical N_2 production due to heterotrophic denitrification was 34% lower than the measured N_2 production (Figure 3.8b) in T1 (PS). These differences indicated that another mechanism was involved in NO_x consumption and N_2 production than heterotrophic denitrification.

ΔsCOD/ΔNO_2^--N ratio was 2 times higher than the theoretical value (1.71) in T1 (PS) (Figure 3.8c). Therefore sCOD was probably removed for the heterotrophic denitrification of nitrate or anaerobic fermentation. Since no methane production was observed in the control and test reactors containing PS in the inoculum, there is no possibility for anaerobic fermentation in these reactors.

Assuming nitrate is removed due to heterotrophic denitrification, ΔsCOD/ΔNO_3^--N ratio in T1 (PS) was calculated to be 2.5 times lower than that of expected with heterotrophic denitrification (2.86) (Figure 3.8d).

The highest nitrite and nitrate consumption were observed in T1 (PS) reactor over the 15-d period. Moreover, in all the reactors containing PS in the inoculum, Damo-Bacteria and Damo-Archaea activity was observed except for T11 and T12 reactors. This is associated with the RS content in the inoculum used in T11 and T12.

The second highest removal rate for nitrite by Damo-Bacteria, nitrate by Damo-Archaea, and methane by DAMO species was observed in T1 (PS). Moreover, the actual methane consumption rate (30.0 μmol/d) was very close to the theoretical methane consumption rate (34.4 μmol/d) in T1 (PS). In consistence with the results of this study, PS was as previously shown to be an optimum inoculum source for the enrichment of Damo-Bacteria (Hatamoto et al., 2014; He et al., 2014). Since fertilization practices to improve agricultural productivity cause an increase in nitrogen load in fields, these areas become habitats for DAMO microorganisms (Wang et al., 2012; Ding et al., 2015; Hu and Ma, 2016). PS used in this study has 162 mg/L sCOD content (Table 3.6). This sCOD source, which is possibly due to plant-derived organic substances, might be the reason for DAMO activity since sCOD might act as a carbon source for methane production in natural ecosystems (Lu, 2005; Wang et al., 2012).

It was observed in the reactors which were inoculated with PS that PS settles and sticks to the bottom of the reactor which prevents the biomass to be homogenously distributed in the reactor during mixing. This situation reduces the contact between

biomass and substrate. Thus, it may affect nitrite and nitrate removal activities in the enrichment culture. This was associated with the sticky and clayey structure of PS. This is another factor to be considered in deciding the appropriate seed sources for the enrichment of DAMO species.

Freshwater Sediment (FS)

In the reactor (T2) inoculated with only FS**,** actual sCOD consumption was 1.6 times the theoretical sCOD consumption calculated based on total nitrite and nitrate consumption assuming that the NO_x was consumed via heterotrophic denitrification (Figure 3.8). Moreover, approximately two times more N_2 gas was produced in T2 (FS) than the amount which can be produced by heterotrophic denitrification (based on the actual sCOD consumption). While no methane production was observed in T2 (FS), T5 (FS-PS), and T8 (FS-PS-AD) reactors, some other reactors inoculated with RS and AD along with FS (i.e T6, T7, T9) showed methane production (Figure 3.7a). Similar to other reactors, in T2 (FS), the actual $\Delta sCOD/\Delta NO_2$-N ratio (6.47) was much higher than the theoretical value (1.71) which is actually the highest among all reactors. Therefore, sCOD should have been consumed with other processes. Since there is no evidence for anaerobic fermentation in reactors containing FS in the inoculum, the only sCOD removal mechanism was heterotrophic denitrification of nitrate.

Heterotrophic denitrification using nitrate as the electron acceptor was assessed by the assumption that all nitrate was removed due to heterotrophic denitrification. Actual $\Delta sCOD/\Delta NO_3^-$-N ratio in T2 was slightly lower than the theoretical value. Among all reactors, the second-highest $\Delta sCOD/\Delta NO_3^-$-N ratio corresponding to 73% of the theoretical value was observed in T2 (FS) (Figure 3.8d). This suggested that most of the NO_x were removed by heterotrophic denitrification.

sCOD content and NO_3^--N content of the FS are 274 mg/L and 1.07 mg/L, respectively. Therefore, FS was considered to be an environment that supports

denitrification in the sediment against DAMO process if the nitrate content was sufficient. However, higher DAMO activity was observed in the reactors that contain FS in the inoculum T2 (FS), T5 (FS-PS), T8(FS-PS-AD) compared to other reactors (Figure 3.7). Therefore, both heterotrophic denitrification and DAMO processes could be active in these reactors.

The highest nitrite consumption rate by Damo-Bacteria, nitrate consumption rate by Damo-Archaea, and methane consumption rates by DAMO microorganisms were observed in the T2 (FS) with a rate of 65.6 μmol N/d, 42.1 μmol N/d, and 42.1 μmol/d, respectively. Moreover, the actual methane consumption rate (42.1 μmol/d) was very close to the theoretical methane consumption rate (43.1 μmol/d) in T2 (FS). This verifies the activities of both Damo-Archaea and Damo-Bacteria observed in the batch reactor inoculated with experiments.

In anoxic environments, carbon is converted to methane which can be utilized by DAMO microorganisms (Chen et al., 2014a). According to the discussion above, this study suggested that the low carbon content of the FS and PS provided an advantage regarding the DAMO activity. The existence of DAMO species in the freshwater sediments was previously detected and successful enrichment cultures have been obtained using freshwater sediments (Raghoebarsing et al., 2006; Ettwig et al., 2009; Hu et al., 2009; Yang et al., 2012; Zhu et al., 2013). Therefore, the results of this study were consistent with the previous studies.

Effect of the combined inoculum

In this study, it was hypothesized that since microbial diversity varies in different ecosystems, the combination of different seed sources might result in the effective enrichment of DAMO species. DAMO activity was detected in the reactors which were inoculated with more than one seed source. However, the nitrite and nitrate consumption rates in these reactors were lower than T1, T2, and T3 reactors which were inoculated with only PS, FS, and AD, respectively. Higher activity was not

detected in the reactors inoculated with combined inoculum. However, since microbial diversity and competition dynamics are different in each inoculum source, using mixed inoculum might still be advantageous for the enrichment of DAMO co-culture (Damo-Bacteria and Damo-Archaea) due to high microbial diversity at the start of the enrichment. In other words, since *M. oxyfera* and *M. nitroreducens* have been presumed to cooperate and coexist, the inoculum consisting of less of one species and more of the other could help the DAMO co-culture enrichment due to the cooperation among them. Moreover, Damo-Bacteria was previously reported to exhibit high competition with other microorganisms, while Damo-Archaea cooperate more with nitrogen cycling microbes (Xie et al., 2020). Thus, the cooperation between nitrogen cycling microorganisms (nitrifying and denitrifying bacteria), which are introduced via one type of inoculum source, with *M. nitroreducens* which is introduced via another inoculum source might improve the enrichment of *M. nitroreducens*. The effect of combined inoculum can be better observed after the acclimation of DAMO species to enrichment conditions and the elimination of the competitive microbes in the inoculum.

To conclude, the results of batch reactor experiments and FISH analyses showed that, among the four seed sources and their combinations tested in this study, PS, FS, and AD and their combinations were found to show potential DAMO activity. All these three seed sources were found to contain both Damo-Archaea and Damo-Bacteria. On the other hand, RS was not observed to be a good choice for the enrichment of Damo-Bacteria or Damo-Archaea due to its high amount of organic matter content which gives denitrifiers and methanogens great advantage over DAMO species. The seed source is very critical to enriching Damo-Bacteria successfully in a short time. Thus, DAMO inoculum should be selected where methane, nitrite, and nitrate existed simultaneously and Damo-Bacteria and Damo-Archaea probably inhabited dominantly. Therefore, although RS was found to be disadvantageous due to potential competition between denitrifiers, methanogens, and DAMO species, it was decided to be used in the combined inoculum of the

further enrichment studies (Chapter 4) due to molecular detection of DAMO species in RS. However, it was decided to wash the combined inoculum with the medium in order to decrease the high initial sCOD content of the RS and AD prior to inoculation. Therefore, the combination of FS, PS, AD, and RS would be used in the enrichment of DAMO species (Chapter 4). Finally, this is the first study to report DAMO process and the occurrence and activity of DAMO microorganisms in Turkey.

CHAPTER 4

ENRICHMENT OF DENITRIFYING ANAEROBIC METHANE OXIDIZING (DAMO) SPECIES

4.1 INTRODUCTION

Climate change and eutrophication are global environmental problems that concern both the ecology and human health (Walther et al., 2002). Eutrophication is caused mainly by nitrogen pollutants, while climate change is due to the emission of GHGs such as methane (Abbasi et al., 2012). Wastewater treatment is one of the areas where; the control strategies can be applied to reduce these pollutants contributing to global environmental problems. One example can be given for recently discovered DAMO microorganisms, namely Damo-Bacteria and Damo-Archaea. Damo-Archaea (*Candidatus* Methanoperedens nitroreducens), utilize methane to reduce nitrate to nitrite (Haroon et al., 2013) while Damo-Bacteria (*Candidatus* Methylomirabilis oxyfera) reduce the nitrite to nitrogen gas with methane oxidation (Ettwig et al., 2010). Therefore, a new concept of wastewater treatment can be developed (Liu et al., 2019b), since nitrogen and methane serve as substrates for DAMO species. To date, utilization of DAMO in wastewater treatment of low carbon wastewaters such as anaerobic digester supernatant, landfill leachate, low carbon industrial wastewaters, and methane-polluted groundwater has been suggested (Hou, 2013).

Before large-scale application of DAMO in wastewater treatment, it is important to know the proper seed sludge, nutrient requirements, reactor configurations, optimal operational and environmental conditions for the DAMO process (Kampman et al., 2012). Moreover, a better understanding of physiology and kinetics is significant to facilitate the application (Allegue et al., 2018). Therefore, DAMO process has been investigated and applied at a laboratory scale. It is reported that pH around 7.5 and

35 °C temperatures are optimal for DAMO microorganisms. The significance of Fe^{2+} and Cu^{2+} was also realized for the growth (He et al., 2015, 2015; Zhao et al., 2017). In the enrichment, synthetic wastewater with trace elements was used as the feed (Wang et al., 2015; Bhattacharjee et al., 2016; Hatamoto et al., 2014) except one study which used the filtered effluent of an activated sludge process (Kampman et al., 2012).

Many enrichment studies focused on Damo-Bacteria, while few studies focused on the enrichment of Damo-Archaea (Vaksmaa et al., 2017; Li et al., 2018). However, since anthropogenic activities and discharges frequently carry a nitrate load to the environment, it is also crucial to include the Damo-Archaea in the enrichment cultures (Li et al., 2018).

DAMO process has not been studied yet due to the slow growth metabolism of DAMO species (doubling time of 1–2 weeks or longer for *M. oxyfera* and several weeks for *M. nitroreducens)* (Zhu et al., 2012; Harb et al., 2021). This causes a long enrichment period and makes the recovery of DAMO from inhibitory effects more difficult. The time required for establishing enrichment cultures for the DAMO is usually 8–16 months (Raghoebarsing et al., 2006; Ettwig et al., 2009; Hu et al., 2009). This long time required for the enrichment might limit the engineering application. Moreover, about 1000 mg N/L·d nitrogen removal is required for the engineering applications (Lu et al., 2020), while the maximum reported nitrite removal rate is lower than 80 mg N/L·d and the maximum average nitrate removal rate is 70–80 mg N/L·d for DAMO process (Allegue et al., 2018; Hatamoto et al., 2017; Hu et al., 2014). Therefore, there is still room for improvement for DAMO process. However, it is to be noted that, higher removal rates have been obtained by combining DAMO process with Anammox and utilizing innovative reactor configurations where nitrite removal rate of 684 mg N/L.d (Cai et al., 2015) and nitrate removal rate of 684-700 mg N/L/d were achieved in a membrane biofilm reactor (MBfR) (Cai et al., 2015; Shi et al., 2013).

One of the main concerns in the application of DAMO is the low solubility of CH_4 (Islas-Lima et al., 2004; Guerrero-Cruz et al., 2018; He et al., 2013). Therefore, in DAMO enrichment studies, excess methane is provided to overcome this concern (Raghoebarsing et al., 2006; Kampman et al., 2014; Chen et al., 2016). In the literature, while some studies provided continuous methane supply (2–10 mL/min) in the continuous enrichment (Hu et al., 2014; Hatamoto et al., 2017; Kampman et al., 2012), others provided methane at high partial pressures to the batch cultivation cultures at the beginning of each cycle (Hatamoto et al., 2014; He et al., 2014).

Biomass loss is also an important factor affecting DAMO (Lai et al., 2018). Due to the slow growth of DAMO cultures, reactor type selection is a controlling factor for the successful enrichment of DAMO species since biomass retention is related to the reactor configuration. Various reactor configurations were used in DAMO enrichment studies such as sequencing batch reactors (SBRs), up-flow continuous reactors, continuously stirred tank reactors (CSTRs), membrane bioreactors (MBRs), and a magnetically stirred gas lift reactor (MSGLR) (Table 4.1). The first successful enrichment of the DAMO was achieved using an SBR (Raghoebarsing et al. 2006). SBR provides the homogeneous substrate and biomass distribution, long-term reliable operation, and robustness under limiting substrate conditions and inhibition conditions (Strous et al., 1999). Thus, as seen in Table 4.1 SBRs were used in many of the enrichment studies (Raghoebarsing et al., 2006; Ettwig et al., 2009; Hu et al., 2009). However, the washout problem was reported in enrichment studies using SBR. This is also supported by the fact that the minimum SRT of DAMO species is in the order of a few weeks (minimum SRT of Damo-Bacteria and Damo-Archaea is 11.1–24.5 days and 29.3 days, respectively) (Chen et al., 2014b; Yu et al., 2017). Strategies such as membrane addition into SBR (Kampman et al., 2012), improvement in the mass transfer of gas-liquid phases, and the mixing of liquid-solid phases by using MSGLR reactor (Hu et al., 2014) are still being investigated to improve solid-liquid transfer between biomass and substrate and gas-liquid transfer of methane coupling high biomass retention.

Table 4.1 DAMO microorganisms enrichment studies and conversion rates (Modified from Harb et al., 2021 and Hu et al., 2009)

Reactor Configuration[a]	**N Source**	**Influent Concentration (mg N/L)**		**Activity/Conversion rate (mg N/L.d)**	
		NO_2^-	**NO_3^-**	**NO_2^-**	**NO_3^-**
SBR[1]	NO_2^-, NO_3^-	Up to 84	Up to 84	14.98	2.52
CSTR[2]	NO_2^-, NO_3^-	42–210	42–140	9.8	0.09
SBR[3]	NO_2^-, NO_3^-	7–280	70	30.1	NP[c]
SBR[4]	NO_3^-		NP[c]	24.2	28.0
SBR[5]	NO_2^-	1.4–84	7–42	5.6	
SBR[6]	NO_2^-	7–21		4.76	
SBR[7]	NO_2^-	0.91–9.13		10.96	
SBR[8]	NO_2^-	40–140		11.4	
CSTR[8]	NO_2^-	30–70		26.4	
MBfBR[9]	NO_2^-	150		14.84	
MBfBR[9]	NO_3^-		100		7.56
SBR[10]	NO_2^-, NO_3^-	16	7	40.32	
DHS[11]	NO_2^-, NO_3^-	7–9.8	7–14	70.4	39.0
DHS[11]	NO_3^-	9.8–14	60.2	84.4	
SBR[12]	NO_3^-		11-34[b]		21.91
SBR[13]	NO_3^-	-	50[b]	<2.0	-
SBR[13]	NO_2^-	10*			32.8

[a]Reactor Configuration: SBR: Sequencing batch reactor, CSTR: Continuously Stirred Tank Reactor, MBfBR: Membrane Biofilm Bioreactor, DHS: Down-flow hanging sponge reactor

[b]Initial concentration inside the reactor [c]NP: Not provided

[1-13]References: [1]Raghoebarsing et al., 2006; [2]Ettwig et al., 2008; [3]Ettwig et al., 2009; [4]Hu et al., 2009; [5]Luesken et al., 2011; [6]He et al., 2014; [7]Kampman et al., 2012; [8]Hu et al., 2014; [9]Wang et al., 2015; [10]Bhattacharjee et al., 2016; [11]Hatamoto et al., 2017; [12]Li et al.,2018; [13]Fu et al., 2017

To overcome both the limited biomass retention and the low solubility of CH_4, the application of granular activated carbon (GAC) was suggested as a strategy in the utilization of DAMO process for nitrogen removal and GHG mitigation (Lu et al., 2020). Previously, carrier application has been suggested to improve the biomass retention of slow-growing microorganisms such as Anammox (Zhang et al., 2015). For the immobilization of biomass, different types of carriers have been applied such as polyurethane sponge carriers (Zhang et al., 2015), polyethylene plastics (Kowalski et al., 2019), polyurethane materials (Chen et al., 2015b), nonwoven fabrics (Wang et al., 2017) and granular activated carbon (GAC) (Chen et al., 2014c). GAC, which is a porous material with a high specific surface area, is commonly used as a microorganism carrier (Lee et al., 2015; Wu et al., 2017). Moreover, it is widely applied to increase direct interspecies electron transfer (DIET) to improve anaerobic digestion and methane production due to its electrical conductivity (Chomiak et al., 2017). Recently, in a study, integration of GAC to an MBR system improved the nitrate and methane removal performance due to the porous structure of GAC which absorbed methane and increase the dissolved methane availability for DAMO microorganisms, and helped microorganisms' retention. Consequently, microorganism retention and metabolic activity were enhanced (Lu et al., 2020). The electron transfer pathway between DAMO species is still unclear. A recent study performed with a microbial fuel cell (MFC) revealed that Damo-Archaea can transfer electrons out of the cells to their bacterial partner with microbial interspecies electron transfer (MIET) (Ding et al., 2017b). Few studies on electrical stimulation effect and conductive nano-magnetite reported an increase in the nitrite and methane removal by Damo-Bacteria due to interspecies electron transfer between complex microbial communities in the culture (Wu et al., 2016; Chang et al., 2021). Therefore, these studies also provided a new direction to stimulate DAMO process by improving MIET.

The lag-phase observed in enrichment studies with high initial concentrations and high HRTs was reported to last shorter (80-90 days) (Fu et al., 2017; Li. et al., 2018) than the studies operated with lower initial concentrations and shorter HRTs

(150-300 days) (Ettwig et al., 2009; Hu et al., 2009; He et al., 2014, Vaksmaa et al.,2017). However, long incubation times and low substrate concentrations were speculated to be crucial for the enrichment of slowly-growing microorganisms, and according to Ettwig et al. (2010), a simple lack of patience might have prevented earlier discovery of DAMO microorganisms. Nevertheless literature is lacking a comparison for the effect of initial nitrite and nitrate concentrations in the enrichment of DAMO microorganisms. Moreover, there is no study conducted to test the effect of HRT on the enrichment of DAMO microorganisms.

The aim of this part of the thesis study is to investigate the enrichment of both Damo-Bacteria and Damo-Archaea. To this purpose, two enrichment studies were carried out, one for a total of 622 days at low influent concentrations and low HRT and the other for a total of 418 days at high influent concentrations and high HRT. During the enrichment studies, the cultivation of DAMO culture was monitored using reactor performances, activity tests, and molecular analysis (FISH). It was also aimed to investigate the effect of granular activated carbon (GAC) on the activity of DAMO co-culture. Thus, GAC was added to the enrichment cultures at the end of the enrichment period and reactors were operated for 1 month under GAC conditions. GAC effect was tested by activity tests performed before and after the GAC addition for the comparison of DAMO activity.

4.2 MATERIALS AND METHODS

To investigate the enrichment of DAMO species, two DAMO cultivation studies (Enrichment-1, Enrichment-2) were carried out simultaneously at different operational conditions. The inocula, reactors, medium, and operational conditions used in these studies are explained in detail below.

4.2.1 Inoculum

This study is the first DAMO culture enrichment study conducted in Turkey. Therefore, there are no previous reports on the occurrence of DAMO species in Turkey and potential seed sources vary in the literature. Thus, prior to the enrichment, occurrence, and the activity of DAMO species in different seed sources (Paddy field soil (PS), Freshwater sediment (FS), Anaerobic digester sludge (AD), Return activated sludge of a WWTP with biological nutrient removal (RS)) was investigated (Chapter 3). The results of this study (Chapter 3) were taken into account in decision-making for the optimum seed source in Enrichment-1 and Enrichment-2 studies.

4.2.1.1 The inoculum used in Enrichment-1 study

Among the four seed sources (Chapter 3); PS, FS, AD was observed to show DAMO activity. However, RS was not observed to be a good choice for the enrichment of DAMO species due to the high amount of organic matter which gives denitrifiers and methanogens a great advantage over DAMO species. Although RS was found as disadvantageous, it was still included in the combined inoculum used in the Enrichment-1 due to molecular detection of DAMO species in RS. Therefore, PS, FS, AD, and RS were used in inoculation for Enrichment-1.

The VS values of PS, FS, AD, and RS samples were 40.3, 20.8, 14.5, and 15.6 g/L, respectively. The inoculum was prepared to contain an equal amount of VS from each seed source. Therefore, the inoculum was prepared using 75, 145, 205 and 190 mL of PS, FS, AD and RS, respectively. 500 mL of this inoculum was taken and used for inoculation of the Reactor E1-0 for Enrichment-1 study. The remaining was stored for the analyses. The TS and VS concentrations of the inoculum used were 105.5 and 19.4 g/L, respectively. The inoculum was washed 3 times under anaerobic conditions with a nitrogen-free medium to remove the COD (Kampman et al., 2011; Hu and Ma et al., 2016). Before being used in inoculation,

the inoculum was sparged with Corgon (95% argon, 5% CO_2 mixture) until the DO content fell below 0.1 mg/L.

The inoculum used in re-inoculation

In Enrichment-1 study, a second inoculation (re-inoculation) was carried out. Previously, in the study presented in Chapter 3 and during the initial stages of the reactor operation for Enrichment-1, it was observed that sludge settles and sticks to the bottom of the reactor which prevented biomass to be homogenously distributed in the reactor during mixing. This situation reduces the contact between biomass and substrate. Thus, it may affect nitrite and nitrate removal activities. This was associated with the sticky and clayey structure of PS in the mixed inoculum. Therefore, PS was decided not to be used in the re-inoculation. At the time of the re-inoculation the population of denitrifiers, which are competing with DAMO species for nitrogen, was assumed to be lower than the initial population in the Enrichment-1 culture since no organic source was added in the medium. Therefore, RS which was used in the first inoculation was decided not to be used in the re-inoculation to prevent the introduction of denitrifiers back to the system. To conclude, for the re-inoculation in Enrichment-1 study, a mixture of only FS and AD was used as the inoculum. Re-inoculation was performed at Cycle-43 (Day-143) of the reactor operation of Enrichment-1. The VS concentrations of FS and AD were 39.8±0.4 and 19.5±0.5 g/L, respectively. The inoculum was prepared to contain an equal amount of VS from each seed source. Therefore, a mixture was prepared using 170 and 340 mL of FS and AD, respectively. TS and VS values of the inoculum used in the re-inoculation are 140.4 and 26.8 g/L, respectively. The inoculum was washed 3 times under anaerobic conditions with a nitrogen-free medium to remove the COD (Kampman et al., 2011; Hu and Ma et al., 2016). Before being used in inoculation, the inoculum was sparged with Corgon (95% argon, 5% CO_2 mixture) until the DO content fell below 0.1 mg/L.

4.2.1.2 The inoculum used in Enrichment-2 study

As mentioned previously, to decide the optimum inoculum for the enrichment of DAMO species, the results of the study presented in Chapter 3 were taken into account. According to the results of this study; PS, FS, and AD were the potential seed sources. However, similar to the Enrichment-1 study, PS was decided not to be used in the inoculation of the Enrichment-2 due to its sticky and clayey structure which prevented biomass to be homogenously distributed in the reactor during mixing. Therefore, the mixture of FS and AD was used as a seed source.

TS, VS, TSS, and VSS concentrations of FS were 380.3±57.4, 18.2±0.7, 359.1±190.4, and 18.0±2.7 g/L, respectively. TS, VS, TSS, and VSS concentrations of AD were 20.8±0.3, 9.5±0, 20.3±0.2, and 9.6±0.1 g/L, respectively. The inoculum mixture was prepared such that the VSS concentration in the reactor was approximately 10 g/L theoretically. Therefore, it was decided to inoculate the reactor with an effective volume of 0.8 L with a mixture of equal volumes of FS (300 mL) and AD (300 mL). The concentrations of TS, VS, TSS, and VSS of the inoculum used in the Enrichment-2 are 200.5, 13.8, 189.7, and 13.8 g/L, respectively.

For the removal of COD, the inoculum was washed 3 times with an N-free medium solution under anaerobic conditions (Kampman et al., 2012; Hu and Ma et al., 2016). Before the inoculation, the inoculum was washed with Argon until the DO content fell below 0.1 mg/L.

4.2.2 Medium

A synthetic medium was used based on the previous enrichment studies (Ettwig et al., 2009; Hatamoto et al., 2014). Medium components are given in Table 4.2.

Table 4.2 Medium used in the DAMO enrichment studies

Medium Components	**Concentration (g/L)**
$KHCO_3$	0.5
KH_2PO_4	0.05
$CaCl_2 \cdot 2H_2O$	0.3
$MgSO_4 \cdot 7H_2O$	0.2
Acidic Trace Element Solution	0.5 mL
Alkaline Trace Element Solution	0.2 mL
Acidic Trace Element Solution	Concentration (g/L)
HCl	100 mM
$FeSO_4 \cdot 7H_2O$	2.085
$ZnSO_4 \cdot 7H_2O$	0.068
$CoCl_2 \cdot 6H_2O$	0.12
$MnCl_2 \cdot 4H_2O$	0.5
$CuSO_4$	0.32
$NiCl_2 \cdot 6H_2O$	0.095
H_3BO_3	0.014
Alkaline Trace Element Solution	Concentration (g/L)
NaOH	10 mM
SeO_2	0.067
$Na_2WO_4 \cdot 2H_2O$	0.050
Na_2MoO_4	0.242

4.2.3 Reactors

4.2.3.1 Reactors used in Enrichment-1 study

In Enrichment-1 study, four different SBRs were used consecutively which are Reactor E1-0 (Figure 4.1), Reactor E1-1 (Figure 4.2a), Reactor E1-2 (Figure 4.2b), and Reactor E1-3 (Figure 4.2c).

All SBRs used in Enrichment-1 study were equipped with 1 liquid valve at the top, 2 gas valves (one extending to the liquid-filled section of the reactor for sparging, the other opening to the headspace for purging), 1 gas sampling point, 1 sludge inlet port (used for feeding). There is a minimum of 1 liquid outlet (for liquid sampling and decanting). In addition, Reactor E1-0 and Reactor E1-2, which are

used in Enrichment-1 study, are equipped with a pressure-resistant glass on the reactor surface (for observation) and a pressure gauge to monitor pressure during operation. Pressure and leakage tests of all reactors used in the enrichment studies were performed prior to usage.

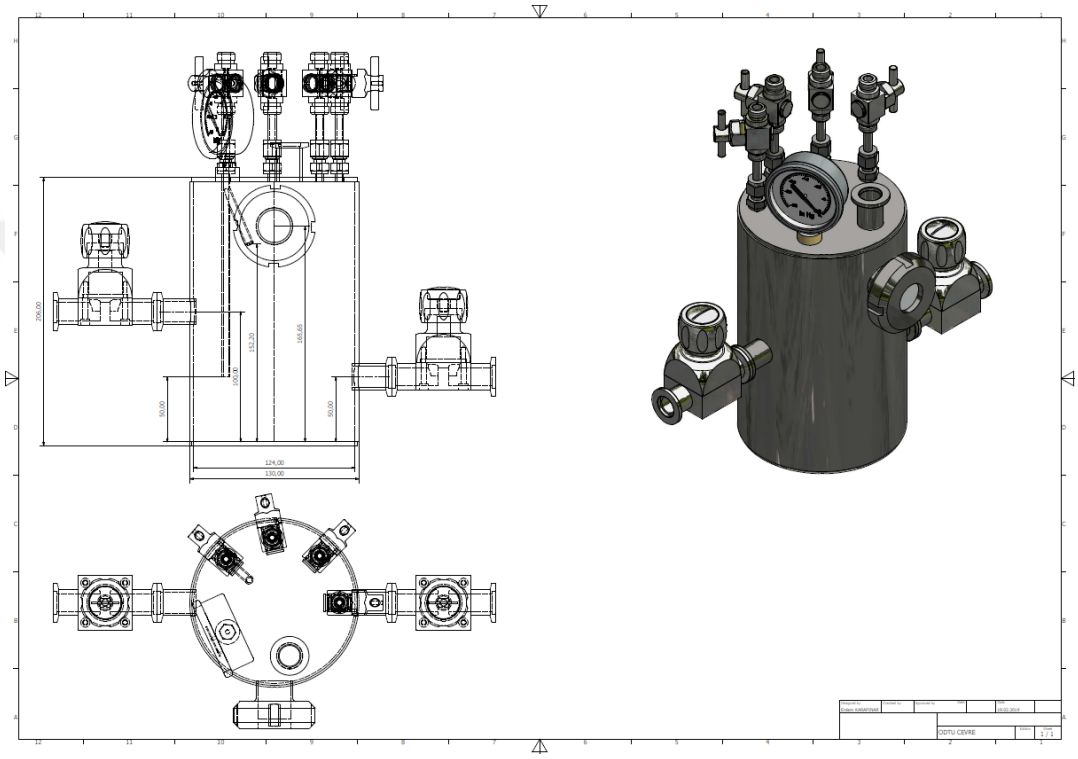

Figure 4.1 Technical drawing of Reactor E1-0

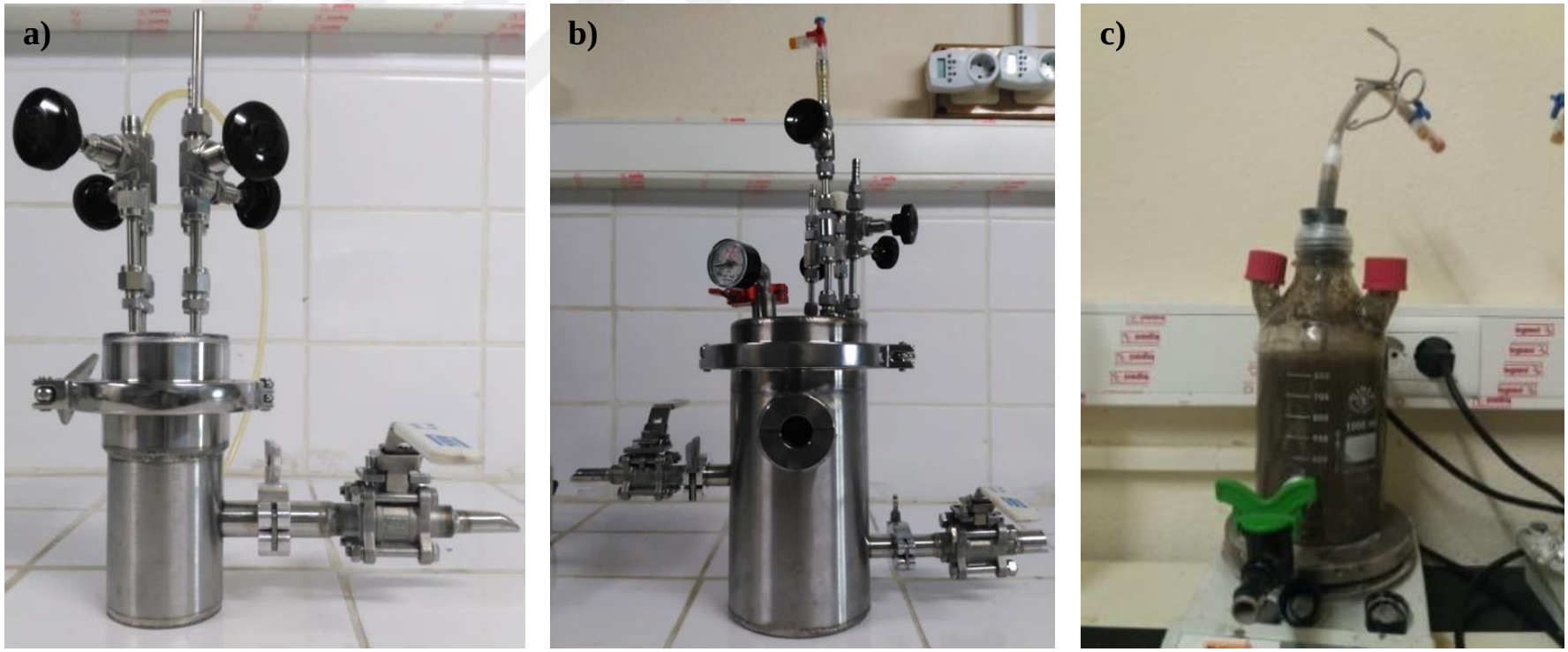

Figure 4.2 a) Reactor E1-1, b) Reactor E1-2 (Modified from Reactor E1-0) and c) Reactor E1-3

Reactor E1-0 was initially planned to be used in the Enrichment-1. However, after a short time of inoculation, various problems were encountered during the operation (Table 4.3). Therefore, it was determined that the design should be improved. Thus, Enrichment-1 was started in Reactor E1-1. This reactor was temporarily used in Enrichment-1 study (Table 4.3) while necessary modifications were made in the Reactor E1-0 design to solve the problems. After the completion of the modifications, Enrichment-1 was carried out in the modified reactor (Reactor E1-2). In the modifications, in order to prevent the liquid from reaching to the valves at the top of the reactor and to prevent leaking, a flange was added to the design. Flange is a construction element that functions to completely open and close the upper part of the reactor and to prevent leakage from the connection point of the top cover and the reactor body. After the flange addition, the volume of the headspace has increased and the distance the liquid travels has been extended. Therefore, the liquid has been prevented from rising up to the top of the reactor. Moreover, with this modification, the upper part of the reactor was able to be fully separated when required to clean the reactor effectively. In the first design (Figure 4.1), the aim was to use as few connections and junction points as possible to ensure the system's tightness and prevent leakages, since the reactor will be operated under pressure and with methane. Therefore, the flange was not included in the original design. Finally, as explained in the results and discussion section, Enrichment-1 study was down-scaled to Reactor E1-3 and continued in this reactor. Table 4.3 presents the details and differences in the reactors used in Enrichment-1 study.

Table 4.3 Reactors used in Enrichment-1 study

Parameters	**Reactors**			
	Reactor E1-0	**Reactor E1-1**	**Reactor E1-2**	**Reactor E1-3**
Inoculum	500 mL mixture of PS, FS, AD, RS	75 mL Concentrated mixture from Reactor E1-0 containing PS, FS, AD, and RS	Inoculum taken from Reactor E1-1 containing PS, FS, AD, and RS	Inoculum taken from Reactor E1-2 containing PS, FS, AD, and RS
Material	Stainless Steel	Stainless Steel	Stainless Steel	Glass
Total volume (L)	2.4	0.4	3.0	1.1 L
Duration of operation	-	Cycles 1-15	Cycles 15-125	Cycles 125-179
Problems encountered with reactor configuration/design	-Liquid outflow from the liquid and gas valves on the top of the reactor during the gas sparging and pressurization -Sludge settling and sticking to the bottom of the reactor due to the clay structure of PS in the inoculum	Temporarily used	-Low DAMO activity and slower enrichment -The possible ineffective mixing leading to low contact between the medium, biomass, and dissolved methane	No problems encountered

4.2.3.2 Reactors used in Enrichment-2 study

Reactor E2 (Figure 4.3) was used in the Enrichment-2 study. Reactor E2 is designed as an SBR with a total volume of 1.1 L and an effective volume of 0.8 L. It is cylindrical and manufactured from glass. It is equipped with 1 inlet cover at the top (for feeding and inoculation) in the reactor, 2 gas inlet-exit points (one extending to the liquid-filled section of the reactor for sparging, the other opening to the headspace for purging and gas sampling). It is equipped with a liquid outlet on the side for liquid sampling. Pressure and leakage tests of the reactor were carried out.

Figure 4.3 Reactor E2

4.2.4 Reactor Start-up and Operation

4.2.4.1 Operation of the reactors used in Enricment-1 study

As mentioned in Section 4.2.3.1, various problems were encountered after the start-up of the Reactor E1-0 (Table 4.3). Therefore, in this section, the operation of the reactors, where no problems were encountered in operation resultant of configuration/design, is presented.

In the studies focusing on the co-enrichment of Damo-bacteria and DAMO-Archaea in the literature (Raghoebarsing et al., 2006; Zhu et al. 2012; Ding et al., 2015), the initial nitrate concentration is usually higher than the nitrite concentration. One of the reasons for this situation is that extra NO_3 is supplied to the reactor taking the possible heterotrophic denitrification that may occur under anaerobic conditions into account. In order to provide an adequate nitrogen source for the enrichment of Damo-Archea, which uses nitrate as an electron acceptor, enough nitrate should be provided Additionally, the toxic effect of nitrite is reported for Damo-Bacteria at a concentration of 14 mg NO_2-N/L (He et al., 2014; Hu et al., 2011; Hatamoto et al., 2014). Therefore, initial concentrations of NO_2-N and NO_3-N in the reactor were adjusted as 5 mg/L and 15 mg/L, respectively. It was aimed to gradually increase these concentrations according to the nitrogen consumption performance of the enrichment culture.

All reactors were operated in the hot room at 35±2°C, with a medium solution adjusted to a pH range of 7-8 (Ettwig et al., 2009; Zhu et al., 2012; He et al., 2014, He et al. ., 2015; Zhao et al., 2017). Differences in the operational parameters of the reactors are presented in Table 4.4.

Reactor E1-1 Operation

In order to temporarily transfer the Enrichment-1 culture from Reactor E1-0 to Reactor E1-1 of 0.4 L, firstly the Reactor E1-0 was emptied and the sludge was let to settle. Then, settled sludge was centrifuged. Reactor E1-1 was inoculated with

75 mL of inoculum (concentrated mixture containing PS, FS, AD, and RS). The medium (Table 4.2) was added after inoculation. Before being used in the inoculation, the inoculum was sparged with Corgon (95% argon, 5% CO_2 mixture) until the DO content fell below 0.1 mg/L. After medium addition, the effective volume is sparged with Corgon (95% Argon, 5%CO_2 mixture) for 15 minutes and then sparged with 95% Methane, 5% CO_2 mixture for 15 minutes after feeding. Since there is no pressure gauge in the reactor, the system was operated at 1.0 atm pressure. The details of the operational conditions of Reactor E1-1 are presented in Table 4.4. A cycle duration of 4 days was temporarily applied in the reactor. This stage in Reactor E1-1 was evaluated as an opportunity for the microorganisms to adapt to the conditions until the modifications in the main reactor were completed and for the organic carbon to be consumed due to heterotopic denitrification. After necessary modifications were made for Reactor E1-2, Enrichment-1 culture in Reactor E-1 was transferred to the Reactor E1-2.

Reactor E1-2 Operation

Effective volume (300 mL) content of Reactor E-1 was transferred to Reactor E1-2. Then, 1.7 L medium was added to make up the effective volume of 2.0 L. The enrichment studies continued in Reactor E1-2 with one cycle time of 3 days (He et al. 2015). The operational conditions of Reactor E1-2 are given in detail in Table 4.4.

Re-inoculation with AD and FS was conducted in this reactor at Cycle-43 (Day-143). Operational conditions were the same after the re-inoculation. After the re-inoculation, the initial TS and VS values in the reactor were 36.5±0.7 and 18.4±0.4 g/L, respectively. The initial TSS and VSS concentrations in the reactor were 21.5±1.1 and 3.7±0.2 g/L, respectively.

Table 4.4 Operational conditions of the reactors used in Enrichment-1 study

Operational Parameters	**Reactor E1-1**	**Reactor E1-2**	**Reactor E1-3**
Inoculum	75 mL concentrated mixture from Reactor E1-0 containing PS, FS, AD, RS	Inoculum taken from Reactor E1-1 containing PS, FS, AD, RS	Inoculum taken from Reactor E1-2 containing PS, FS, AD, RS
Total volume (L)	0.4	3.0	1.1 L
Effective volume (L)	0.3	2.0	0.8 L
Duration of operation	Cycles 1-15	Cycles 15-125	Cycles 125-179
HRT (d)	8	6	12
Cycle time(d)	4	3	3
Feeding	1 min	1 min	1 min
Reaction	92.5 h	68.5 h	68.5 h
Settling	3 h	3 h	3 h
Decanting	0.5 h	0.5 h	0.5 h
Pressure (atm)	1.0	1.2	1.0
Exchange ratio (%)	50	50	50
Mixing	Orbital shaker (120 rpm)	Orbital shaker (120 rpm)	Magnetic stirrer (250 rpm)
Initial TSS (g/L)	48.1±0.7	11.3±1.3	69.1±0.8
Initial VSS (g/L)	7.6±0.02	3.0±0.3	15.4±1.1

Reactor E1-3 Operation

Enrichment-1 system was down-scaled at Cycle-125 (Day-442). To this purpose, Reactor E1-3 of 1.1 L (Figure 4.2c) was started to be operated. The operational conditions of Reactor E1-3 are given in detail in Table 4.4. In order to transfer the Enrichment-1 culture from Reactor E1-2 to Reactor E1-3, firstly the Reactor E1-2 was emptied and the sludge was let to settle. Then, settled sludge was transferred to Reactor E1-3 and the medium was added to make up an effective volume of 0.8 L. Before inoculation, the medium was washed with Argon until the DO content was below 0.1 mg/L, and then with CO_2 until the pH was around 7.5. After the inoculation and the addition of the medium solution (Table 4.2), the effective volume was sparged with Argon for 15 minutes. Since there was no pressure gauge in the reactor, the system was operated at 1.0 atm pressure.

As seen in Table 4.4, HRT value was increased to 12 d and the volume exchange ratio was decreased to 25%. The reason for the reduction of the exchange ratio from 50% to 25% is taking both the time required for the sludge to settle and the ease of reactor operation into account. In Reactor E1-3, which continued to be operated with a cycle of 3 days, the settling time was determined as 3 hours. The volume of the sludge settled at the end of the settling period was approximately 0.6 L, and the reactor had an effective volume of 0.8 L. Therefore, Reactor E1-3 was operated with an exchange ratio of 25%.

It should be noted that the period between Cycle 85-94 (Day 295-343) coincided with the global pandemic period. The cycle period for the Enrichment-1 system, which has a cycle period of 3 days and HRT of 12 days in routine operation, has been increased. This was decided in order to minimize the time spent in the laboratory during this period and due to the national curfew. The cycle duration varied during this period (3-8 days), and accordingly, the HRT values in these cycles vary between 6-16 days.

During the operation of all reactors, the following procedure was applied to fix the initial NO_2 and NO_3 concentrations in the next cycle: Two samples were taken per

day, one for the measurement of the initial concentrations (t=0) at the beginning of the cycle, and the second from the effluent at the end of the cycle. Nitrite and nitrate analyses were performed for the samples. According to the effluent NO_2 and NO_3 concentrations, the N contents of the (next) cycle's feed solution was adjusted taking into account the desired initial theoretical concentrations in the next cycle.

4.2.4.2 Operation of the reactors used in Enricment-2 study

Reactor E2 (Figure 4.3) was used in the Enrichment-2 study. 0.6 L inoculum was added to Reactor E2. After inoculation, 0.2 L medium (Table 4.2) was added to make up an effective volume of 0.8 L. Before inoculation, the medium was washed with Argon until the DO content was below 0.1 mg/L, and then with CO_2 until the pH was around 7.5. After the inoculation and the addition of the medium solution, the effective volume was sparged with Argon for 15 minutes. Then, the effective volume was washed with a mixture of 95% CH4, 5% CO_2 for 15 minutes, and the reactor internal pressure was adjusted to be 1.0 atm. The initial TS, VS, TSS, and VSS concentrations in the reactor were 135.3±4.0, 11.5±0.9, 134.9±12.4, and 9.5±1.2 g/L, respectively.

Enrichment-2 was run at very different operational conditions than those of Enrichment-1 study. First of all, the HRT of Reactor E2 was adjusted to 120 days. Accordingly, one cycle lasted 30 days (Fu et al., 2017; Li et al., 2018). The feeding, reaction, settling, and decanting periods were set to 0.5 h, 716 h, 3 h, and 0.5 h, respectively. The reason for studying such long HRT was to shorten the lag-phase observed in the enrichment of DAMO microorganisms. In the literature, the DAMO enrichment studies were obtained either at low HRTs as 1.4-15 days (Hu et al., 2014; Kampman et al., He et al., 2014; Etttwig et al., 2009; Hatamoto et al., 2014) or at long HRTs such as 90-120 days with high initial N concentrations. The latter was attributed to fast consumption of other electron donors used in autotrophic and heterotrophic denitrification, improved methane availability in the reactor due to periodical methane supply during one cycle, and more stable

operation of the system without disturbance, as in the natural habitat where DAMO microorganisms are detected. Accordingly, high concentrations were applied; NO_2-N was 10 mg/L while NO_3-N was 50 mg/L (Fu et al., 2017; Li. et al., 2018). The reactor was operated in the hot room fixed at 35±2 ^{0}C, magnetic stirrer (500 rpm) with a medium solution adjusted to pH 7.5. (Ettwig et al., 2009; Zhu et al., 2011; He et al., 2014, He et al., 2015; Zhao et al., 2017). The volume exchange ratio was 25%. In order to increase the dissolved methane availability, effective volume was sparged with a mixture of 95% methane and 5% CO_2 at 2-3 day intervals throughout the cycle (Fu et al., 2017; Li et al., 2018).

Although cycle duration was set to 30 days, NO_2 and NO_3 in the reactor were depleted before 30 days due to heterotrophic denitrification at the beginning of the enrichment study. Therefore, liquid samples were taken once every 2-3 days for nitrite and nitrate analyses. When one of them depleted, a new cycle was started. Following the depletion of COD, which is used as an electron donor in heterotrophic denitrification, Enrichment-2 system was started to be operated with a cycle time of 30 days. Initial concentrations of NO_2-N (mg/L) and NO_3-N (mg/L) in the reactor were adjusted as 10 mg/L and 50 mg/L, respectively, as mentioned previously (Fu et al., 2017; Li et al., 2018).

There was no change in the operational conditions of the Enrichment-2 system due to the pandemic.

During the operation, a similar procedure as that of Enrichment-1 stıudy was applied to adjust the initial NO_2 and NO_3 concentrations of each cycle: According to the effluent NO2 and NO3 concentrations, the N contents of the (next) cycle's feed solution was adjusted taking into account the desired initial theoretical concentrations in the next cycle.

.

4.2.5 Activity Tests

4.2.5.1 Concept and calculations used in the activity tests

In order to monitor the enrichment process and activity increase in Enrichment-1 and Enrichment-2 studies, activity tests were carried out periodically. Activity tests were performed using two different reactors (control reactors and test reactors). Nitrite and nitrate were added to both the control reactor and test reactor. However, methane was only added to the test reactor. Activity tests were also performed using the same batch reactor and dividing the experimental period into two phases. In other words, once the reactor was conducted, it was run as a control reactor and thus no methane was added (control phase). At the end of a specific duration, the second phase (the test phase) started and methane was added to the same reactor. The period conducted with methane indicated conditions similar to that of a test reactor.

In the control reactor/phase, nitrite and nitrate removal depend on the heterotrophic and autotrophic denitrification mechanisms different than the DAMO process. However, nitrite and nitrate removal in the test reactor/phase was attributed to both DAMO process and other heterotrophic and autotrophic denitrification mechanisms (He et al., 2015). A conceptual schematic of the DAMO activity calculation is presented in Figure 3.3. Therefore, nitrite and nitrate consumptions in the test reactors were considered to be the total denitrification consisting of heterotrophic and autotrophic denitrification and DAMO activity. Moreover, Damo-Archaea converts nitrate to nitrite which results in an increase in the nitrite concentration in the reactor. Produced nitrite was included in the calculations of nitrite consumption by Damo-Bacteria as additional nitrite input (Figure 3.3).

NO_2 and NO_3 consumption rates

Formulas, which were used in the calculations to determine the activity (mmol/L.d) of Damo-Bacteria and Damo-Archaea, are given in Equation 4.1 and Equation 4.2 below. Rate calculations were performed for the data only showing a linear trend ($R^2 > 0.90$). The graphs showing the nitrite and nitrate consumption/production trends in test and control reactors/phases obtained from the activity tests are presented in Appendix G.

$$r_{NO_3,\text{Damo-Arch}} = r_{NO_3,\text{test}} - r_{NO_3,\text{control}} \quad \text{(Equation 4.1)}$$

$$r_{NO_2,\text{Damo-Bact}} = r_{NO_2,\text{test}} - r_{NO_2,\text{control}} + r_{NO_2,\text{Damo-Arch}} \quad \text{(Equation 4.2)}$$

Where;

$r_{NO_3,\text{test}}$: consumption rate of nitrate in the test reactor/phase

$r_{NO_3,\text{control}}$: consumption rate of nitrate in the control reactor/phase

$r_{NO_2,\text{test}}$: consumption rate of nitrite in the test reactor/phase

$r_{NO_2,\text{control}}$: consumption rate of nitrite in the test/control reactor

$r_{NO_2,\text{Damo-Bact}}$: nitrite consumption rate of Damo-Bacteria

$r_{NO_3,\text{Damo-Arch}}$: nitrate consumption rate of Damo-Archaea

$r_{NO_2,\text{Damo-Arch}}$: nitrite production rate of Damo-Archaea

Methane consumption rates

Methane analyses were performed throughout the study. However, due to the high partial pressure of methane (0.95 to 1.14 atm in Enrichment-1, 0.95 atm in

Enrichment-2, and 0.95 atm in activity tests), no significant change in methane value was detected. In other words, even if methane was consumed, the methane concentration in the headspace did not change noticeably. Therefore, related data was not included in this thesis study. However, it should be noted that since the nitrogen source concentrations are low, the amount of methane is not limiting.

The method of calculation to know the availability of methane in the reactors is presented below as an example. The period between Cycle-147 and 169 in the Enrichment-1 where the highest NO_2-N and NO_3-N concentrations were fed while headspace was pressurized to 1.0 (0.95 atm CH_4) was taken into account as a worst-case scenario for the availability of methane. In this period, the initial concentrations of NO_2-N and NO_3-N were 10 mg/L (0.71 mmol/L) and 40 mg/L (2.86 mmol/L) which corresponds to 0.57 mmol and 2.29 mmol of NO_2-N and NO_3-N, respectively (Note that effective volume: 0.8 L). For Damo-Bacteria stoichiometric ratio of CH_4:NO_2 is 3:8 and for Damo-Archaea stoichiometric ratio of CH_4:NO_3 is 1:4 (Figure 3.3). Therefore, the removal of 0.57 mmol NO_2-N requires 0.21 mmol CH_4 and the removal of 2.29 mmol NO_3-N requires CH_4 0.6 mmol CH_4, resulting in the total amount of 0.81 mmol CH_4.

Using the universal gas law, moles of methane in the headspace were calculated as presented in Equation 4.3.

$$CH_{4\,\text{headspace}}\ (\mu\text{mol}) = \frac{P \times V}{R \times T} \qquad \text{(Equation 4.3)}$$

$$CH_{4\,\text{headspace}}\ (\mu\text{mol}) = \frac{0.95\ \text{atm} \times 0.3\ \text{L}}{0.085057\ \frac{\text{L. atm}}{\text{mol} \times \text{K}} \times 308\ \text{K}} = 0.011\ \text{moles}$$

Where;

n: the amount of CH_4 in the headspace, moles

P: Pressure, atm

V: volume, L

R: the universal gas constant, 0.082057 $\frac{\text{L.atm}}{\text{mol}\times\text{K}}$

T: temperature, K

Assuming that the liquid and gas phase were in equilibrium, dissolved methane content in the effective liquid volume was calculated based on the measured methane content in the headspace (µmol) and the mole fraction solubility coefficient (0.000021) for CH_4 (Wilhelm et al., 1977) using the Equation 4.4 presented below. Calculation of mole fraction solubility coefficient of CH_4 is given in Appendix B.

$\text{CH}_{4\,\text{liquid}}$ (µmol) = $\text{CH}_{4\,\text{headspace}}$ (µmol) x MFSC (Equation 4.4)

Dissolved CH_4(mol) = 0.011 (mol) × 0.000021 = 2.4×10^{-7} moles

Where;

- $\text{CH}_{4\,\text{liquid}}$ (µmol) is the amount of methane dissolved in the liquid phase in equilibrium with the headspace
- $\text{CH}_{4\,\text{headspace}}$ is the amount of methane in the gas phase
- MFSC is the ratio of dissolved methane to methane in the gas phase at temperatures from 0 to 75 ^{0}C and at 1 atm pressure.

Then, the total amount of methane in moles in liquid and headspace was calculated as presented below in Equation 4.5.

Total $\text{CH}_{4\,\text{in reactor}}$ (µmol) = $\text{CH}_{4\,\text{headspace}}$ (µmol) + $\text{CH}_{4\,\text{liquid}}$ (µmol) (Equation 4.5)

Total CH_4 = 0.011 moles + 2.4×10^{-7} moles = 0.011 moles

Since a total of 11 mmol of methane is available in the reactor and the required amount is only 0.81 mmol, methane is considered to be not limiting during the enrichment studies, even at the most needed conditions where the highest N amount was applied to the reactors.

4.2.5.2 Operational conditions used in the activity tests

In Enrichment-1 system, 4 activity tests were performed, namely En1-AT1, En1-AT2 (Cycle-125, Day 442), En1-AT3 (Cycle-169, Day-592) (Figure 4.4) and En1-GAC (Cycle-179, Dat-622). For Enrichment-2 system, 3 activity tests were performed, namely En2-AT1 (Cycle-13, Day 174) (Figure 4.5), En2-AT2 (Cycle-20, Day-388) and En2-GAC (Cycle-22, Day 418).

En1-AT1, En1-GAC, and En2-GAC activity tests were performed as an in-reactor (with the whole culture) activity test (Ettwig et al., 2008; Kampman et al., 2011; Zhu et al., 2012) (Table 4.5). The other activity tests (En1-AT2, En1-AT3, En2-AT1, En2-AT2) were performed as batch reactor activity tests. In batch reactor activity tests, inoculum withdrawn from Enrichment-1 and Enrichment-2 systems were washed 3 times with nitrite and nitrate-free medium to remove residual nitrite and nitrate and were seeded to the batch reactors (Kampman et al., 2011; Hu and Ma et al., 2016). Batch reactors were used with a total volume of 55 mL and an effective volume of 35 mL (He et al., 2014; He et al., 2015). The reactors were inoculated with 15 mL of inoculum. 20 mL of medium was added to the reactors to set the initial theoretical concentrations of NO_2-N and NO_3-N (Table 4.5). The medium solution was washed with Argon until the DO content fell below 0.1 mg/L, and then with CO_2 at a pH of 7.5. After feeding, the effective volume was flushed with Argon. Liquid samples and gas samples were taken from the reactors at 12-hour intervals. The reactors were operated in a fixed hot room at 35±2°C and pH range of 7.0-7.5 (He et al., 2014, He et al., 2015; Zhao et al., 2017). The operational differences and details of the activity tests are given below in Table 4.5.

Table 4.5 Operational conditions of activity tests for Enrichment-1 and Enrichment-2 studies

Parameters	Enrichment-1				Enrichment-2		
	En1-AT1	**En1-AT2**	**En1-AT3**	**En1-GAC**	**En2-AT1**	**En2-AT2**	**En2-GAC**
Cycle	Cycle-72	Cycle-125	Cycle-169	Cycle-179	Cycle-13	Cycle-20	Cycle-22
Day	Day-247	Day-442	Day-592	Day-622	Day-174	Day-388	Day-418
Type	In-reactor	Serum bottle	Serum bottle	In-reactor	Serum bottle	Serum bottle	In-reactor
N feed	NO_2 and NO_3	NO_2 and NO_3	NO_2 or NO_3	NO_2 and NO_3	NO_2 and NO_3	NO_2 or NO_3	NO_2 and NO_3
Initial NO_2-N	5 mg/L	7 mg/L	10 mg/L	10 mg/L	7 mg/L	10 mg/L	10 mg/L
Initial NO_3-N	20 mg/L	7 mg/L	40 mg/L	40 mg/L	7 mg/L	50 mg/L	50 mg/L
Total Volume	3.0 L	55 mL	55 mL	3.0 L	55 mL	55 mL	1.1 L
Effective Volume	2.0 L	35 mL	35 mL	2.0 L	35 mL	35 mL	0.8 L
Inoculum	Whole biomass	15 mL	15 mL	Whole biomass	15 mL	15 mL	Whole biomass
Phasing [a]	Yes	Yes	No	Yes	Yes	No	Yes
Medium addition [b]	No	Yes	-	Yes	Yes	-	Yes
Methane purging	No	Yes	Yes	Yes	Yes	Yes	No
Duration	72 h	72 h	72 h	144 h	72 h	Yes	144 h
Control phase	36 h	36 h	72 h	72 h	36 h	Yes	72 h
Test phase	36 h	36 h	72 h	72 h	36 h	72 h	72 h
Liquid sampling	10 mL	1 mL	1 mL	10 mL	1 mL	1 mL	10 mL
Pressure	1.2 atm.	1.2 atm.	1.2 atm.	1.2 atm.	1.2 atm.	1.2 atm.	1.0 atm
Gas sampling	-	100 µL	100 µL	-	100 µL	100 µL	-
Mixing	120 rpm	120 rpm	120 rpm	120 rpm	120 rpm	120 rpm	250 rpm*

[a] Control and test phases were applied consequently in the same batch reactor

[b] Fresh medium was added at the end of the control phase before starting the test phase according to the effluent nitrite and nitrate concentration

Figure 4.4 Batch reactors set-up for En1-AT3

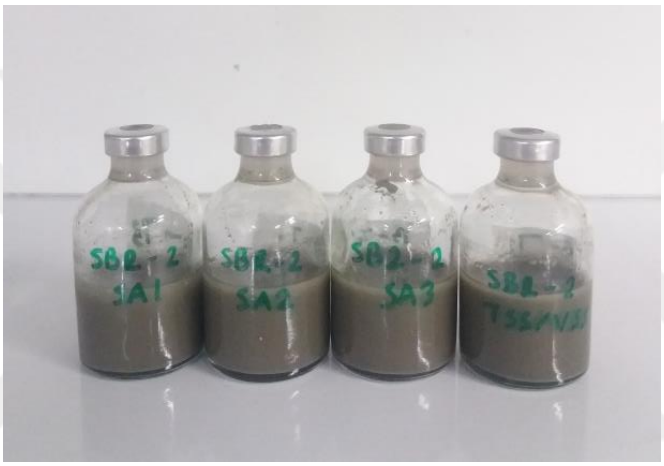

Figure 4.5 Batch reactors set-up for En2-AT1

4.2.6 GAC Addition

GAC was added to the Enrichment-1 and Enrichment-2 systems in order to observe its effect on the activity and reactor performance. GAC carbon was added to the Enrichment-1 at Cycle-170 and to Enrichment-2 at the Cycle-21, and reactors were operated for 10 cycles and 2 cycles (approximately 30 days), respectively after GAC addition. Before its addition to the reactors, GAC (1.5 mm, Merck) was boiled in water and washed 3 times until the supernatant was completely colorless (Lu et al., 2020; Yang et al., 2017). Four g of GAC was added

to the reactors and the concentration of GAC in the reactor was adjusted to 5 g/L (Lu et al., 2020).

4.2.7 Analytical methods

4.2.7.1 Physiochemical analyses

TS, VS, TSS, and VSS content were determined according to the Standard Methods (APHA, AWWA, WEF, 2005) with triplicate analysis.

Nitrite, nitrate, phosphate, and sulfate were determined with Ion chromatography (IC) (Dionex) (Reino et al., 2018). For the routine analysis during enrichment studies and in the activity tests, nitrite, nitrate, and ammonia analyses were conducted in duplicates. The Nessler Method (Hach Nessler Reagent) was used for the ammonia analysis when the sample amount was sufficient. Ammonia was measured with test kits (Lovibond, VARIO Ammonia Test Kits) when the sample volume is low. IC method and calibration curves for the ions analyzed by IC and ammonia calibration conducted for the Nessler Method are presented in Appendix H.

Dissolved COD analysis was conducted according to the USEPA approved reactor digestion method using medium range COD kits (Hach, 2012). Total Organic Carbon (TOC) measurements were made with a combustion type TOC analyzer (Shimadzu). TOC device was used in Non-Purgeable Organic Carbon (NPOC) mode with combustion catalytic oxidation method at 680°C. All TOC concentrations presented in this study represent the remaining TOC value (NPOC) after the volatilization of inorganic carbon and volatile organic carbon (such as CO_2 and CH_4). Therefore, the TOC values measured and displayed in this thesis study are the organic carbon content that causes the sCOD. The calibration curve for TOC (NPOC) is presented in Appendix H. The relationship between TOC concentrations of 0-15 mg/L and sCOD was theoretically calculated by Equation

4.6 and higher than TOC concentrations of 15 mg/L was theoretically calculated by Equation 4.7 both of which are presented below (Dubber and Gray, 2010).

$$sCOD\ (mg/L) = 7.25 + 2.99 \times TOC\ (mg/L) \quad \text{(Equation 4.6)}$$

$$sCOD\ (mg/L) = 49.2 + 3.00 \times TOC\ (mg/L) \quad \text{(Equation 4.7)}$$

All samples were filtered through a 0.45 μm filter (Sartorius) prior to ammonia, COD, and TOC analyses. For IC analysis, the samples were filtered through a 0.22 μm filter (Sartorius). TS, VS, TSS, VSS, COD, TOC, and NH_3-N analyses were run in triplicates for each measurement.

Elemental analyses (S, Mn, Fe) of samples were performed at METU Central Laboratory with an Inductively Coupled Plasma Optical Emission Spectrometer. Samples were filtered through a 0.45 μm paper filter (Sartorius). As a pre-treatment, for the analysis of the elements in solid and liquid phase separately, nitric acid was added to the liquid samples at pH <2, solid samples were dried at 105 ^{0}C.

CO_2, CH_4, N_2 gases were measured with a GC equipped with a Thermal Conductivity Detector (Trace GC Ultra: Thermo Electron Corporation) (Ettwig et al. 2008). Calibration curves and methods used in GC analysis were given in Appendix H.

DO and pH were analyzed by DO meter and pH meter, respectively. The temperature of the hot room used was measured with a thermometer.

Medium (Table 4.2) components except acidic and alkaline trace metal solutions were sterilized by autoclaving. Acidic and alkaline trace metal solutions were sterilized by filtration through 0.22 μm filter paper.

Calibration and analytical method validation was carried out for the IC, GC, TOC analyze and Nessler Method. The limit of detection (LOD) and limit of quantification (LOQ) were calculated using Equations 4.8 and 4.9; as presented below (Magnusson and Örnemark, 2014; Dettmer-Wilde and Engewald, 2014).

$$\mathrm{LOD} = \frac{3.3\sigma}{s} \quad \text{(Equation 4.8)}$$

$$\mathrm{LOQ} = \frac{10\sigma}{s} \quad \text{(Equation 4.9)}$$

Where;

s: the slope of the calibration curve

σ: standard deviation of the lowest analyte concentration

4.2.7.2 Fluorescence In Situ Hybridization (FISH)

Fluorescence In Situ Hybridization (FISH) analyses was performed for the biomass samples (Figure 4.6a) taken periodically from Enrichment-1 and Enrichment-2 systems to identify and quantify the (targeted) species in the biomass. The principle of the FISH technique is based on the hybridization of rRNA-targeted oligonucleotides (probes) to the rRNA in the target microorganism in the biomass (Amann et al., 1995). One of the aspects of the FISH method is that it is possible to directly detect and quantify non-culturable and non-isolable species in complex systems (Daims et al., 2009) such as DAMO microorganisms.

To this purpose, approximately 5 ml of samples were used. Biomass was separated by centrifugation (10000 g for 5 min) and then the supernatant was discarded. Collected samples were fixed with an equal volume of 4% paraformaldehyde (PSA) in phosphate-buffered saline (PBS) and left overnight at 4°C. PSA and biomass were separated by centrifugation (10000 g for 5 min) and fixed biomass was dissolved in 5 mL 1:1 PBS/EtOH. Dehydration was carried out with sequential wash with 50%, 80%, and 99% ethanol. Permeabilization was performed using

lysozyme and incubation for 1 hr at 37 ^{0}C. Five different hybridization mixtures composed of different probes were used in the FISH analyses of the biomass samples taken periodically from Enrichment-1 and Enrichment-2 systems. Therefore, for each biomass sample, 4 slides were prepared. The hybridization mix contents used on these slides are given in Figure C.1. Hybridization was carried out in a hybridization buffer (40% formamide) at 46°C for at least 5 h (He et al., 2014; Hatamoto et al., 2014). After hybridization, the biomass on slides was washed at 48°C for 20 min with a washing buffer containing the same components as the hybridization buffer. The 16S rRNA-targeted oligonucleotide probes used in this study and the targeted species are given in Table 4.6.

Prepared slides (Figure 4.6b) were observed via Carl Zeiss Axio Vision A1 UV microscope and at least 3 representative microscopy images were captured for each slide. Microscopic visualization is explained in detail in Appendix D.

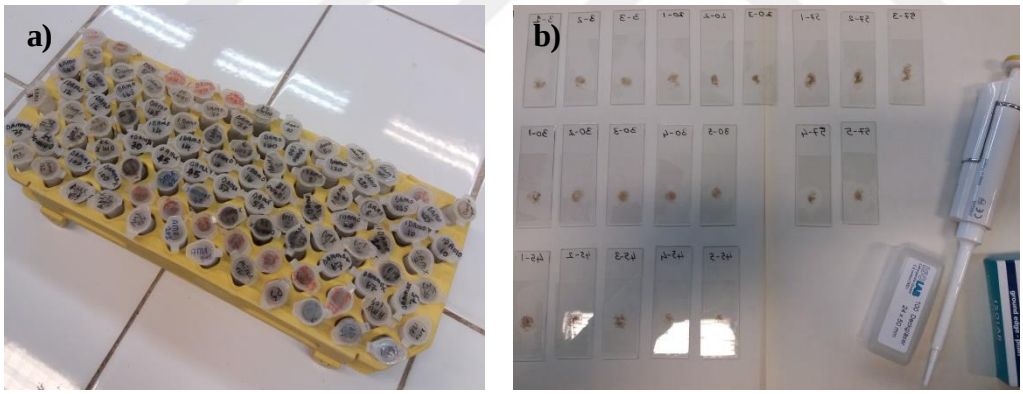

Figure 4.6 a) Samples used in FISH analyses and b) Prepared slides for FISH analyses

Table 4.6 The 16S rRNA-targeted oligonucleotide probes used in this study

Probe	Label	Target Species	Reference
EUB Mix (EUB338, EUB338 II, EUB338 III)	GFP	General Bacteria	(Knittel et al., 2005)
DARCH-915 (S-Darc-0915-a-A-20-GTG CTC CCC CGC CAA TTC CT)	GFP	General Archaea	(Ettwig et al., 2009)
NC10-1027 (S-*-DBACT-1027-a-A-18-TCT CCA CGC TCC CTT GCG)	Cy5	NC10 phylum bacteria	(Ettwig et al., 2009)
DBACT-193 (S-*-DBACT-0193-a-A-18-CGC TCG CCC CCT TTG GTC)	Alexa Fluor 350	Damo-Bacteria (*M. oxyfera*)	(Ettwig et al., 2009)
DARCH-872 (S-*-Darc-872-a-A-18- GGC TCC ACC CGT TGT AGT)	GFP and Cy5	Damo-Archaea (*M. nitroreducens*)	(Hu et al., 2015)

For quantitative determination of General Bacteria, General Archaea, NC10 Phylum bacteria, Damo-Archaea, and Damo-Bacteria, images captured for each slide were analyzed via ImageJ software. Pixel areas were determined using ImageJ for specific probes using 3 representative images (captured from the same slide). The average pixel area obtained from image analysis of 3 representative images was used in the quantification of the target microorganisms. A visual summary of ImageJ analysis is represented in Figure D.1. Methods used in quantification are given in Appendix D in detail. Summary quantification data are presented in Appendix D.

4.3 RESULTS AND DISCUSSION

In this study, 2 alternative systems (Enrichment-1 and Enricment-2) were operated in order to accelerate the enrichment of DAMO microorganisms. The main differences used in the start-up and operations of the 2 systems are summarized in Table 4.7.

Table 4.7 Start-up and operational differences between Enrichment-1 and Enrichment-2 systems

Parameters	**Enrichment-1**	**Enrichment-2**
Inoculum	1st inoculation: PS, FS, AD, RS 2nd inoculation: FS, AD	FS, AD
TSS in the reactor	1st inoculation: 12.9 g/L 2nd inoculation: 21.5 g/L	134.9 g/L
VSS in the reactor	1st inoculation: 6.1 g/L 2nd inoculation: 3.7 g/L	9.5 g/L
Cycle Time	3 days	30 days
Initial NO_2-N concentration	5-10 mg/L	10 mg/L
Initial NO_3-N concentration	5-40 mg/L	50 mg/L

As seen in Table 4.7, Enrichment-1 system was initially inoculated with PS, FS, AD, and RS and re-inoculated with FS and AD due to low biomass content in the reactor which is discussed further in Section 4.3.1. Enrichment-2 system was inoculated with only FS and AD. Therefore, the only difference in the inoculum is the biomass introduced from AD and RS to the Enrichment-1 system. One of the main differences is that Enrichment-2 system had more TSS and VSS content than that of Enrichment-1 system even after the 2nd inoculation performed for the Enrichment-1 system. Therefore, initial biomass concentration was also higher in the Enrichment-2 system. Moreover, as seen in Table 4.7, one cycle of Enrichment-2 system is 30 days which is ten times more than that of Enrichment-1 system. With this strategy, sludge was decanted from the reactor at longer intervals; therefore, biomass was only contact in the air every 30 days. Finally, since Enrichment-2 system was operated with a longer cycle time, initial concentrations of nitrite and nitrate in the system was also higher while in Enrichment-1 system, enrichment was started with very low initial concentrations and gradually increased based on the activity increase and the system's response to operational changes which is also discussed in detail below. This strategy was adopted since it was observed that the lag-phase in enrichment studies with high initial concentrations and long cycle time (Fu et al., 2017; Li. et al., 2018) lasted shorter (80-90 days). In comparison, the lag-phase in studies with lower initial concentrations and shorter cycle times lasted between 150-300 days (Ettwig et al., 2009; Hu et al., 2009; He et al., 2014, Vaksmaa et al.,2017). However, long incubation times and low substrate concentrations were speculated to be crucial for the enrichment of slowly-growing microorganisms, and according to Ettwig et al. (2010), simple lack of patience might have prevented earlier discovery of DAMO microorganisms.

4.3.1 Results of Enrichment-1 study

Enrichment-1 system was evaluated using reactor performance, activity tests and FISH analysis conducted periodically for the system.

As explained in Section 4.2.4, Enrichment-1 study was performed in Reactor E1-1 from Cycle-0 to Cycle-15. Enrichment-1 system was scaled up to a modified reactor named Reactor E1-2 (total volume: 3.0 L), where the operation lasted from Cycle-15 to Cycle-125. Enrichment-1 studies were later down-scaled and continued in Raector E1-3 (total volume: 1.1 L) from Cycle-125 to Cycle-169.

4.3.1.1 Performance of Enrichment-1 system

sCOD and pH trends observed during the Enrichment-1 system are presented in Figure 4.7 and 4.8, respectively. Figure 4.9 shows the theoretical initial, experimental initial, and effluent NO_2-N and NO_3-N concentrations measured for Enrichment-1 system. Finally, the change in NO_2-N and NO_3-N removal rates and removal efficiencies are shown in Figure 4.10 and 4.11, respectively.

During the enrichment, it was aimed that the dissolved methane, which is used as an electron donor in DAMO process, becomes the only carbon source in the reactor. For this reason, the sCOD concentration was monitored to observe the decrease resultant of heterotrophic denitrification (Figure 4.7). It was observed that high sCOD due to the organic content of the AD and RS sludge in the inoculum decreased in the first 5 cycles from 284.19±2.80 mg/L to 21.67.19±0.9 mg/L (Figure 4.7). At the end of Cycle-5, sCOD content was measured as 6.95±1.20 mg/L and it was assumed to be a negligible concentration for heterotrophic denitrification. After re-inoculation at Cycle-43, sCOD concentration increased and then decreased again due to heterotrophic denitrification and dilution of sCOD. As seen in Figure 4.10, the initial sCOD of the Cycle-76 was measured as 2859.2±36.1 mg/L. This is thought to be the result of the addition of an external carbon source to the reactor as a result of a mistake made during the feeding. As seen in Figure 4.8, it was also observed that the effluent pH for Cycle-76 suddenly decreased (pH 6.1). In this cycle, it was seen that that NO_2-N and NO_3-N removal efficiencies suddenly increased (Figure 4.11) The short-term (Cycles 74-78) increase in NO_2-N and NO_3-N removal efficiencies is due to heterotrophic denitrification. The mistake was

realized at the end of Cycle-78 and before starting Cycle-79. After that, the sludge in the reactor was washed 3 times with a nutrient solution under anaerobic conditions for the removal of sCOD (Kampman et al., 2012; Hu and Ma, 2016). Following the washing process, it was determined that the initial and effluent sCOD of Cycle-79 decreased (24.3±0.2 and 20.2±0.4 mg/L, respectively) (Figure 4.7). To fasten the consumption of sCOD remaining in the reactor, at Cycle-80 (for once), the initial concentrations of NO_2-N and NO_3-N were doubled and fed to the reactor as 10 mg/L and 40 mg/L (Figure 4.9). The latter analysis showed that sCOD was maintained in the reactor at concentrations between 30-35 mg/L until the end of the Enrichment-1 (Cycle-169).

A significant increase in pH value was detected especially in the first 10 cycles (Figure 4.8). This increase, at the end of the cycle, is due to heterotrophic denitrification in the first stages of the operation when sCOD was present in the reactor. It is known that the optimum pH for DAMO microorganisms is between 7.0 and 8.0 (Ettwig et al., 2009; Luesken et al., 2011; He et al., 2014). However, in a study investigating the effect of a wide pH range (6.0-9.0) on DAMO activity, it was proven that the pH value of 7.6 was optimum in the DAMO process (He et al., 2015). As a result, as of Cycle-11 cycle, Enrichment-1 was operated with an initial pH between 7.2-7.6. After downscaling in Cycle-125 (Day-442) (transfer of biomass to Reactor E1-3), it was observed that the initial and effluent pH values increased. This increase was reduced again with the modifications made in the purging times to adjust the pH value and the system was operated with the initial pH value between 7.2-7.6 (Figure 4.8). It was observed that the pH generally increases slightly during overall operation (Figure 4.8). This can be associated with Damo-Bacteria activity since *M.oxyfera* uses 8/3 moles H+ ion for the removal of 1 mol of CH_4 resulting in acidity consumption. On the other hand, since CH_4 is converted to CO_2 by both DAMO microorganisms, produced CO_2 can also dissolve in the water resulting in a pH decrease. However, interestingly, there is no reported pH trend during the previous DAMO enrichment studies in the literature.

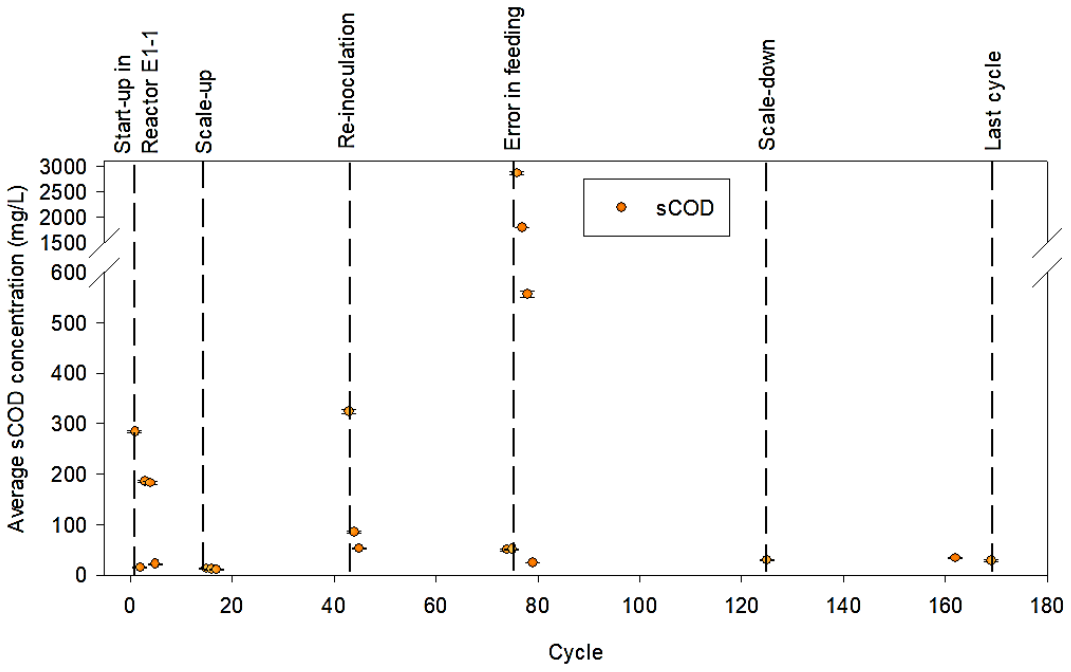

Figure 4.7 sCOD trend in Enrichment-1 system

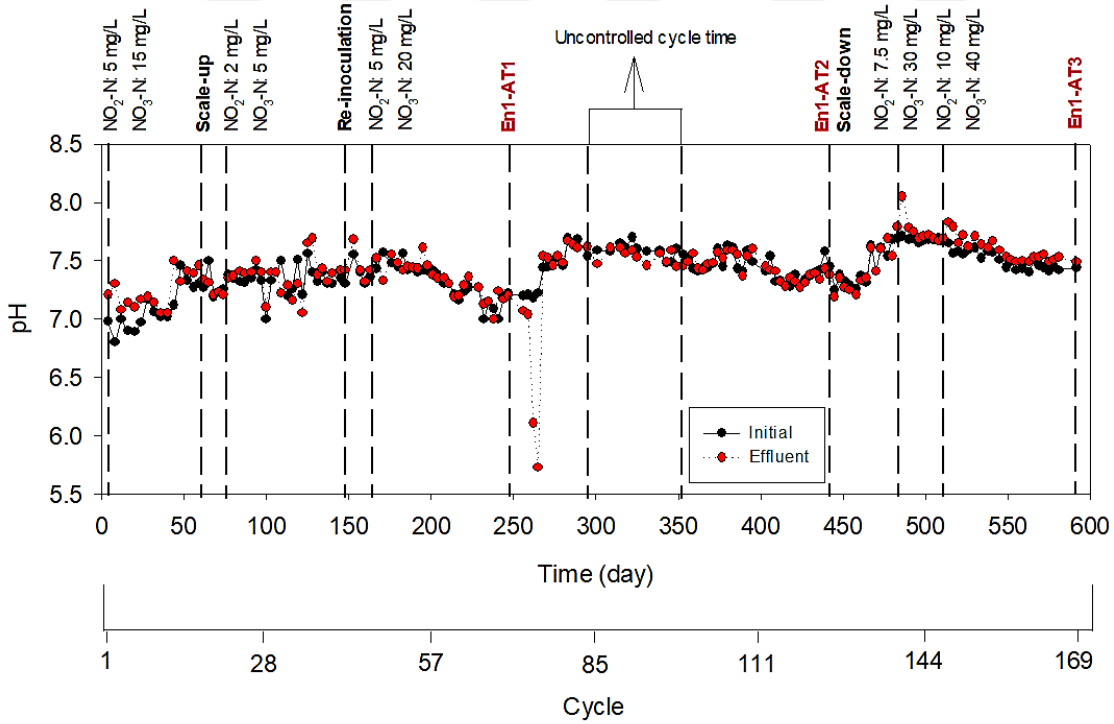

Figure 4.8 Initial and effluent pH values in the Enrichment-1 system

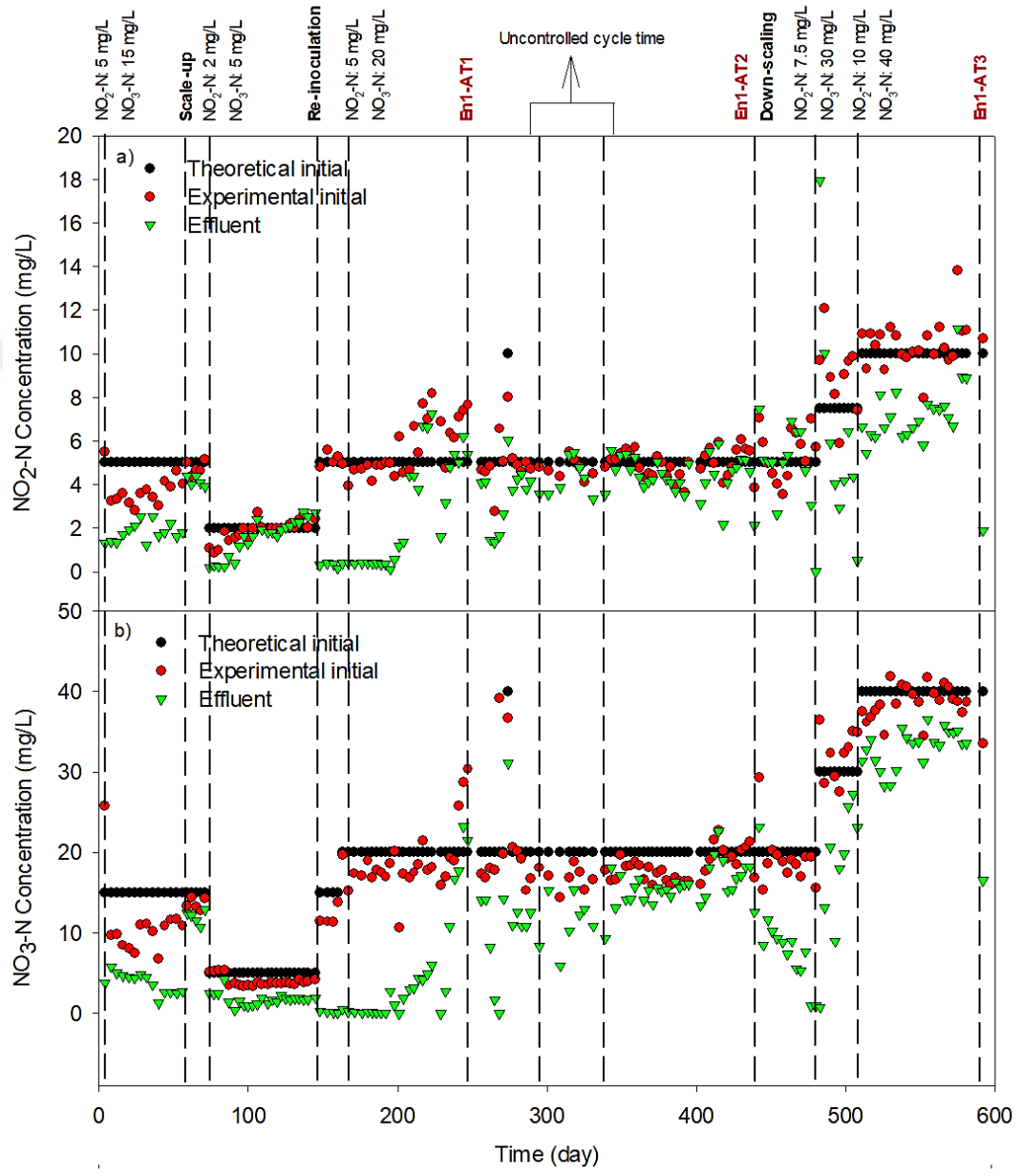

Figure 4.9 Theoretical initial, experimental initial and effluent concentrations of a) NO_2-N and b) NO_3-N in Enrichment-1 system

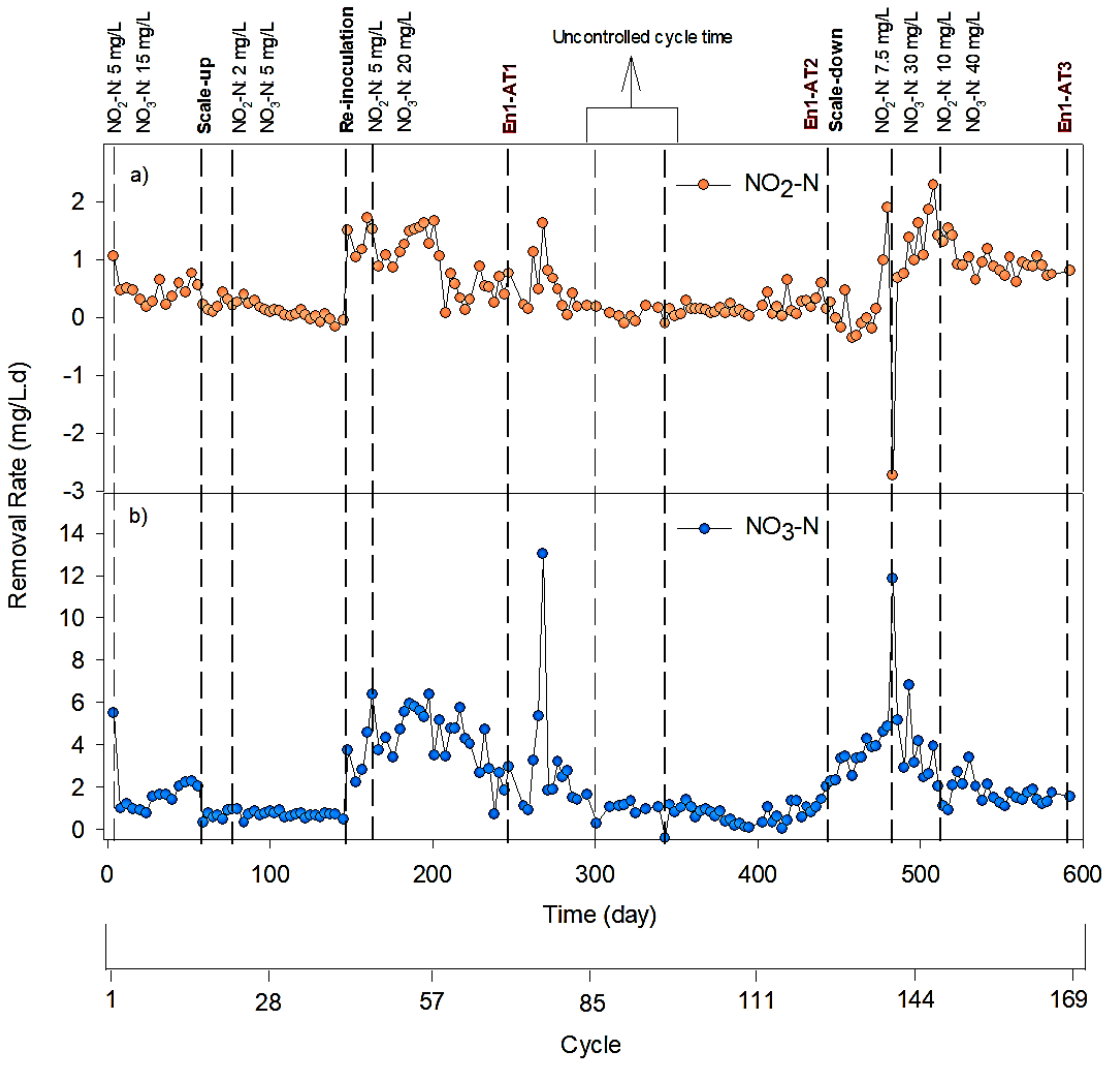

Figure 4.10 a) NO_2-N and b) NO_3-N removal rate in Enrichment-1 system

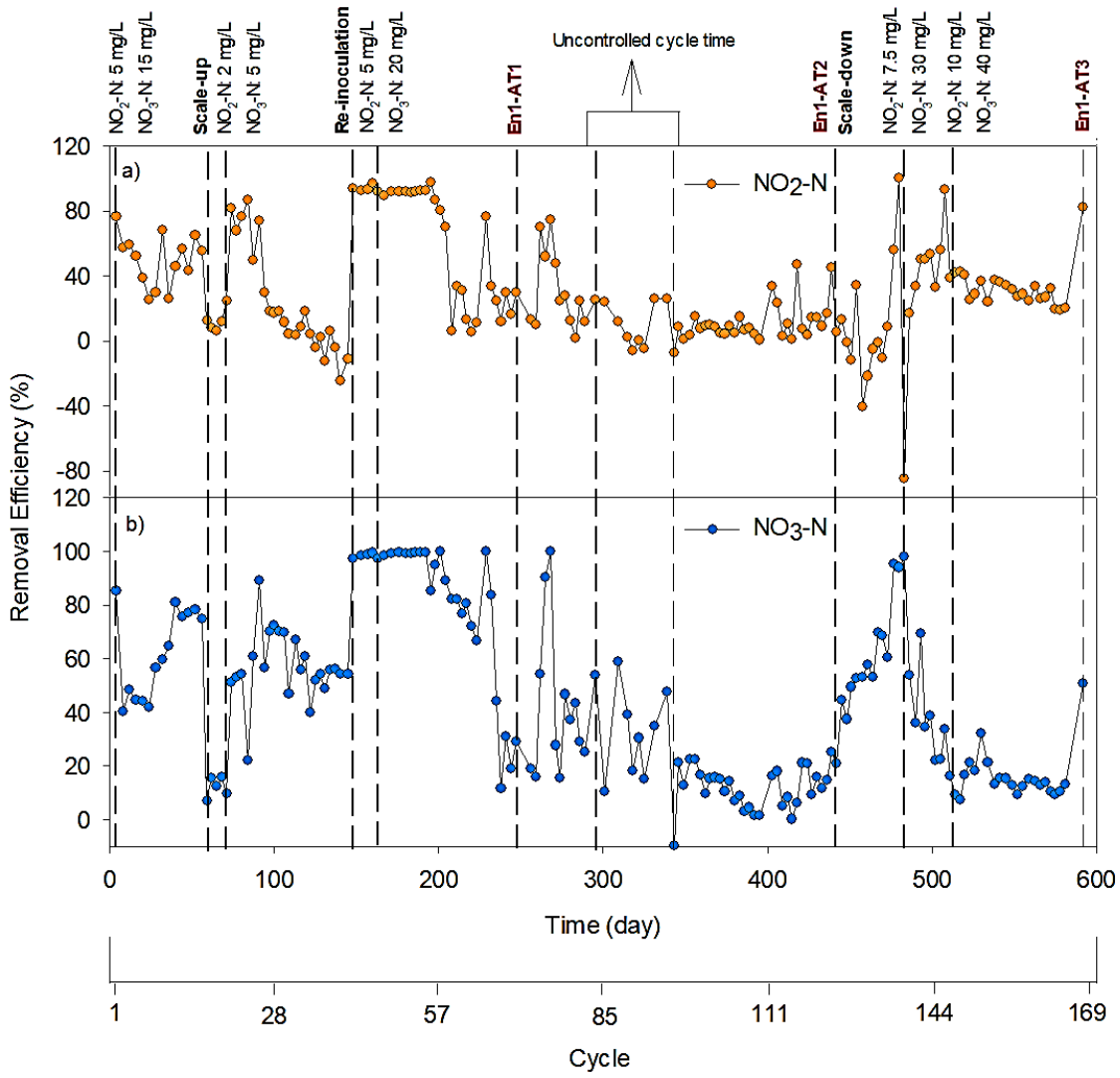

Figure 4.11 a) NO_2-N and b) NO_3-N removal efficiencies in Enrichment-1 system

As seen in Figure 4.10, in the first cycles (Cycles 1-6), both nitrite and nitrate consumption rates decreased due to the decrease in sCOD in the reactor which was used in nitrite and nitrate consumption by heterotrophic denitrification. After this decrease, starting with Cycle-7, an increase in both nitrite and nitrate consumption was observed. This is associated with the adaptation of DAMO microorganisms to enrichment conditions and a decrease in the competition between heterotrophic denitrifiers. As of Cycle-14, nitrite and nitrate consumption rates increased to 0.04 mmol/L.d and 0.14 mmol/L.d, respectively. In Cycle-15, biomass was transferred from the temporarily used reactor (Reactor E1-1 with 300 mL effective volume) to Reactor E1-2 with 2.0 L effective volume and the operation continued in this reactor. Upon transfer, it was observed that NO_2-N and NO_3-N removal rates sharply decreased to 0.03 and 0.012 mmol/L.d, respectively (Figure 4.10). In the temporary reactor (with 300 mL effective volume) VSS concentration was higher compared to the Reactor E1-2 (with 2.0 L effective volume) (Table 4.8). Therefore, a decrease in removal rates was associated with the 2.5-fold increase in the substrate to inoculum (S/I) ratio. Therefore, as of Cycle-20, the initial concentrations of NO_2-N and NO_3-N in the reactor were also reduced to 2 mg/L and 5 mg/L, respectively, to be gradually increased based on the removal rates (Figure 4.10). With the decrease in the initial concentration, nitrite and nitrate removal efficiency increased from 25% to 82% and 10% to 50% (Figure 4.11), however, no apparent increase was observed in the removal rates (Figure 4.10). Low removal rates were considered to be due to the decrease in the in-reactor concentrations of sCOD used in heterotrophic denitrification in the reactor or other electron donors (Fe, Mn, S, etc.) used in autotrophic denitrification. Therefore, a low trend in removal rates was observed between Cycle-20 and Cycle-43. As a matter of fact, in DAMO enrichment studies, Damo-Bacteria and Damo-Archaea activity are evidenced by an increasing trend following a decreasing trend of NO_2-N and NO_3-N removal rates (Hu et al., 2009; He et al., 2014; Fu et al., 2017; Li et al., 2018). This is due to the decrease in the activities of microorganisms involved in other processes competing with DAMO. In other words, following the

consumption of other electron donors, DAMO culture is expected to grow since dissolved methane becomes the only carbon source in the reactor. However, nitrite and nitrate removal rates from Cycle-20 to Cycle-43 has fluctuated between 0-0.04 mmol/L.d and 0.03-0.07 mmol/L.d, and no increasing trend was detected.

Re-inoculation

In order to increase the biomass concentration (11.3±3.0 g VSS/L)(Table 4.8) and DAMO activity, re-inoculation was performed with a mixture of FS and AD. The initial concentration of NO_3-N in the reactor, which was previously provided with an initial concentration of 5 mg/L NO_3-N, was started to be added as 15 mg/L (Cycle-43) in order to fasten the sCOD consumption. After re-inoculation, the TSS and VSS content increased to 21.5±1.1 g/L and 3.7±0.2 g/L, respectively. Following re-inoculation, NO_2-N removal efficiency suddenly increased ranging in 70-98% between Cycle 43-60, while NO_3-N removal efficiency approached almost 100% (Figure 4.11). Due to its consumption, the initial NO_3-N concentration was again increased to 20 mg/L (Cycle-47) (Figure 4.9). In the following cycles (until Cycle-138), the initial NO_2-N and NO_3-N concentrations were adjusted as 5 and 20 mg/L, respectively (Figure 4.9).

Table 4.8 Summary of solid analysis results for Enrichment-1 system

Parameter	**Cycle-1**	**Cycle-15**	**Cycle-43**	**Cycle-125**
Stage	Start-up	Up-scale	Re-inoculation	Down-scale
Total Volume	0.4 L	3 L	3 L	1.1 L
Effective Volume	0.3 L	2 L	2 L	0.8 L
Reactor	Reactor E1.2	Reactor E1.1	Reactor E1.1	Reactor E1.3
TSS (g/L)	48.1±0.7	11.3±1.3	21.5±1.1	69.1±0.8
VSS (g/L)	7.6±0.02	3.0±0.3	3.7±0.2	15.4±1.1
VSS/TSS (%)	15.6	26.5	17.2	22.3

Elemental analysis

After re-inoculation, the nitrite and nitrate removal rates were still high at Cycle-50 probably due to other denitrification mechanisms besides DAMO. At this period, elemental analysis (for electron donors commonly used in autotrophic denitrification: manganese, iron, and sulfur) was conducted for the sample taken from the reactor. It was previously reported that competition and cooperation between nitrogen cycling microorganisms and DAMO species can affect the relationships between *M. oxyfera* and *M. nitroreducens* (Xie et al., 2020). Therefore, the results were used to comment on the possible other mechanisms taking place in the enrichment culture which can also cause competition with DAMO microorganisms.

Elemental analyses results were evaluated based on manganese (Mn), iron (Fe) and sulfur (S) amounts in the reactor at the beginning of Cycle-50 and other presence of other electron donors used in autotrophic denitrification. A detailed discussion on potential reactions is given in Appendix J. Results indicated that one or more of the HS^-, $S_2O_3^{2-}$, SCN^- ions and sediment-derived pyrite (FeS_2) may be involved in autotrophic denitrification (Appendix J). In the metabolic reactions involving the afore-mentioned electron donors, SO_4 is produced theoretically. The initial and effluent SO_4 analyzes of Cycle-50 showed that there was a decrease in the sulfate instead of an increase in Cycle-50. However, in other cycles where SO_4 concentrations increased, it is possible to observe HS^-, $S_2O_3^{2-}$, SCN^-, FeS_2-related autotrophic denitrification. So, DAMO process seems to be effective in NO_x removal in Enrichment-1 system, at least during the cycles, where SO_4 was not produced.

Possible heterotrophic denitrification specific to Cycle-50 was also investigated. sCOD consumption was 4.8 mg/L. It is known that there is a total of 4.3 mg/L NO_2-N removal (7.4 mg/L sCOD equivalents, using Table 3.8 and 17.0 mg/L of NO_3-N removal (48.7 mg/L sCOD equivalents, using Table 3.8) in Cycle-50. For heterotrophic denitrification of nitrite and nitrate, a total of 55.9 mg/L sCOD is

required. Actual sCOD consumption is only 8.6% of the theoretical value needed for heterotrophic denitrification. In other words, it appears that 91.4% of the nitrogen content in Cycle-50 was also not removed by either heterotrophic denitrification. Moreover, both pyrite (FeS_2) oxidation and sulfur-driven autotrophic denitrification is reported as nitrate-dependent (Shao et al., 2010; Bosch et al., 2012). This might suggest that reduced forms of sulfur that can be found in the AD and sediment-derived pyrite (FeS_2) could cause a competition between Damo-Archaea until they are completely consumed in the enrichment culture.

There is an increase in the initial concentrations of NO_3-N and especially NO_2-N between Cycle-60 and 73 (Figure 4.9). This is due to a break in the nitrite and nitrate analysis conducted via IC. Since the analysis could not be performed due to a failure in IC, nitrite, and nitrate were added without the results of the effluent analysis, based on the amount added in the last cycle before the device malfunctioned. Therefore, theoretical and experimental concentrations are not consistent with each other and there is an accumulation of nitrite and nitrate between Cycle 60-73. After IC analyzes were restarted as of Cycle-74, the feeding was again carried out based on the effluent analysis, therefore the theoretical and experimental initial concentrations were close to each other.

The removal rate and removal efficiencies gradually decreased between Cycle 60-111. In order to follow the enrichment process of the culture at this stage, the first activity test (En1-AT1) of Enrichment-1 system was performed at Cycle 72 (day 247). The graphs showing the nitrite and nitrate trends during the activity test are presented in Appendix G (Figure G.1 and G.2). According to the results of this test, the NO_2-N and NO_3-N removal rates were found as 0.04 mmol/L.day (0.56 mg/L.day) and 0.06 mmol/L.day (0.84 mg/L.day), respectively. However, it was observed from the results of the control phase (without methane) that, apparent heterotrophic and autotrophic denitrification mechanisms were taking place in the reactor (Appendix G; Figure G.1 and G.2).

Table 4.9 Summary of activity test results for Enichment-1 system

Activity Tests	NO_2-N removal rate of Damo-Bacteria		NO_3-N removal rate of Damo-Archaea	
	mmol/L.d	µmol/d.g VSS[a]	mmol/L.d	µmol/d.g VSS[a]
En1-AT1	0.04	12.1	0.06	18.2
En1-AT2	0.12	18.8	0.04	6.3
En1-AT3	0.07	6.4	0.07	6.4

[a] Calculated using the results of solid (TSS and VSS) analysis performed for each activity test

A decrease in the removal rate and removal efficiency observed between Cycles 60-111 was associated with the decrease in other electron donors (sCOD, Fe, Mn, S, etc.) used in other denitrification processes besides DAMO. In previous DAMO enrichment studies, removal rates ranged between 0-0.1 mmol/L.day for NO_2-N and 0-0.5 mmol/L.day for NO_3-N before the expected increase was recorded (Ettwig et al., 2009; Hu et al., 2009; He et al., 2014; Hatamoto et al., 2014; Fu et al., 2017; Li et al. 2018). In Cycle-111, NO_2-N and NO_3-N removal rates decreased to approximately 0.001 mmol/L.day and 0.01 mmol/L.day (Day-395), respectively. Following this, as expected, NO_2-N and NO_3-N removal rates started to increase by Cycle-111 (Figure 4.10). Therefore, Cycle-111 was a critical turning point in the Enrichment-1 study.

Between Cycle-111 and Cycle-124, although there were fluctuations in the NO_2-N removal rate, an increasing trend was observed (Figure 4.10). The removal rate reached 0.58 mg/L.day (0.041 mmol/L.day) and the removal efficiency reached 45% on Cycle-124. At this stage of the enrichment process, the increase in NO_3-N removal performance was quite significant. The removal rate and removal efficiency were measured as 0.1 mg/L.day (0.01 mmol/L.day) and 2% at Cycle-111, reached to 1.4 mg/L.day (0.1 mmol/L.day) and 25% respectively, in Cycle-124. This increase showed that from re-inoculation (Cycle-43) to Cycle-111, other electron donors in the reactor were consumed, and, in turn, the activities of microorganisms involved in other denitrification processes competing with DAMO decreased. Therefore, NO_2-N and NO3-N consumption by Damo-Bacteria and

Damo-Archaea both started to increase following Cycle-111. Therefore, the second activity test (En1-AT2) was performed on Cycle-125 (Day-442). The graphs showing the nitrite and nitrate trends during the activity test are presented in Appendix G (Figure G.3 and G.4). According to the results of this test, the NO_2-N and NO_3-N removal rates were 1.68 mg/L.day (0.12 mmol/L.day) and 0.56 mg/L.day (0.04 mmol/L.day), respectively. The results were consistent with the removal rates obtained in the reactor at Cycle-124. The activity test also revealed the existence of other denitrification mechanisms; however, their effect was less than observed in the first activity test (En1-AT1).

In Enrichment-1, there are approximately 250 days between re-inoculation(Cycle-43) and the start of the activity increase (Cycle-111). This period is defined as the lag period and it can vary between 80 days (Li et al., 2018; Hatamoto et al., 2014; Fu et al., 2017) to 200 days (Ettwig et al., 2008; Hu et al., 2009). Therefore, the factors resulting in the low DAMO activity and slower enrichment in this study compared to other studies were evaluated. Consequently, this was attributed to the fact that the reactor is not mixed well enough in the orbital mixer (120 rpm). Therefore, it was hypothesized that the contact between the medium, biomass, and dissolved methane should be improved. In this context, it was decided to reduce the reactor size and change the method of mixing in Enrichment-1 system. To do this, culture was transferred to a smaller-sized reactor (Reactor E1-3) with a 0.8 L effective volume and this reactor was mixed via a magnetic stirrer instead of an orbital mixer. In this way, it was aimed to enrich the DAMO microorganisms faster by increasing the contact of DAMO microorganisms with the substrate.

Down-scaling

The down-scaling was carried out at Cycle-125 (Day 442). Due to the transfer of biomass to a smaller effective volume TSS and VSS contents increased to 69.1±0.8 and 15.4±1.1 g/L, respectively (Table 4.8). The initial concentrations of NO_2-N and NO_3-N were continued to be fed as 5 mg/L and 20 mg/L, respectively until Cycle-138 (Figure 4.9). After down-scaling, a temporary decrease was observed in the

NO_2-N removal rate until Cycle-130. Subsequently, the NO_2-N removal rate started to increase again and at Cycle-137 the removal efficiency was 100% (Figure 4.11), and the removal rate reached 1.9 mg/L (0.14 mmol/L.day) (Figure 4.10). The increase in NO_3-N removal, which started by Cycle-111, continued after down-scaling, and the removal efficiency at Cycle-137 was measured as 94% (Figure 4.11), and the removal rate was 4.9 mg/L.day (Figure 4.10).

Since the removal efficiency of both NO_2-N and NO_3-N at Cycle-137 (Day-480) is approximately 100%, the initial concentrations of both are increased by 1.5 times as of Cycle-138 to 7.5 mg/L and 30 mg/L, respectively (Figure 4.9). In Cycle-138 (First cycle using increased initial concentrations), the NO_3-N consumption efficiency reached 98% (Figure 4.11), and the removal rate reached 11.9 mg/L.day (Figure 4.10). On the contrary, the NO_2-N removal rate was measured as -2.74 mg/L.day, in other words, nitrite accumulated in the system (Figure 4.10). This indicated that a mechanism that causes nitrite production in the reactor occurred. Considering that nitrite and nitrate removal rates started to increase as of Cycle-111, this increase in nitrite production may indicate Damo-Archaea activity. Assuming that other electron donors in the reactor were completely consumed until the Cycle-111, it was thought that the Damo-Archaea, which is involved in the consumption of nitrate with increased initial concentration, may be better adapted to high initial concentrations applied. For NO_3-N, where the highest removal performance was observed at Cycle-138 (11.9 mg/L.d), the removal rate decreased in the next cycle, then continued to decrease fluctuating between Cycles-138 and 147. The average NO_3-N removal rate between Cycle-138 and Cycle-147 was 4.8 mg/L.d (Figure 4.10), and the average removal efficiency was 45% (Figure 4.11). On the contrary to nitrate, after the nitrite production observed at Cycle-138, the NO_2-N removal rate recovered and started to increase again, and the removal efficiency was 93% (Figure 4.11) and the removal rate was 2.29 mg/L.d (Figure 4.10) at Cycle-146. This removal performance observed for NO_2-N at Cycle-146 is the highest since the onset of activity increase at Cycle-111.

Competition for methane

The increase in nitrite removal rate and the simultaneous decrease observed in nitrate removal rates were associated with a competition between Damo-Bacteria and Damo-Archaea for dissolved methane. Although these two microorganisms live in syntrophy in nature (the nitrite produced by the archaea is consumed by the bacteria), it has been reported that the two microorganisms may compete for dissolved methane in the enrichment cultures (Guerrero-Cruz et al., 2019; Lu et al., 2019). Essentially, methane was added in excess for the enrichment of DAMO microorganisms at the beginning of a cycle. On the other hand, 0.43 mmol of NO_2-N and 1.71 mmol NO_3-N were present in the reactor at the beginning of a cycle between Cycle-138 and Cycle-146 which requires a total of 0.54 mmoles of methane for the removal of all nitrite and nitrate. Therefore, the total amount of methane provided at the beginning of a cycle (i.e 0.011 moles) is enough for the removal of all the nitrite and nitrate provided to the reactor. However, when nitrite and nitrate consumption rates increase, dissolved methane consumption also increases. Although methane, which is in the headspace is constantly dissolving in the liquid after the consumption of methane in liquid by DAMO activity, the amount of dissolved methane in the liquid part also decreases, as time progresses during one cycle. Therefore there is a possibility of competition between Damo-Bacteria and Damo-Archaea over dissolved methane. Since methane affinity of Damo-Archaea (0.5 mM) (Lu et al., 2019) is reported to be much lower than that of Damo-Bacteria (2.6 ± 0.7 μM) (Ding and Zheng, 2021), which explains the decreased nitrate removal rates.

Due to the increase in nitrite removal performance, it was decided to increase the initial concentration again. However, at this stage, it was thought that already declining Damo-Archaea activity might get worse with the nitrite increase since an increase in nitrite would cause an increase in the activity of Damo-Bacteria since the methane affinity of Damo-Archaea is lower than that of Damo- Bacteria. For this reason, it was decided to simultaneously increase the nitrate concentration which is used by Damo-Archaea as an electron acceptor in order to prevent the

already declining Damo-Archaea activity from being adversely affected by the competition with Damo-Bacteria. Therefore, at Cycle-147, the initial concentrations were increased by 1.3 times, and NO_2-N and NO_3-N were started to be fed as 10 mg/L and 40 mg/L, respectively (Figure 4.9).

With the increase in initial concentrations, removal efficiency and removal rate decreased for nitrite. Nitrate removal was not observed to be affected negatively or positively by the nitrite increase. After the decrease occurred at Cycle-147 in the removal rates, it was observed that nitrite removal stabilized at lower rates. Between Cycle-147 and Cycle-169, the average removal rate and removal efficiency for NO_2-N were measured as 0.97 mg/L.day and 33%, respectively (Figure 4.10 and Figure 4.11). In this period, NO_3-N was consumed with an average removal rate of 1.7 mg/L.day and average removal efficiency of 16% (Figure 4.10 and Figure 4.11). Therefore, Damo-Bacteria could not adapt to the high initial NO_2-N concentration (10 mg/L), and already declining Damo-Archaea activity was not recovered possibly due to nitrite inhibition.

Nitrite inhibition

It has been previously observed in the literature that nitrite causes a toxic effect on Damo-Bacteria at a concentration of 14 mg/L NO_2-N (He et al., 2014; Hu et al., 2011; Hatamoto et al., 2014). However, this level of nitrite did not inhibit the activities of *M. oxyfera* in other previous studies (Ettwig et al., 2009; Ettwig et al., 2010). Moreover, recently in a study investigating the effect of nitrite on both Damo-Bacteria and Damo-Archaea activity, 950 mg/L NO_2-N was reported to completely inhibit the activity in a short-term exposure and the nitrogen removal performance of DAMO co-culture was completely inhibited at concentrations of 650 mg/L NO_2-N in the long-term inhibition experiments (Lou et al., 2019). Therefore, the inhibitory effect of nitrite might depend on what extent has the culture has been enriched or the removal performance of the culture. Moreover, there might be indirect factors taking part in this inhibition such that Damo-Archaea is reported to transform 10% of the produced nitrite to ammonium,

preventing nitrite accumulation and the caused toxicity (Ettwig et al., 2016). Therefore, the reasons for the difference among observations concerning nitrite toxicity are unclear and require further investigation. In this study, between Cycle 147 and Cycle-169, nitrite concentration was 10 mg/L and it was lower than the lowest concentration reported for inhibition (14 mg/L). However, since the activity was slowly increasing and DAMO culture was not stable, nitrite toxicity is still a possibility. It should be noted that there are no previous studies on the toxic effect of nitrate. However, it is thought that overloading may have negatively affected both DAMO species in the culture.

After approximately 80 days of operation since the last increase of the initial concentrations (Cycle 147, Day-511), the third activity test (En1-AT3) was carried out at Cycle 169 (Day 592) (Figure 4.12). The graphs showing the nitrite and nitrate trends during the activity test are also presented in Appendix G (Figure G.5 and Figure G.6). According to the results of this test, the NO_2-N and NO_3-N removal rates were 0.98 mg/L.day (0.07 mmol/L.day) and 0.98 mg/L.day (0.07 mmol/L.day), respectively. It was observed compared to En1-AT2 that, Damo-Bacteria activity increased while Damo-Archaea activity slightly decreased. However, the activities obtained for 592 days of the operating period (by Cycle-169) were lower than those given in other enrichment studies (Table 4.1).

a) **b)**

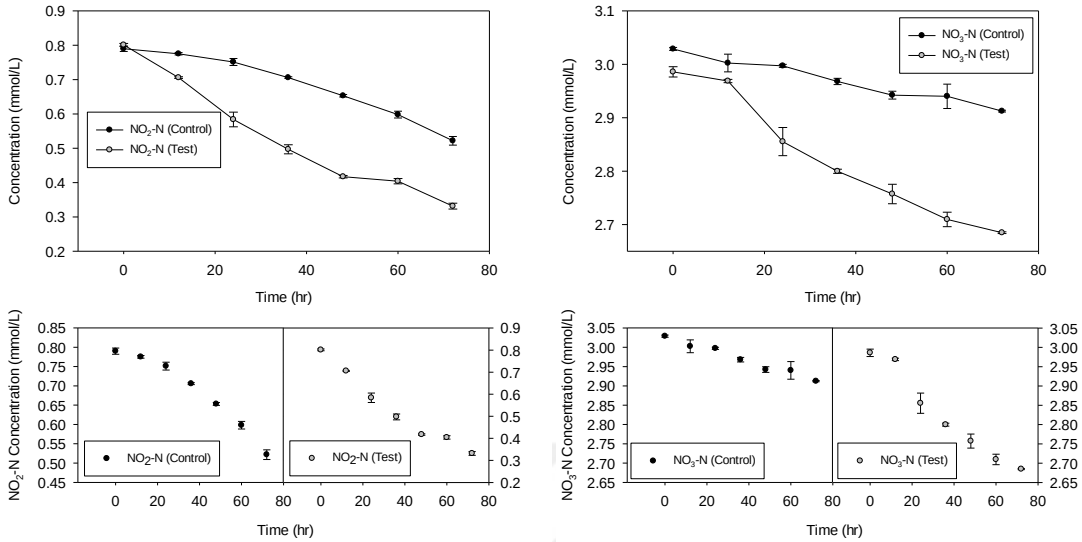

Figure 4.12 a) Nitrite trend observed in En1-AT3 and b) Nitrate trend observed in En1-AT3

Sulfate concentrations were followed (Appendix I) to monitor autotrophic denitrification with other electron donors. According to the elemental analysis results, these donors were speculated to be sulfur in the liquid phase and pyrite in the solid phase due to inoculum (Appendix J). It would be expected to observe a sulfate accumulation in the reactor due to autotrophic denitrification mechanisms via these electron donors. However, no obvious trend was observed to support the possibility of autotrophic denitrification. Therefore, nitrite and nitrate removal after the lag-phase (Cycle 43-111) was attributed to DAMO microorganisms.

4.3.1.2 Molecular identification of target species in Enrichment-1 culture

FISH analysis was used to investigate the relative abundance and compositional changes of targeted species such as *M. oxyfera*, *M. nitroreducens*, and NC10 Phylum bacteria in the total microbial population of Enrichment-1 culture. The relative % compositions of target species to total microbial population were

determined based on FISH analyses as shown Figure 4.13. Sample FISH images of Cycle-165 (the latest cycle FISH analysis was conducted) are shown in Figure 4.14. As seen in the Figure 4.13, general archaea % composition (64%) was higher than general bacteria % composition (36%) at the beginning of the enrichment (Cycle-10) probably due to high methanogenic archaea existed in the AD sludge. Then, it was observed that the composition of general archaea and *M. nitroreducens* decreased to 42% and 13%, respectively at Cycle-28 while *M. oxyfera* increased to 23% from 7% (Cycle-10). However, after the re-inoculation (Cycle-43), general archaea and *M.nitroreducens* increased again due to their high abundance in the inoculum (AD). It has been observed that starting with Cycle-100 (%27) there has been an increase in the composition of NC10 phylum, which consists of methane-oxidizing bacteria until Cycle-165 (40%). This increase was majorly parallel with the nitrite removal performance of the Enrichment-1 culture since, after Cycle-11, an increase in the nitrite reduction was detected which was associated with the enrichment of Damo-Bacteria. As mentioned before, after the first increase in the initial concentrations of nitrite and nitrate (Cycle-138), nitrite removal increased until the second increase in the initial concentrations (Cycle-147) while nitrate removal decreased after the first increase in the initial concentrations. It was thought that due to competition over methane, Damo-Archaea activity decreased after Cycle-138 which is also in line with the FISH analysis where there was a decrease observed in *M. nitroreducens* composition between Cycle-145(22%) and Cycle-165(11%). Although nitrite removal rate decreased after the second increase in the concentrations (Cycle 147), the %composition of NC10 continued to increase in the culture while the composition of *M.oxyfera* decreased. The reason behind the decrease in nitrite removal was associated with a possible nitrite inhibition (Cycle 147). It can be speculated that while *M.oxyfera* was more susceptible to nitrite inhibition, other NC10 phylum bacteria were not majorly affected.

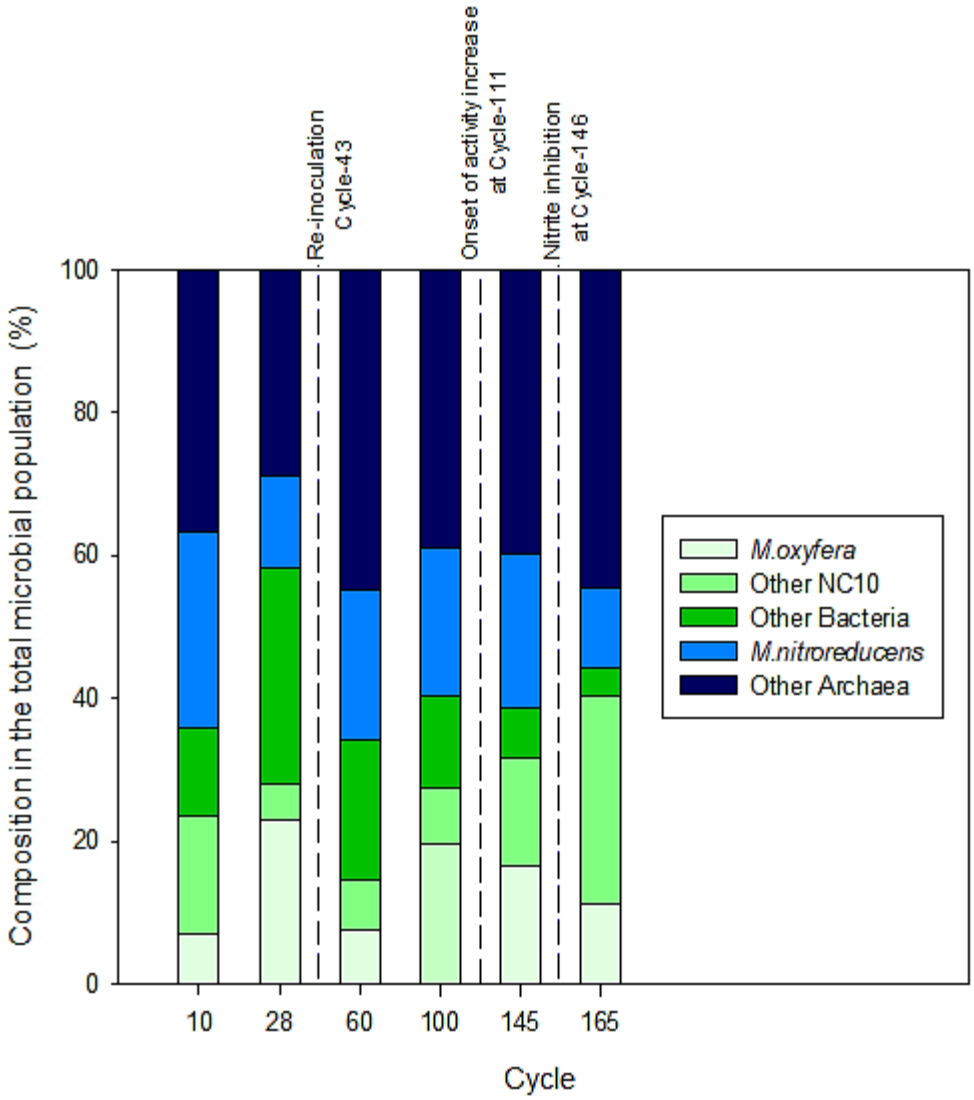

Figure 4.13 Compositions of target microorganisms in Enrichment-1 culture ("Other Bacteria" refers to bacteria composition in total microbial population excluding NC10 phylum bacteria; "Other NC10" refers to NC10 phylum bacteria composition in total microbial population excluding *M.Oxyfera* (Damo-Bacteria); "Other Archaea" refers to archaea composition in total microbial population excluding Damo-Archaea; Shades of green shows the total bacterial composition in the microbial population; Shades of blue shows the total archaeal composition in the microbial population, see Appendix D for the detailed method of calculation of each species)

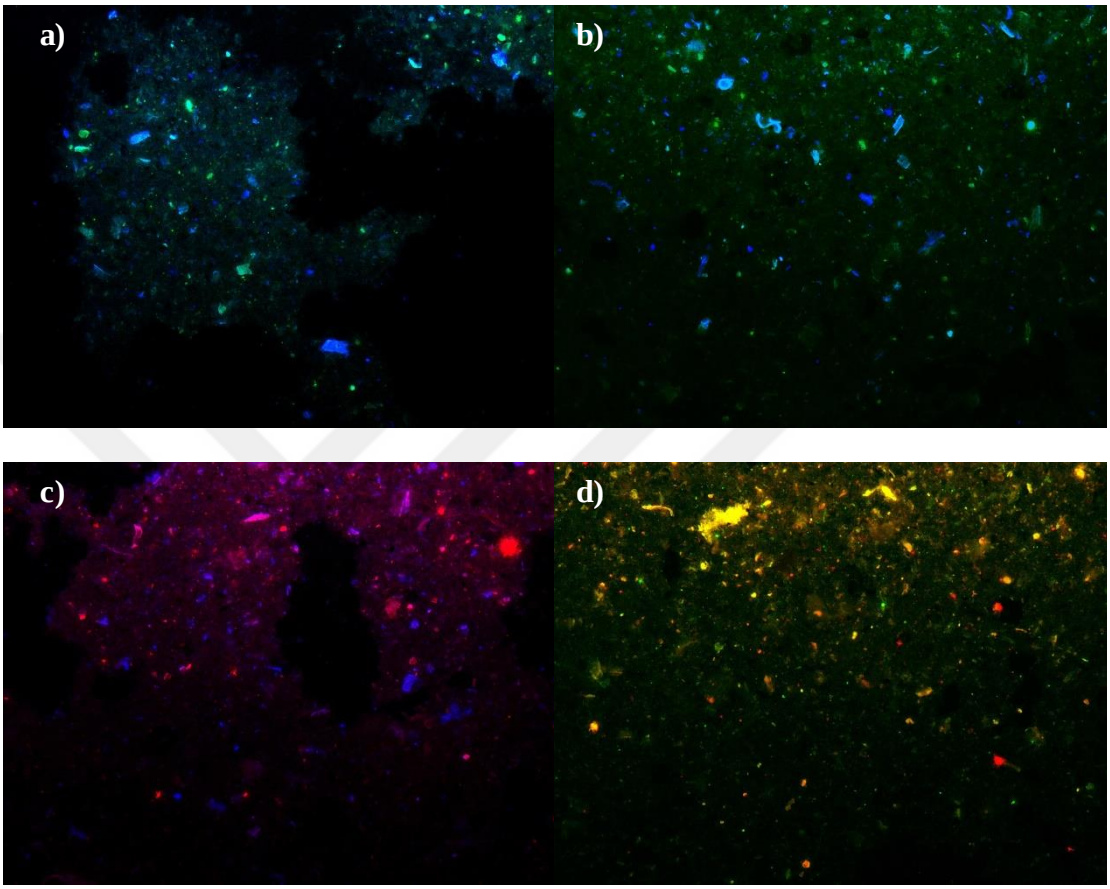

Figure 4.14 FISH images of the biomass taken on Cycle-165 a) Damo-Bacteria hybridized with DBACT-193 probe (Alexa Fluor 350, blue) and Damo-Archaea (*M. nitroreducens*) hybridized with DARCH-915 probe (GFP, green) b) Damo-Bacteria hybridized with DBACT-193 probe (Alexa Fluor 350, blue) and General Bacteria hybridized with EUBMix (GFP, green) c) Damo-Bacteria hybridized with DBACT-193 probe (Alexa Fluor 350, blue) and The NC10 phylum bacteria hybridized with NC10-1027 probe (Cy5, red), and d) Damo-Archaea (*M. nitroreducens*) hybridized with DARCH-915 probe (GFP, green)

4.3.2 Results of Enrichment-2 study

Enrichment-2 system was operated for 20 cycles (388 days) evaluated using reactor performance, activity tests, and FISH analyses conducted periodically for the system.

4.3.2.1 Performance of Enrichment-2 system

sCOD trends observed during the Enrichment-2 system are presented in Figure 4.15. Moreover, Figure 4.16 shows the pH trend and theoretical initial, experimental initial, and effluent NO_2-N and NO_3-N concentrations measured during the Enrichment-2 study. Finally, the change in NO_2-N and NO_3-N removal rates and removal efficiencies are shown in Figure 4.17.

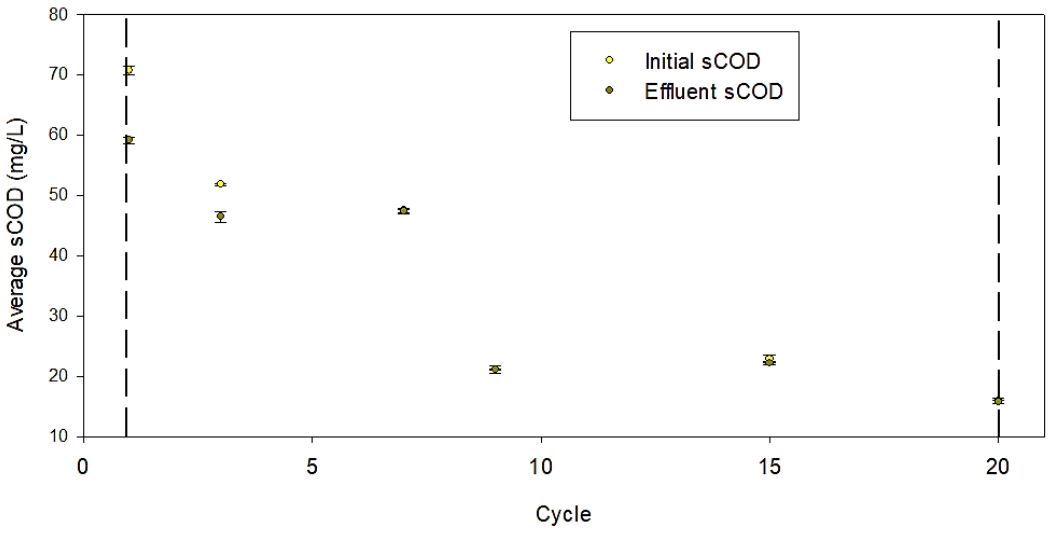

Figure 4.15 sCOD trend in Enrichment-2 system

Sludge used in the inoculation (even after washing) had a sCOD of 248.7±22.7 mg/L, so it was expected that heterotrophic denitrification would predominate at the beginning of the operation. In order to consume the organic carbon source in

the environment, a sufficient amount of nitrogen source must be available. Therefore, at the beginning of the enrichment process, NO_2 and NO_3 consumption, which is expected to occur due to heterotrophic denitrification, was followed. When one of the NO_2 or NO_3 in the reactor was depleted, settling and decanting periods were applied. Then, with a feeding period, a new cycle was started even though 30 days of cycle duration was not reached. In other words, at the beginning of the operation, the cycle time was determined according to the consumption of NO_2 and NO_3 in the reactor for the fast depletion of sCOD by heterotrophic denitrification. Following the depletion of sCOD (Figure 4.15) and the decrease in the activity of heterotrophic denitrifiers (after the first 9 cycles), Enrichment-2 system was started to be operated with a cycle time of 30 days (in 120-day HRT) as of Cycle-10. The latter sCOD analysis showed that sCOD was maintained in the reactor at concentrations between 15-22 mg/L until the end of the Enrichment-2 study indicating that after Cycle-9, heterotrophic denitrification was not occurring. This was also verified by pH analysis. The initial and effluent pH values during a cycle were examined. The big difference of (0.8 pH unit) observed between the initial and final pH values in the first cycles of the operation may have resulted from heterotrophic denitrification due to the high amount of electron donor existence (sCOD). However, as of Cycle-7, with the depletion of sCOD the initial and effluent pH values got closer. This was due to the decrease in heterotrophic denitrification activity. It should be noted that the reactor was also purged with a mixture of 95% CH_4 and 5% CO_2 at 2-3 day intervals throughout each cycle (Fu et al., 2017; Li et al., 2018) to increase the dissolved CH_4 in the liquid which simultaneously increases CO_2 concentration in the reactor and lower the pH. Therefore, considering that the pH would decrease as a result of regular purging applied, the reactor was operated with an initial pH of 7.5-7.8 through the rest of the operation (Cycle-8 to Cycle-20).

Using the sCOD measured in the reactor, the nitrogen expected to be removed with sCOD removal (45.7 mg/L) between Cycle-2 and Cycle-10 was calculated using Table 3.8 (Chapter 3, Section 3.3.3) If sCOD was used in the removal of nitrite (i.e

maximum consumption), the theoretical NO_2-N to be consumed is calculated as 26.7 mg/L. However, between Cycle-2 and Cycle-10, a total of 693.0 mg/L nitrogen was consumed, consisting of 102.2 mg/L NO_2-N and 590.7 mg/L NO_3-N. This indicates that the consumption of all nitrite and nitrate was not only via heterotrophic denitrification. In other words, nitrite and nitrate were removed using other electron donors, Possibly CH_4 was used as an electron donor via DAMO process.

The increase in the initial concentrations of NO_2-N and NO_3-N between Cycle-2 and Cycle-4 (Figure 4.16) was due to the failure of the IC device. In this period, NO_2-N and NO_3-N in the effluent could not be analyzed. Therefore, NO_2-N and NO_3-N were added based on Cycle-1, and this caused accumulation in the reactor. As of Cycle-4, the initial concentrations started to decrease and approached theoretical initial concentrations of 10 mg/L NO_2-N and 50 mg/L NO_3-N.

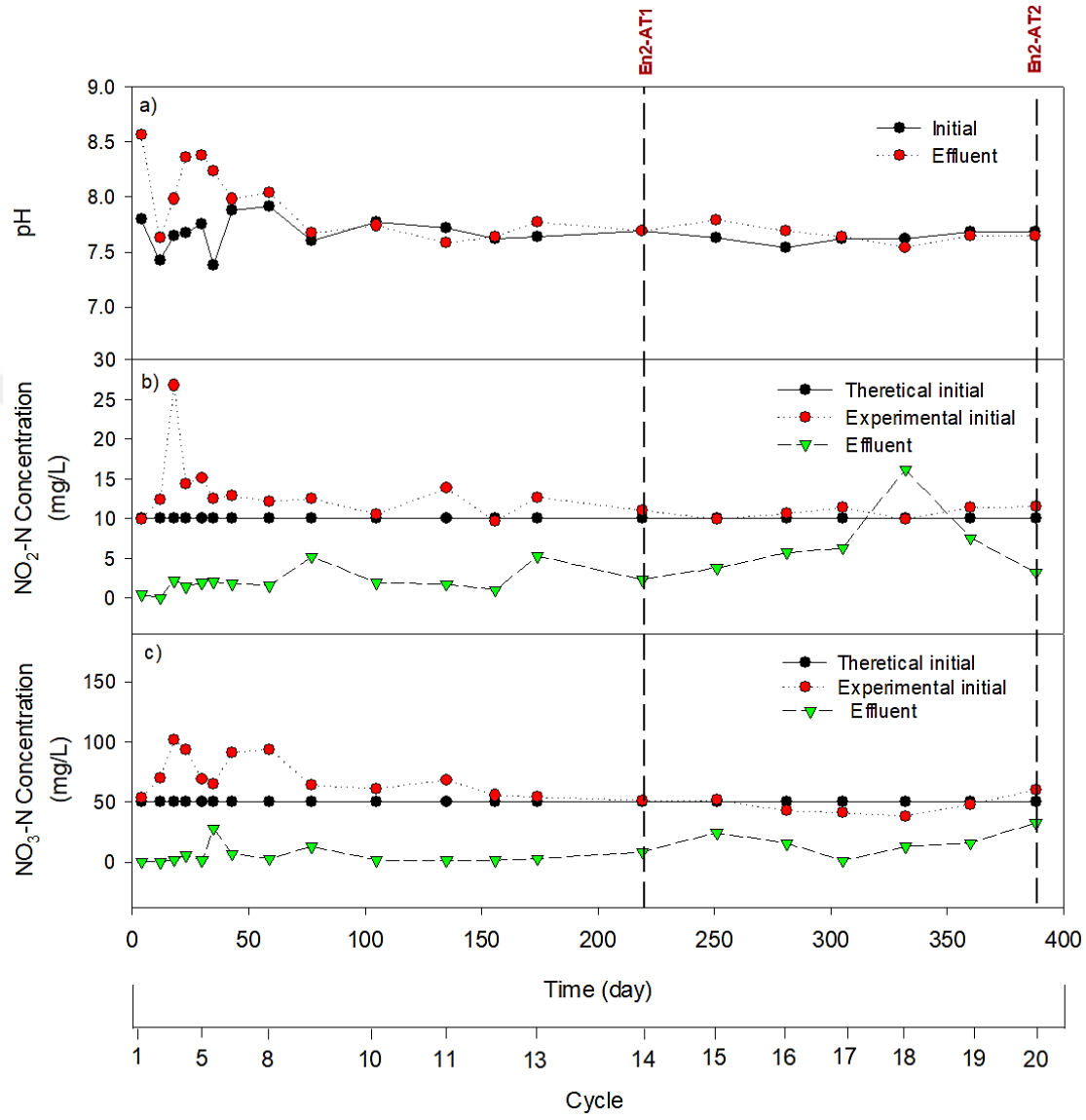

Figure 4.16 Theoretical initial, experimental initial and effluent concentrations of a) NO_2-N and b) NO_3-N in Enrichment-2 system

The NO_2-N and NO_3-N removal efficiencies were calculated using initial and effluent concentrations and are shown based on the consumption at the end of a cycle (Figure 4.17). On the other hand, in order to follow the possible change in removal rate in one cycle (long-lasting cycles) (for example, possible nitrite increase or activity increase), the change in nitrite and nitrate concentrations and even the removal rates were monitored by taking samples and nitrite and nitrate analysis at certain intervals throughout the cycle. As expected, the removal rates calculated within one cycle decrease as the concentration decreases. The removal rates shown in Figure 4.17a and Figure 4.17b were calculated according to the initial slope of nitrite and nitrate concentration graphs which showed a linear trend (linear trend: $R^2 > 0.90$).

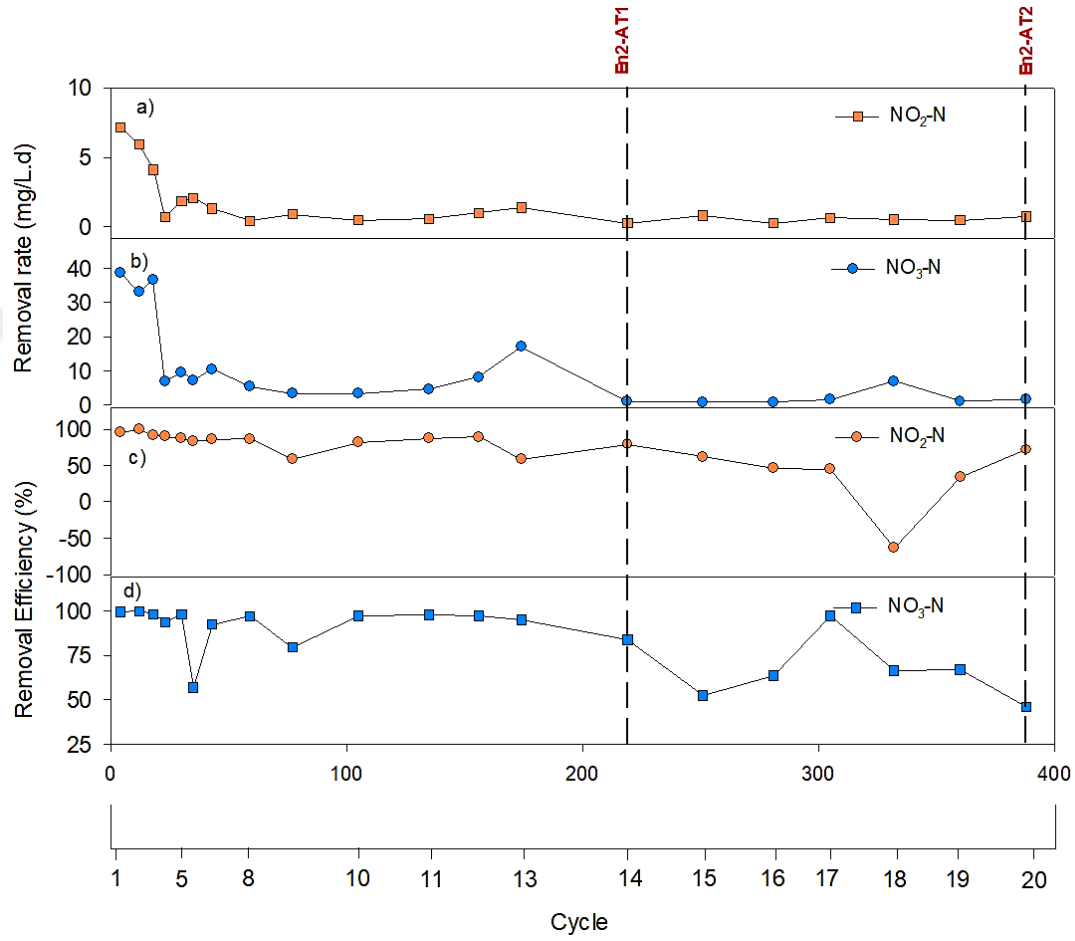

Figure 4.17 Removal rates of a) NO_2-N and b) NO_3-N, and removal efficiencies of c) NO_2-N and d) NO_3-N in Enrichment-2 system

It was observed that the NO_2-N removal rate (4-7 mg/L.day) of the first 3 cycles (total of 17 days) was higher than the removal rates in the following cycles (Figure 4.17a and b). This was due to heterotrophic denitrification using as mentioned above. The NO_2-N removal rate decreased at Cycle-4 (0.72 mg/L.day) due to the decrease in the concentration of the organic carbon involved in the removal of nitrite/nitrate in the reactor. Afterward, a slight increase in removal rates (1.32-2.08 mg/L.day) was observed between Cycle-4 and Cycle-7, which was associated with the adaptation of microorganisms present in the inoculum to temperature and operating conditions. It was observed that the NO_2-N removal rate, which decreased to 0.43 mg/L.day at Cycle-8, fluctuated for a while and then increased to 1.40 mg/L.day at Cycle-13. NO_3-N removal was recorded at much higher rates than nitrite (Figure 4.17). Nitrate removal rate ranged from 33-39 mg/L.day in the first 3 cycles (first 17 days). In the following cycles, similar to the trend observed in nitrite removal rates, as the heterotrophic denitrification decreased, the nitrate removal rate also decreased. Between Cycle-4 and Cycle-5, the nitrate removal rate was between 6.86-10.48 mg/L.day. It then decreased to 5.32 mg/L.day at Cycle-8. Similar to the NO_2-N removal efficiency, it increased again at Cycle-12 and Cycle-13 and reached 17.03 mg/L.day at Cycle-13. Since nitrate was consumed within 18 days in Cycle 13, a new cycle was started before the 30-day cycle period was completed.

In addition to the increase in nitrite and nitrate removal performance, when the concentration trends in the Cycle-9 are examined, there is an increase in nitrite concentration while nitrate concentration decreases in parallel. This situation in nitrite continued for most of the analyses at Cycles 11, 12, and 13. This observation may be due to the activity of Damo-Archaea, which converts nitrate to nitrite. In order to understand the role of Damo-Archaea and to observe the growth of Damo-Bacteria and Damo-Archaea separately, the first activity test (En2-AT1) was performed for Enricment-2 cultures at the end of the Cycle-13 (Day-174) (Figure 4.18). According to the results of this test, average NO_2-N and NO_3-N removal rates were 0.84 mg/L.day (0.06 mmol/L.day) and 0.28 mg/L.day (0.02

mmol/L.day), respectively. The NO_2-N and NO_3-N removal rates obtained in the reactor in Cycle-13 were 1.40 mg/L.day (0.1 mmol/L.day) and 17.03 mg/L.day (1.22 mmol/L.day), respectively. In addition, the activity test results point out that other heterotrophic and autotrophic denitrification mechanisms still taking place in the reactor (Figure 4.18). The graphs showing the nitrite and nitrate trends during the activity test are also presented in Appendix G (Figure G.7 and G.8)

a) b)

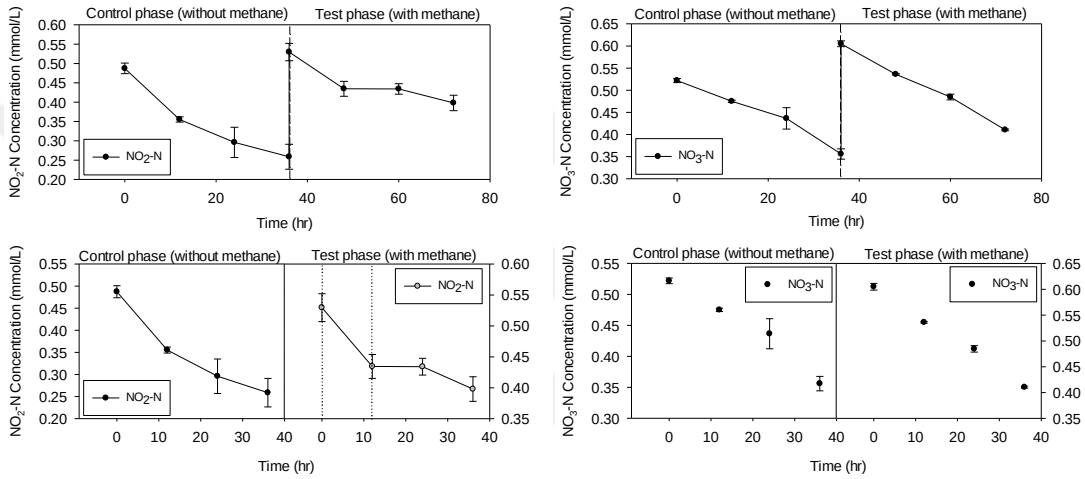

Figure 4.18 a) Nitrite trend observed in En2-AT1 and b) Nitrate trend observed in En2-AT1

In Cycle-14, both NO_2-N and NO_3-N removal rates decreased, respectively, to 0.27 mg/L.day and 1.0 mg/L.day. This may be due to the removal of microbial sludge (80 mL) from the reactor at the end of Cycle-13 to be used in the activity test. Biomass taken from the reactor was re-added to the system on the 6th operating day of Cycle-14 (after the end of the activity test). Cycle-14 was terminated at the end of the 45 days since neither nitrite nor nitrate was consumed at the end of 30 days. No significant increase or decrease in NO_2-N and NO_3-N removal rates was observed between cycles 14 and 20, and the average NO_2-N and NO_3-N removal rates were 0.54 mg/L.d and 2.01 mg/L.d, respectively.

As seen in Figure 4.17, the removal efficiencies were high as expected where heterotrophic denitrification was speculated to be dominant. NO_2-N and NO_3-N were removed by 86% and 92% on average within cycles 1-13. Both nitrite and nitrate removal efficiencies decreased after Cycle-13 in parallel with the decrease in the removal rates. The average NO_2-N removal efficiency of 39% and NO_3-N removal efficiency of 68% were observed between Cycle-13 and Cycle-20. The reason for the decrease in the high removal efficiencies (%) observed until Cycle-13 was attributed to the change in the population dynamics and the enrichment of the target microorganisms as a result of the decrease in the concentrations of electron donors used in heterotrophic and autotrophic denitrification in the reactor. Yet, while the heterotrophic denitrification activity is decreasing, the DAMO activity may be increasing. Therefore, to understand the contribution of Damo-Archaea and Damo-Bacteria to nitrite and nitrate removal, the second activity test (En2-AT2) was performed at the end of Cycle-20. The graphs showing the nitrite and nitrate trends during the activity test are presented in Appendix G. According to the results of this test, the NO_2-N and NO_3-N removal rates of Damo-Bacteria and Damo-Archaea were 1.68 mg/L.day (0.12 mmol/L.day) and 0.98 mg/L.day (0.06 mmol/L.day). Compared to the results of En1-AT1, both Damo-Bacteria and Damo-Archaea activity increased (Table 4.10). It was previously reported that nitrate removal is the rate-limiting step in the combined cultures of Damo-Bacteria and Damo-Archaea (Li et al., 2018). The nitrite removal rate is previously observed to be 2 times higher than the nitrate removal rate, and the enrichment of Damo-Archaea is more difficult than that of Damo-Bacteria (Hu et al., 2009; Hu et al., 2011; Fu et al., 2017). Accordingly, Enrichment-2, Damo-Bacteria activity was 2 times higher than that of Damo-Archaea by Cycle-20 (Day-388). It should be noted that despite the higher activities of Enrichment-2 culture compared to Enrichment-1 culture, the activities obtained at the end of the Cycle-20 were lower than those obtained in the literature (2-40 mg/L.d NO_2-N and 2-40 mg/L.d NO_3-N)(Table 4.1).

Table 4.10 Summary of activity test results for Enichment-2 system

Activity Tests	NO_2-N removal rate of Damo-Bacteria		NO_3-N removal rate of Damo-Archaea	
	mmol/L.d	µmol/d.g VSS[a]	mmol/L.d	µmol/d.g VSS[a]
En2-AT1	0.06	11.8	0.02	3.9
En2-AT2	0.12	21.8	0.06	10.9

[a] Calculated using the results of solid (TSS and VSS) analysis performed for each activity test

The results of the solid analysis performed during the enrichment study are presented in Table 4.11. Compared to Cycle-1, it was observed that VSS/TSS(%) content in the reactor has doubled although TSS content decreased due to the washout. However, although the activity of both Damo-Bacteria and Damo-Archaea increased from En2-AT1(Cycle-13) to En2-AT2(Cycle-20) (Table 4.10), a decrease in VSS/TSS(%) ratio was observed at Cycle-20, which can be explained by the death of other microorganisms than DAMO.

Table 4.11 Summary of solid analysis results for Enichment-2 system

Parameter	Cycle-1	Cycle-15	Cycle-20
TSS (g/L)	134.9±12.4	88.2±0.1	64.4±2.9
VSS (g/L)	9.5±1.2	13.8±0.2	6.6±0.3
VSS/TSS (%)	7.0	15.6	10.3

Sulfate concentrations were followed (Appendix İ) to monitor autotrophic denitrification with other electron donors (maybe sulfur in the liquid phase and pyrite in the solid phase due to inoculum based on the elemental analysis results in Enrichment-1) and no obvious trend was observed to support the possibility of autotrophic denitrification.

4.3.2.2 Molecular identification of target species in Enrichment-2 culture

The relative compositions of target species to total microbial population determined based on FISH analyses as shown Figure 4.18. Sample FISH images of Cycle-20 (the latest cycle FISH analysis was conducted) are shown in Figure 4.19. As seen in the Figure 4.19, general archaea (59%) was higher in abundance compared to general bacteria (41%) at the beginning of the enrichment (Cycle-3) due to the methanogenic archaea content of AD sludge used in the inoculation. It was observed that the composition of general archaea and *M. nitroreducens* decreased until Cycle-10 and it was 35% by Cycle-10 while *M. oxyfera* started to increase in the culture from 6% at Cycle-3 to 22% at Cycle-10. Starting with Cycle-10 until the end of the operation, an increasing trend was observed in NC10 phylum bacteria which were 50% of the total microbial population at Cycle-20, while *M. Oyfera* remained the same (16-17%). Moreover, *Nitroreducens* did not show any increasing or decreasing trend in the FISH analysis while general archaeal composition in the culture decreased. Thus, FISH analyses revealed the enrichment of NC10 Phlym bacteria in Enrichment-2 study supporting higher Damo-Bacteria activity in the activity tests compared to Damo-Archaea.

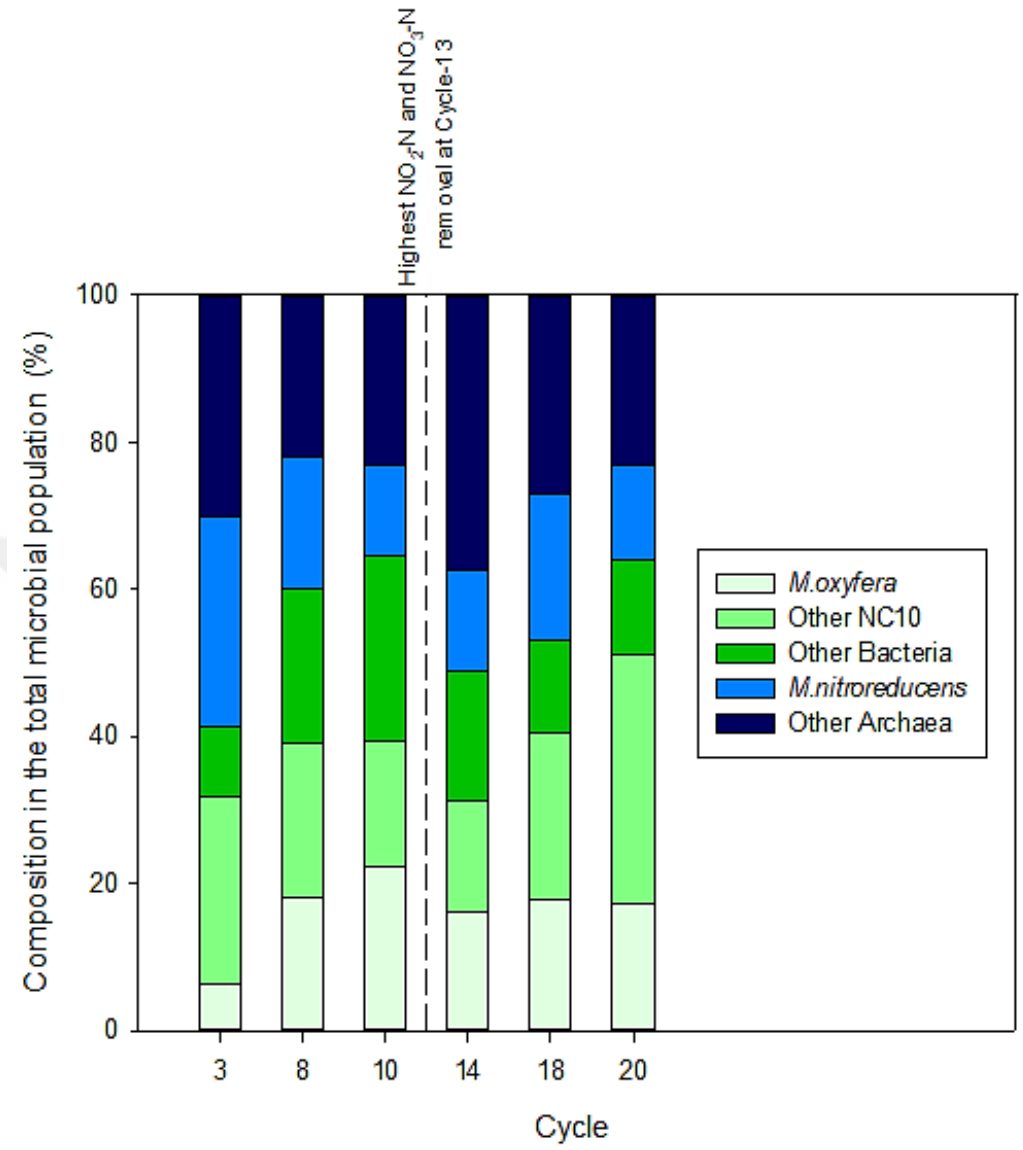

Figure 4.19 Compositions of target microorganisms in Enrichment-2 culture ("Other Bacteria" refers to bacteria composition in total microbial population excluding NC10 phylum bacteria; "Other NC10" refers to NC10 phylum bacteria composition in total microbial population excluding M.oxyfera (Damo-Bacteria); "Other Archaea" refers to archaea composition in total microbial population excluding Damo-Archaea; Shades of green shows the total bacterial composition in the microbial population; Shades of blue shows the total archaeal composition in the microbial population, see Appendix D for the detailed method of calculation of each species)

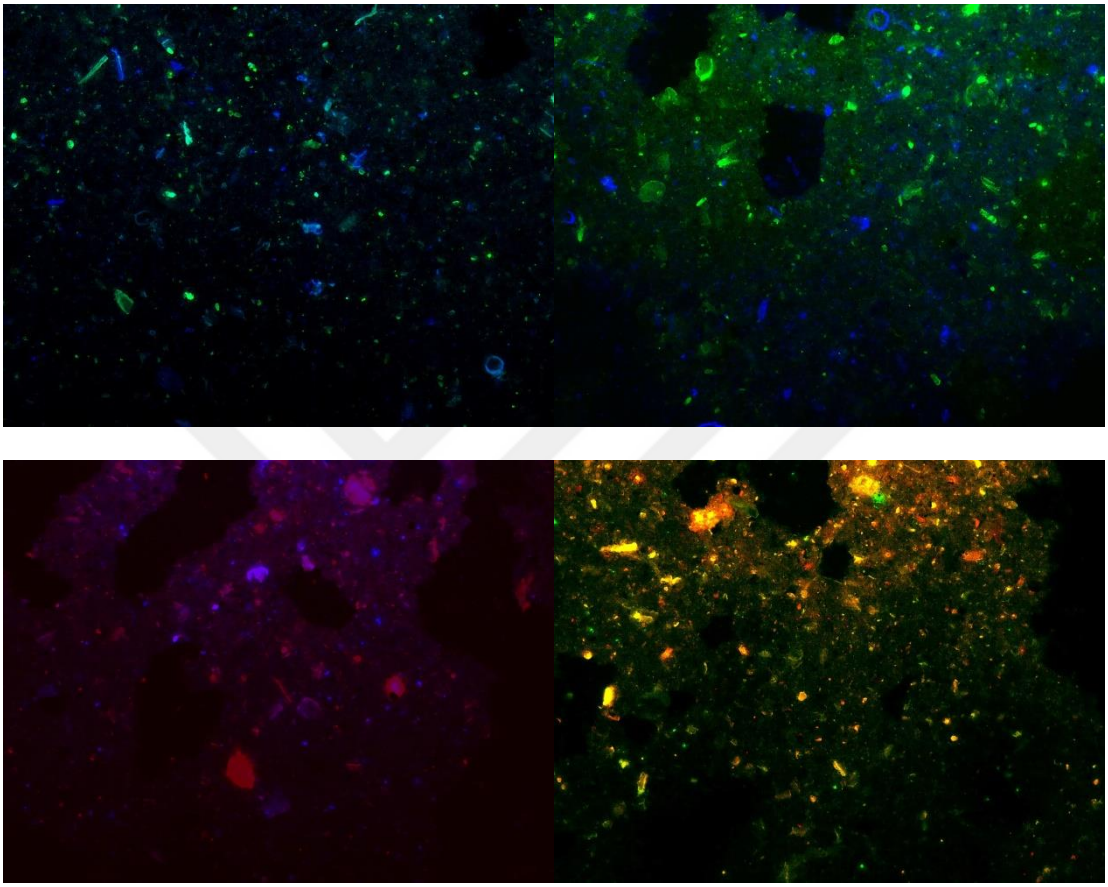

Figure 4.20 FISH images of the biomass taken on Cycle-20 a) Damo-Bacteria hybridized with DBACT-193 probe (Alexa Fluor 350, blue) and Damo-Archaea (*M. nitroreducens*) hybridized with DARCH-915 probe (GFP, green) b) Damo-Bacteria hybridized with DBACT-193 probe (Alexa Fluor 350, blue) and General Bacteria hybridized with EUBMix (GFP, green) c) Damo-Bacteria hybridized with DBACT-193 probe (Alexa Fluor 350, blue) and The NC10 phylum bacteria hybridized with NC10-1027 probe (Cy5, red), and d) Damo-Archaea (*M. nitroreducens*) hybridized with DARCH-915 probe (GFP, green)

4.3.3 Effect of GAC on Enrichment-1 and Enrichment-2 cultures

GAC was added to Enrichment-1 and Enrichment-2 cultures at the end of 592 (Cycle-169) and 388 days (Cycle-20) of operation, respectively. The results were evaluated based on the reactor performance (removal rates of nitrite and nitrate) and activity tests which were conducted before and after GAC addition (En1-GAC and En2-GAC). The graphs showing the reactor performance based on nitrite and nitrate removal rates are presented for Enrichment-1 and Enrichment-2 cultures in Table 4.12 and Table 4.13, respectively. Moreover, a comparison of Damo-Bacteria and Damo-Archaea activity observed in the activity tests before and after GAC addition for Enrichment-1 and Enrichment-2 cultures are given in Figure 4.20 and Figure 4.21, respectively. The graphs showing the nitrite and nitrate trends in En1-GAC and En2-GAC are also presented in Appendix G (Figure G.11 and Figure G.12)

Enrichment-1

It can be seen from Table 4.12 that, the average NO_2-N removal rate has doubled from 0.97 mg/L.d to 1.94 mg/L at the end of 30 days of operation after GAC addition. This increase was also observed in the activity tests (Figure 4.20). In Figure 4.20, it can be seen that the increase in Damo-Bacteria activity at the end of 30 days operation after GAC addition was even higher than the increase recorded between activity tests En1-AT1 and En1-AT3 conducted during Enrichment-1. This period corresponds to 345 days of operation. Therefore, the positive effect of GAC was quite observable in Damo-Bacteria activity.

Interestingly, there has been a decrease in nitrate removal rate. Prior to GAC addition, methane competition between Damo-Archaea and Damo-Bacteria was questioned for the culture in Enrichment-1 resulting in the Damo-Archaea being out-competed by Damo-Bacteria. Therefore, the decrease in Damo-Archaea activity coupling with the increase in Damo-Bacteria activity suggests that, although GAC addition may have helped the availability of dissolved methane and

improved the contact of biomass with dissolved methane, Damo-Bacteria benefited from GAC addition more than Damo-Archaea due to its higher affinity for methane (Ding et al., 2021). Moreover, it can be said that the conductivity of methane, which was hypothesized to contribute to the interspecies electron transfer, was overshadowed by the methane limitation and already existing competition between DAMO species.

Table 4.12 Effect of GAC on the performance of Enrichment-1 system

Cycle No	NO_2-N[a]		NO_3-N[a]	
	Average Removal Efficiency (%)	**Average Removal Rate (mg/L.d)**	**Average Removal Efficiency (%)**	**Average Removal Rate (mg/L.d)**
147-169	Before GAC Addition to Enrichment-1			
	32.99±7.28	0.97±0.26	16.18±5.40	1.70±0.57
170-179	After GAC Addition to Enrichment-1			
	53.30±10.74	1.94±0.34	7.76±7.13	1.14±0.54

[a] NO_2-N and NO_3-N initial theoretical concentration in Enrichment-1 was 10 mg/L and 40 mg/L for the data covering before and after GAC addition

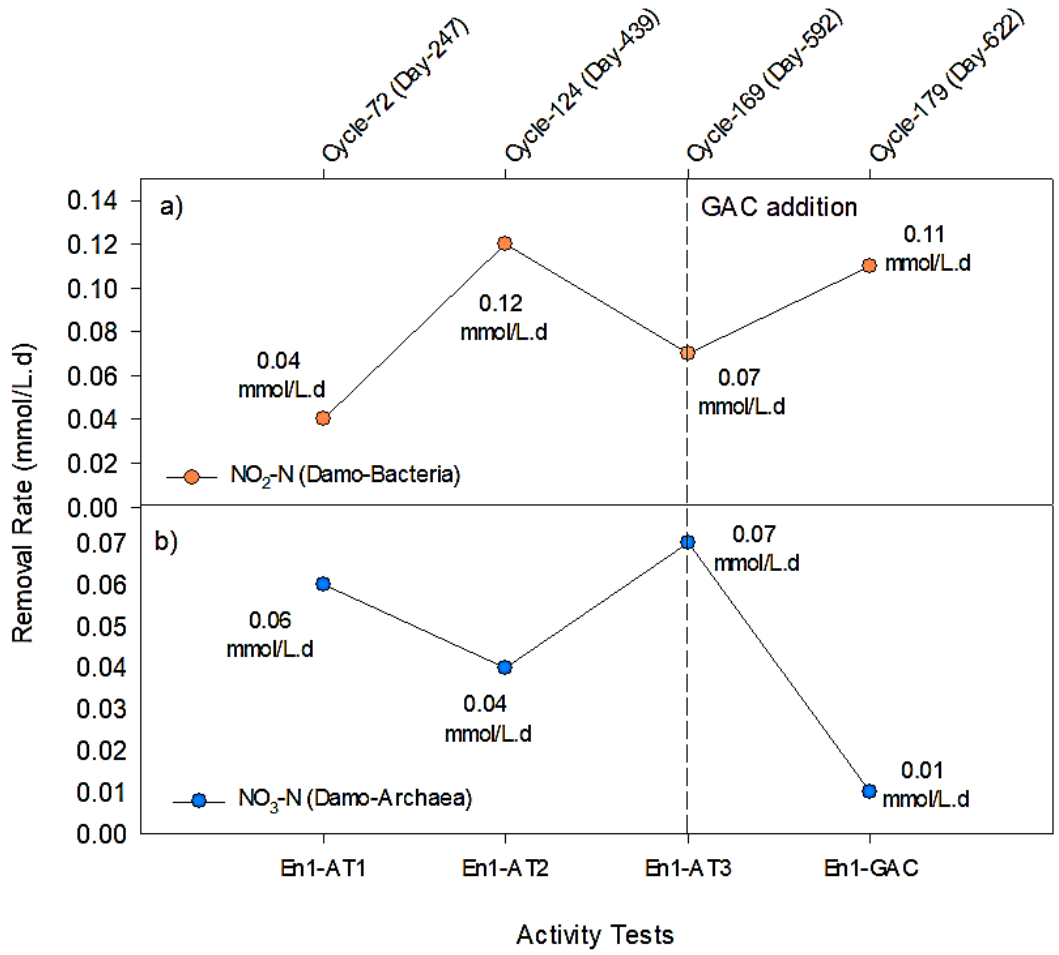

Figure 4.21 Damo-Bacteria and Damo-Archaea activities observed in the activity tests before and after GAC addition in Enrichment-1

Enrichment-2

It can be seen from Table 4.13 that, a slight reduction was observed in the removal rates in Enrichment-2 for both NO_2-N and NO_3-N removal after GAC addition. However, activity test comparison showed that both Damo-Archaea and Damo-Bacteria activity was improved after the GAC addition (Figure 4.21). Similar to Enrichment-1, Damo-Bacteria activity, at the end of 30 days operation after GAC addition, was even very close to the increase observed between activity tests En2-AT1 and En2-AT2. This period corresponds to 284 days of operation, much higher than the operation under GAC conditions. The Damo-Bacteria activity increased from 0.04 to 0.12 mmol/L.d in 248 days, and then to 0.21 after GAC addition. Application of GAC decreased the time required by enrichment by 3-fold. Similarly, Damo-Archaea, which maintained a low activity during Enrichment-2, was observed to have much higher activity after GAC addition. Its activity, which increased to 0.06 mmol/L.d from 0.02 mmol/L.d through 248 days, almost doubled (0.13 mmol/L.d) after GAC addition only in 30 days. It was discussed before that, methane availability is a factor in the enrichment of DAMO species which might have caused the low activities of Damo-Archaea. However, since this reactor was purged with methane every 2-3 days during the operation, it can be expected that the availability of dissolved methane was higher in Enrichment-2 compared to Enrichment-1. Therefore, the porous structure and conductivity of GAC may have resulted in an enhanced microbial activity by absorption of methane and adsorption of biomass in addition to the improved microbial electron transfer.

Table 4.13 Effect of GAC on the performance of Enrichment-2 system

Cycle No	Day	NO_2-N*				NO_3-N*			
		Removal Efficiency (%)	Average Removal Efficiency (%)	Removal Rate (mg/L.d)	Average Removal Rate (mg/L.d)	Removal Efficiency (%)	Average Removal Efficiency (%)	Removal Rate (mg/L.d)	Average Removal Rate (mg/L.d)
Before GAC addition to Enricment-2									
19	360	33.86	52.82	0.48	0.61	66.99	56.48	1.15	1.40
20	388	71.78		0.74		45.97		1.64	
After GAC addition to Enricment-2									
21	403	73.44	74.85	0.65	0.54	20.80	20.32	1.24	1.08
22	418	76.27		0.43		19.84		0.92	

* NO_2-N and NO_3-N initial theoretical concentration in Enrichment-2 was 10 mg/L and 50 mg/L for the data covering before and after GAC addition

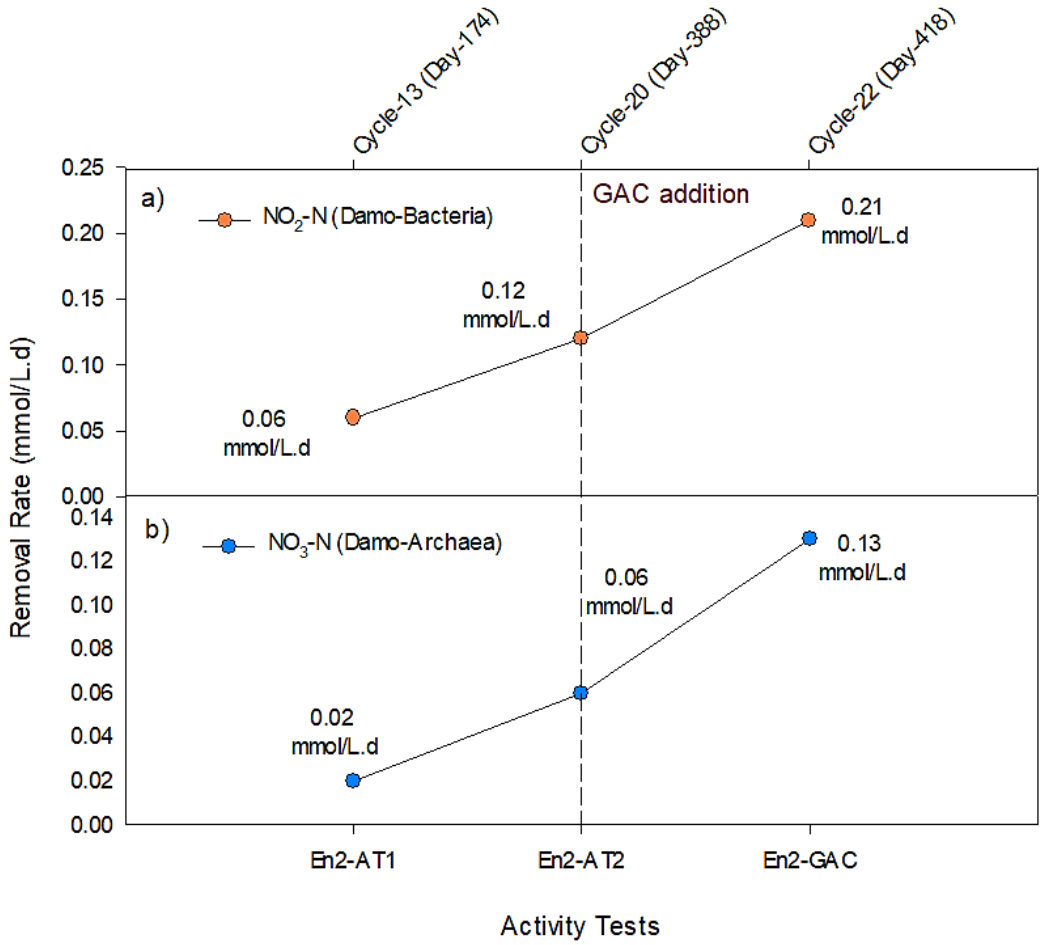

Figure 4.22 Damo-Bacteria and Damo-Archaea activity observed in the activity tests before and after GAC addition in Enrichment-2

4.3.4 Comparison of Enrichment-1 and Enrichment-2 systems

As discussed before (Section 4.3.1 and 4.3.2), the enrichment cultures cultivated in this study showed very low nitrite and nitrate removal activity although the molecular evidence supported their presence in the cultures. Previously in DAMO enrichment studies using SBR, nitrite removal rates were reported as 2-40 mg N/L.d and nitrate removal rates were between 2-40 mg N/L.d for DAMO microorganisms (Table 4.1). In this study, maximum nitrite and nitrate removal rates, since the onset of activity increase at Cycle-111, were estimated as 2.29 mg NO_2-N/L.d and 11.9 mg NO_3-N/L.d in Enrichment-1. In Enrichment-2, after the first ten cycles where heterotrophic denitrification was detected, maximum nitrite and nitrate removal rates were estimated as 1.40 mg NO_2-N/L.d and 17.03 mg NO_3-N/L.d. On the other hand, according to the activity test results, the highest removal rate observed for NO_2-N by Damo-Bacteria was 1.68 mg/L.d for both Enrichment-1 (En1-AT2) and Enrichment-2 (En2-AT3). The highest removal rate of NO_3-N by Damo-Archaea was 0.98 mg/L.d in Enrichment-1 (En1-AT3) and 0.84 mg/L.d in Enrichment-2 (En2-AT2). Despite the low removal rates, activity test results for Enrichment-2 system showed an increasing trend in the activity of both DAMO species. FISH results also revealed an increase in NC10 phylum bacteria in the enrichment culture, although no increase was detected for *M.nitroreducens*. On the other hand, despite the strategies applied to improve the activities in Enrichment-1 system, activity increase was detected at Cycle-111 corresponding to 247 days of lag period after re-inoculation (Cycle-43).

According to the activity test results of Enrichment-1 system, it was observed that Damo-Bacteria activity increased 3-fold between the En1-AT1 and En1-AT2. This period corresponded to 192 days. Then, a loss of activity was observed, which was attributed to increasing nitrite initial concentrations. In Enrichment-2 system, it is seen that the activity doubled in the 214 days between the En2-AT1 and En2-AT2 activity tests. As a result of this comparison, it was seen that there was a period in

which the increase of Damo-Bacteria was faster in Enrichment-1 system than that of Enrichment-2 system. However, the inhibition observed when the initial NO_2-N concentration was increased to 10 mg/L was unexpected since an increasing trend in Damo-Bacteria activity was observed in Enrichment-2 system, which was operated with an initial concentration of 10 mg/L. To investigate the reason for this difference, the substrate/inoculum (S/I) ratio was compared for the two reactors. In Enrichment-1 system, at Cycle-147 where NO_2-N concentration started to be fed as 10 mg/L, S/I ratio was calculated as 0.0015 g NO_2-N/g VSS. On the other hand, at the beginning of the Enrichmenr-2, where NO_2-N concentration started to be fed as 10 mg/L, the S/I ratio was calculated as 0.001 g NO_2-N/g VSS. Accordingly, inhibition might be prevented in Enrichment-2 system due to the lower S/I ratio. Nevertheless, in the literature, nitrite toxicity is not yet correlated with biomass concentration, and the effect of S/I is unknown. However, this might be the reason behind the differences observed in nitrite inhibition mentioned earlier. Moreover, long HRT may have facilitated the adaptation of DAMO microorganisms to 10 mg/L NO_2-N.

There was no significant increase in the activity of Damo-Archaea in Enrichment-1 system. However, in Enrichment-2, a 3-fold increase was observed in Damo-Archaea activity in the 214 days operation. Thus, high initial nitrate concentrations may have a positive effect on the enrichment of Damo-Archaea. The application of high nitrate concentrations may have caused faster depletion of electron donors used in other heterotopic and autotrophic denitrification mechanisms, leading to a reduction in competition with Damo-Archaea.

Accordingly, specific activities of Damo-Bacteria and Damo-Archaea in Enrichment-1 (Table 4.9) and Enrichment-2 (Table 4.10) were compared. Enrichment-2 system reached much higher specific activities (606.32 μmol/L.d.g VSS for Damo-Bacteria and 303.16 μmol/L.d.g VSS for Damo-Archaea) in 388 days, compared to maximum specific activities obtained in Enrichment-1 study (535.71 μmol/L.d.g VSS for Damo-Bacteria and 173.16 μmol/L.d.g VSS for Damo-Archaea).

Another possible reason for better enrichment observed in Enrichment-2 system can be related to the growth factors which might be absent in the synthetic wastewater fed to the systems. It was reported that Damo-Bacteria can utilize the growth factors excreted by other heterotrophic bacteria (He et al., 2018). Therefore, the accumulation of substances that are missing in the synthetic wastewater fed to the system might have supported DAMO microorganisms indirectly in Enrichment-2 system. However, this effect was not observed in Enrichment-1 due to possible washout of the growth factors every 3 days via relatively short SBR cycles. Moreover, a decrease in DAMO microorganisms was reported when COD concentrations increased from 24 mg/L to 140 mg/L suggesting that high COD can support heterotrophic denitrifiers over DAMO due to the competition over nitrite (He et al., 2018). sCOD concentration was between 30-35 mg/L and 15-22 mg/L, respectively in Enrichment-1 study and in Enrichment-2 study. Although the difference is not very high, higher sCOD in Enrichment-1 culture might have supported heterotrophic denitrification activity. Another possible reason can be that dissolved methane availability was probably higher in Enrichment-2 since it was provided with methane every 2-3 days via purging. This might have slightly increased the dissolved methane in the reactor.

In this study, SBR configuration was selected in the enrichment of DAMO microorganisms due to its reported advantages for the enrichment of slowly-growing microorganisms such as homogeneous distribution of substrate and biomass, stability under limiting conditions, and reliable operation (Strous et al., 1999). Moreover, SBRs were previously used in successful enrichment of DAMO microorganisms (Raghoebarsing et al., 2006; Ettwig et al., 2009; Hu et al., 2009; Luesken et al., 2011). However, in this study, low activity of DAMO species in both Enrichment-1 and Enrichment-2 systems operated using SBRs was attributed to the possibility that the SBR configuration did not facilitate dissolved methane availability and gas transfer.

Finally, GAC addition was also observed to be more effective in Enrichment-2 system, which led to an increase in both Damo-Archaea and Damo-Bacteria

activity. However, in Enrichment-1 system, the GAC effect was overshadowed by the methane limitation, nitrite inhibition, and already existing competition between DAMO species.

CHAPTER 5

CONCLUSIONS AND RECOMMENDATIONS

This thesis study revealed that it is possible to enrich DAMO microorganisms from different seed sources. Moreover, the effects of different operational conditions and GAC on the enrichment of DAMO microorganisms were investigated. The results are summarized as follows;

- Among the four seed sources and their combinations tested in this study, PS, FS, and AD and their combinations were observed to show potential DAMO activity. However, RS was not observed to be a good choice for the enrichment of Damo-Bacteria or Damo-Archaea due to the high amount of organic matter which gives denitrifiers and methanogens a great advantage over DAMO species.
    - Low carbon content in the FS and PS provided an advantage regarding the DAMO activity since, in the anoxic environments; carbon is converted to methane which can be utilized by DAMO microorganisms.
    - DAMO species were detected in RS, however, DAMO activity was not observable in the reactors containing RS, suggesting that DAMO process was overshadowed by other predominant microorganisms in the RS.
    - Reduced forms of sulfur (HS^-, $S_2O_3^{2-}$, SCN^-) that can be found in the AD and sediment-derived pyrite (FeS_2) could cause a competition between Damo-Archaea and autotrophic denitrifiers until they are completely consumed in the enrichment culture.
- Enrichment of both Damo-Bacteria and Damo-Archaea was achieved in SBRs. Maximum nitrite and nitrate removal rates, since the onset of activity increase, were 2.29 mg NO_2-N/L.d and 11.9 mg NO_3-N/L.d in Enrichment-

1 and 1.40 mg NO_2-N/L.d and 17.03 mg NO_3-N/L.d in Enrichment-2. However, the maximum nitrite removal rate by Damo-Bacteria (1.68 mg/L.d for both Enrichment-1 and Enrichment-2 and nitrate removal rate by Damo-Archaea (0.98 mg/L.d in Enrichment-1 and 0.84 mg/L.d in Enrichment-2) detected with activity tests were lower compared to some literature data.

- Despite the advantages concerning the homogeneous distribution of substrate and biomass, long-term reliable operation, improved sludge settleability, the SBR configuration did not support the fast enrichment of DAMO species. The main reason for the low activity of DAMO species in the cultures was associated with the SBR configuration which did not facilitate availability of dissolved methane and gas transfer.
- Higher DAMO specific activities (606.32 μmol/L.d.g VSS for Damo-Bacteria and 303.16 μmol/L.d.g VSS for Damo-Archaea) were obtained using high HRT (120 days) and higher initial substrate concentrations (10 mg/L NO_2-N and 50 mg/L NO_3-N). This was attributed to the faster depletion of electron donors used by other heterotopic and autotrophic denitrification mechanisms which might have prevented the competition between *M.nitroreducens* and other denitrifying microorganisms. Additionally, the accumulation of missing growth factors may have resulted in the activity increase of *M.oxyfera*.
- Enough evidence was collected to support that there is competition between Damo-Bacteria and Damo-Archaea for dissolved methane. In methane-limited conditions, Damo-Bacteria was more active compared to Damo-Archaea.
- Despite being lower than the previously reported concentrations for nitrite inhibition of DAMO species, in this study, 10 mg/L NO_2-N concentration inhibited the activity of DAMO species in one

enrichment study while no inhibition was detected in the other. The inhibitory effect of nitrite might depend on the operational conditions used in the enrichment. Long HRT may have facilitated the adaptation of DAMO microorganisms to 10 mg/L NO_2-N.

  - The positive effect of GAC was observed on both Damo-Bacteria and Damo-Archaea activity. Application of GAC decreased the enrichment period by 3-fold. GAC addition may have helped the availability of dissolved methane and improved the contact of biomass with dissolved methane. The conductivity of methane may have contributed to the interspecies electron transfer between DAMO species.

- DAMO co-culture enrichment is critical for possible future application of DAMO process in wastewater treatment. This study showed that DAMO co-culture can be enriched by using SBR fed with nitrite and nitrate using mixed inoculum sources. Nevertheless, nitrite and nitrate removal rates of DAMO microorganisms should be improved by further modifications in reactor configurations to overcome the problems related to the slow growth of DAMO microorganisms and the availability of dissolved methane.

RECOMMENDATIONS

- Microbial community analysis, quantitative PCR, and phylogenetic analysis of the 16S rRNA genes could be helpful for the identification and quantification of *M. nitroreducens*, *M. oxyfera*, and to assess the relative abundance of DAMO species in different seed sources prior to enrichment.
- Carbon isotope tracer technology could be helpful to quantify the potential methane consumption and activity of DAMO species.
- DAMO enrichment can be improved by the continuous supply of methane in SBRs, MBR configurations, and bio-carrier applications.

- The effect of initial substrate concentrations and HRTs should be investigated further to shorten the time of enrichment for DAMO species.
- Reducing the inhibition of the DAMO process could improve the efficiency of nitrogen removal. To prevent possible nitrite inhibition, the effect of S/I on DAMO microorganisms could be investigated.
- To understand the contribution of GAC to different mechanisms that could improve DAMO activity, the effect of non-conductive biocarriers and conductive biocarriers on the activity of DAMO species should be investigated.

REFERENCES

Ahn, Y. (2006). Sustainable Nitrogen Elimination Biotechnologies: A Review. Process Biochemistry, vol. 41, no. 8, pp. 1709–1721., doi:10.1016/j.procbio.2006.03.033

Allegue, T., Arias, A., Fernandez-Gonzalez, N., Omil, F., & Garrido, J. M. (2018). Enrichment of nitrite-dependent anaerobic methane oxidizing bacteria in a membrane bioreactor. Chemical Engineering Journal, 347, 721–730. https://doi.org/10.1016/j.cej.2018.04.134

Angenent, L. T., Karim, K., Al-Dahhan, M. H., Wrenn, B. A., & Domıguez-Espinosa, R. (2004). Production of bioenergy and biochemicals from industrial and agricultural wastewater. Trends in Biotechnology, 22(9), 477–485

Bandara, W. M., Satoh, H., Sasakawa, M., Nakahara, Y., Takahashi, M., & Okabe, S. (2011). Removal of residual dissolved methane gas in an upflow anaerobic sludge blanket reactor treating low-strength wastewater at low temperature with degassing membrane. Water Research, 45(11), 3533–3540

Barnard, R, X Le Roux, BA Hungate et al. (2006). Several components of global change alter nitrifying and denitrifying activities in an annual grassland. Functional Ecology 20: 557-564

Bastviken, D., Tranvik, L. J., Downing, J. A., Crill, P. M., Enrich-Prast, A. (2011). Freshwater methane emissions offset the continental carbon sink. Science, 331(6013), 50-50. doi:10.1126/science.1196808

Beal, E.J., House, C.H., Orphan, V.J. (2009). Manganese- and iron-dependent marine methane oxidation. Science 325 (5937), 184–187. https://doi.org/10.1126/ science.1169984

Beklioğlu, M., Bucak, T., Coppens, J., Bezirci, G., Tavşanoğlu, Ü, Çakıroğlu, A., Özen, A. (2017). Restoration of eutrophic lakes with fluctuating water levels: a 20-year monitoring study of two inter-connected lakes. Water, 9(2), 127. doi:10.3390/w9020127

Berner, R. A. (2003). The long-term carbon cycle, fossil fuels and atmospheric composition. Nature, 426(6964), 323–326. https://doi.org/10.1038/nature02131

Bhattacharjee, A. S., Motlagh, A. M., Jetten, M. S., and Goel, R. (2016). Methane dependent denitrification- from ecosystem to laboratory-scale enrichment for engineering applications. Water Research, 99, 244-252. doi:10.1016/j.watres.2016.04.070

Bodelier PL (2011) Toward understanding, managing, and protecting microbial ecosystems. Front Microbiol 2:80. doi:10.3389/fmicb. 2011.00080

Boetius A., K. Ravenschlag, C. J. Schubert, D. Rickert, F. Widdel, A. Gieseke, (2000). A marine microbial consortium apparently mediating anaerobic oxidation of methane. Nature 407:623–626

Boetius, A., & Wenzhöfer, F. (2013). Seafloor oxygen consumption fuelled by methane from cold seeps. Nature Geoscience, 6(9), 725–734. https://doi.org/10.1038/ngeo1926

Bogner, J., Pipatti, R., Hashimoto, S., Diaz, C., Mareckova, K., Diaz, L.,Gregory, R. (2008). Mitigation of global GHG emissions from waste: Conclusions and strategies from the Intergovernmental panel on climate Change (IPCC) Fourth assessment Report. Working Group III (mitigation). Waste Management & Research: The Journal for a Sustainable Circular Economy, 26(1), 11-32. doi:10.1177/0734242x07088433

Boley, A., Muller, W.R., Haider, G. (2000). Biodegradable polymers as solid substrate and biofilm carrier for denitrification in recirculated aquaculture

systems. Aquac. Eng. 22, 75‑85. https://doi.org/10.1016/S0144-8609(00)00033-9

Britannica, The Editors of Encyclopaedia. "Nitrogen cycle". Encyclopedia Britannica, 27 May 2020. Accessed on 10 June 2021 from https://www.britannica.com/science/nitrogen-cycle

Cai, C., Hu, S., Chen, X., Ni, B., Pu, J., Yuan, Z. (2018a). Effect of methane partial pressure on the performance of a membrane biofilm reactor coupling methane-dependent denitrification and anammox. Science of The Total Environment,639, 278-285. doi:10.1016/j.scitotenv.2018.05.164

Cai, C., Hu, S., Guo, J., Shi, Y., Xie, G., Yuan, Z. (2015). Nitrate reduction by denitrifying anaerobic methane oxidizing microorganisms can reach a practically useful rate. Water Res. 87, 211–217. https://doi.org/10.1016/j.watres.2015.09.026

Cai, C., Leu, A.O., Xie, G.J., Guo, J.H., Feng, Y.X., Zhao, J.X., Tyson, G.W., Yuan, Z.G., Hu, S.H. (2018b). A methanotrophic archaeon couples anaerobic oxidation of methane to Fe(III) reduction. ISME J. 12 (8), 1929–1939. https://doi.org/10.1038/s41396- 018-0109-x

Campos, J. L., Valenzuela-Heredia, D., Pedrouso, A., Val del Río, A., Belmonte, M., Mosquera-Corral, A. (2016). Greenhouse gases emissions from wastewater treatment plants: Minimization, treatment, and prevention. Journal of Chemistry, 2016, 1–12. https://doi.org/10.1155/2016/3796352

Castro-Barros, C. M., Ho, L. T., Winkler, M. K., & Volcke, E. I. (2017). Integration of methane removal in aerobic anammox-based granular sludge reactors. Environmental Technology, 39(13), 1615–1625. https://doi.org/10.1080/09593330.2017.1334709

Chang, J., Wu, Q., Yan, X., Wang, H., Lee, L. W., Liu, Y., Liang, P., Qiu, Y., & Huang, X. (2021). Enhancement of nitrite reduction and enrichment Of

methylomonas via conductive materials in A nitrite-dependent anaerobic methane oxidation system. Environmental Research, 193, 110565. https://doi.org/10.1016/j.envres.2020.110565

Chen H., Ma C., Yang G., Wang H., Yu Z. and Jin R. (2014c). Floatation of flocculent and granular sludge in a high-loaded anammox reactor, Biores. Technol., 169, 409-415

Chen, F., Zheng, Y., Hou, L., Zhou, J., Yin, G., & Liu, M. (2019). Denitrifying anaerobic methane oxidation in marsh sediments of Chongming eastern intertidal flat. Marine Pollution Bulletin, 110681. doi:10.1016/j.marpolbul.2019.1106

Chen, G., Li, J., Deng, H., Dong, Q., Zhang, Y., Zheng, Z., Hou, A., (2015b). Study on Anaerobic ammonium oxidation (ANAMMOX) sludge immobilized in different gel carriers and its nitrogen removal rerformance. J. Residuals Sci. Technol. 12, S47–S54

Chen, J., Zhou, Z., Gu, J.D., (2015a). Complex community of nitrite-dependent anaerobic methane oxidation bacteria in coastal sediments of the Mai Po wetland by PCR amplification of both 16S rRNA and pmoA genes. Applied Microbiology and Biotechnology 99, 1463–1473

Chen, J., Zhou, Z.C., Gu, J.D., (2014a). Occurrence and diversity of nitrite-dependent anaerobic methane oxidation bacteria in the sediments of the South China Sea revealed by amplification of both 16S rRNA and pmoA genes. Applied Microbiology and Biotechnology 98, 5685–5696

Chen, X., Guo, J., Shi, Y., Hu, S., Yuan, Z., and Ni, B. (2014b). Modeling of Simultaneous Anaerobic Methane and Ammonium Oxidation in a Membrane Biofilm Reactor. Environmental Science and Technology, 48(16), 9540-9547. doi:10.1021/es502608s

Chen, X., Liu, Y., Peng, L., Yuan, Z., & Ni, B.-J. (2016). Model-Based Feasibility Assessment of Membrane Biofilm Reactor to Achieve Simultaneous

Ammonium, Dissolved Methane, and Sulfide Removal from Anaerobic Digestion Liquor. Scientific Reports, 6(1). doi:10.1038/srep25114

Conrad R. (2009). The global methane cycle: recent advances in understanding the microbial processes involved. Environ Microbiol Rep 1(5):285–292. doi:10.1111/j.1758-2229.2009.00038.x

Cookney, J., Mcleod, A., Mathioudakis, V., Ncube, P., Soares, A., Jefferson, B., Mcadam, E., 2016. Dissolved methane recovery from anaerobic effluents using hollow fibre membrane contactors. J. Membr. Sci. 502, 141–150, 2016

Cui, M., Ma, A., Qi, H., Zhuang X., and Zhuang, G. (2015) Anaerobic oxidation of methane: an "active" microbial process. Microbiology Open, 4(1), 1–11. doi: 10.1002/mbo3.232

Daelman, M. R., Van Voorthuizen, E. M., Van Dongen, L. G., Volcke, E. I., & Van Loosdrecht, M. C. (2013). Methane and nitrous oxide emissions from municipal wastewater treatment – results from a long-term study. Water Science and Technology, 67(10), 2350-2355. doi:10.2166/wst.2013.109

Denman KL, (2007) Couplings between changes in the climate system and biogeochemistry. Climate change 2007: The physical Science Basis. Contribution of Working Group I to the Fourth Assessment Report of the Intergovernmental Panel on Climate Change, eds Solomon S, et al. (Cambridge Univ Press, Cambridge, UK)

Dettmer-Wilde, K., Engewald, W. (2014) "Practical gas chromatography a comprehensive reference", Berlin: Springer-Verlag.

Deutzmann, J.S., Schink, B. (2011) Anaerobic oxidation of methane in sediments of Lake Constance, an oligotrophic freshwater lake. Appl Environ Microbiol 77(13):4429–4436

Di Capua, F. D., Pirozzi, F., Lens, P. N., & Esposito, G. (2018). Electron donors for autotrophic denitrification. Chemical Engineering Journal, 362, 922–937.

Ding, J., Fu, L., Ding, Z.-W., Lu, Y.-Z., Cheng, S. H., Zeng, R. J. (2015). Environmental evaluation of coexistence of denitrifying anaerobic methane-oxidizing archaea and bacteria in a paddy field. Applied Microbiology and Biotechnology, 100(1), 439–446. https://doi.org/10.1007/s00253-015-6986-2

Ding, J., Lu, Y.-Z., Fu, L., Ding, Z.-W., Mu, Y., Cheng, S. H., & Zeng, R. J. (2017b). Decoupling of DAMO archaea from DAMO bacteria in a methane-driven microbial fuel cell. Water Research, 110, 112–119. doi:10.1016/j.watres.2016.12.006

Ding, J., Zeng, R.J. (2021). Fundamentals and potential environmental significance of denitrifying anaerobic methane oxidizing archaea. Sci. Total Environ. 757, 143928. https://doi.org/10.1016/j.scitotenv.2020.143928.

Ding, Z., Lu, Y., Fu, L., Ding, J., and Zeng, R. J. (2016). Simultaneous enrichment of denitrifying anaerobic methane-oxidizing microorganisms and anammox bacteria in a hollow-fiber membrane biofilm reactor. Applied Microbiology and Biotechnology, 101(1), 437-446. doi:10.1007/s00253-016-7908-7

Ding, Z., Lu, Y., Fu, L., Ding, J., Zeng, R.J. (2017a). Simultaneous enrichment of denitrifying anaerobic methane-oxidizing microorganisms and anammox bacteria in a hollow-fiber membrane biofilm reactor. Appl. Microbiol. Biotechnol. 101 (1), 437–446. https://doi.org/10.1007/s00253-016-7908-7.

Ding, Z., W., Ding, J., Fu, L., Zhang, F., & Zeng, R. J. (2014). Simultaneous enrichment of denitrifying methanotrophs and anammox bacteria. Applied Microbiology and Biotechnology, 98(24), 10211–10221. doi:10.1007/s00253-014-5936-8

Du, R., Peng, Y., Ji, J., Shi, L., Gao, R., Li, X., 2019. Partial denitrification providing nitrite: opportunities of extending application for anammox. Environ. Int. 131, 105001. https://doi.org/10.1016/j.envint.2019.105001

Duce, R. A., LaRoche, J., Altieri, K., Arrigo, K. R., Baker, A. R., Capone, D. G.,Zamora, L. (2008). Impacts of Atmospheric Anthropogenic Nitrogen on the Open Ocean. Science, 320(5878), 893–897. doi:10.1126/science.1150369.

El-Fadel, M., & Massoud, M. (2001). Methane emissions from wastewater management. Environmental Pollution, 114(2), 177-185. doi:10.1016/s0269-7491(00)00222-0

Environmental Protection Agency (EPA). Global Anthropogenic Emissions of Non-CO2 Greenhouse Gases: 1990–2020 (EPA Report 430-R-06-003). Office of Athospheric Programs Climate Change Division.

Estefan, G., R. Sommer and J. Ryan. (2013). Methods of soil, plant, and water analysis. A manual for the West Asia and North Africa region

Ettwig, K. F., Alen, T. V., Pas-Schoonen, K. T., Jetten, M. S., and Strous, M. (2009). Enrichment and Molecular Detection of Denitrifying Methanotrophic Bacteria of the NC10 Phylum. Applied and Environmental Microbiology, 75(11), 3656-3662. doi:10.1128/aem.00067-09

Ettwig, K. F., Butler, M. K., Paslier, D. L., Pelletier, E., Mangenot, S., Kuypers, M. M., Schreiber, F., Dutilh, B. E., Zedelius, J., de Beer, D., Gloerich, J., Wessels, H. J. C. T., van Alen, T., Luesken, F., Wu, M. L., van de Pas-Schoonen, K. T., Op den Camp, H. J. M., Janssen-Megens, E. M., Francoijs, K. J., Stunnenberg, H., Weissenbach, J., Jetten, M. S. M., and Strous, M. (2010). Nitrite-driven anaerobic methane oxidation by oxygenic bacteria. Nature, 464(7288), 543-548. doi:10.1038/nature08883

Ettwig, K. F., Shima, S., van de Pas-Schoonen, K. T., Kahnt, J., Medema, M. H., Op den Camp, H. J. M., Jetten, M. S., and Strous, M. (2008). Denitrifying

bacteria anaerobically oxidize methane in the absence of Archaea. Environmental Microbiology, 10,3164–3173.

Ettwig, K. F., Zhu, B., Speth, D., Keltjens, J. T., Jetten, M. S. M., & Kartal, B. (2016). Archaea catalyze iron-dependent anaerobic oxidation of methane. Proceedings of the National Academy of Sciences, 113(45), 12792–12796. doi:10.1073/pnas.1609534113

Dahab, F. M., Lee, Y. W. (1988). Nitrate Removal from Water Supplies Using Biological Denitrification . Water Pollution Control Federation WPCF Annual Conference Issue , 60(9), 1670–1674.

Fu, L., Ding, J., Lu, Y., Ding, Z., and Zeng, R. J. (2017a). Nitrogen source effects on the denitrifying anaerobic methane oxidation culture and anaerobic ammonium oxidation bacteria enrichment process. Applied Microbiology and Biotechnology, 101(9), 3895-3906. doi:10.1007/s00253-017-8163-2

Fu, L., Ding, J., Lu, Y., Ding, Z., Bai, Y., Zeng, R.J., (2017b). Hollow fiber membrane bioreactor affects microbial community and morphology of the DAMO and Anammox co-culture system. Bioresour. Technol. 232, 247–253. https://doi.org/10.1016/j.biortech.2017.02.048.

Fu, L., Ding, Z., Ding, J., Zhang, F., and Zeng, R. J. (2015). The role of paraffin oil on the interaction between denitrifying anaerobic methane oxidation and Anammox processes. Applied Microbiology and Biotechnology,99(19), 7925-7936. doi:10.1007/s00253-015-6670-6

Fu, L., Zhang, F., Bai, Y., Lu, Y., Ding, J., Zhou, D., Liu, Y., Zeng, R.J. (2019). Mass transfer affects reactor performance, microbial morphology, and community succession in the methane-dependent denitrification and anaerobic ammonium oxidation coculture. Sci. Total Environ. 651, 291–297. https://doi.org/10.1016/j. scitotenv.2018.09.184.

Galloway, J. N., Townsend, A. R., Erisman, J. W., Bekunda, M., Cai, Z., Freney, J. R., Sutton, M. A. (2008). Transformation of the Nitrogen Cycle: Recent

Trends, Questions, and Potential Solutions. Science, 320(5878), 889–892. doi:10.1126/science.1136674

Gambelli, L., Guerrero-Cruz, S., Mesman, R. J., Cremers, G., Jetten, M. S., Op den Camp, H. J., Kartal, B., Lueke, C., & van Niftrik, L. (2018). Community Composition and Ultrastructure of a Nitrate-Dependent Anaerobic Methane-Oxidizing Enrichment Culture. Applied and Environmental Microbiology, 84(3). https://doi.org/10.1128/aem.02186-17

Ge, S., Wang, S., Yang, X., Qiu, S., Li, B., Peng, Y., 2015. Detection of nitrifiers and evaluation of partial nitrification for wastewater treatment: a review. Chemosphere 140, 85-98. https://doi.org/10.1016/j.chemosphere.2015.02.004

Glass, J. B., & Orphan, V. J. (2012). Trace Metal Requirements for Microbial Enzymes Involved in the Production and Consumption of Methane and Nitrous Oxide. Frontiers in Microbiology,3. doi:10.3389/fmicb.2012.00061

Gonzalez-Fernandez, C., Sialve, B., & Molinuevo-Salces, B. (2015). Anaerobic digestion of microalgal biomass: Challenges, opportunities and research needs. Bioresource Technology, 198, 896–906. https://doi.org/10.1016/j.biortech.2015.09.095

Graf, J. S., Mayr, M. J., Marchant, H. K., Tienken, D., Hach, P. F., Brand, A., et al. (2018). Bloom of a denitrifying methanotroph, "Candidatus Methylomirabilis limnetica", in a deep stratified lake. Environ. Microbiol. doi: 10.1111/1462-2920.14285

Guerrero-Cruz, S., Stultiens, K., Van Kessel, M.A., Versantvoort, W., Jetten, M.S., Op den Camp, H.J., Kartal, B. (2019). Key physiology of a nitrite-dependent methane-oxidizing enrichment culture. Appl. Environ. Microbiol. 85 (8) https://doi.org/ 10.1128/aem.00124-19.

Guisasola, A., de Haas, D., Keller, J., and Yuan, Z., (2008). Methane formation in sewer systems. Water Research 42 (6-7), 1421-1430

Guo, J. H., Liu, X. J., Zhang, Y., Shen, J. L., Han, W. X., Zhang, W. F., Zhang, F. S. (2010). Significant Acidification in Major Chinese Croplands. Science, 327(5968), 1008–1010. doi:10.1126/science.1182570

Gupta, D., and Singh, S. K. (2012). Greenhouse Gas Emissions from Wastewater Treatment Plants: A Case Study of Noida. Journal of Water Sustainability, 1(2), 131–140. https://doi.org/10.11912/jws.2.2.131-139

Haddadi, S., Elbeshbishy, E., & Lee, H. S. (2013). Implication of diffusion and significance of anodic pH in nitrogen-recovering microbial electrochemical cells. Bioresource Technology, 142, 562–569.

Hansen, J., Fung, I., Lacis, A., Rind, D., Lebedeff, S., Ruedy, R., Russell, G., & Stone, P. (1988). Global climate changes as forecast by Goddard Institute for Space Studies three-dimensional model. Journal of Geophysical Research, 93(D8), 9341. https://doi.org/10.1029/jd093id08p09341.

Harb, R., Laçin, D., Subaşı, I., & Erguder, T. H. (2021). Denitrifying anaerobic methane oxidation (damo) cultures: Factors affecting their enrichment, performance and integration with anammox bacteria. Journal of Environmental Management, 295, 113070. https://doi.org/10.1016/j.jenvman.2021.113070

Haroon, M. F., Hu, S., Shi, Y., Imelfort, M., Keller, J., Hugenholtz, P., Yuan, Z., and Tyson, G. W. (2013). Anaerobic oxidation of methane coupled to nitrate reduction in a novel archaeal lineage. Nature, 500(7464), 567-570. doi:10.1038/nature12375

Hatamoto, M., Kimura, M., Sato, T., Koizumi, M., Takahashi, M., Kawakami, S., Araki, N., and Yamaguchi, T. (2014). Enrichment of Denitrifying Methane-Oxidizing Microorganisms Using Up-Flow Continuous Reactors and Batch Cultures. PLoS ONE, 9(12). doi:10.1371/journal.pone.0115823

Hatamoto, M., Sato, T., Nemoto, S., Yamaguchi, T., (2017). Cultivation of denitrifying anaerobic methane-oxidizing microorganisms in a continuous-flow sponge bioreactor. Appl. Microbiol. Biotechnol. 101 (14), 5881–5888. https://doi.org/ 10.1007/s00253-017-8315-4.

He, Z., Cai, C., Shen, L., Lou, L., Zheng, P., Xu, X., and Hu, B. (2014). Effect of inoculum sources on the enrichment of nitrite-dependent anaerobic methane-oxidizing bacteria. Applied Microbiology and Biotechnology, 99(2), 939-946. doi:10.1007/s00253-014-6033-8

He, Z., Cai, C., Wang, J., Xu, X., Zheng, P., Jetten, M. S. M., et al. (2016). A novel denitrifying methanotroph of the NC10 phylum and its microcolony. Sci. Rep. 6, 10–20. doi: 10.1038/srep32241

He, Z., Feng, J., Wei, Z., Wu, S., Zou, J., Pan, X., (2018). Optimization of methane-dependent oxygenic denitrification in sequencing batch reactors by insights into the microbial interactions. Sci. Total Environ. 643, 623–631. https://doi.org/10.1016/j. scitotenv.2018.06.238.

He, Z., Geng, S., Pan, Y., Cai, C., Wang, J., Wang, L., Hu, B. (2015a). Improvement of the trace metal composition of medium for nitrite-dependent anaerobic methane oxidation bacteria: Iron (II) and copper (II) make a difference. Water Research, 85, 235-243. doi:10.1016/j.watres.2015.08.040

He, Z., Geng, S., Shen, L., Lou, L., Zheng, P., Xu, X., & Hu, B. (2015b). The short- and long-term effects of environmental conditions on anaerobic methane oxidation coupled to nitrite reduction. Water Research, 68, 554-562. doi:10.1016/j.watres.2014.09.055

Hinrichs, K.-U., J. M. Hayes, S. P. Sylva, P. G. Brewer, and E. F. DeLong. (1999). Methane-consuming archaebacteria in marine sediments. Nature 398:802–805.

Hou, Y. (2013). Study of the anaerobic methane oxidation coupled to nitrate denitrification. MS Thesis. Department of Civil Engineering, University of Waterloo, Waterloo, Ontario, Canada, 2013

Houghton, R. A. (2003). The contemporary carbon cycle. Treatise on Geochemistry, 473–513. https://doi.org/10.1016/b0-08-043751-6/08168-8.

Hu, B., He, Z., Geng, S., Cai, C., Lou, L., Zheng, P., and Xu, X. (2014a). Cultivation of nitrite-dependent anaerobic methane-oxidizing bacteria: Impact of reactor configuration. Applied Microbiology and Biotechnology, 98(18), 7983-7991. doi:10.1007/s00253-014-5835-z

Hu Z, Lotti T, Lotti T, de Kreuk M, Kleerebezem R, van Loosdrecht M, Kruit J, Jetten MSM, Kartal B (2013) Nitrogen removal by a nitritation-anammox bioreactor at low temperature. Appl Environ Microbiol. doi:10.1128/ AEM.03987-12

Hu, B.L., Shen, L.D., Lian, X., Zhu, Q., Liu, S., Huang, Q., He, Z.F., Geng, S., Cheng, D.Q., Lou, L.P., (2014b). Evidence for nitrite-dependent anaerobic methane oxidation as a previously overlooked microbial methane sink in wetlands. Proc. Natl. Acad. Sci. 111 (12), 4495–4500.

Hu, S., Zeng, R. J., Burow, L. C., Lant, P., Keller, J., and Yuan, Z. (2009). Enrichment of denitrifying anaerobic methane oxidizing microorganisms. Env. Microbiol. Rep., 1, 377-384.

Hu, S., Zeng, R. J., Haroon, M. F., Keller, J., Lant, P. A., Tyson, G. W., and Yuan, Z. (2015). A laboratory investigation of interactions between denitrifying anaerobic methane oxidation (DAMO) and anammox processes in anoxic environments. Scientific Reports, 5, 1–9. https://doi.org/10.1038/srep08706

Hu, S., Zeng, R. J., Keller, J., Lant, P. A., and Yuan, Z. (2011). Effect of nitrate and nitrite on the selection of microorganisms in the denitrifying anaerobic methane oxidation process. Env. Microbiol. Rep., 3, 315-319.

Hu, Z., & Ma, R. (2016). Distribution and characteristic of nitrite-dependent anaerobic methane oxidation bacteria in wastewater treatment plants and agriculture fields of northern China. doi:10.7287/peerj.preprints.2421

Intergovernmental Panel on Climate Change (IPCC). Climate Change 2014: Mitigation of Climate Change. Contribution of Working Group III to the Fifth Assessment Report of the Intergovernmental Panel on Climate Change. Cambridge University Press, Cambridge, United Kingdom and New York, NY, USA.

Intergovernmental Panel on Climate Change (IPCC). Climate Change 2013: The Physical Science Basis. Contribution of Working Group I to the Fifth Assessment Report of the Intergovernmental Panel on Climate Change. Cambridge University Press, Cambridge, United Kingdom and New York, NY, USA.

Islas-Lima, S., Thalasso, F., and Gómez-Hernandez, J. (2004). Evidence of anoxic methane oxidation coupled to denitrification. Water Research, 38(1), 13–16. https://doi.org/10.1016/j.watres.2003.08.024

Jetten, M. S. M. (2008). The microbial nitrogen cycle. Environmental Microbiology, 10(11), 2903–2909. doi:10.1111/j.1462-2920.2008.01786.x

Jiang, L., Hu, Z., Wang, Y., Ru, D., Li, J., and Fan, J. (2018). Effect of trace elements on the development of co-cultured nitrite-dependent anaerobic methane oxidation and methanogenic bacteria consortium. Bioresource Technology,268, 190-196. doi:10.1016/j.biortech.2018.07.139

Kampman, C., Hendrickx, T. L., Luesken, F. A., Alen, T. A., Camp, H. J., Jetten, M. S., Zeeman, G., Buisman, C. J. N., and Temmink, H. (2012). Enrichment of denitrifying methanotrophic bacteria for application after direct low-temperature anaerobic sewage treatment. Journal of Hazardous Materials, 227-228, 164-171. doi:10.1016/j.jhazmat.2012.05.032.

Kampman, C., Temmink, H., Hendrickx, T. L. G., Zeeman, G., and Buisman, C. J. N. (2014). Enrichment of denitrifying methanotrophic bacteria from municipal wastewater sludge in a membrane bioreactor at 20 °C. J Hazard Mater 274:428–435.

Keller, J., & Hartley, K. (2003). Greenhouse gas production in wastewater treatment: Process selection is the major factor. Water Science and Technology, 47(12), 43–48. https://doi.org/10.2166/wst.2003.0626

Kirschke, S., P. Bousquet, P. Ciais, M. Saunois, J.G. Canadell, E.J. Dlugokencky, P. Bergamaschi, D. Bergmann, D.R. Blake, L. Bruhwiler, P. Cameron-Smith, S. Castaldi, F. Chevallier, L. Feng, A. Fraser, M. Heimann, E.L. Hodson, S. Houweling, B. Josse, P.J. Fraser, P.B. Krummel, J.-F. Lamarque, R.L. Langenfelds, C. Le Quéré, V. Naik, S. O'Doherty, P.I. Palmer, I. Pison, D. Plummer, B. Poulter, R.G. Prinn, M. Rigby, B. Ringeval, M. Santini, M. Schmidt, D.T. Shindell, I.J. Simpson, R. Spahni, L.P. Steele, S.A. Strode, K. Sudo, S. Szopa, G.R. van der Werf, A. Voulgarakis, M. van Weele, R.F. Weiss, J.E. Williams, and G. Zeng, 2013: Three decades of global methane sources and sinks. Nat. Geosci., 6, 813-823, doi:10.1038/ngeo1955.

Knittel, K., & Boetius, A. (2009). Anaerobic Oxidation of Methane: Progress with an Unknown Process. Annual Review of Microbiology, 63(1), 311–334. doi:10.1146/annurev.micro.61.0807

Knittel, K., Lösekann, T., Boetius, A., Kort, R., & Amann, R. (2005). Diversity and distribution of methanotrophic archaea at cold seeps. Applied and Environmental Microbiology, 71(1), 467-479. doi:10.1128/aem.71.1.467-479.2005

Kojima, H., Tsutsumi, M., Ishikawa, K., Iwata, T., Mußmann, M., and Fukui, M. (2012). Distribution of putative denitrifying methane oxidizing bacteria in

sediment of a freshwater lake, Lake Biwa. Systematic and Applied Microbiology, 35(4), 233–238. https://doi.org/10.1016/j.syapm.2012.03.005

Kowalski, M. S., Devlin, T. R. & Oleszkiewicz, J. A. (2019) Attachment of anaerobic ammonium-oxidizing bacteria to augmented carrier material. Environmental Technology 40 (5), 576–583.

Lai, C.Y., Dong, Q.Y., Chen, J.X., Zhu, Q.S., Yang, X., Chen, W.D., Zhao, H.P., Zhu, L. (2018). Role of extracellular polymeric substances in a methane based membrane biofilm reactor reducing vanadate. Environ. Sci. & Technol. 52 (18), 10680‑10688.

Lee, H.,S., Tang, Y., Rittmann, B. E., Zhao, H.P. (2018). Anaerobic oxidation of methane coupled to denitrification: Fundamentals, challenges, and potential. Critical Reviews in Environmental Science and Technology, 48(19-21), 1067–1093. https://doi.org/10.1080/10643389.2018.1503927

Lee, R., McCarty, P.L., Bae, J., Kim, J. (2015). Anaerobic fluidized membrane bioreactor polishing of baffled reactor effluent during treatment of dilute wastewater. J. Chem. Technol. Biotechnol. 90 (3), 391‑397.

Li, J., Lou, J., Lv, J., (2020a). The effect of sulfate on nitrite-denitrifying anaerobic methane oxidation (nitrite-DAMO) process. Sci. Total Environ. 731, 139160. https:// doi.org/10.1016/j.scitotenv.2020.139160.

Li, W., Lu, P., Chai, F., Zhang, L., Han, X., and Zhang, D. (2018). Long-term nitrate removal through methane-dependent denitrification microorganisms in sequencing batch reactors fed with only nitrate and methane. AMB Express,8(1). doi:10.1186/s13568-018-0637-9

Li-dong, S., Qun, Z., Shuai, L., Ping, D., Jiang-ning, Z., Dong-qing, C., Xiang-yang, X., Ping, Z., & Bao-lan, H. (2014). Molecular evidence for nitrite-dependent Anaerobic methane-oxidising bacteria in THE JIAOJIANG estuary of the East SEA (CHINA). Applied Microbiology and

Biotechnology, 98(11), 5029–5038. https://doi.org/10.1007/s00253-014-5556-3

Liu Y, Zhang J, Zhao L, Li Y, Yang Y, Xie S. (2014). Aerobic and nitrite-dependent methane-oxidizing microorganisms in sediments of freshwater lakes on the Yunnan Plateau. Applied Microbiology and Biotechnology 99:23712381 DOI 10.1007/s00253-014-6141-5.

Liu, T., Hu, S., Guo, J. (2019a). Enhancing mainstream nitrogen removal by employing nitrate/nitrite-dependent anaerobic methane oxidation processes. Crit. Rev. Biotechnol. 39 (5), 732–754. https://doi.org/10.1080/07388551.2019.1598333

Liu, T., Hu, S., Yuan, Z., Guo, J. (2019b). High-level nitrogen removal by simultaneous partial nitritation, anammox and nitrite/nitrate-dependent anaerobic methane oxidation. Water Res. 166.

Liu, Y., Wang, X., Chen, Y., Zhang, L., Xu, K., & Du, Y. (2020). Anaerobic methane-oxidizing bacterial communities in sediments of a drinking reservoir, beijing, china. annals of microbiology, 70(1). doi:10.1186/s13213-020-01578-5

Liu, Y., Whitman, W. B. (2008). Metabolic, phylogenetic, and ecological diversity of the methanogenic archaea. Annals of the New York Academy of Sciences, 1125(1), 171–189. https://doi.org/10.1196/annals.1419.019

Lou, J., Wang, X., Li, J., Han, J. (2019). The short- and long-term effects of nitrite on denitrifying anaerobic methane oxidation (DAMO) organisms. Environ. Sci. Pollut. Control Ser. 26 (5), 4777–4790. https://doi.org/10.1007/s11356-018-3936-4.

Lu, P., Liu, T., Ni, B., Guo, J., Yuan, Z., Hu, S., (2019). Growth kinetics of Candidatus ‘Methanoperedens nitroreducens’ enriched in a laboratory reactor. Sci. Total Environ. 659, 442–450. https://doi.org/10.1016/j.scitotenv.2018.12.351.

Lu, P., Wang, X., Tang, Y., Ding, A., Yang, H., Guo, J., Cui, Y., & Ling, C. (2020). Granular activated carbon assisted nitrate-dependent anaerobic methane oxidation-membrane bioreactor: Strengthening effect and mechanisms. Environment International, 138, 105675. https://doi.org/10.1016/j.envint.2020.105675

Lu, Y. (2005). In situ stable Isotope probing Of methanogenic archaea in the Rice Rhizosphere. Science, 309(5737), 1088–1090. https://doi.org/10.1126/science.1113435

Lu, Y., and Conrad, R. (2005). In situ stable isotope probing of methanogenic archaea in the rice rhizosphere. Science 309, 1088–1090. doi: 10.1126/science.1113435

Lu, Y., Fu, L., Li, N., Ding, J., Bai, Y., Samaras, P., Zeng, R.J., 2018. The content of trace element iron is a key factor for competition between anaerobic ammonium oxidation and methane-dependent denitrification processes. Chemosphere 198, 370–376. https://doi.org/10.1016/j.chemosphere.2018.01.172.

Lu, Y.-Z., Fu, L., Ding, J., Ding, Z.-W., Li, N., Zeng, R. J. (2016). Cr(VI) reduction coupled with anaerobic oxidation of methane in a laboratory reactor. Water Research, 102, 445–452. doi:10.1016/j.watres.2016.06.065

Luesken, F., van Alen, T., Biezen, E., Frijters, C., Toonen, G., Kampman, C., Hendrickx, T., Zeeman, G., Temmink, H., Strous, M., Op den Camp, H., and Jetten, M. (2011). Diversity and enrichment of nitrite-dependent anaerobic methane oxidizing bacteria from wastewater sludge. Applied Microbiology and Biotechnology, 92(4), 845-854. doi:10.1007/s00253-011-3361-9.

Luesken, F., Wu, M., Op den Camp, H., Keltjens, J., Stunnenberg, H., Francoijs, K., Strous, M., and Jetten, M. (2012). Effect of oxygen on the anaerobic methanotroph “Candidatus Methylomirabilis oxyfera”: Kinetic and

transcriptional analysis. Environmental Microbiology, 14(4), 1024–1034. https://doi.org/10.1111/j.1462-2920.2011.02682.x

Luo, J., Chen, H., Yuan, Z., and Guo, J. (2018). Methane-supported nitrate removal from groundwater in a membrane biofilm reactor. Water Research,132, 71-78. doi:10.1016/j.watres.2017.12.064

Luo, J.-H., Chen, H., Hu, S., Cai, C., Yuan, Z., & Guo, J. (2018). Microbial Selenate Reduction Driven by a Denitrifying Anaerobic Methane Oxidation Biofilm. Environmental Science & Technology, 52(7), 4006–4012. doi:10.1021/acs.est.7b05046

Luque-Almagro, V. M., Cabello, P., Sáez, L. P., Olaya-Abril, A., Moreno-Vivián, C., & Roldán, M. D. (2017). Exploring anaerobic environments for cyanide and cyano-derivatives microbial degradation. Applied Microbiology and Biotechnology, 102(3), 1067–1074. https://doi.org/10.1007/s00253-017-8678-6

Maaz, M., Yasin, M., Aslam, M., Kumar, G., Atabani, A. E., Idrees, M., Anjum, F., Jamil, F., Ahmad, R., Khan, A. L., Lesage, G., Heran, M., & Kim, J. (2019). Anaerobic membrane bioreactors for wastewater treatment: Novel configurations, fouling control and energy considerations. Bioresource Technology, 283, 358–372. https://doi.org/10.1016/j.biortech.2019.03.061

Malyan, S. K., Bhatia, A., Kumar, A., Gupta, D. K., Singh, R., Kumar, S. S., Jain, N. (2016). Methane production, oxidation and mitigation: A mechanistic understanding and comprehensive evaluation of influencing factors. Science of The Total Environment, 572, 874-896. doi:10.1016/j.scitotenv.2016.07.182

Magnusson, B., Örnemark, U. (2014). Eurachem Guide: The Fitness for Purpose of Analytical Methods – A Laboratory Guide to Method Validation and Related Topics, 2nd ed.

Matsuyama, N., Saigusa, M., Sakaiya, E., Tamakawa, K., Oyamada, Z., Kudo, K. (2005). "Acidification and Soil Productivity of Allophanic Andosols Affected by Heavy Application of Fertilizers", Soil Science and Plant Nutrition, 51(1), 117–123.

Mayr, M.J., Zimmermann, M., Guggenheim, C., Brand, A., Buergmann, H. (2020). Niche partitioning of methane-oxidizing bacteria along the oxygen-methane counter gradient of stratified lakes. ISME J. 14 (1), 274–287.

McCarty, P. L. (2018). What is the Best Biological Process for Nitrogen Removal: When and Why? Environmental Science & Technology, 52(7), 3835–3841. doi:10.1021/acs.est.7b05832

McCarty, P. L., Bae, J., & Kim, J. (2011). Domestic wastewater treatment as a net energy producer–can this be achieved? Environmental Science & Technology, 45(17), 7100–7106.

Modin, O., Fukushi, K., and Yamamoto, K., (2007). Denitrification with methane as external carbon source. Water Research, 41(12), 2726-2738.

Mulder, A. (2003). The quest for sustainable nitrogen removal technologies. Water Science and Technology, 48(1), 67–75. doi:10.2166/wst.2003.0018

Murrell, J. C., & Jetten, M. S. M. (2009). The microbial methane cycle. Environmental Microbiology Reports, 1(5), 279–284. doi:10.1111/j.1758-2229.2009.00089.x

Nauhaus, K., Boetius, A., Kruger, M., and Widdel, F. (2002). In vitro demonstration of anaerobic oxidation of methane coupled to sulphate reduction in sediment from a marine gas hydrate area. Environmental Microbiology, 4(5), 296-305. doi:10.1046/j.1462-2920.2002.00299.x

Nie, W., Xie, G., Ding, J., Lu, Y., Liu, B., Xing, D., Wang, Q., Han, H., Yuan, Z., Ren, N., 2019. High performance nitrogen removal through integrating denitrifying anaerobic methane oxidation and Anammox: from enrichment

to application. Environ. Int. 132 (May), 105107. https://doi.org/10.1016/j.envint.2019.105107.

Nielsen, P. H., Daims, H., & Lemmer, H. (2009). FISH Handbook for Biological Wastewater Treatment. IWA Publishing. https://doi.org/10.2166/9781780401775

Nikolausz, M., & Kretzschmar, J. (2020). Anaerobic digestion in the 21st century. Bioengineering, 7(4), 157. https://doi.org/10.3390/bioengineering7040157

Öğün, E. (2012). Determınatıon of the reactıve nıtrogen cycle at lake eymir (Master's thesis, Hacettepe University, 2012). Ankara: Hacettepe University.

Okoro, O. V., & Sun, Z. (2019). Desulphurisation of Biogas: A Systematic Qualitative and Economic-Based Quantitative Review of Alternative Strategies. ChemEngineering, 3(3), 76. doi:10.3390/chemengineering3030076

Orcutt, B. N., LaRowe, D. E., Biddle, J. F., Colwell, F. S., Glazer, B. T., Reese, B. K., Kirkpatrick, J. B., Lapham, L. L., Mills, H. J., Sylvan, J. B., Wankel, S. D., & Wheat, C. G. (2013). Microbial activity in the marine deep biosphere: Progress and prospects. Frontiers in Microbiology, 4. https://doi.org/10.3389/fmicb.2013.00189

Pan, X., Angelidaki, I., Alvarado-Morales, M., Liu, H., Liu, Y., Huang, X., & Zhu, G. (2016). Methane production from formate, acetate and h2/co2; focusing on kinetics and microbial characterization. Bioresource Technology, 218, 796–806. https://doi.org/10.1016/j.biortech.2016.07.032

Prinn, R. G. (2003). The cleansing capacity of the atmosphere. Annual Review of Environment and Resources, 28(1), 29–57. https://doi.org/10.1146/annurev.energy.28.011503.163425

Raghoebarsing, A., Pol, A., van de Pas-Schoonen, K., Smolders, A., Ettwig, K., Rijpstra, W., Schouten, S., Sinninghe Damsté, J., Op den Camp, H., Jetten, M., and Strous, M. (2006). A microbial consortium couples anaerobic methane oxidation to denitrification. Nature, 440, 918–921.

Rahimi, S., Modin, O., & Mijakovic, I. (2020). Technologies for biological removal and recovery of nitrogen from wastewater. Biotechnology Advances, 107570. doi:10.1016/j.biotechadv.2020.107

Rasigraf, O., Kool, D. M., Jetten, M. S., Damste, J. S., and Ettwig, K. F. (2014). Autotrophic Carbon Dioxide Fixation via the Calvin-Benson-Bassham Cycle by the Denitrifying Methanotroph "Candidatus Methylomirabilis oxyfera". Applied and Environmental Microbiology, 80(8), 2451-2460. doi:10.1128/aem.04199-13

Reeburgh, W. S. (1996). "Soft Spots" in the global methane budget. pp. 334-342. In M. E. Lidstrom and F. R. Tabita (eds.) 8th International Symposium on Microbial Growth on C-1 Compounds, Kluwer, Dordrecht.

Reeburgh, W. S. (2007). Oceanic methane Biogeochemistry. ChemInform, 38(20). https://doi.org/10.1002/chin.200720267

Reino C., Suarez-Ojeda M. E., Perez J., Carrera J. (2018). “Stable long-term operation of an upflow anammox sludge bed reactor at mainstream conditions”, Water Research,128(2018), 331-341.

Rigby, M., Prinn, R. G., Fraser, P. J., Simmonds, P. G., Langenfelds, R. L., Huang, J., Cunnold, D. M., Steele, L. P., Krummel, P. B., Weiss, R. F., O'Doherty, S., Salameh, P. K., Wang, H. J., Harth, C. M., Mühle, J., & Porter, L. W. (2008). Renewed growth of atmospheric methane. Geophysical Research Letters, 35(22). https://doi.org/10.1029/2008gl036037

Schneider, C. A., Rasband, W. S., & Eliceiri, K. W. (2012). NIH Image to ImageJ: 25 years of image analysis. *Nature Methods, 9*(7), 671–675.

Shen L., Liu S., Zhu Q., Li X., Cai C., Cheng D. , Lou L., Xu X. , Zheng P, Hu, B. (2013) Distribution and diversity of nitrite-dependent anaerobic methane-oxidising bacteria in the sediments of the Qiantang River. Microb Ecol doi:10.1007/s00248-013-0330-0

Shen, L., He, Z., Zhu, Q., Chen, D., Lou, L., Xu, X., Zheng, P., and Hu, B. (2012). Microbiology, ecology, and application of the nitrite-dependent anaerobic methane oxidation process. Frontiers in Microbiology, 3, 1-5. doi:10.3389/fmicb.2012.00269

Shen, L., Hu, B., Liu, S., Chai, X. P., He, Z. F., Ren, H. X., Zheng, P. (2016). Anaerobic methane oxidation coupled to nitrite reduction can be a potential methane sink in coastal environments. Applied Microbiology and Biotechnology, 100(16), 7171–7180.

Shen, L., Liu, S., Huang, Q., Lian, X., He, Z., Geng, S., Hu, B. (2014). Evidence for the co-occurrence of nitrite-dependent anaerobic ammonium and methane oxidation processes in a flooded paddy field. Applied and Environmental Microbiology, 80(24), 7611-7619. doi:10.1128/aem.02379-14.

Shen, L.D., Ouyang, L., Zhu, Y., Trimmer, M. (2019). Active pathways of anaerobic methane oxidation across contrasting riverbeds. The ISME journal 13 (3), 752.

Shen, L.-dong, Wu, H.-sheng, & Gao, Z.-qiu. (2014). Distribution and environmental significance of nitrite-dependent anaerobic methane-oxidising bacteria in natural ecosystems. Applied Microbiology and Biotechnology, 99(1), 133–142. https://doi.org/10.1007/s00253-014-6200-y

Shi, Y., Hu, S., Lou, J., Lu, P., Keller, J., Yuan, Z. (2013). Nitrogen removal from wastewater by coupling anammox and methane-dependent denitrification in a membrane biofilm reactor. Environ Sci Technol 47(20): 11577–11583

Shin, C., Kim, K., McCarty, P. L., Kim, J., & Bae, J. (2016). Integrity of hollow-fiber membranes in a pilot-scale anaerobic fluidized membrane bioreactor (AFMBR) after twoyears of operation. Separation and Purification Technology, 162, 101–105.

Shoda, M., (2017). Heterotrophic nitrification and aerobic denitrification by Alcaligenes faecalis No. 4. Nitrification Denitrification 31.

Smith, A. L., Skerlos, S. J., & Raskin, L. (2013). Psychrophilic anaerobic membrane bioreactor treatment of domestic wastewater. Water Research, 47(4), 1655–1665.

Strous, M., Kuenen, J. G., & Jetten, M. S. (1999). Key physiology of anaerobic ammonium oxidation. Applied and Environmental Microbiology, 65(7), 3248–3250. https://doi.org/10.1128/aem.65.7.3248-3250.1999

Tate, K. R. (2015). Soil methane oxidation and land-use change – from process to mitigation. Soil Biology and Biochemistry, 80, 260–272. doi:10.1016/j.soilbio.2014.10.010

Tchobanoglous, G., Burton, F. L., & Stensel, H. D. (2014). Wastewater engineering: Treatment and reuse.

Tchobanoglous, G., Stensel, H.D., Tsuchihashi, R., Burton, F., 2014. Wastewater Engineering: Treatment and Resource Recovery, fifth ed. McGraw Hill Education, McGraw-Hill, New York

Thauer, R. K. (1998). Biochemistry of methanogenesis: A tribute to Marjory Stephenson:1998 Marjory Stephenson prize lecture. Microbiology, 144(9), 2377–2406. https://doi.org/10.1099/00221287-144-9-2377.

Thauer, R. K. (2010). Functionalization of Methane in Anaerobic Microorganisms. Angewandte Chemie International Edition, 49(38), 6712–6713. doi:10.1002/anie.201002967.

Thauer, R. K., & Shima, S. (2006). Methane as Fuel for Anaerobic Microorganisms. Annals of the New York Academy of Sciences, 1125(1), 158–170. doi:10.1196/annals.1419.000

Torres, C. I., Kato Marcus, A., Lee, H. S., Parameswaran, P., Krajmalnik-Brown, R., & Rittmann, B. E. (2010). A kinetic perspective on extracellular electron transfer by anoderespiring bacteria. FEMS Microbiology Reviews, 34(1), 3–17.

Vaksmaa, A., Guerrero-Cruz, S., Van Alen, T. A., Cremers, G., Ettwig, K. F., Lüke, C., & Jetten, M. S. (2017). Enrichment Of Anaerobic Nitrate-Dependent Methanotrophic 'Candidatus Methanoperedens Nitroreducens' Archaea From An Italian Paddy Field Soil. Applied Microbiology and Biotechnology, 101(18), 7075-7084. doi:10.1007/s00253-017-8416-0

Valenzuela, E. I., Prieto-Davó, A., López-Lozano, N. E., Hernández-Eligio, A., Vega-Alvarado, L., Juárez, K., Cervantes, F. J. (2017). Anaerobic methane oxidation driven by microbial reduction of natural organic matter in a tropical wetland. Applied and Environmental Microbiology, 83(11). doi:10.1128/aem.00645-17

van Kessel, M. A., Stultiens, K., Slegers, M. F., Cruz, S. G., Jetten, M. S., Kartal, B., and Op den Camp, H. J. (2018). Current perspectives on the application of N-damo and anammox in wastewater treatment. Current Opinion in Biotechnology, 50, 222-227. doi:10.1016/j.copbio.2018.01.031

Velasco, P., Jegatheesan, V., & Othman, M. (2018). Recovery of dissolved methane from anaerobic membrane bioreactor using degassing membrane contactors. Frontiers in Environmental Science, 6. https://doi.org/10.3389/fenvs.2018.00151

Wahlen, M. (1997). The global methane cycle. Annual Review of Earth and Planetary Sciences Vol. 21:407-426, https://doi.org/10.1146/annurev.ea.21.050193.002203.

Wang, D., Wang, Y., Liu, Y., Ngo, H. H., Lian, Y., Zhao, J., Chen, F., Yang, Q., Zeng, G., and Li, X. (2017). Is denitrifying anaerobic methane oxidation-centered technologies a solution for the sustainable operation of wastewater treatment Plants. Bioresource Technology, 234, 456-465. doi:10.1016/j.biortech.2017.02.059

Wang, S., Wu, Q., Lei, T., Liang, P., Huang, X., 2015. Enrichment of denitrifying methanotrophic bacteria from Taihu sediments by a membrane biofilm bioreactor at ambient temperature. Environ. Sci. Pollut. Res. Int. 23 (6), 5627–5634.

Wang, X., Wang, S., Xue, T., Li, B., Dai, X., & Peng, Y. (2015). Treating low carbon/nitrogen (C/N) wastewater in simultaneous nitrification-endogenous denitrification and phosphorous Removal (sndpr) systems by strengthening Anaerobic intracellular carbon storage. Water Research, 77, 191–200. https://doi.org/10.1016/j.watres.2015.03.019

Wang, Y., Huang, P., Ye, F., Jiang, Y., Song, L.Y., Op den Camp, H.J.M., Zhu, G.B., Wu, S.J., (2016). Nitrite-dependent anaerobic methane oxidizing bacteria along the water level fluctuation zone of the Three Gorges Reservoir. Applied Microbiology and Biotechnology 100, 1977–1986.

Wang, Y., Zhu, G., Harhangi, H. R., Zhu, B., Jetten, M. S., Yin, C., & Op den Camp, H. J. (2012). Co-occurrence and distribution of nitrite-dependent anaerobic ammonium and methane-oxidizing bacteria in a paddy soil. FEMS Microbiology Letters, 336(2), 79-88. doi:10.1111/j.1574-6968.2012.02654.x

Westerholm, M., & Schnürer, A. (2019). Microbial Responses to Different Operating Practices for Biogas Production Systems. In J. R. Banu (Ed.), *Anaerobic Digestion* (Issue September, p. 13). IntechOpen. https://www.intechopen.com/books/advanced-biometric-technologies/liveness-detection-in-biometrics

Wilhelm, E., Battino, R., & Wilcock, R. J. (1977). Low-pressure solubility of gases in liquid water. Chemical Reviews, 77(2), 219-262. doi:10.1021/cr60306a003

Winkler, M., Ettwig, K., Vannecke, T., Stultiens, K., Bogdan, A., Kartal, B., Volcke, E., 2015. Modelling simultaneous anaerobic methane and ammonium removal in a granular sludge reactor. Water Res. 73, 323–331. https://doi.org/10.1016/j. watres.2015.01.039

Wu, B., Zamani, F., Lim, W., Liao, D., Wang, Y., Liu, Y., Chew, J.W., Fane, A.G. (2017). Effect of mechanical scouring by granular activated carbon (GAC) on membrane fouling mitigation. Desalination 403, 80‑87.

Wu, M. L., van Teeseling, M. C., Willems, M. J., van Donselaar, E. G., Klingl, A., Rachel, R., Geerts, W. J., Jetten, M. S., Strous, M., and van Niftrik, L. (2012b). Ultrastructure of the denitrifying methanotroph "Candidatus Methylomirabilis oxyfera", a novel polygon-shaped bacterium. J. Bacteriol., 194, 284-291.

Wu, M., Ettwig, K., Jetten, M., Strous, M., Keltjens, J., van Niftrik, L. (2011). A new intraaerobic metabolism in the nitrite-dependent anaerobic methane-oxidizing bacterium Candidatus 'Methylomirabilis oxyfera. Biochem. Soc. Trans. 39 (1), 243–248.

Wu, M., van Alen, T.A., van Donselaar, E., Strous, M., Jetten, M., van Niftrik, L., (2012a). Co-localization of particulate methane monooxygenase and cd1 nitrite reductase in the denitrifying methanotroph 'Candidatus Methylomirabilis oxyfera'. FEMS Microbiol. Lett. 334 (1), 49–56..

Wu, Q., Chang, J., Yan, X., Ailijiang, N., Fan, Q., Wang, S., Huang, X. (2016). Electrical stimulation enhanced denitrification of nitrite-dependent anaerobic methane-oxidizing bacteria. Biochemical Engineering Journal, 106, 125–128. doi:10.1016/j.bej.2015.11.014

Xie, F., Ma, A., Zhou, H., Liang, Y., Yin, J., Ma, K., Zhuang, G. (2020). Niche differentiation of denıtrıfyıng anaerobic methane oxidizing bacteria and archaea leads to effectıve methane filtration in a tibetan alpıne wetland. Environment International, 140, 105764. doi:10.1016/j.envint.2020.105764.

Xie, G., Cai, C., Hu, S., & Yuan, Z. (2016). Complete nitrogen removal from synthetıc anaerobic sludge digestion liquor through ıntegrating anammox and denitrifying anaerobic methane oxidation in a membrane biofilm reactor. Environmental Science & Technology, 51(2), 819-827. doi:10.1021/acs.est.6b04500

Xie, G.-J., Liu, T., Cai, C., Hu, S., Yuan, Z., 2018. Achieving high-level nitrogen removal in mainstream by coupling anammox with denitrifying anaerobic methane oxidation in a membrane biofilm reactor. Water Res. 131, 196-204.

Xu, S., Lu, W., Muhammad, F. M., Liu, Y., Guo, H., Meng, R., & Wang, H. (2018). New molecular method to detect denitrifying anaerobic methane oxidation bacteria from different environmental niches. Journal of Environmental Sciences,65, 367-374. doi:10.1016/j.jes.2017.04.016

Xu, S., Lu, W., Mustafa, M. F., Caicedo, L. M., Guo, H., Fu, X., & Wang, H. (2017). Co-existence of Anaerobic Ammonium Oxidation Bacteria and Denitrifying Anaerobic Methane Oxidation Bacteria in Sewage Sludge: Community Diversity and Seasonal Dynamics. Microbial Ecology,74(4), 832-840. doi:10.1007/s00248-017-1015-x

Yang, J., Jiang, H., Wu, G., Hou, W., Sun, Y., Lai, Z., & Dong, H. (2012). Co-occurrence of nitrite-dependent anaerobic Methane oxidizing and anaerobic AMMONIA oxidizing bacteria in two qinghai-tibetan saline lakes. Frontiers of Earth Science, 6(4), 383–391. https://doi.org/10.1007/s11707-012-0336-9

Yu, H., Kashima, H., Regan, J.M., Hussain, A., Elbeshbishy, E., Lee, H., 2017. Kinetic study on anaerobic oxidation of methane coupled to denitrification. Enzym. Microb. Technol. 104, 47–55. https://doi.org/10.1016/j.enzmictec.2017.05.005

Zhang, L., Yang, J., Hira, D., Fujii, T., Zhang, W., & Furukawa, K. (2011). High-rate nitrogen removal from anaerobic digester liquor using an up-flow anammox reactor with polyethylene sponge as a biomass carrier. Journal of Bioscience and Bioengineering, 111(3), 306–311. https://doi.org/10.1016/j.jbiosc.2010.10.010

Zhang, M., Luo, Y., Lin, L.a., Lin, X., Hetharua, B., Zhao, W., et al., (2018). Molecular and stable isotopic evidence for the occurrence of nitrite-dependent anaerobic methaneoxidizing bacteria in the mangrove sediment of Zhangjiang Estuary, China. Appl. Microbiol. Biotechnol. 102, 2441–2454.

Zhang, W., Jin, Y., & D. Rouse, J. (2015). Granular activated carbon as nucleus for formation of anammox granules in an expanded granular-sludge-bed reactor. Global Nest Journal, 17(3), 508–514. https://doi.org/10.30955/gnj.001444

Zheng, Y., Hou, L., Chen, F., Zhou, J., Liu, M., Yin, G., Gao, J., Han, P. (2020). Denitrifying anaerobic methane oxidation in intertidal marsh soils: Occurrence and environmental significance. Geoderma 357, 113943

Zhou, L., Wang, Y., Long, X.E., Guo, J., Zhu, G. (2014). High abundance and diversity of nitrite-dependent anaerobic methane-oxidizing bacteria in a paddy field profile. FEMS Microbiol. Lett. 360 (1), 33–41.

Zhou, L., Wang, Y., Long, X.E., Guo, J., Zhu, G. (2014). High abundance and diversity of nitrite-dependent anaerobic methane-oxidizing bacteria in a paddy field profile. FEMS Microbiol. Lett. 360 (1), 33–41.

Zhu Q, Shen L, Baolan HU, Lou L. (2013) Molecular detection of denitrifying anaerobic methane oxidizing bacteria in the sediment of West Lake. Hangzhou, Acta Scientiae Circumstantiae

Zhu, B., Dijk, G. V., Fritz, C., Smolders, A. J., Pol, A., Jetten, M. S., and Ettwig, K. F. (2012). Anaerobic Oxidization of Methane in a Minerotrophic Peatland: Enrichment of Nitrite-Dependent Methane-Oxidizing Bacteria. Applied and Environmental Microbiology, 78(24), 8657-8665. doi:10.1128/aem.02102-12

Zhu, B., Sánchez, J., van Alen, T. A., Sanabria, J., Jetten, M. S., Ettwig, K. F., and Kartal, B. (2011). Combined anaerobic ammonium and methane oxidation for nitrogen and methane removal. Biochemical Society Transactions, 39(6), 1822-1825. doi:10.1042/bst20110704

Zhu, G., Wang, M., Li, Y., Wang, Y., Fei, H., & Wang, S. (2018). Denitrifying anaerobic methane oxidizing in global upland soil: Sporadic and non-continuous distribution with low influence. Soil Biology and Biochemistry, 119, 90-100. doi:10.1016/j.soilbio.2018.01.011

Zhu, G.B., Zhou, L.L., Wang, Y., Wang, S.Y., Guo, J.H., Long, X.E., Sun, X.B., Jiang, B., Hou, Q.Y., Jetten, M.S.M., Yin, C.Q. (2015). Biogeographical distribution of denitrifying anaerobic methane oxidizing bacteria in Chinese wetland ecosystems. Environmental Microbiology Reports 7, 128–138.

Zhu, Q., Shen, L., Hu, B., Lou, L., and Cheng, D. (2013). Molecular detection of denitrifying anaerobic methane oxidizing bacteria in the sediment of West Lake. Acta Sci. Circumst., 33, 1321-1325.

APPENDICES

A. Sampling Locations

Figure A.1 a) Freshwater sediment sampling locations in Eymir Lake, Ankara and, b) Paddy Field soil sampling locations from paddy field in Kızılırmak District, Çankırı

Table A.1 Calculation of the VS of the inoculum sources containing 600 mg of each seed sources

Seed stock	PS			FS			AD			RS			Seed stock		
	VS of the seed source (g/L)	Volume in the seed stock (ml)	VS in the seed stock (mg)	VS of the seed source (g/L)	Volume in the seed stock (ml)	VS in the seed stock (mg)	VS of the seed source (g/L)	Volume in the seed stock (ml)	VS in the seed stock (mg)	VS of the seed source (g/L)	Volume in the seed stock (ml)	VS in the seed stock (mg)	Total VS (mg)	Total volume (ml)	VS(g/L)
1	40.3	14.9	600	-			-			-			600	14.9	40.3
2	-			20.8	28.8	600	-			-			600	28.8	20.8
3	-			-			14.5	41.3	600	-			600	41.3	14.5
4	-			-			-			15.6	38.4	600	600	38.4	15.6
5	40.3	14.9	600	20.8	28.8	600	-			-			1200	43.7	27.5
6	-			20.8	28.8	600	14.5	41.3	600	-			1200	70.2	17.1
7	-			20.8	28.8	600	15.6	38.4	600	-			1200	67.2	17.8
8	40.3	14.9	600	20.8	28.8	600	14.5	41.3	600	-			1800	85.1	21.2
9	40.3	14.9	600	20.8	28.8	600				15.6	38.4	600	1800	82.1	21.9
10	-			-			14.5	41.3	600	15.6	38.4	600	1200	79.7	15
11	40.3	14.9	600	-						15.6	38.4	600	1200	53.3	22.5
12	40.3	14.9	600	-			14.5	41.3	600	15.6	38.4	600	1800	94.6	19

B. Calculation of the Mole Fraction Solubility Coefficient of Methane

Table B.1 Coefficients in the equation

Gas no.	Gas	Temp range T/K	A cal K^{-1} mol^{-1}	B cal mol^{-1}	C cal K^{-1} mol^{-1}	D cal K^{-2} mol^{-1}	% σ [b]	Ref (no. data pts used [c])
1	Helium	273–334	−233.163	8737.84	32.2652	−0.0119726	0.67	72(6), 75(3), 76(5), 73(29), 74(3)
2	Neon	273–339	−310.827	12766.8	43.6185	−0.0127534	0.58	72(6), 76(12), 73(28)
3	Argon	274–347	−336.760	16170.1	46.2117	−0.00608793	0.53	*j*(9), 85(6), 77(15), 72(8), *d*(5), 78(8), 71(1)
4	Krypton	274–348	−270.967	15992.9	33.2892	0.0260485	0.47	72(10), 79(19)
5	Xenon	285–345	−360.119	18744.6	49.0332	−0.00311323	0.67	72(8), 80(3)
6	Radon	276–370	−499.309	25864.2	69.3241	0.00101227	1.6	81d(9), 81e(37)
7	Hydrogen	274–339	−357.802	13897.5	52.2871	−0.0298936	0.44	82(9), *e*(2), 83(5), *f*(1), 84(14)
8	Nitrogen	273–346	−327.850	16757.6	42.8400	0.0167645	0.94	85(5), 86(6), 77(32), 82(7), 87(10)
9	Oxygen	274–348	−286.942	15450.6	36.5593	0.0187662	0.31	77(15), 90(16), 82(7), 87(13), 91(22)
10	Ozone [g]	277–293	*−29.7374*	*3905.44*				*h*(2)
11	Carbon monoxide	273–353	−341.325	16487.3	46.3757		0.68	92(8), 93(1)
12	Carbon dioxide [i]	273–353	−317.658	17371.2	43.0607	−0.00219107	0.54	82(8), 95(8), 94(1)
13	Methane	275–353	−365.183	18106.7	49.7554	−0.000285033	1.8	98(6), *k*(3), 82(7), 92(5), 99(4), 251(4), 304(5), 100(5)
14	Ethane	275–353	−533.392	26565.0	74.6240	−0.00457313	1.6	98(4), 82(6), 92(5), 99(4), 101(5), 100(5)

$$R \times \ln x_2 = A + \frac{B}{T} + C \times \ln\frac{T}{K} + D \times T$$

Where;
R is the gas constant, T is the thermodynamic temperature, x_2 is the mole fraction solubility at 1 atm partial pressure of the gas

C. FISH Procedure

Figure C.1 Probe content of each hybridization mix used in slides

Hybridization mix preparation to be used for 1 sample for each slide is given below;

Slide 1: 8 µl FA(40%) + 2 µl D-BACT 193+ 2 µl EUB Mix + 2 µl NC10-1027

Slide 2: 8 µl FA(40%) + 2 µl D-ARCH 872 + 2 µl D-ARCH 915

Slide 3: 8 µl FA(40%) + 2 µl EUB Mix

Slide 4: 8 µl FA(40%) + 2 µl D-ARCH 915

D. Quantification of Target Microorganisms

Microscopic Visualization

Stained slides which are stored at -20°C were brought to room temperature in the dark room for microscopic visualization. Carl Zeiss Axio Vision A1 UV was used to observe the prepared slides. The microscope had objective lenses of 4x/0.1, 10x/0.25, 40x/0.65 and 100x/1. General Bacteria, General Archaea, and Damo-Archaea (*M.nitroreducens*) hybridized with GFP-labeled probes were visualized as green through blue colored filter. Damo-Bacteria (*M.oxyfera*) hybridized with Alexa-Fluor 350 probes were visualized as blue through UV filter. NC10 phylum bacteria and Damo-Archaea hybridized with Cy5-labeled probes were visualized as green through blue filter. All microorganisms stained with DAPI were visualized as blue in color through UV filter. Slides were viewed at 40x magnification. At least 3 representative microscopic images were captured for each slide. Pixel areas were determined using ImageJ for specific probes using 3 representative images (captured from the same slide). Average pixel area obtained from image analysis of 3 representative images were used in the quantification of the target microorganisms.

Image Analysis

Microscopic images were disposed and analyzed with ImageJ 1.52a software (Schneider et al., 2012). During ImageJ analysis the microorganisms are classified depending on their fluorescence signal intensity. Target microorganisms were determined in comparison to threshold intensity (Zhou et al., 2007). Threshold value of 8-bit image was used to cover microorganisms with reference to the original image which is also converted to 8-bit. Finally, pixel area analysis of the image was performed and extracted from the summary table of imageJ as shown in Figure D.2.

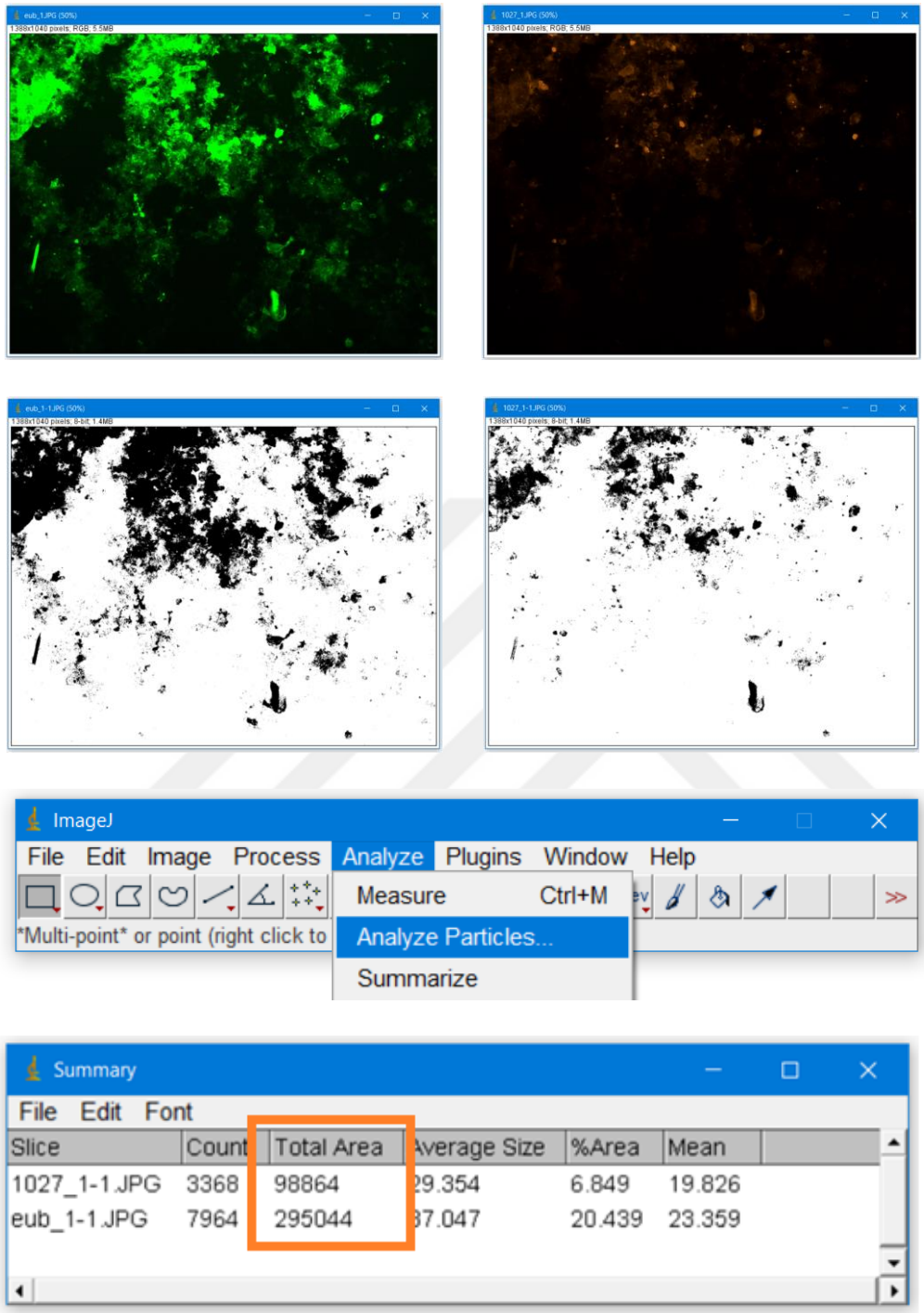

Figure D.1 A sample screenshot of image analyses performed by ImageJ

Microbial composition of target species

In the calculations, relative abundances of microbial communities were calculated by assuming that total microbial population includes Bacteria and Archaea summing up as 100%.

Using the images captured, General Bacteria to DAPI ratio and General Archaea to DAPI ratio was calculated. Then, these ratios were used in the normalization to determine the content of General Bacteria and General Archaea in the total microbial population (100%). Formulas used in the calculations are presented below;

$$\frac{\text{General Bacteria}}{\text{DAPI}}(\%) = \frac{\text{Pixel area of General Bacteria}}{\text{Pixel area of DAPI}} \times 100 \text{ (Equation D.1)}$$

$$\frac{\text{General Archaea}}{\text{DAPI}}(\%) = \frac{\text{Pixel area of General Archaea}}{\text{Pixel area of DAPI}} \times 100 \text{ (Equation D.2)}$$

$$\frac{\text{General Bacteria}}{\text{Total Microbial Population}}(\%) = \frac{\frac{\text{General Bacteria}}{\text{DAPI}}(\%)}{\frac{\text{General Bacteria}}{\text{DAPI}}(\%) + \frac{\text{General Archaea}}{\text{DAPI}}(\%)} \times 100 \text{ (Equation D.3)}$$

$$\frac{\text{General Archaea}}{\text{Total Microbial Population}}(\%) = \frac{\frac{\text{General Archaea}}{\text{DAPI}}(\%)}{\frac{\text{General Bacteria}}{\text{DAPI}}(\%) + \frac{\text{General Archaea}}{\text{DAPI}}(\%)} \times 100 \text{ (Equation D.4)}$$

Using the images captured from Slide 3, ratio of Damo-Archaea to General Archaea in the total microbial population (%) was calculated as shown below.

$$\frac{\text{Damo-Archaea}}{\text{General Archaea}}(\%) = \frac{\text{Pixel area of Damo-Archaea}}{\text{Pixel area of General Archaea}} \times 100 \quad \text{(Equation D.5)}$$

Using the images captured from Slide 2, Ratio of NC10 Phylum to General Bacteria (%), ratios of Damo-Bacteria to NC10 Phylum (%) and Ratio of Damo-Bacteria to General Bacteria (%) are calculated as shown below;

$$\frac{\text{NC10 Phylum}}{\text{General Bacteria}}(\%) = \frac{\text{Pixel area of NC10 Phylum}}{\text{Pixel area of General Bacteria}} \times 100 \quad \text{(Equation D.6)}$$

$$\frac{\text{Damo-Bacteria}}{\text{General Bacteria}}(\%) = \frac{\text{Pixel area of Damo-Bacteria}}{\text{Pixel area of General Bacteria}} \times 100 \quad \text{(Equation D.7)}$$

$$\frac{\text{Damo-Bacteria}}{\text{NC10 Phylum}}(\%) = \frac{\text{Pixel area of Damo-Bacteria}}{\text{Pixel area of General Bacteria}} \times 100 \quad \text{(Equation D.8)}$$

Finally, content of target species (Damo-Bacteria, Damo-Archaea and NC10 Pylum) in the total microbial population (%) was calculated using the formulas given below;

$$\frac{\text{Damo-Bacteria}}{\text{Total Microbial Population}}(\%) = \frac{\frac{\text{General Bacteria}}{\text{Total Microbial Population}}(\%) \times \frac{\text{Damo-Bacteria}}{\text{General Bacteria}}(\%)}{100}$$

Equation D.9

$$\frac{\text{Damo-Archaea}}{\text{Total Microbial Population}}(\%) = \frac{\frac{\text{General Archaea}}{\text{Total Microbial Population}}(\%) \times \frac{\text{Damo-Archaea}}{\text{General Archaea}}(\%)}{100}$$

Equation D.10

$$\frac{\text{NC10 Phylum}}{\text{Total Microbial Population}}(\%) = \frac{\frac{\text{General Bacteria}}{\text{Total Microbial Population}}(\%) \times \frac{\text{NC10 Phylum}}{\text{General Bacteria}}(\%)}{100}$$

Equation D.11

Additionally,

Archaea content in total microbial population excluding Damo-Archaea is defined as "Other Archaea" and its' content in the total microbial population is calculated as shown below;

$$\frac{\text{Other Archaea}}{\text{Total Microbial Population}}(\%) = \frac{\text{General Archaea}}{\text{Total Microbial Population}}(\%) - \frac{\text{Damo-Archaea}}{\text{Total Microbial Population}}$$

Equation D.12

Bacteria content in total microbial population excluding NC10 phylum bacteria is defined as "Other Bacteria" its' content in the total microbial population is calculated as shown below;

$$\frac{\text{Other Bacteria}}{\text{Total Microbial Population}}(\%) = \frac{\text{General Bacteria}}{\text{Total Microbial Population}}(\%) - \frac{\text{Damo-Bacteria}}{\text{Total Microbial Population}}(\%)$$

Equation D.13

NC10 Phylum bacteria content excluding Damo-Bacteria is defined as "Other NC10" and its' content in the total microbial population is calculated as shown below;

$$\frac{\text{Other NC10}}{\text{Total Microbial Population}}(\%) = \frac{\text{NC10 Phylum}}{\text{Total Microbial Population}}(\%) - \frac{\text{Damo-Bacteria}}{\text{Total Microbial Population}}(\%)$$

Equation D.14

Table D.1 Summary of the data calculated using the areas obtained for 3 representative images in FISH analyses of the seed sources

Seed Source		NC10 Phylum/ T.M.P[a]	Damo-Bacteria/ T.M.P[a]	Damo-Archaea/ T.M.P[a]	NC10 Phylum/ General Bacteria	Damo-Bacteria/ General Bacteria	Damo-Bacteria/ NC10 Phylum	Damo-Archaea/ General Archaea	General Bacteria/ DAPI	General Archaea/ DAPI
AD	Average (%)	74.4	72.4	25.6	34.0	28.5	82.6	35.9	27.5	33.8
	Standard Deviation (%)	4.1	7.7	4.1	5.9	8.2	10.3	2.8	4.3	6.4
	Coefficient of Variation (%)	5.5	10.6	16.0	17.4	28.8	12.4	7.9	15.7	18.8
FS	Average (%)	53.7	39.5	46.3	43.5	14.4	33.1	30.8	35.4	19.2
	Standard Deviation (%)	5.3	5.6	5.3	4.9	1.4	2.0	4.5	3.9	0.9
	Coefficient of Variation (%)	9.8	14.1	11.4	11.2	9.9	6.0	14.7	11.2	4.6
PS	Average (%)	76.4	20.5	23.6	25.0	7.6	30.2	37.4	6.4	4.6
	Standard Deviation (%)	4.8	3.8	4.8	3.5	1.8	3.2	2.0	1.2	1.5
	Coefficient of Variation (%)	6.3	18.6	20.4	13.9	23.3	10.7	5.5	19.4	31.7
RS	Average (%)	59.4	19.3	40.6	43.7	26.2	59.8	24.5	36.2	36.9
	Standard Deviation (%)	6.2	4.4	6.2	5.5	4.5	6.8	2.8	8.8	6.4
	Coefficient of Variation (%)	10.5	22.8	15.4	12.6	17.1	11.4	11.3	24.4	17.2

[a] T.M.P refers to Target Microbial Population

Table D.2 Summary of the data calculated using the areas obtained for 3 representative images in FISH analyses in Enrichment-1

Cycle		General Archaea/ DAPI	General Bacteria/ DAPI	Damo-Archaea/ General Archaea	NC10 Phylum/ General Bacteria	Damo-Bacteria/ General Bacteria	Damo-Bacteria/ NC10 Phylum
10	Average (%)	51.20	28.70	42.88	65.44	19.31	29.68
	Standard Deviation (%)	5.40	0.80	3.99	3.12	3.20	5.97
	Coefficient of Variation (%)	10.55	2.79	9.31	4.76	16.55	20.11
28	Average (%)	58.20	39.40	34.57	67.73	48.60	71.67
	Standard Deviation (%)	3.80	5.80	5.02	3.79	4.33	2.48
	Coefficient of Variation (%)	6.53	14.72	14.53	5.60	8.90	3.46
60	Average (%)	54.80	34.60	35.16	81.76	42.59	52.43
	Standard Deviation (%)	11.40	3.10	2.66	4.78	4.49	8.47
	Coefficient of Variation (%)	20.80	8.96	7.57	5.85	10.54	16.15
100	Average (%)	56.35	29.27	31.91	42.60	22.12	51.64
	Standard Deviation (%)	9.01	4.98	3.19	7.50	7.03	13.73
	Coefficient of Variation (%)	15.98	17.00	10.00	17.60	31.79	26.58
145	Average (%)	15.94	12.66	20.23	90.77	25.49	28.04
	Standard Deviation (%)	2.57	8.14	1.34	2.28	4.31	4.39
	Coefficient of Variation (%)	16.11	64.28	6.64	2.51	16.92	15.65
165	Average (%)	19.91	27.90	30.43	48.00	39.23	81.44
	Standard Deviation (%)	1.79	1.23	0.80	6.62	7.03	3.76
	Coefficient of Variation (%)	8.98	4.42	2.64	13.79	17.93	4.62

Table D.3 Summary of the data calculated using the areas obtained for 3 representative images in FISH analyses in Enrichment-2

Cycle		General Archaea/ DAPI	General Bacteria/ DAPI	Damo-Archaea/ General Archaea	NC10 Phylum/ General Bacteria	Damo-Bacteria/ General Bacteria	Damo-Bacteria/ NC10 Phylum
3	Average (%)	43.70	49.50	42.59	76.05	33.31	43.58
	Standard Deviation (%)	8.00	1.40	1.51	8.31	7.88	8.12
	Coefficient of Variation (%)	18.31	2.83	3.55	10.92	23.66	18.63
8	Average (%)	44.00	78.60	35.76	79.61	26.84	33.94
	Standard Deviation (%)	7.90	3.50	1.78	6.38	4.20	6.52
	Coefficient of Variation (%)	17.95	4.45	4.98	8.01	15.65	19.22
10	Average (%)	20.49	37.23	34.66	60.93	34.75	57.58
	Standard Deviation (%)	1.60	4.41	2.15	5.07	3.12	10.01
	Coefficient of Variation (%)	7.80	11.84	6.19	8.32	8.99	17.39
14	Average (%)	29.16	27.78	27.26	64.03	32.87	51.41
	Standard Deviation (%)	0.11	3.93	1.68	1.68	3.45	6.34
	Coefficient of Variation (%)	0.38	14.14	6.18	2.62	10.49	12.33
18	Average (%)	16.61	24.89	45.38	65.01	29.94	45.77
	Standard Deviation (%)	2.81	3.08	2.42	4.35	6.80	7.92
	Coefficient of Variation (%)	16.89	12.37	5.34	6.69	22.73	17.31
20	Average (%)	50.97	35.93	48.57	76.61	15.10	19.72
	Standard Deviation (%)	1.90	4.24	3.84	2.46	3.00	3.90
	Coefficient of Variation (%)	3.74	11.80	7.91	3.21	19.89	19.76

E. Nitrite and Nitrate Concentrations for Test and Control Reactors in Batch Reactor Experiments

Table E.1 Nitrite and nitrate concentrations of test reactors in batch reactor experiments using different seed sources

Reactors	t= 0 d [a]		t= 5 d [a]		t= 8 d [a]		t= 8 d [b]		t=10 d [a]		t=15 d [a]	
	NO_2-N	NO_3-N	NO_2-N	NO_3-N	NO_2-N	NO_3-N	NO_2-N	NO_3-N	NO_2-N	NO_3-N	NO_2-N	NO_3-N
T-1	10.13	31.16	1.8	7.2	0.3	0.7	10.3	30.7	3.7	7.3	1.7	6.0
T-2	10.05	31.93	0.4	7.3	0.4	0.8	10.4	30.7	0.1	0.1	1.0	3.0
T-3	9.55	32.70	0.0	0.1	0.0	0.1	10.0	30.1	0.0	2.7	0.2	0.1
T-4	11.74	26.10	0.2	0.1	0.1	0.1	10.1	30.1	4.8	2.0	0.1	0.1
T-5	10.82	19.50	7.3	0.0	1.3	0.0	11.2	30.0	11.0	18.4	0.0	0.0
T-6	9.39	20.60	0.0	0.0	0.1	0.0	10.1	30.0	0.0	0.1	0.0	0.0
T-7	11.13	21.69	0.0	0.0	0.1	0.0	10.1	30.0	10.1	4.6	0.0	0.0
T-8	10.23	27.72	0.0	0.1	0.0	0.1	10.0	30.1	7.9	19.4	0.0	0.1
T-9	8.43	33.74	0.0	13.0	0.5	0.5	10.5	30.5	0.2	0.8	2.1	2.8
T-10	6.14	34.01	0.1	13.0	0.4	0.4	10.3	30.4	0.7	16.4	1.1	1.4
T-11	6.80	34.27	0.1	0.0	0.0	0.0	10.0	30.0	3.8	22.8	0.0	0.0
T-12	6.51	28.14	0.0	0.0	0.0	0.0	10.0	30.0	8.4	24.1	0.0	0.0

[a] Average results of replicate analyses

[b] Theoretical initial concentration after the second feeding of the reactors on Day 8. (Note that feeding was performed assuming the final concentrations at Day 8 are 0 mg/L based on the consumption between Day 0 and Day 5. Therefore, equal amount of nitrogen source was added to the reactors in the second feeding to set the initial concentrations of NO_2-N and NO_3-N to 10 and 30 mg/L respectively. This approach was taken to save time, since the nitrite and nitrate analysis for the samples taken on Day-8 would have taken more than 1 day. After the feeding on Day 8, liquid samples taken on Day 8 were analyzed for nitrite and nitrate. Theoretical initial concentration was calculated based on the actual nitrite and nitrate analysis results for Day 8.)

Table E.2 Nitrite and nitrate concentrations of control reactors in batch reactor experiments using different seed sources

Reactors	t= 0 d [a]		t= 5 d [a]		t= 8 d [a]		t= 8 d [b]		t=10 d [a]		t=15 d [a]	
	NO_2-N	NO_3-N	NO_2-N	NO_3-N	NO_2-N	NO_3-N	NO_2-N	NO_3-N	NO_2-N	NO_3-N	NO_2-N	NO_3-N
C-1	10.13	31.16	8.2	30.6	7.1	30.3	16.8	59.0	15.5	58.0	7.4	38.6
C-2	10.05	31.93	1.1	0.2	0.4	0.1	10.4	30.1	2.6	28.1	1.8	5.0
C-3	9.55	32.70	0.0	0.2	0.1	0.1	10.1	30.1	0.5	14.2	0.0	0.3
C-4	11.74	26.10	0.2	0.1	0.1	0.0	10.1	30.0	0.2	0.1	0.1	0.1
C-5	10.82	19.50	0.4	0.2	0.1	0.0	10.1	30.0	11.9	25.9	10.6	18.5
C-6	9.39	20.60	0.0	0.1	0.0	0.0	10.0	30.0	7.6	7.6	0.1	0.2
C-7	11.13	21.69	0.0	0.1	0.1	0.0	10.1	30.0	0.0	0.0	0.0	0.0
C-8	10.23	27.72	0.0	0.0	0.1	0.1	10.1	30.1	10.0	27.8	1.1	1.4
C-9	8.43	33.74	0.0	0.1	0.1	0.0	10.0	30.0	3.7	2.6	0.0	0.1
C-10	6.14	34.01	0.0	0.1	0.0	0.1	10.0	30.1	0.2	2.3	0.0	0.0
C-11	6.80	34.27	0.1	0.1	0.0	0.0	10.0	30.0	0.0	0.1	0.0	0.0
C-12	6.51	28.14	0.0	0.1	0.0	0.1	10.0	30.1	2.8	7.5	0.0	0.1

[a] Average results of replicate analyses

[b] Theoretical initial concentration after the second feeding of the reactors on Day 8. (Note that feeding was performed assuming the final concentrations at Day 8 are 0 mg/L based on the consumption between Day 0 and Day 5. Therefore, equal amount of nitrogen source was added to the reactors in the second feeding to set the initial concentrations of NO_2-N and NO_3-N to 10 and 30 mg/L respectively. This approach was used to save time, since the nitrite and nitrate analysis for the samples withdrawn on Day-8 would have last more than 1 day. After the feeding on Day 8, liquid samples withdrawn on Day 8 were analyzed for nitrite and nitrate. Theoretical initial concentration was calculated based on the actual nitrite and nitrate analysis results for Day 8.)

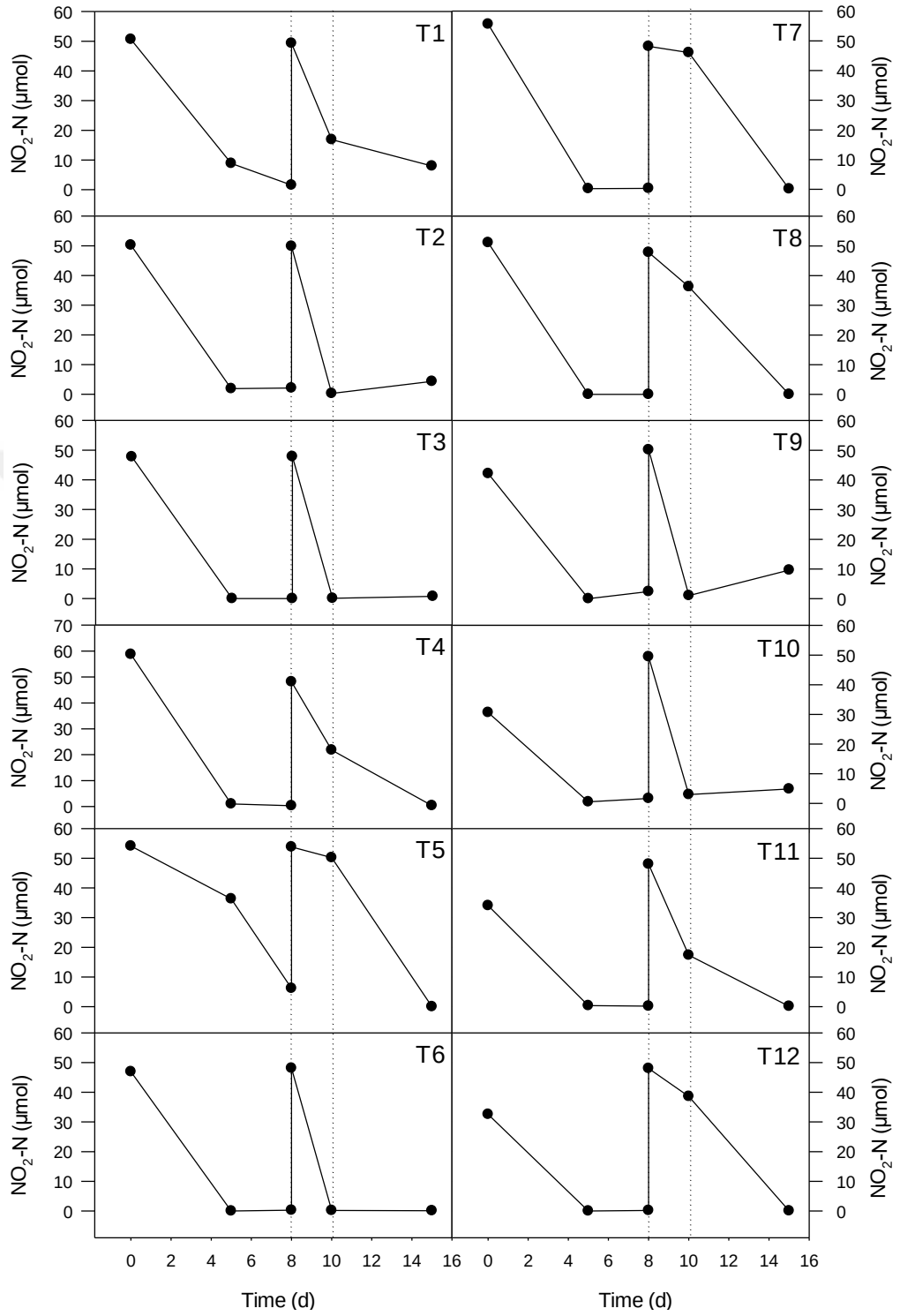

Figure E-1 Graphs showing the nitrite consumption trend in test reactors (NO_2 consumption rates in test reactors were calculated between dotted lines (Day 8-10). Sudden increase in concentration on Day 8 indicates the second feeding)

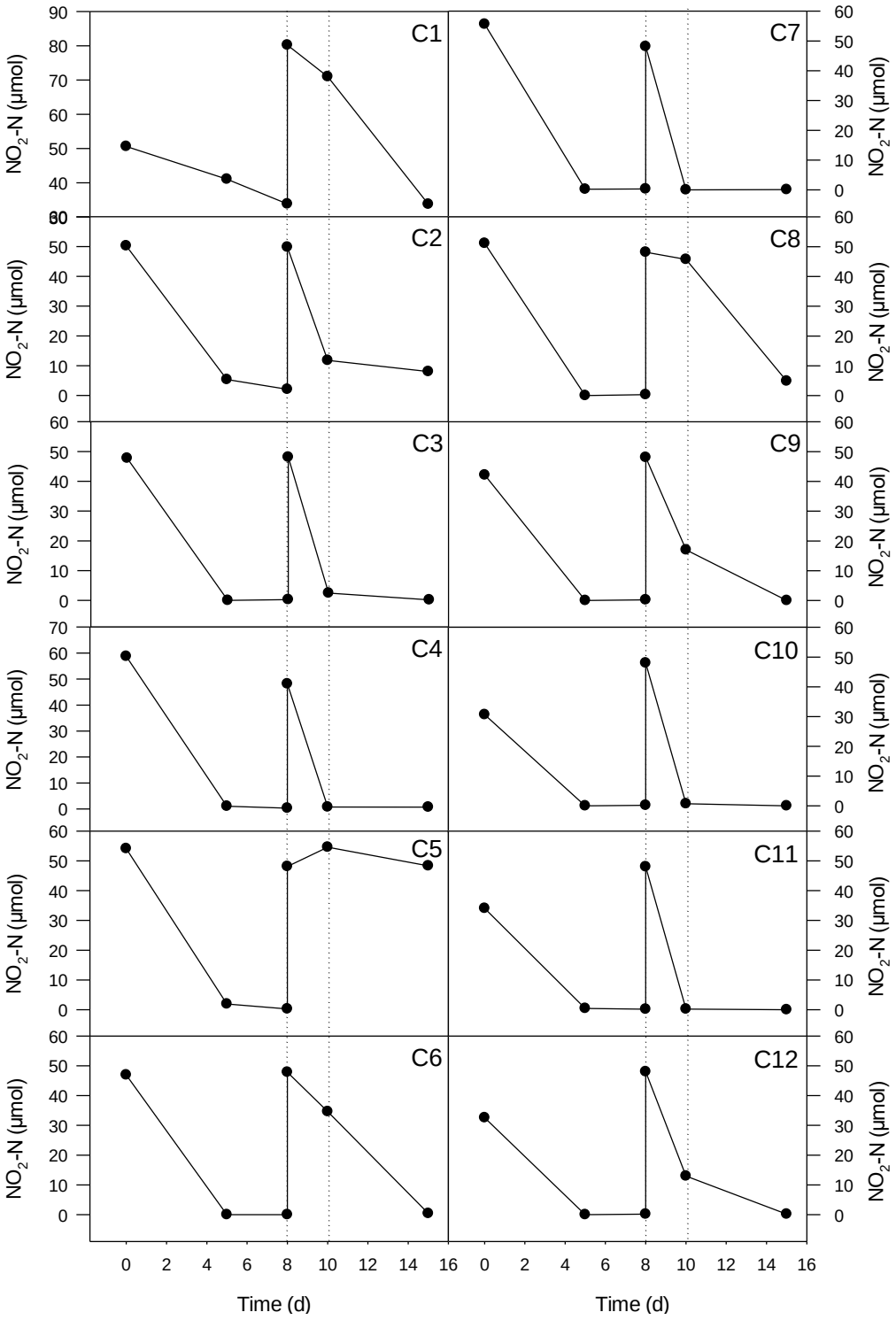

Figure E.2 Graphs showing the nitrite consumption trend in control reactors (NO_2 consumption rates in control reactors were calculated between dotted lines (Day 8-10). Sudden increase in concentration on Day 8 indicates the second feeding)

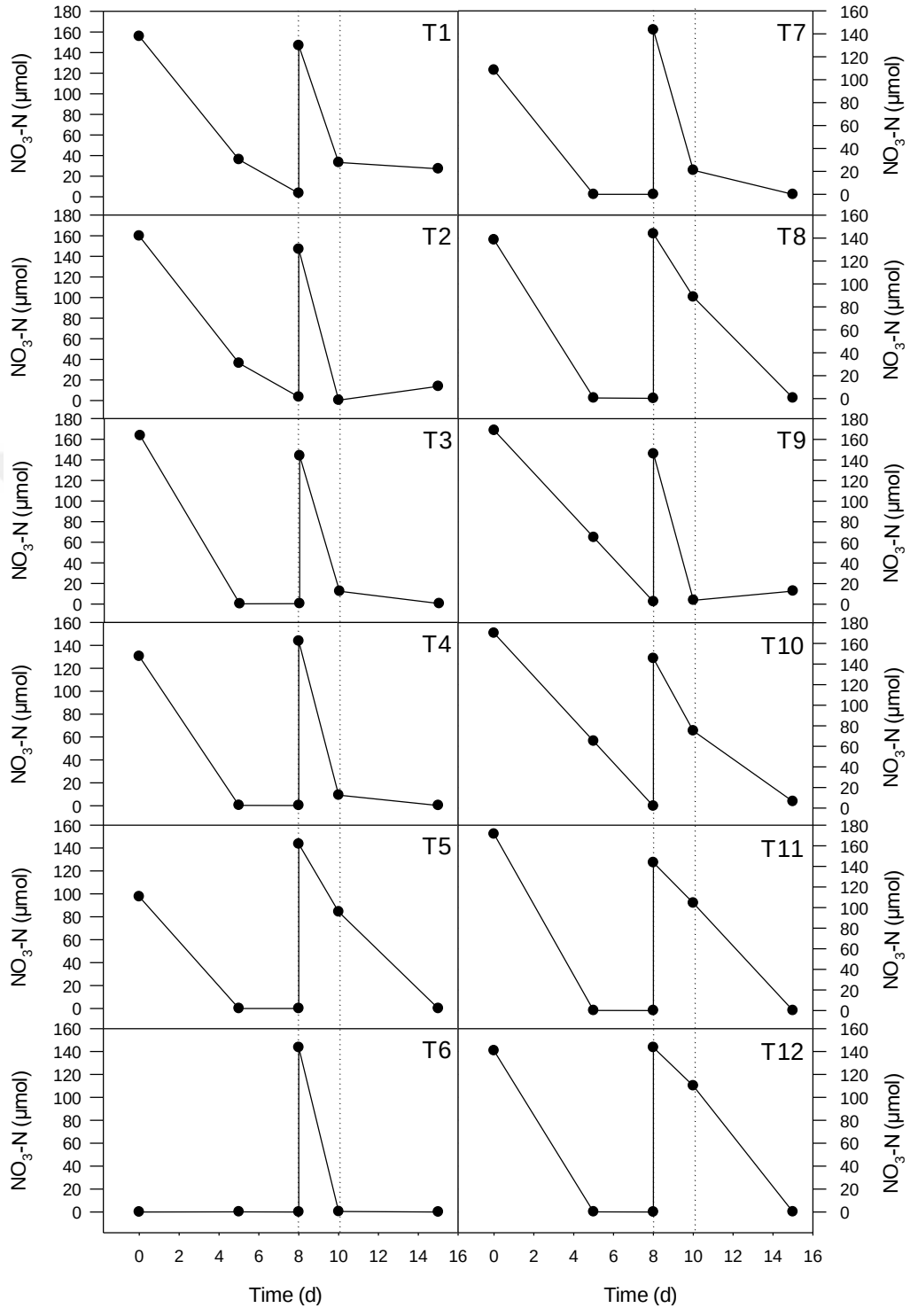

Figure E.3 Graphs showing the nitrate consumption trend in test reactors (NO_3 consumption rates in test reactors were calculated between dotted lines (Day 8-10). Sudden increase in concentration on Day 8 indicates the second feeding)

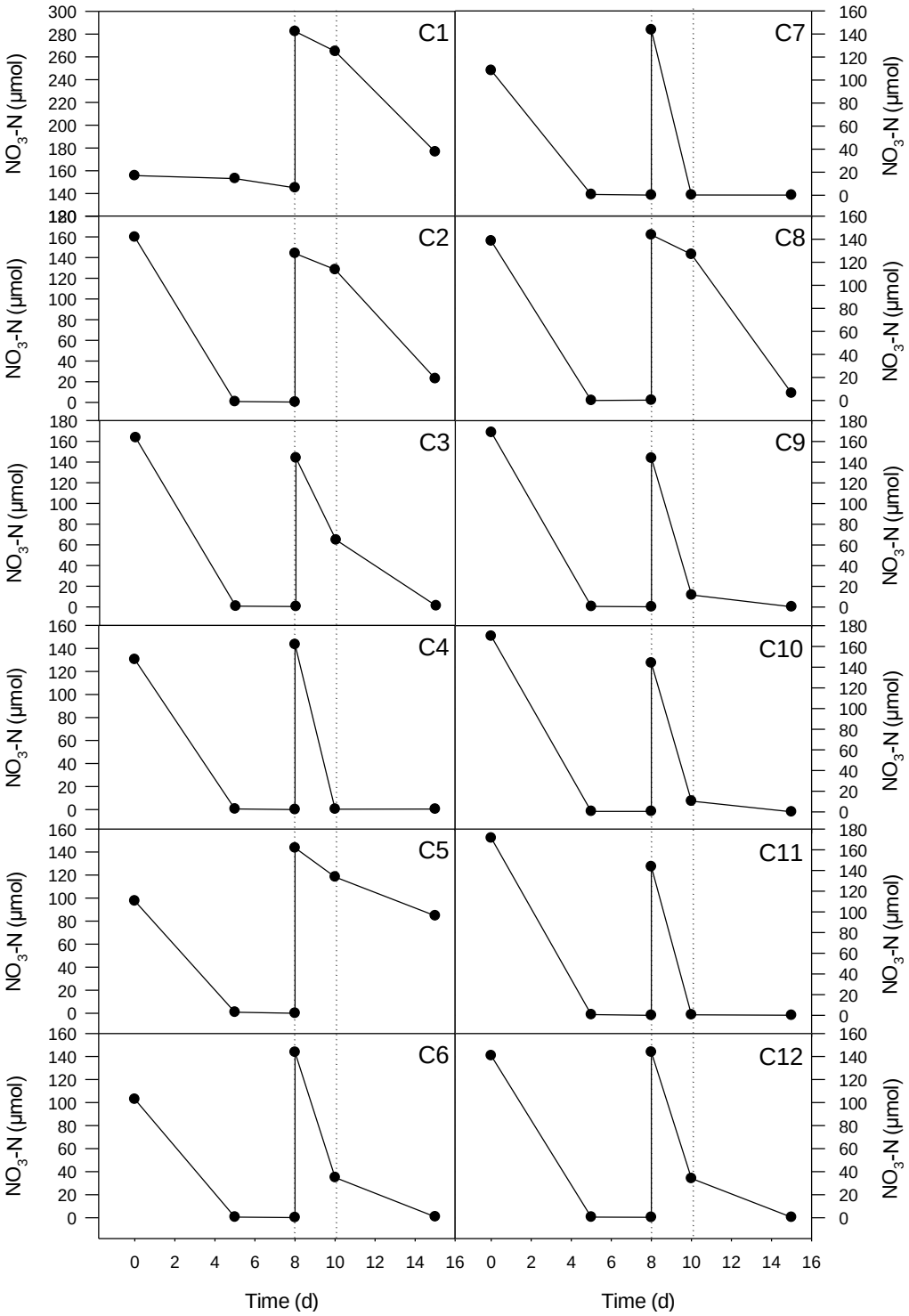

Figure E.4 Graphs showing the nitrate consumption trend in control reactors (NO_3 consumption rates in control reactors were calculated between dotted lines (Day 8-10). Sudden increase in concentration on Day 8 indicates the second feeding)

F. Methane Analyses Results for Test and Control Reactors in Batch Reactor Experiments

Table F.1 Methane analysis results for test and control reactors over the 15-day incubation

No	Inoculum Source	Test Reactors					Control Reactors				
		Total CH_4 in the reactor (µmol)[a]				Δ CH_4	Total CH_4 in the reactor (µmol) [a]				Δ CH_4
		Day 0	Day 5	Day 10	Day 15	(µmol)	Day 0	Day 5	Day 10	Day 15	(µmol)
1	PS	968	797	684	505	-463	0	0	0	0	0
2	FS	1185	863	721	531	-654	0	0	0	0	0
3	AD	1225	1038	941	810	-415	0	179	265	345	345
4	RS	1210	1029	1209	1377	167	0	179	503	1216	1216
5	FS-PS	1133	844	786	602	-531	0	0	0	0	0
6	FS-AD	1272	984	954	1024	-247	0	41	128	227	227
7	FS-RS	998	945	473	759	61	0	108	243	436	436
8	FS-PS-AD	1246	1036	1016	872	-375	0	0	0	0	0
9	FS-PS-RS	1141	889	802	668	-474	0	38	124	221	221
10	RS-AD	1182	1129	1045	991	-191	0	261	352	468	468
11	RS-PS	1036	845	889	920	-116	0	102	230	493	493
12	PS-AD-RS	1176	1001	950	844	-332	0	180	263	384	384

[a] Based on the average results of replicate analysis

[b] Refer to Sectio 3.2.3 Calculation methods section for the calculation method of total CH_4 in the reactor

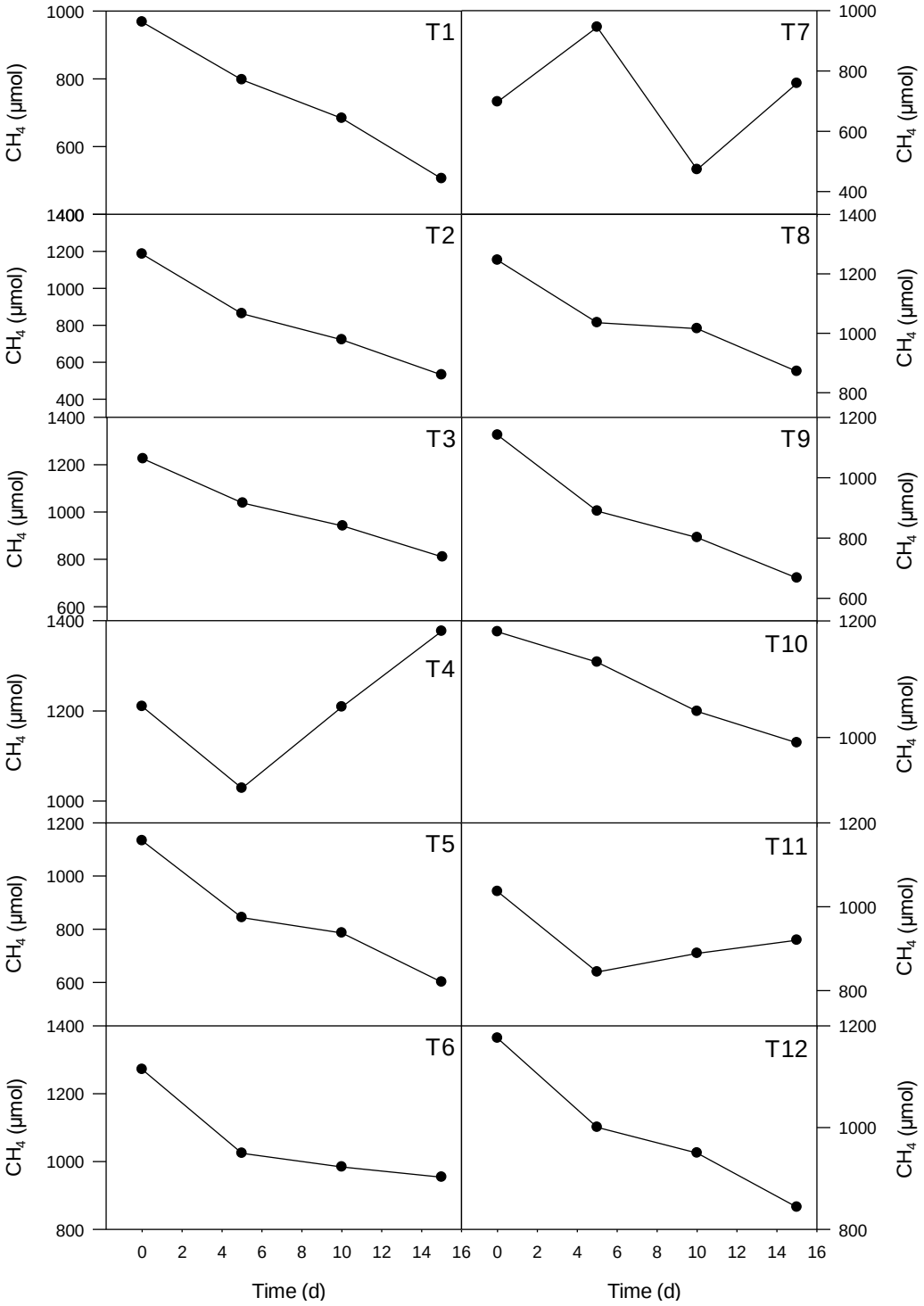

Figure F.1 Graphs showing the methane trend in test reactors. CH_4 consumption rates were calculated using the data only showing a linear trend (where $R^2 > 0.90$).

G. Nitrite and Nitrate Trends of The Activity Tests for Enrichment-1 and Enrichment-2.

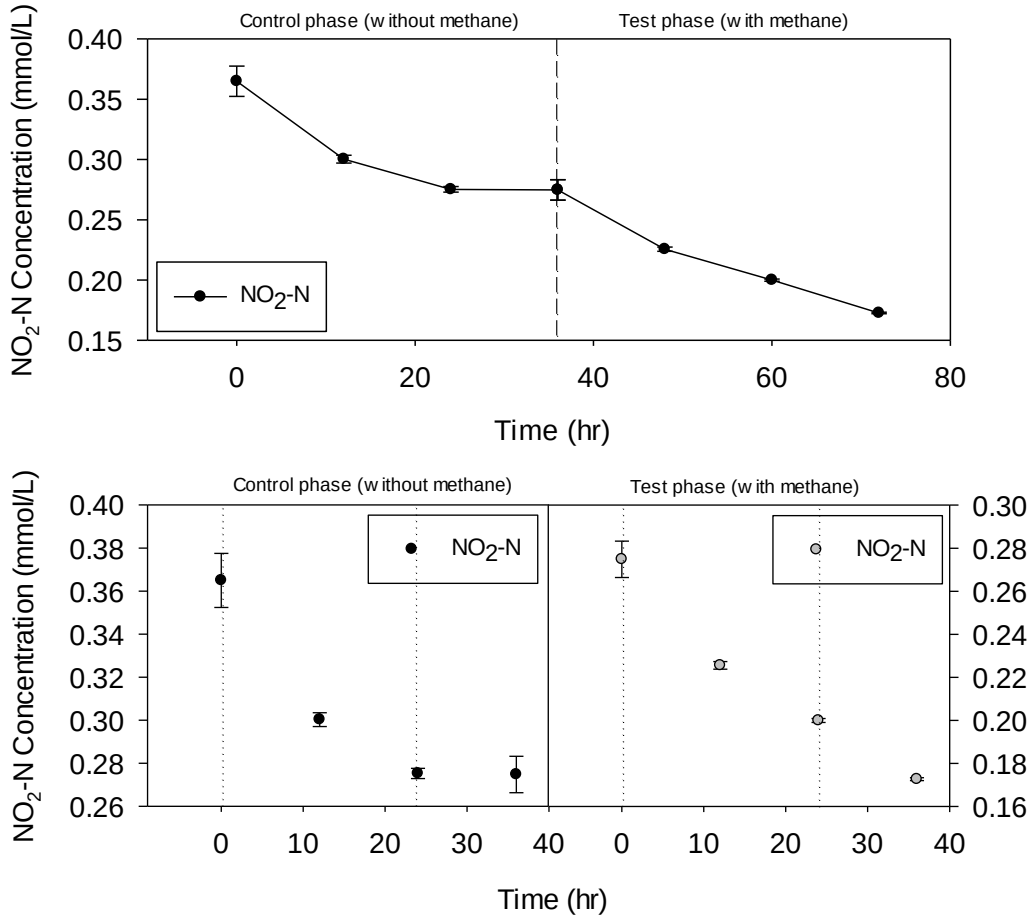

Figure G.1 Nitrite trend observed in En1-AT1

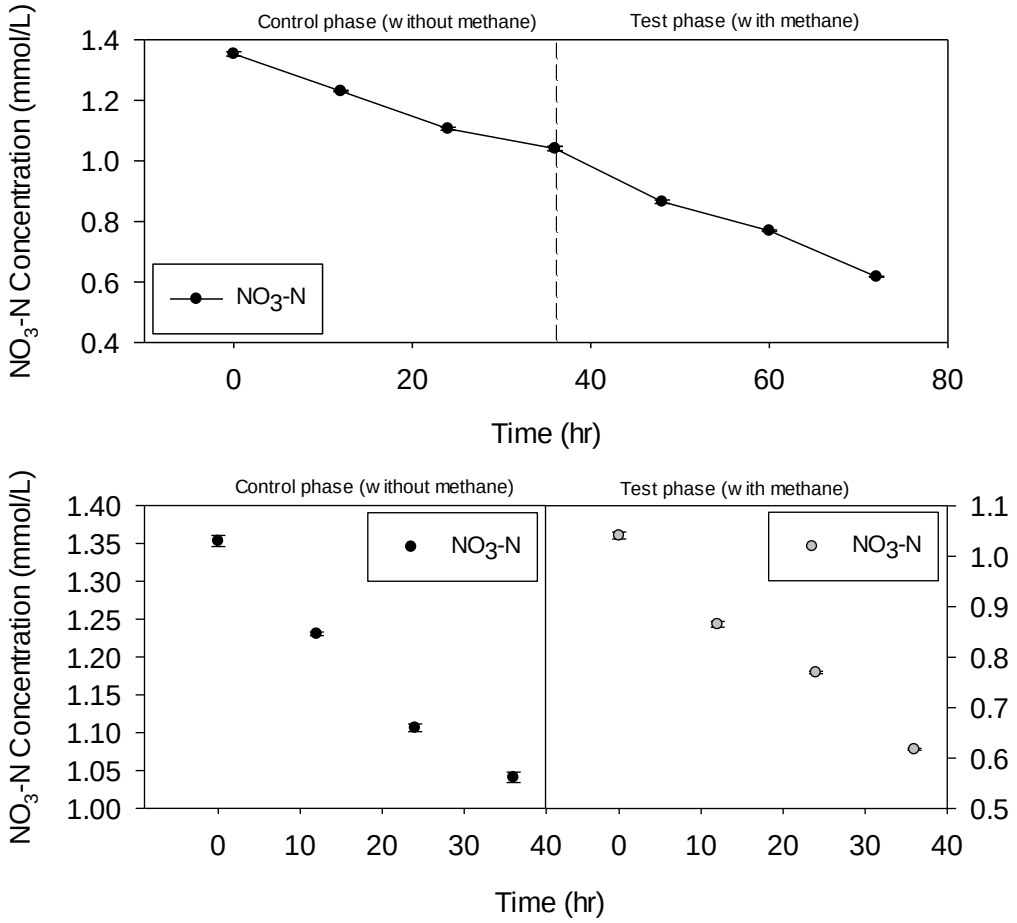

Figure G.2 Nitrate trend observed in En1-AT1

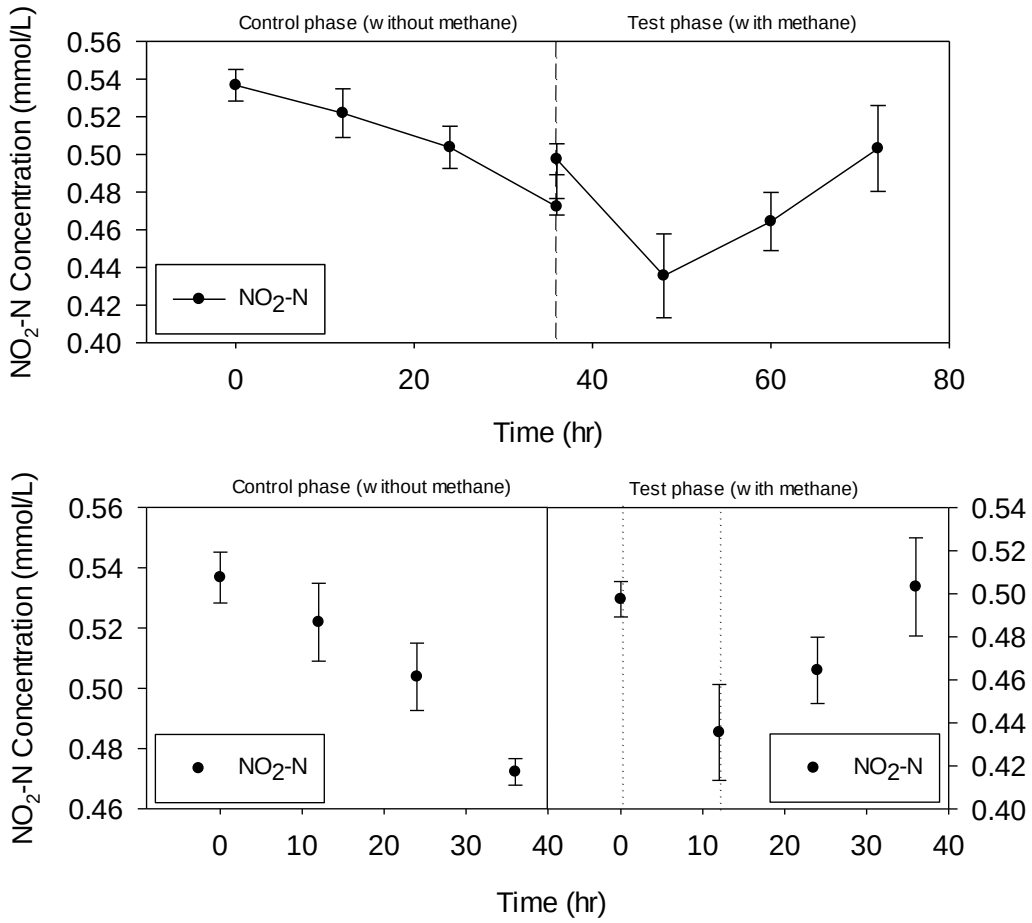

Figure G.3 Nitrite trend observed in En1-AT2

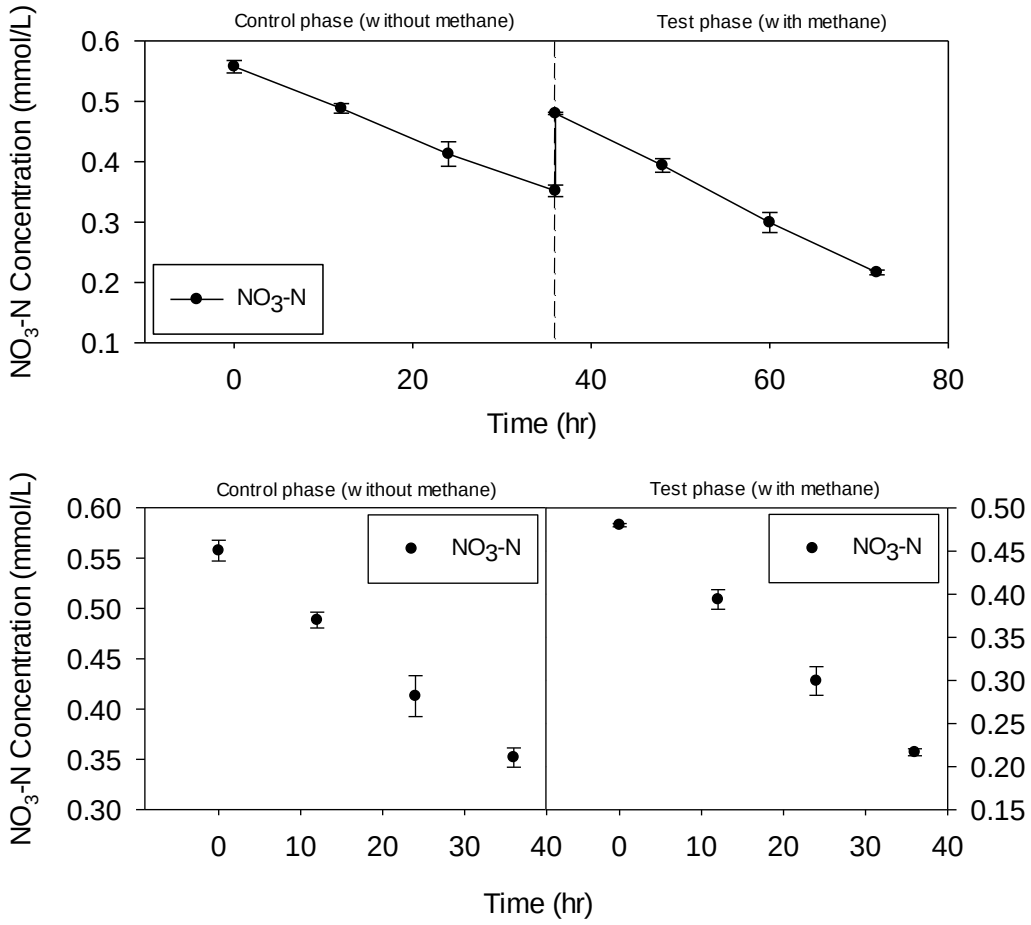

Figure G.4 Nitrate trend observed in En1-AT2

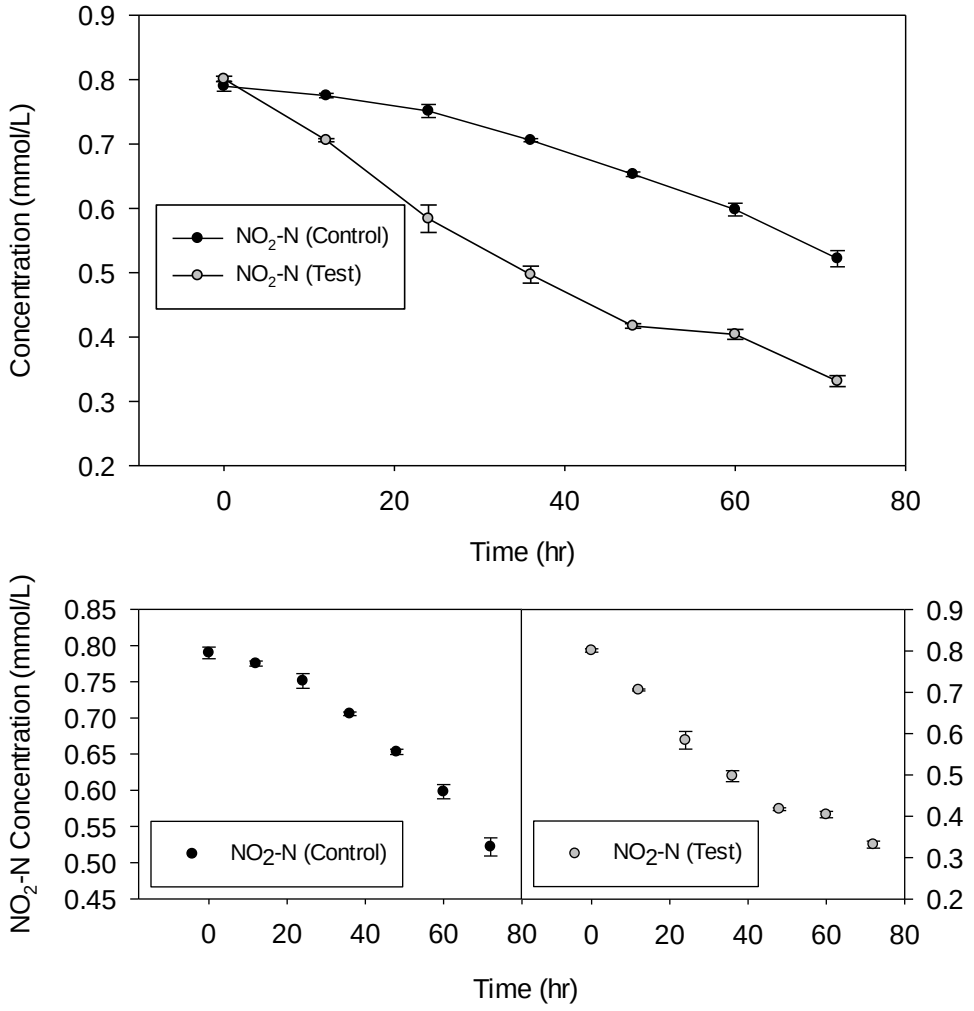

Figure G.5 Nitrite trend observed in En1-AT3

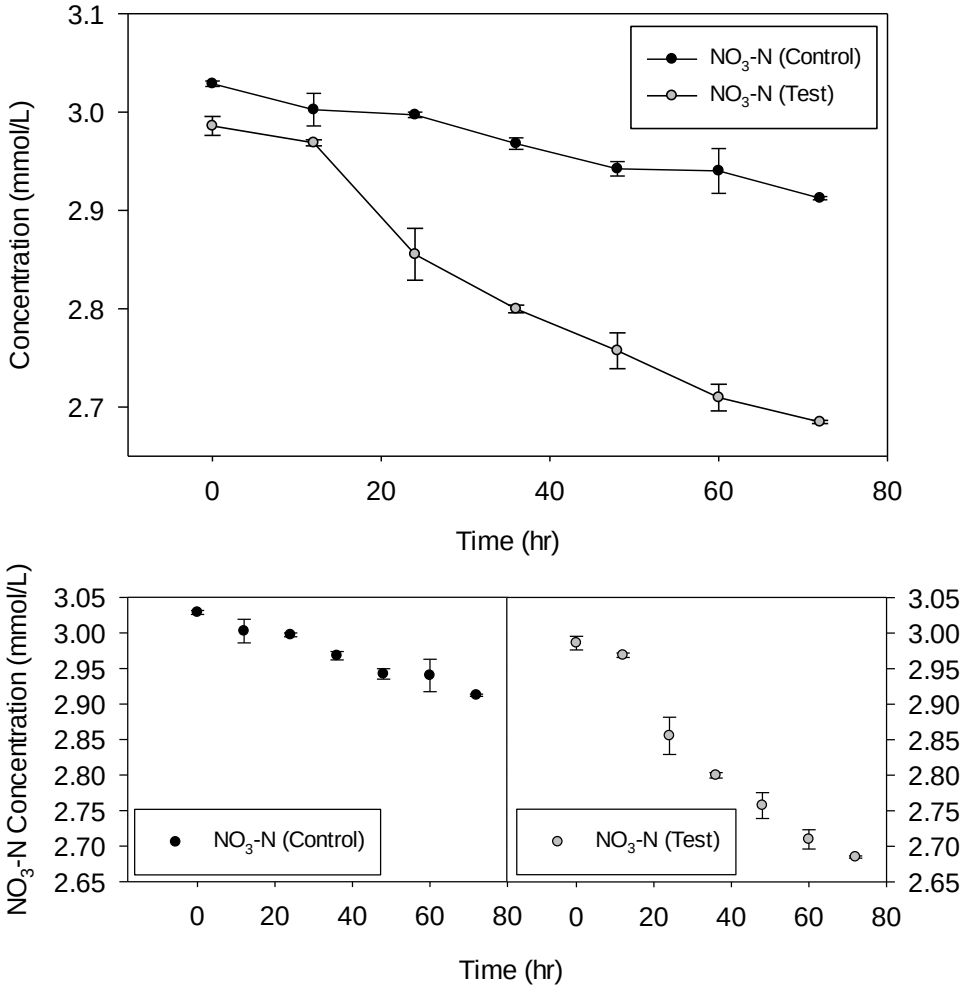

Figure G.6. Nitrate trend observed in En1-AT3

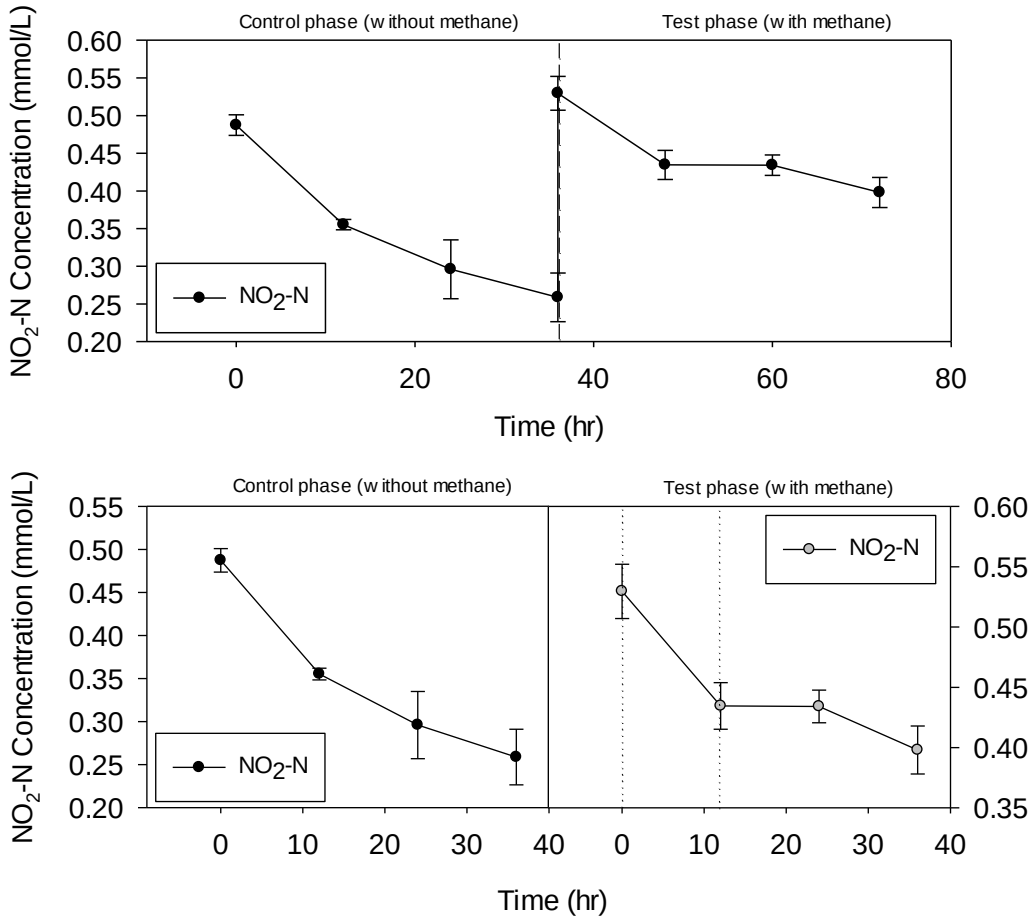

Figure G.7 Nitrite trend observed in En2-AT1

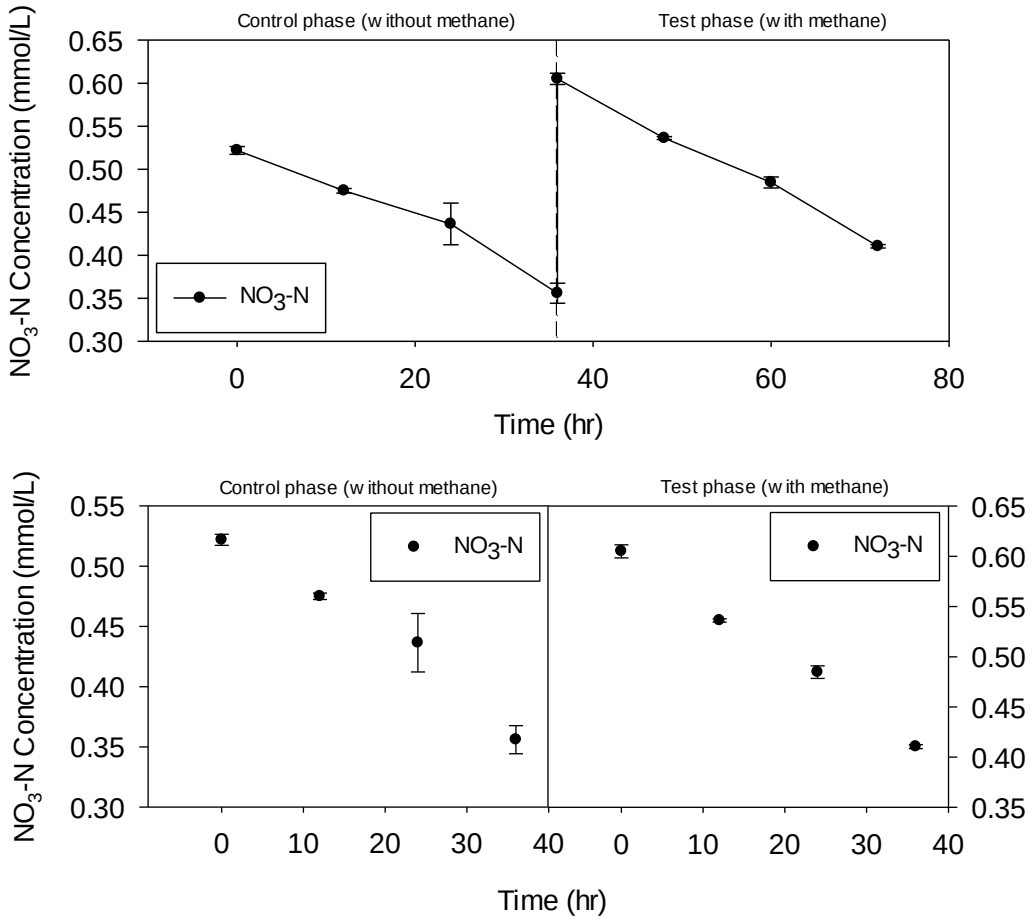

Figure G.8 Nitrate trend observed in En2-AT1

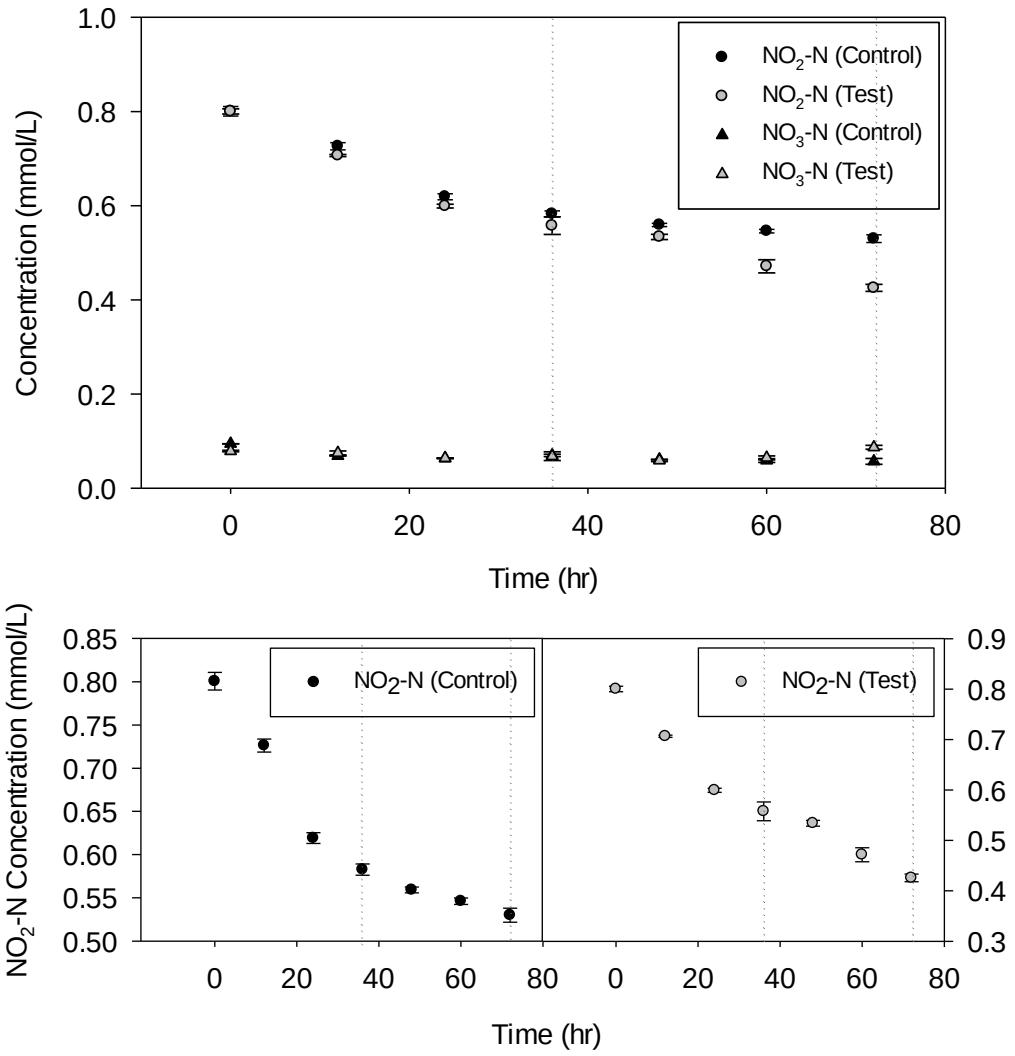

Figure G.9 Nitrite trend observed in En2-AT2

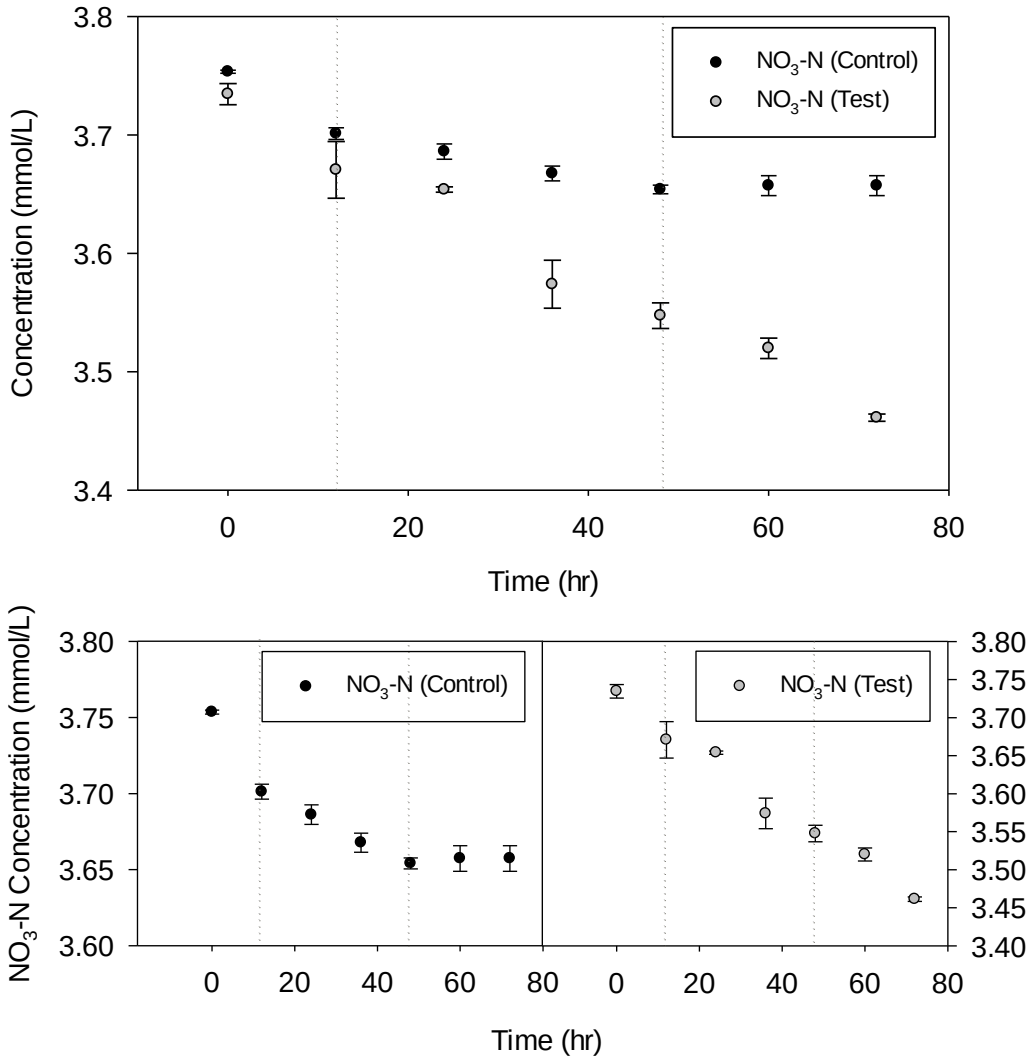

Figure G.10 Nitrate trend observed in En2-AT2

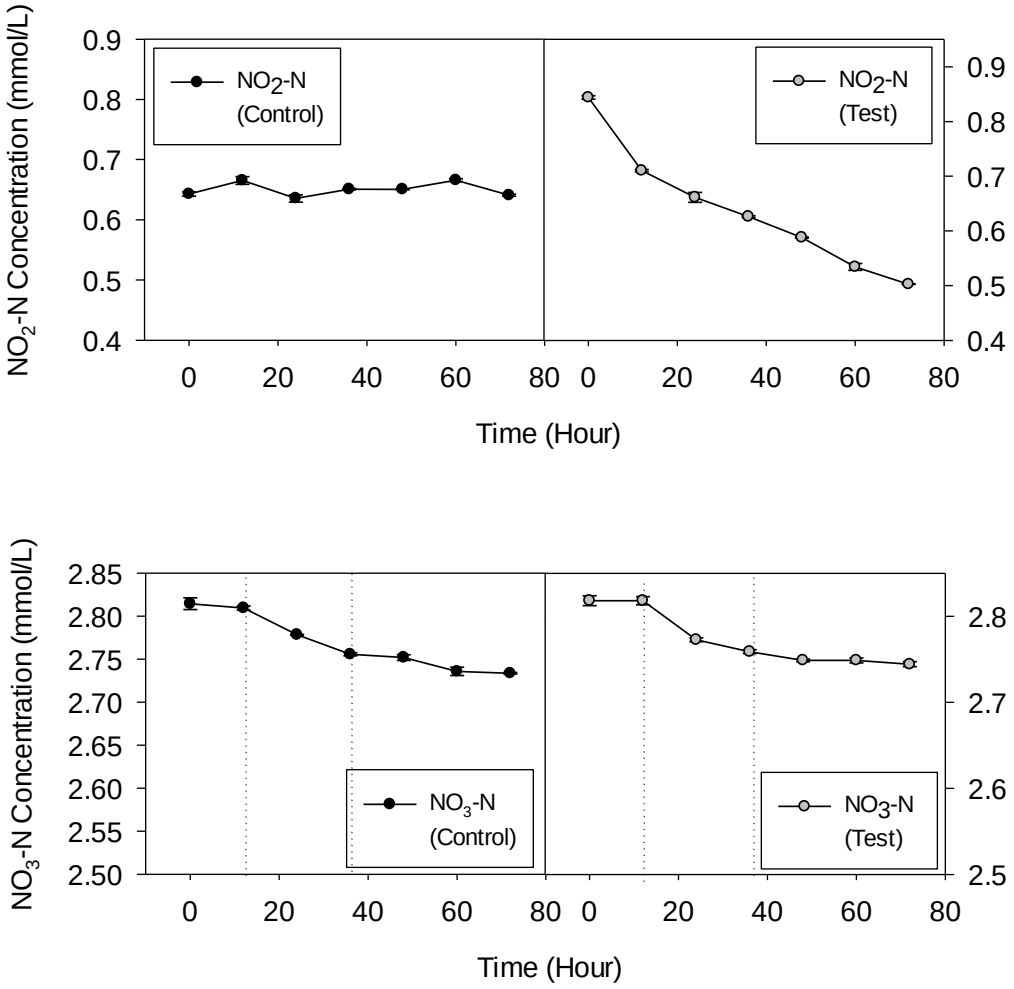

Figure G.11 Nitrite and nitrate trends observed in En1-GAC

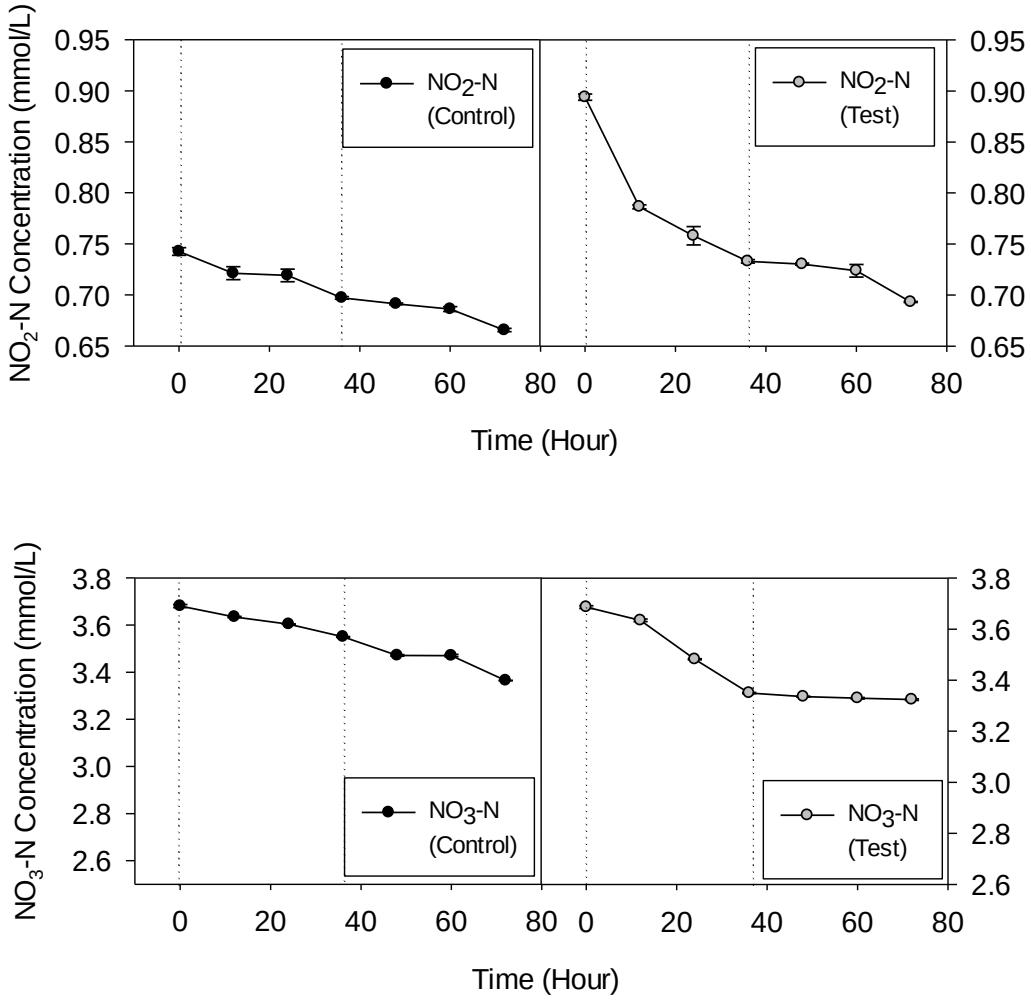

Figure G.12 Nitrite and nitrate trends observed in En2-GAC

H. Calibration Curves Used in Ion Chromatograph, Gas Chromatograph, TOC analyses and Nessler Method

Calibration curves obtained as a result of low and high range calibration using anion standard solutions (Shimadzu PIA Std. Sample Anion and High Purity Standards Anion Std.) for NO_2^-, NO_3^- PO_4^{-2} and SO_4^{-2} ions in IC analyses are presented in Figure H.1, Figure H.2, Figure H.3 and Figure H.4, respectively.

The ion chromatography device was adjusted to have a maximum pressure limit of 150 bar, an oven temperature of 45 ^oC and a flow rate of 0.8 mL/min. LOD for nitrite, nitrate, phosphate and sulfate measured with IC are 0.015, 0.09, 0.024 and 0.003 mg/L, respectively; LOQ are 0.045, 0.027, 0.024 and 0.01 mg/L, respectively.

a)

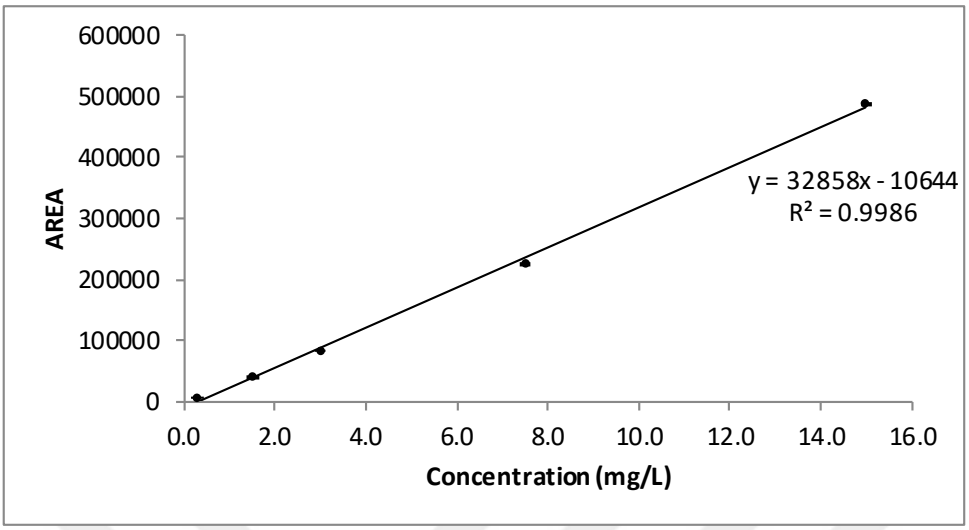

b)

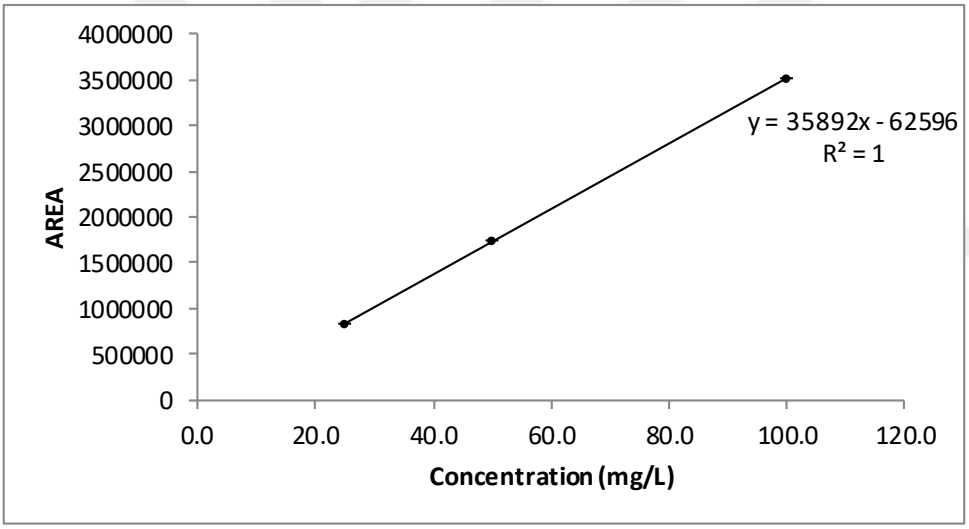

Figure H.1 NO_2 a) low and b) high range calibration curve

a)

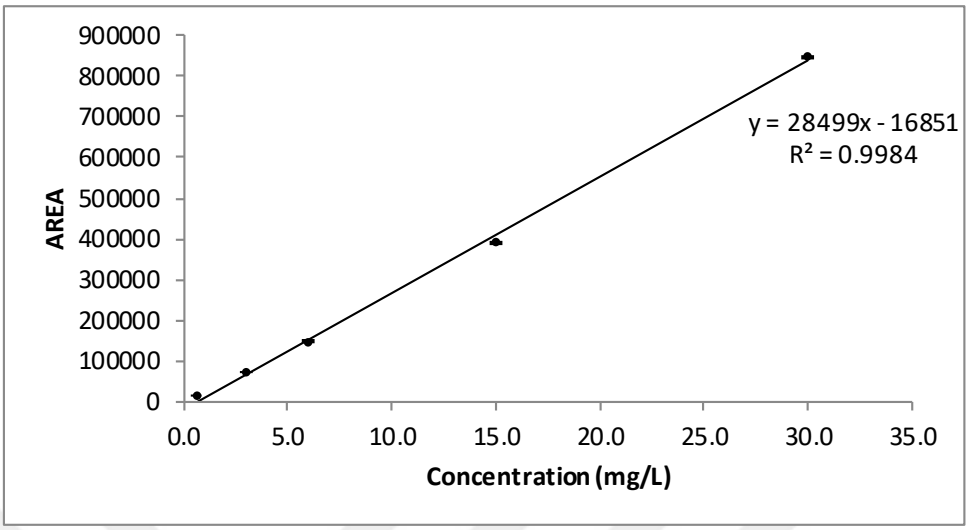

b)

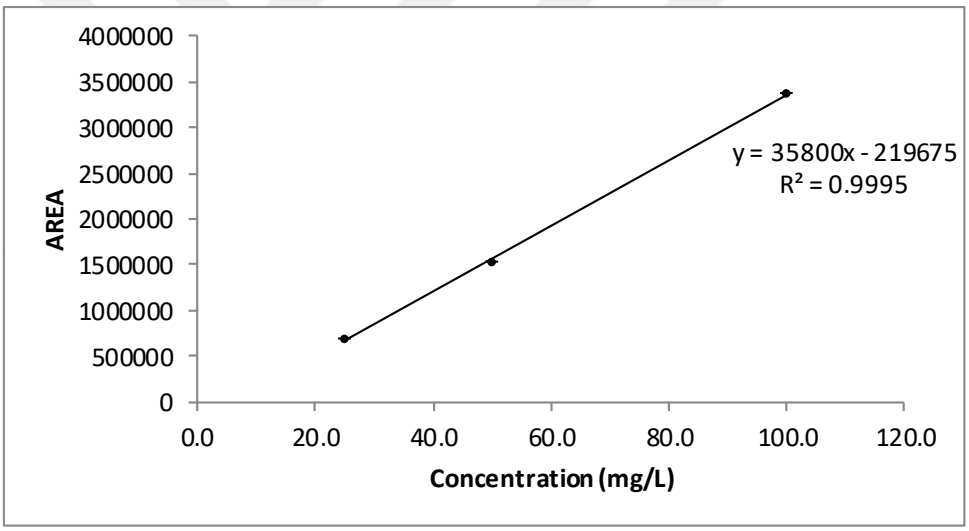

Figure H.2 NO_3 a) low and b) high range calibration curve

a)

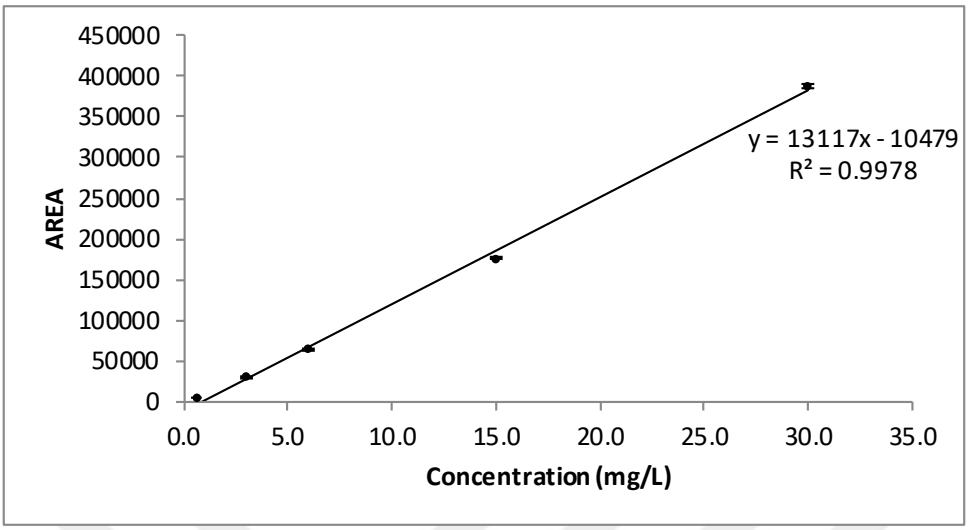

b)

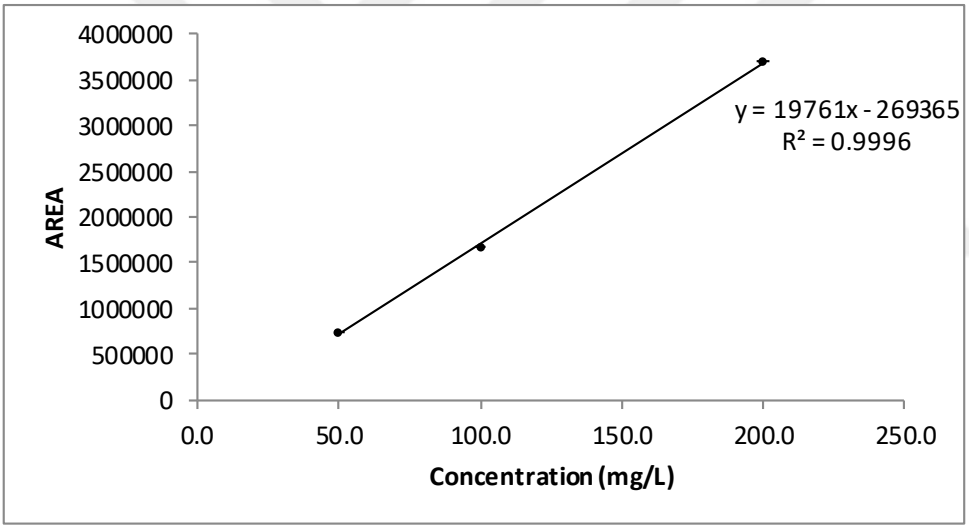

Figure H.3 PO_4 a) low and b) high range calibration curve

a)

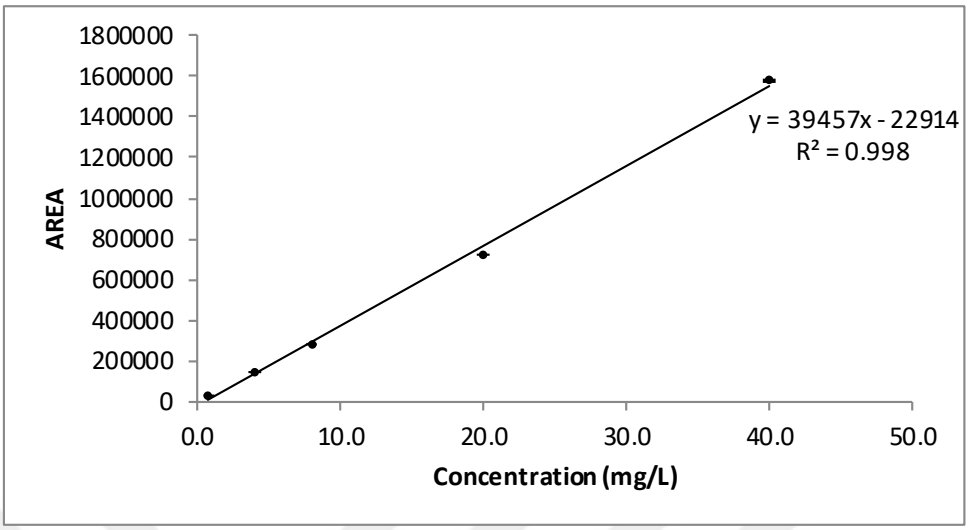

b)

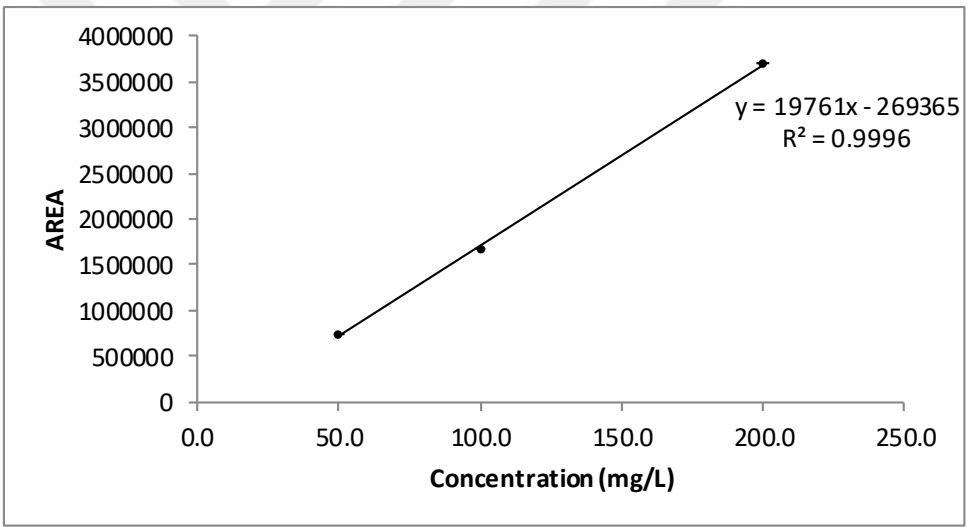

Figure H.4 SO_4 a) low and b) high range calibration curve

The calibration curves obtained using GC and calibration gas (10% H_2, 10% N_2 30% CO_2, 50%CH_4) for CO_2, CH_4, and N_2 gases in gas chromatograph analyzes are presented in Figure H.5, Figure H.6 and Figure H.7.

The injector temperature was set at 80°C, the furnace temperature at 40°C, and the detector temperature at 80°C, and helium was used as the carrier gas at constant pressure of 100 kPa. The column used is the serial connected CP7429: CP-molsieve 5A/CP-porabond Q column. Calibration curves for CO_2, CH_4, N_2 are given in below.

LOD for CO_2, CH_4, N_2 measured by GC are 0.07, 0.38 and 0.04 µmol, respectively; LOQ are 0.21, 1.15 and 0.11 µmol, respectively.

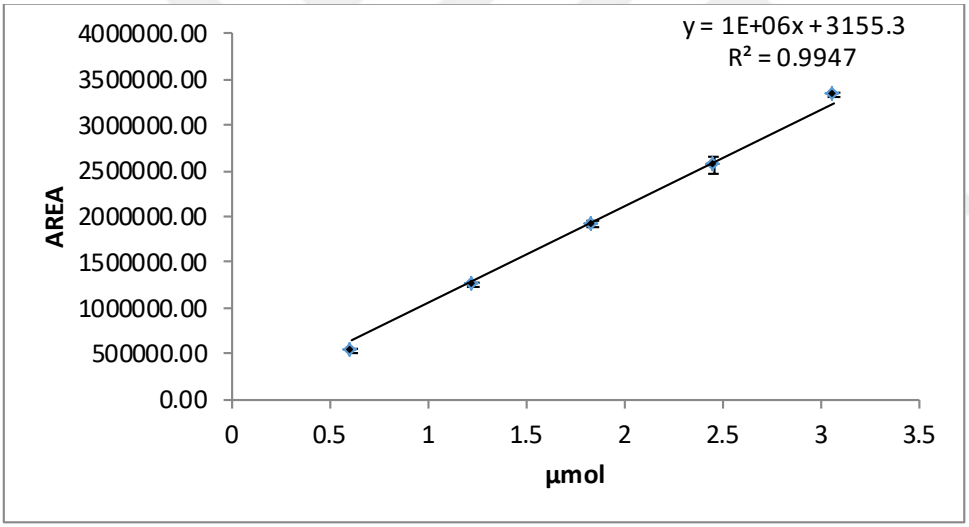

Figure H.5 CO_2 calibration curve

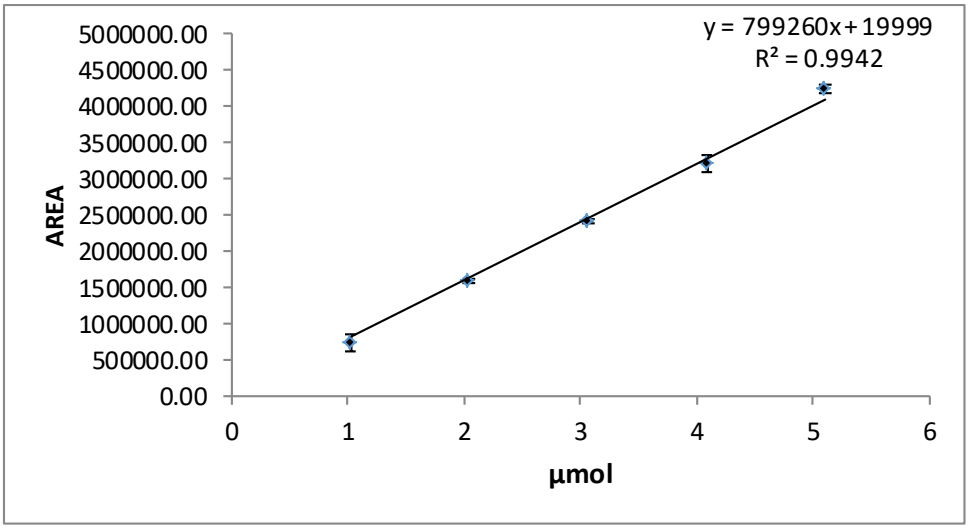

Figure H.6 CH_4 calibration curve

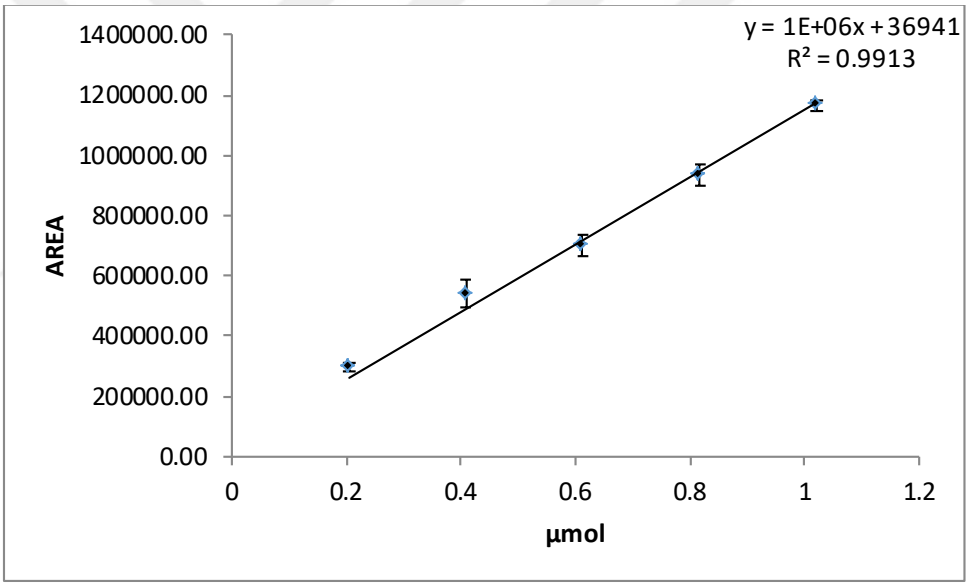

Figure H.7 N_2 calibration curve

The calibration curve obtained with potassium hydrogen phthalate ($C_8H_5KO_4$) in the analysis performed with the Total Organic Carbon (TOC) Analyzer is shown in Figure H.8. The LOD and LOQ for total carbon (TC) measured with a TOC analyzer are 0.1 and 1.2 mg/L, respectively.

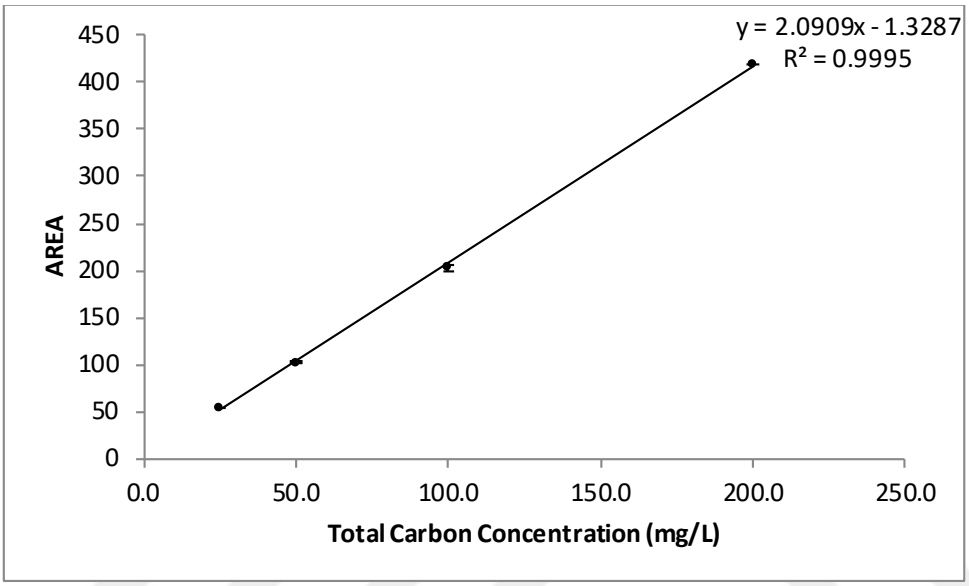

Figure H.8 Total Carbon (Specified as non-purgeable organic carbon (NPOC)) calibration curve

The calibration curve obtained using NH_4Cl stock solution in NH_3-N analyzes performed with the Nessler Method (HACH) is shown in Figure H.9. LOD and LOQ for ammonia measurements using the Nessler method are 0.02 and 0.02 mg/L, respectively.

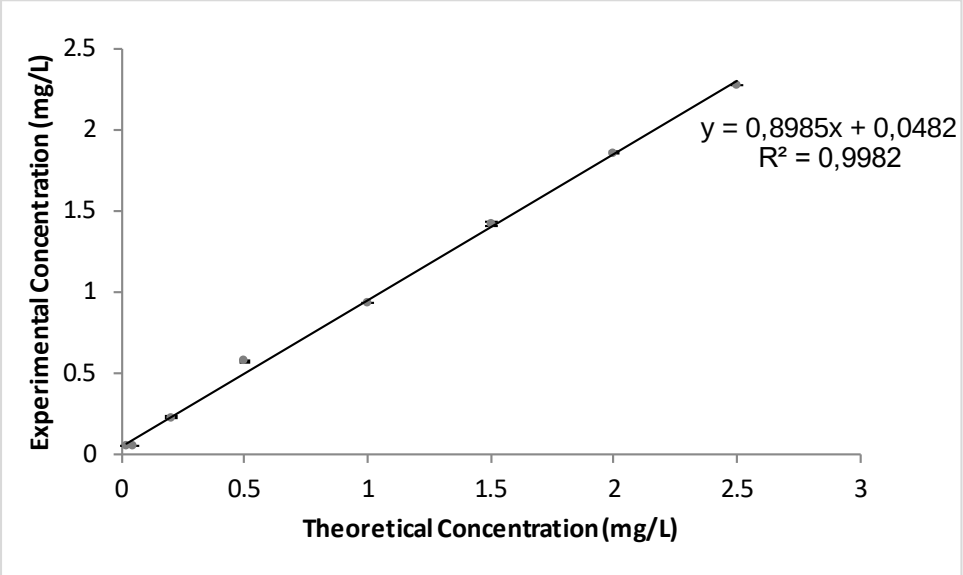

Figure H.9 NH_3-N calibration curve

İ. Sulfate Trends in Enrichment-1 and Enrichment-2

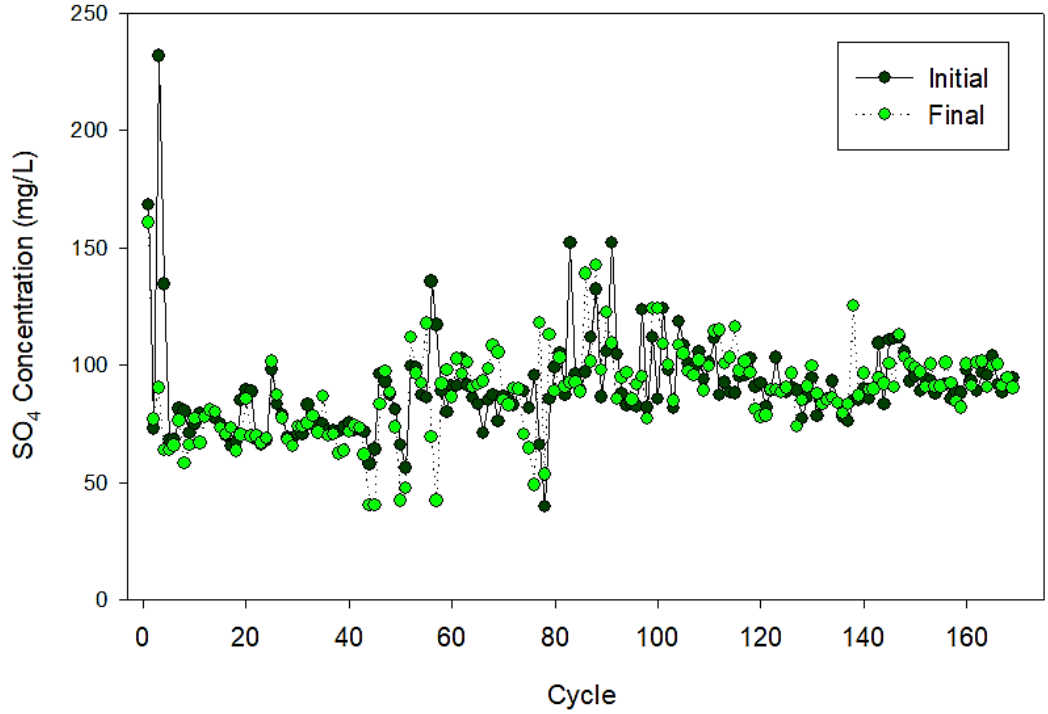

Figure I.1 SO_4 trend in Enrichment-1

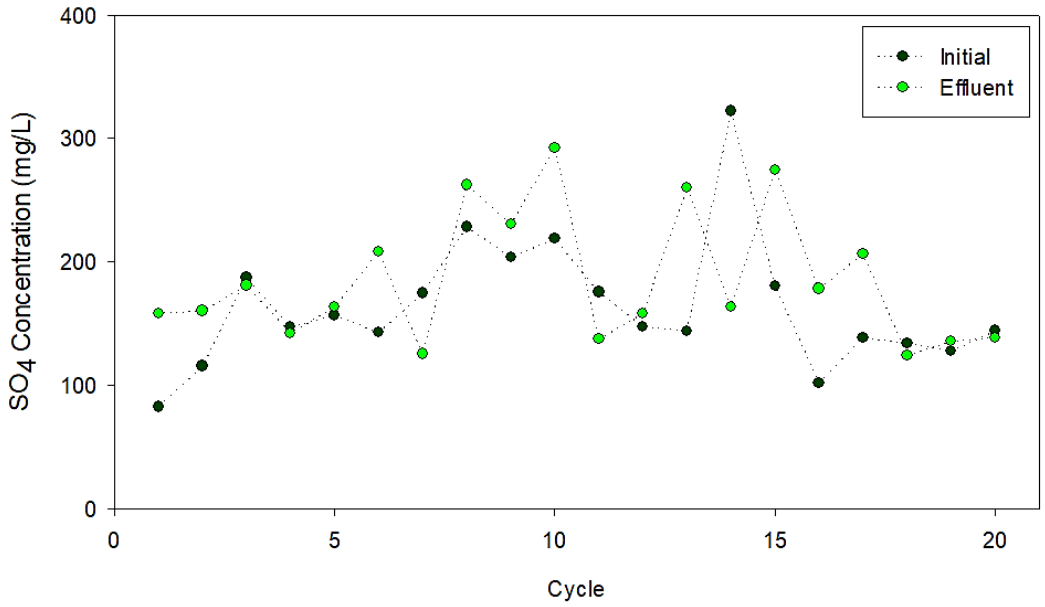

Figure I.2 SO_4 trend in Enrichment-2

J. Evaluation of Autotrophic Denitrification Possibilities in Enrichment-1

Possible electron donors used in denitrification (NH_4^+, H_2, Mn^{2+}, Fe^{2+}, Fe^0, S^0, HS^-) and related stoichiometric reactions are presented in the table below.

Table J.1 Stoichiometric reactions of commonly used electron donors in autotrophic denitrification

$NH_4^+ + 1.32\ NO_2^- + 0.066\ HCO_3^- + 0.13\ H^+ \rightarrow 1.02\ N_2 + 0.26\ NO_3^- + 0.066\ CH_2O_{0.5}N_{0.15} + 2.03\ H_2O$.	Equation J.1
$H_2 + 0.355\ NO_3^- + 0.049\ CO_2 + 0.355\ H^+ \rightarrow 0.010\ C_5H_7O_2N + 0.172\ N_2 + 1.143\ H_2O$	Equation J.2
$Mn^{2+} + 0.4\ NO_3^- + 0.8\ H_2O \rightarrow MnO_2 + 0.2\ N_2 + 1.6\ H^+$	Equation J.3
$Fe^{2+} + 0.2\ NO_3^- + 2.4\ H_2O \rightarrow Fe(OH)_3 + 0.1\ N_2 + 1.8\ H^+$	Equation J.4
$Fe^0 + 0.4\ NO_3^- + 1.2\ H_2O \rightarrow Fe^{2+} + 0.2\ N_2 + 2.4\ OH^-$	Equation J.5
$S^0 + 0.876\ NO_3^- + 0.343\ H_2O + 0.379\ HCO_3^- + 0.023\ CO_2 + 0.080\ NH_4^+ \rightarrow 0.080\ C_5H_7O_2N + 0.824H^+ + 0.44\ N_2 + SO_4^{2-}$	Equation J.6
$HS^- + 1.23\ NO_3^- + 0.573\ H^+ + 0.438\ HCO_3^- + 0.027\ CO_2 + 0.093\ NH_4^+ \rightarrow 0.093\ C_5H_7O_2N + 0.866H_2O + 0.614\ N_2 + SO_4^{2-}$	Equation J.7
$S_2O_3^{2-} + 1.24\ NO_3^- + 0.45\ HCO_3^- + 0.09\ NH_4 + + 0.11\ H_2O \rightarrow 0.09\ C_5H_7O_2N + 0.40\ H^+ + 0.62\ N_2 + 2SO_4^{2-}$	Equation J.8
$SCN^- + 1.6\ NO_3^- + 0.2\ H_2O + 1.6\ H^+ + HCO_3 - \rightarrow SO_4^{2-} + NH_3 + 2\ CO_2 + 0.8\ N_2$	Equation J.9
$FeS_2 + 3\ NO_3^- + 2\ H_2O \rightarrow Fe(OH)_3 + 1.5\ N_2 + 2\ SO_4^{2-} + H^+$	Equation J.10
$H_3AsO_3 + 0.4\ NO_0^- \rightarrow 1.6\ H^+ + HASO_4^{2-} + 0.2\ N_2 + 0.2\ H_2O$	Equation J.11

Autotrophic denitrification possibility due to specific electron donors was evaluated below;

- Anammox reaction (Equation J.1) was not expected since there was no ammonium in the medium solution as electron donor and seed sludge used in re-inoculation was already washed.
- H_2 dependent autotrophic denitrification (Equation J.2) was not expected as there was no H_2 in the headspace.
- There was no arsenic in the acidic trace element solution contained in the medium; therefore, denitrification in which arsenic acid (H_3AsO_3) was used as electron donor is also not expected (Equation J.11).
- The initial amounts of Fe^{2+}, Mn^{2+} added to the reactor (0.0037 and 0.0013 mmol, respectively) with the medium solution were quite low.

Nevertheless, $\Delta NO_3/\Delta Fe^{+2}$ and $\Delta NO_3/\Delta Mn^{+2}$ molar ratios were calculated based on the NO_3 amount (mmol) consumed in the reactor, and assuming that all of the iron and manganese amount added at the beginning of the cycle with the medium solution was used in autotrophic denitrification. These values were 656 for $\Delta NO_3/\Delta Fe^{+2}$ and 1866 for $\Delta NO_3/\Delta Mn^{+2}$ at Cycle-50. Experimental ratios are quite high when compared to the theoretical $\Delta NO_3/\Delta Fe^{+2}$ (0.2) and $\Delta NO_3/\Delta Mn^{+2}$ (0.4) ratios calculated using stoichiometric reactions of Fe^{+2} and Mn^{+2} (Equations J.3 and J.4). Therefore, the amount of nitrate removed in the reactor is much higher than the amount which can be consumed with Fe^{+2} and Mn^{+2} added in the medium. This eliminates the possibility of autotrophic denitrification from iron and manganese due to addition via medium solution.

- An autotrophic denitrification scenario due to Fe^0, Fe^{+2} and Mn^{+2}, which may have been added to the reactor as a result of inoculation(i.e. with inoculum source) was also evaluated; this time with elemental analyses.
- Nitrate removal due to reduced sulfur compounds (Equation J.6-7-8-9) such as elemental sulfur, sulfide and thiosulfate, which can be found in anaerobic digester sludge (Di Capua et al., 2018) used in the re-inoculation was evaluated with respect to elemental analyses, as discussed below.

The possibilities of autotrophic denitrification in which iron (Fe), manganese (Mn) and elemental S are used as electron donors were evaluated for Cycle-50 via elemental analysis, the results of which are given below.

Table J.2. Results of elemental analysis for Enrichment-1 Cycle-50[a]

Sample	**Mn (%)**	**Fe (%)**	**S (%)**
Solid phase (Sludge)	0,079	4	0,73
Sample	**Mn (mg/L)**	**Fe (mg/L)**	**S (mg/L)**
Liquid phase	0,0084	0,06	40

[a] The sample was filtered through a 0.45 µm filter for separate analysis of solid and liquid phase elements.

In the evaluation of the elemental analysis, results some assumptions were made which are presented below:

- ✓ Manganese (Mn^{+2}), which is used as an electron donor in autotrophic denitrification, is an ion dissolved in water, and the results of the analysis in the liquid phase were evaluated in calculating the theoretical nitrate removal due to manganese (Equation J.3).
- ✓ The iron exists in solid form as free (Fe^0) or precipitates of iron compounds, and in liquid form as one of two oxidative types (ferrous state; Fe^{2+} or ferric state; Fe^{3+}). In autotrophic denitrification reactions involving iron, iron is in the form of Fe^{2+} (Equation J.4), Fe^0 (Equation J.5) and pyrite (FeS_2) (Equation J.10). In order to evaluate the possible maximum nitrate removal due to iron in the liquid phase (Fe^{3+} cannot be used as an electron donor), it is assumed that all of the iron species in the liquid phase are Fe^{2+} (Equation 1.10). Fe^0 and FeS_2 are insoluble in water. Therefore, when the scenario, where all the solid iron is in the form of Fe^0 and FeS_2, are evaluated separately, it is seen that the donor that can contribute more to nitrate removal is FeS_2. Since iron is very rare in nature as free form (Fe^0) and is usually found in sediments in the form of mineral compounds (Heyden and Roychoudhury, 2015), FeS_2 was assumed to be used as electron donor when evaluating solid iron-dependent autotrophic denitrification (Equation J.10).
- ✓ While evaluating the results of the sulfur (S) analysis, the solid-phase sulfur was taken into account in autotrophic denitrification since elemental sulfur (S^0) is not dissolved in water. All of the sulphur compounds (HS^-, $S_2O_3^{2-}$, SCN^-) present in water as ions can be found in the anaerobic digester sludge and can be converted to each other by microbial reactions (Okoro and Sun, 2019; Luque-Almagro et al. 2017). When the reactions in which these three possible sulfur compounds are used as electron donors are evaluated separately, it is seen that the donor that can contribute more to nitrate removal is SCN-. In order to evaluate the probability of maximum nitrate

consumption, the dominant electron donor based on liquid sulfur was assumed to be SCN- (Equation J.9).

In line with the assumptions explained above, for the maximum possible autotrophic denitrification, the cases where Mn^{+2}, Fe^{2+} and SCN^- in the liquid phase and FeS_2 and S^0 compounds/elements in the solid phase were considered as electron donors. In Enrichment-1 system, in order to evaluate the contribution of these ions as electron donors to the nitrate removal, the theoretical nitrate removal and sulfate production of the relevant processes are calculated and presented in Table J.3. It is to be noted that the initial concentrations of these ions at the beginning of Cycle-50 were calculated using elemental analysis results (Table J.2).

Table J.3. Comparison of the actual values with the amount of NO_3 to be consumed and SO_4 to be produced when possible electron donors are used in Cycle-50

Theoretical and Actual Values			**Amounts of NO_3 and SO_4 consumed / produced based on specific electron donor[a]**		
			Mn	**Fe**	**S**
Theoretical [b]	Liquid	NO_3 consumption (g)	0.000008	0.000027	0.29
		SO_4 production (g)	-	-	0.24
	Solid[c]	NO_3 consumption (g)	0	0.45	0.04
		SO_4 production (g)	-	-	0.07
	Total	NO_3 consumption (g)	0.000008	0.45	0.29
		SO_4 production (g)	-	-	0.31
Actual		NO_3 consumption (g)		0.15	
		SO_4 production (g)		0.05	

[a] Calculations were made assuming that Mn^{+2}, Fe^{2+} and SCN^- ions in the liquid phase and FeS^2 and S^0 compounds/elements in the solid phase were used as electron donors.
[b] Theoretical nitrate consumption was calculated using the stoichiometry in Table J.1
[c] TS concentration (0.4%) and density (1501.8 g/L) of the sludge sample taken from the reactor were used in solid phase calculations.

Nitrate consumption that can occur with autotrophic denitrification due to manganese, iron and sulfur and actual nitrate consumption observed in Cycle-50 (Table J.3) was in Figure J.1.

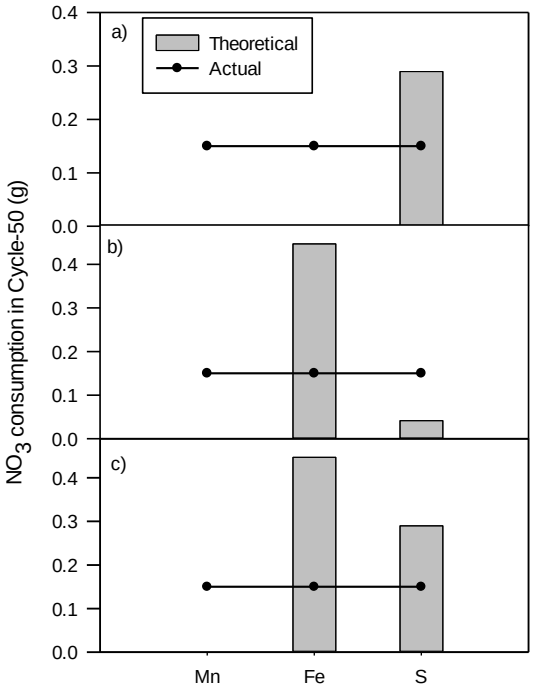

Figure J.1 Comparison of the theoretical the NO_3 consumption that can be consumed in a) liquid phase, b) solid (sludge) phase and c) total (liquid and solid) consumption, and the actual NO_3 consumption according to the elemental analysis results of the sample taken at the beginning of the Cycle-50

In the autotrophic denitrification scenario, where the total (liquid and solid phase) manganese is used as electron donor, the total nitrate amount that can be consumed is considerably lower than the actual amount consumed (Figure J.1). This corresponds to only 0.005% of the actual consumption. This result shows that Mn^{+2} –derived autotrophic denitrification was not effective in nitrogen consumption in the system.

On the other hand, the comparison shown in Figure J.1a and Figure J.1b indicates the possibilities of autotrophic denitrification due to iron in the solid (sludge) phase and sulfur-induced denitrification in the liquid phase. In autotrophic denitrification, in which the sulfur ion is used as an electron donor in the liquid phase, the amount

of nitrate that can be consumed theoretically corresponds to approximately twice the actual value (193%). This indicates that one or more of the HS^-, $S_2O_3^{2-}$, SCN^- ions may be involved in denitrification. Similarly, when the solid phase FeS_2 compound is used as an electron donor in autotrophic denitrification, the amount of nitrate that would be consumed theoretically corresponds to about three times (298%) the actual value. Since iron is very rare in free form (Fe^0) in nature, this indicates that sediment-derived pyrite (FeS2) may be involved in denitrification.

In reactions involving HS^-, $S_2O_3^{2-}$, SCN^- and FeS_2, which can be used as electron donors in autotrophic denitrification (Table J.1), the amount of SO_4 (g) that should be produced theoretically has been calculated (Table J.3). However, no sulfate production was observed in Cycle-50 (Figure I.1) in the Enrichment-1 system. Therefore, autotrophic denitrification via these reactions was observed not to be occurring in Enrichment-1 system. At least in Cycle-50, nitrate removal was due to DAMO process. However, in other cycles where SO_4 concentrations increased, it is possible to observe these electron donors-raelated autotrophic denitrification. Yet, as seen in Figue İ.1 increase in SO_4 concentrations during each cycle was not that common. So, DAMO process seems to be effective in NO_x removal in Enrichment-1 system, at least during the cycles, where SO_4 was not produced or was produced in low amounts.